Valorization of sédiments in bio-based materials : Application to fluvial sediments with incorporation of natural fibers

Mazhar Hussain

Normandie Université

UNIVERSITÉ DE ROUEN NORMANDIE

THÈSE

Pour obtenir le diplôme de doctorat

Spécialité **GENIE CIVIL**

Préparée au sein de l'**Université de Rouen Normandie**

Valorization of sédiments in bio-based materials-Application to fluvial sediments with incorporation of natural fibers

Présentée et soutenue par

MAZHAR HUSSAIN

Thèse soutenue le 26/10/2022

devant le jury composé de :

M. KENICHI SATO	Professeur des Universités - Université de Fukuoka	Rapporteur du jury
MME DELMA VIDAL	Professeur des Universités - Instituto Tecnológico de Aeronáutica	Rapporteur du jury
MME LUSMEILIA AFRIANI	Professeur des Universités - Université de Lampung	Membre du jury
M. ANDRY RICO RAZAKAMANANTSOA	Chargé de Recherche - UNIVERSITE NANTES	Membre du jury
MME HAFIDA ZMAMOU	Chargé de Recherche - UniLaSalle	Membre du jury
MME IRINI DJERAN-MAIGRE	Professeur des Universités - INSTITUT NATIONAL DES SCIENCES APPLIQUEES DE LYON	Président du jury
MME NATHALIE LEBLANC	Maître de Conférences HDR - UniLaSalle	Directeur de thèse
M. DANIEL LEVACHER	Professeur des Universités - Université de Caen Normandie	Co-directeur de thèse

Thèse dirigée par **NATHALIE LEBLANC** (TRANSFORMATIONS ET AGRO-RESSOURCES) et **DANIEL LEVACHER** (MORPHODYNAMIQUE CONTINENTALE ET COTIERE)

ED 497 NBISE
Normande de Biologie Intégrative, Santé, Environnement

Transformations & Agro-Ressources
UniLaSalle

Normandie Université

Pour obtenir le diplôme de doctorat

Spécialité Physico-chimie des matériaux

Préparée au sein de l'Université de Rouen Normandie

Sustainable reuse of sediments in bio-based materials - Application to fluvial sediments with incorporation of natural fibers

Présentée et soutenue par
Mazhar HUSSAIN

Thèse soutenue publiquement le 26 octobre 2022 devant le jury composé de		
Mme Lusmeilia AFRIANI	Professeure, Université de Lampung, Indonésie	Examinatrice
Mme Irini DJERAN-MAIGRE	Professeure, INSA Lyon	Examinatrice
Mme Natahlie LEBLANC	Enseignante-Chercheure, HDR, UniLaSalle, Rouen	Directrice de thèse
M. Daniel LEVACHER	Professeur émérite, Université de Caen Normandie	Co-directeur de thèse
M. Andry R. RAZAKAMANANTSOA	Chargé de recherches, Dr, Université Gustave Eiffel, Nantes	Examinateur
M. Kenichi SATO	Professeur, Université de Fukuoka, Japon	Rapporteur
Mme Delma VIDAL	Professeure, ITA, São José dos Campos, Brasil	Rapporteure
Mme Hafida ZMAMOU	Chercheure, Dr, UniLaSalle, Rouen	Co-encadrante

Thèse dirigée par Nathalie LEBLANC et Daniel LEVACHER
Unité de recherche Transformations & Agro-ressources (ULR 7519) et
Laboratoire Morphodynamique Continentale et Côtière M2C UMR 6143 CNRS

Acknowledgments

First of all, I would like to express my sincere thanks to my PhD supervisors Nathalie Leblanc, Daniel Levacher and Hafida Zmamou for their guidance, support, encouragement and suggestions which helped me to complete this work. I am also thankful to Prof. François Buyle-Bodin and Michele t' Kint for their valuable suggestions during CSI meetings.

I would like to thank to Magalie Legrain, Jean Baptiste and Marianne Rosa for their technical assistance in experimentation. Special thanks to Leo Saouti and Raphaelle Del Negro for their experimental work and cooperation. I am also thankful to all my colleagues in M2C Lab and Unilasalle for their help and suggestions throughout my thesis.

I greatly acknowledge the financial support from HEC Pakistan and funding by the project "From traditional uses to an integrated valorisation of sediments in the Usumacinta River basin (VAL-USES)" from the Agence Nationale de la Recherche of France (ANR-17-CE03-0012-01) and the Consejo Nacional de Ciencia y Tecnología of Mexico (FONCICYT-290792).

I am also thankful to my family and friends for their support and encouragement.

Mazhar Hussain

Abstract

This research is focused on sediment reuse in fired bricks, earth bricks and agronomy in the context of the circular economy. Usumacinta River sediments are dredged from Tabasco state of Mexico. Characteristics of these sediments were investigated for their reuse. Sediment suitability for bricks was observed with industrial approaches and standards. Fired bricks were manufactured with sediments mixing, moulding, drying and firing. Cubic (20*20*20 mm^3) and prismatic (15*15*60 mm^3) brick specimens were made for compressive and tensile strength test of fired bricks. Bricks were fired at a temperature range of 700 °C to 1100°C to optimize the use of energy. Strength of bricks was also optimized with different moulding moisture contents. Scale effect on strength of bricks was observed by varying the dimensions of fired bricks.

Similarly, earth bricks were manufactured by using Usumacinta River sediments (J3) and palm fibers which are local agro-industry waste. Characteristics of palm oil fibers such as morphology, tensile strength, biochemical composition etc. were investigated for their reuse in earth bricks. Palm oil flower fibers were used to make earth bricks due to their suitable morphology and strength. These fibers were extracted with a knife mill by using grids of 2cm (G-2cm) and 3cm (G-3cm). Earth bricks were manufactured with 0%, 1%, 2%, 3%, 4% and 5% fiber addition by mass and compacted dynamically. Earth bricks were dried in oven at 40°C. Tensile and compressive strength tests were performed on bricks to observe the influence of fiber addition. Brick's durability was also assessed with inundation, water absorption and abrasion test.

For Usumacinta River sediments use in agronomy, their agronomic characteristics such as presence of nutrients, pH, electrical conductivity and sodium absorption ratio were investigated. Experimental study was conducted in greenhouse to observe the growth of ryegrass with Usumacinta sediments and potting soil. Three soil compositions with 0% sediments, 50% sediments+50% potting soil and 100% sediments were used. Growth and germination of ryegrass were observed in different soil compositions to assess the agronomic potential of sediments.

Furthermore, the findings of Usumacinta sediments were replicated for local French sediments from Dunkirk port and Garonne River to make earth bricks with hemp shiv as reinforcement.

Contents

General introduction

Sediments are dredged to smoothly run the navigation and water flow operations. Dredged sediments are considered as waste material. Recovery of sediments as a natural resource in construction materials, roads, beach nourishment, land reclamation and agronomy etc. is possible after the removal of contaminants and excessive water. For sediment reuse, their characteristics and social aspects are important. Characteristics of sediments include their physico-chemical, mineralogical, hydromechanical and environmental characteristics. Furthermore, the quantity of dredged sediments, their proximity to the urban areas and local demands are some additional aspects that decide the sediments recovery sector.

Sediments reuse in construction materials is helpful to preserve the soil resources. Fired bricks are manufactured with clayey soils but excessive use of soil in fired bricks has a devastating impact on agriculture soil due to the limitation of these soils in some regions of the world. Dredged sediments reuse in fired bricks has the potential to save natural resources and valorize sediment waste. Different industrial approaches can be considered to evaluate the potential of sediments for fired bricks which includes Winkler approach, Casagrande diagram, Gippini diagram and Augustinik diagram. Granulometry, organic matter, Atterberg limits and chemical composition of sediments have a significant influence on the strength of fired bricks.

Reuse of waste sediments and fibers in earth bricks contributes to the manufacturing of sustainable and ecological building materials. Earth bricks are manufactured with clayey soils and natural fibers. Sediment characteristics, fiber content, compaction and moulding moisture content have a substantial influence on the strength, durability and performance of earth bricks. The influence of different manufacturing parameters on earth bricks is observed through mechanical testing of bricks. For the valorization of sediments in earth bricks, the use of local fibers is essential to limit the transportation of raw materials and reduce carbon footprints. Local tropical natural fibers in Tabasco include palm oil flower and fruit fibers, coconut coir, banana spines fibers and sugarcane bagasse fibers which are local waste from the agro-industry in Tabasco. Figure 1 shows the waste sediments and fibers recovery in earth bricks.

Figure 1. Earth bricks made with sediments and natural fibers.

Sediments reuse in agronomy is relatively unexplored. Dredged sediments have the potential to be used in the reconstitution of agronomic soil, landscaping and vegetation of riverbanks to limit the erosion. Sediments are generally rich in nutrients and act as fertilizing agents which improve the quality of soil and the yield of crops. Performance and fertilizing effects of sediments in crops can be observed by monitoring the germination and growth of plants.

Val uses project

This study is a part of Val- Uses project on sustainable recovery of Usumacinta River sediments in local applications. Usumacinta River sediments have been dredged from the Tabasco state of Mexico and these sediments constitute a valuable resource as reuse of sediments in construction materials *i.e. fired and earth bricks* and agronomy has a potential to contribute to the socio-economic development of the region.

Objective

The objective of this research is the recycling of Usumacinta River sediments in fired bricks, earth bricks and agronomy. A manufacturing process is to be implemented to manufacture fired and earth bricks and assess the Usumacinta River sediment's potential for agronomy through experimentation.

Usumacinta River sediments characteristics will be investigated for their reuse in fired bricks, earth bricks and agronomy. Laboratory scale experiments will be conducted to manufacture fired brick at different firing temperatures and manufacturing conditions. In case of earth bricks, characteristics of tropical waste fibers *i.e palm oil flower and fruit fibers* will be investigated, and earth bricks will be manufactured with different fiber content. Sediment's agronomic potential will be evaluated with greenhouse tests by mixing Usumacinta River sediments with potting soil to grow ryegrass.

In addition to the Usumacinta sediments, recovery of French sediments from Dunkirk port and Garonne River in earth bricks is envisaged along with hemp shiv. Finding from Usumacinta sediments are to be implemented on local sediments by replicating the manufacturing conditions of Usumacinta bricks.

Structure of thesis

This thesis is divided into 5 chapters which are bibliography, characterization of sediments, sediments reuse in fired bricks, sediments reuse in earth bricks and local applications. Chapter 1 gives the overview of dredged sediments and natural fibers characteristics for their valorization in bricks. Furthermore, recent developments in manufacturing of earth and fired bricks are also reviewed.

In chapter 2, characteristics of Usumacinta River sediments are investigated for their recovery in fired bricks, earth bricks and agronomy. In chapter 3, Usumacinta River sediments suitability for fired bricks is discussed and fired bricks are manufactured with different industrial approaches. In chapter 4, Usumacinta River sediments suitability for earth bricks is examined and earth bricks are made with Usumacinta River sediments along with palm oil flower fibers. In chapter 5, Usumacinta River sediments agronomic characteristics are investigated, and these

sediments are used with potting soil to grow ryegrass in greenhouse to observe the germination and growth of plants with Usumacinta River sediments. Chapter 5 also discusses the reuse of local French sediments in earth bricks along with hemp shiv.

Chapter 1. Literature review

This section consists of a bibliographic study about dredged sediment characterization and valorization. Rules and regulations for reuse of polluted sediments are also reviewed. The review study focuses on the characteristics of sediments and their reuse in construction materials such as fired and earth bricks. Suitability of sediments for bricks is discussed in the light of industrial approaches and standards. Manufacturing of earth bricks involves the incorporation of natural fibers for reinforcement. Characteristics of natural fibers are also reviewed for their recovery in earth bricks. Modern trends and methodologies in manufacturing of fried bricks and earth bricks are discussed and their typical physical and mechanical characteristics are also examined

1.1. Dredged sediments

Sediments are accumulated in the ports, dams and lakes due to the transportation of sediments by water channels and erosion of coastal areas. These sediments are dredged to preserve navigation and water flow operations. Dredged sediments stored on land sites are treated as waste. A large portion of these sediments is discharged into the sea by immersion. However, the disposal of waste sediments has environmental concerns as the presence of pollutants in sediments has devastating effects on the aquatic system and marine life.

Dredged sediments are separated into polluted sediments, slightly polluted and non-polluted sediments. Rules and regulations for the management and recovery of sediments vary according to the nature of sediments. Non-polluted marine sediments can be discharged into the sea and estuaries which is the most economical way. However, the suspension of fine particles in water disrupts the aquatic system. Slightly polluted and polluted sediments are stored on land sites. The storage, disposal and recovery of polluted sediments are implemented after analysis of contaminants and sediments characteristics. Treatment of highly polluted sediments is essential for their recycling.

1.1.1. Composition of sediments

Sediments consist of elements such as Si, Al, K, Na, Mg etc. which constitute 80% mass of sediments. Similarly remaining mass is occupied by water, organic and inorganic materials. Inorganic compounds include silicates (quartz, mica, feldspar etc.) clay minerals (kaolinite, illite and montmorillonite), carbonates (calcium carbonate, dolomite), iron oxides, phosphates and sulfides. Heavy metals such as Hg, Pb, Cd, Ni, Zn are usually trace elements in dredged sediments (Sahfi, 2020; Samara, 2007). 20% to 90% volume of sediments is occupied by water. Water in sediments is present in the form of pore water, by capillarity and inherent water. The initial water content of dredged sediments is very high and sometimes ranges up to 300% (Sahfi, 2020). Dehydration of sediments is time-consuming and costly which makes their recovery operations complicated.

1.1.2. Polluted sediments

Sediments are polluted with heavy metals and chemicals due to industrial affluents and agricultural waste from fertilizers and pesticides. Nature of pollutants in dredged sediments can be organic (PCBs, PAHs, TBT, dioxins) and inorganic (As, Pb, Cu, Zn, Cr, etc.) (Agostini et al., 2007). Release of sediments into the sea is banned if they are polluted with heavy metals such as Ni, Cr, Pb, Cu etc. and organic compounds such as hydrocarbons, PAH and PCB etc. The environmental regulations have made the disposal of sediments difficult. Polluted sediments are stored in land sites for their treatment and reuse. However, the presence of pollutants such as heavy metals and organic compounds needs attention.

Tables 1.1 and 1.2 show the concentration levels and thresholds for heavy metals in dredged sediments. Levels N1 and N2 in Table 1.1 show the low and high concentrations of heavy metals according to French recommendations (MEDD, 2020). Heavy metal concentration is considered negligible below the N1 level. Between N1 and N2 levels, investigation of pollutants

is obligatory for their disposal and reuse and their concentration above N2 can be harmful and sediments must be treated.

Table 1. 1. Level of contamination in dredged sediments in mg/kg (MEDD, 2020)

Elements	Cd	Cr	Cu	Pb	Zn	As	Ni	Hg
Level N1	1.2	90	45	100	276	25	37	0.4
Level N2	2.4	180	90	200	552	50	74	0.8

Table 1.2 shows the heavy metals concentration in fluvial sediments according to French standards (MEDD, 2020). Metals concentration above the S1 threshold is dangerous.

Table 1. 2 Contaminants threshold for sediments

Elements	Cd	Cr	Cu	Pb	Zn	As	Ni	Hg
S1 (mg/kg)	2	150	100	100	300	30	50	1

Removal of contaminants from dredged sediments is done by different techniques. Treatment of polluted sediments can be done by Novosol process which decreases organic matter by calcination and stabilizes heavy metals by adding phosphoric acid to the sediments. Leaching of sediments is also done to remove the contaminants. Burning of sediments for their recovery in clinker and fired bricks removes organic impurities by decomposition of organic matter at high temperatures (Samara et al., 2009).

Sediments with pollutants above N2 level and S1 threshold are stored on land sites. Land storage of sediments is expensive, and its cost varies with the land cost, pollutants and distance of the storage site. Therefore, sediments treatment is important to reuse them.

1.2. Sediment's characteristics

Sediment storage and recovery are decided after analyzing sediments characteristics and level of contamination (Hayet et al., 2017) as explained in the flowchart in Figure 1.1.

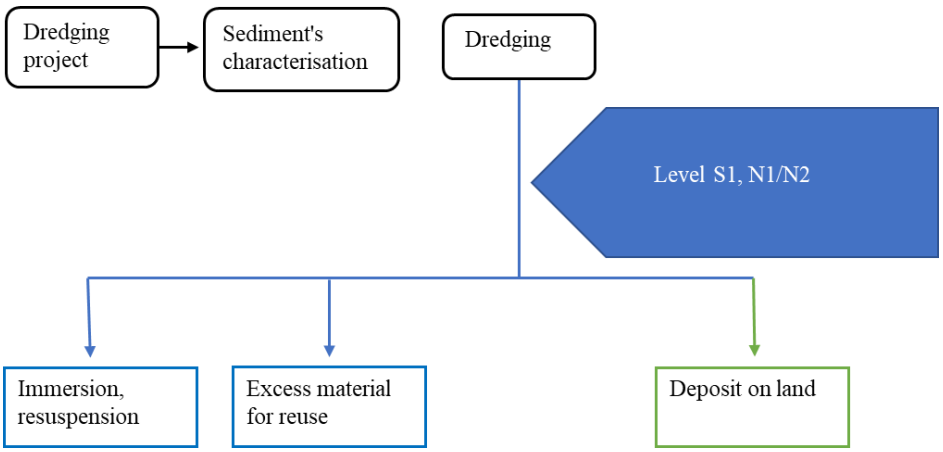

Figure 1. 1. Flowchart for decisions for sediments management (Hayet et al., 2017).

Sediment's physical, chemical and mineralogical characteristics are important to decide their reuse in different sectors. Chemical, thermal and mineralogical characteristics of sediments can

be found with different tests such as X-ray fluorescence (XRF), thermo gravimetry and X-ray diffraction etc. (Xu et al., 2014).

1.2.1.1. Physical characteristics of sediments

Physical properties of sediments include granulometry, Atterberg limits, density etc. These properties are found by tests such as laser granulometry, methylene blue test, Casagrande test.

Grain size analysis of sediments is useful to observe soil classification and its suitability for different applications such as fired and earth bricks, roads etc. Soil granulometry is correlated with porosity and permeability to better understand the sediment's behavior.

Atterberg limits of sediments include liquidity limit and plasticity limit. The liquidity limit of a clayey soil is very high, and they have high plasticity. On the other hand, sandy soil has very low plasticity. Atterberg limits of sediments are helpful to observe moulding characteristics of sediments for construction materials. Low plasticity of sandy soils makes them unsuitable for fired and earth bricks applications as fired and earth bricks with sandy soils are usually fragile and have low strength.

1.2.1.2. Hydromechanical characteristics of sediments

Hydromechanical properties of sediments include consolidation, permeability and decantation. Consolidation and permeability of sediments are important for their use in applications such as embankments, dykes etc. Consolidation is slow in clayey soils, and they have low permeability. Decantation of sediments is important for their dehydration as initial water content of dredged is usually very high.

1.2.1.3. Mineralogical analysis of sediments

Mineralogical analysis of sediments is performed with XRD and SEM to observe the mineralogical phases and morphology of sediments (Sedilab, 2015). The presence of oxides such as MgO, SiO_2, Cao, alkalis and alumina is observed to see sediments suitability for bricks, concrete and other applications. Mineralogical analysis of sediments shows the presence of different minerals in the soil such as quartz, kaolinite, muscovite, illite, montmorillonite etc. (Bhatnagar et al., 1994).

1.2.1.4. Chemical characteristics of sediments

Chemical properties of sediments include organic matter, soluble salts, carbonate content, pH, elemental and oxide composition of sediments etc. Organic content in sediments induces the porosity in fired bricks on burning and decreases their strength. However, certain number of pores in the sediment matrix is necessary to control the temperature and humidity of the building structure. The water absorption of bricks increases with porosity.

1.3 Sediments dredging and valorization in France

Due to the lack of natural resources and the proximity of big cities near the rivers and ports, the use of dredged sediments is increasing. Moreover, strict environmental regulations have

encouraged the reuse of sediments. Characteristics of sediments play and important role for their valorization in different applications. Dredged sediments can partially or fully replace the non-renewable clay resources in construction materials. Sediments mixing with sand and clay change the mineralogy of these sediments and improve sediment's characteristics and suitability for their specific reuse.

Many studies have been conducted on the reuse of dredged sediments in civil engineering applications such as roads, concrete and embankments, backfilling of quarries etc. Dredged sediments have diverse nature and granulometry of sediments vary from region to region and the percentage of clay, silt and sand fluctuates. Therefore, most of the research on these sediments is concentrated only on their specific use based on the demands of local industry (Rakshith et al., 2016).

In France, every year 50 million m^3 of sediments are dredged from marine ports and 6 million m^3 of estuarine sediments are dredged. The important quantity of sediments is dredged from the estuarine ports of Rouen, Nantes, St-Nazaire and Bordeaux and from the maritime ports of Dunkirk, Calais, Boulogne, le Havre and la Rochelle (Sahfi, 2020). The marine dredged sediments are mostly discharged into the sea. The remaining sediments are stored in sea and land sites depending on the level of contaminants. Sediments stored in the sea are used for beach refilling.

Figure 1.2 shows the dredged port sediment management and reuse in France from the English Channel, Atlantic and Mediterranean Sea. The dredged sediments from these ports of France are mostly immersed in the sea and used for beach nourishment but a small quantity is stored on land sites also.

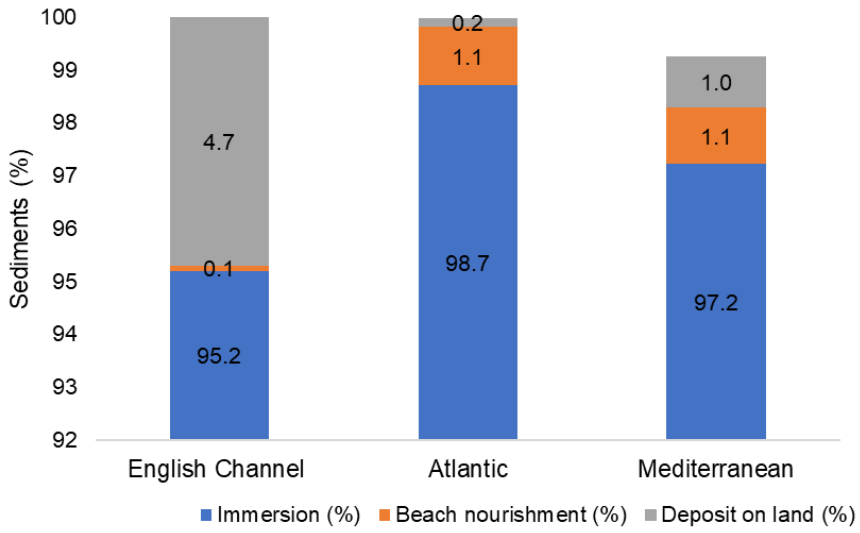

Figure 1. 2. Port dredged sediments management and use in France (Sedilab, 2015).

Figure 1.3. shows the quantity of sediments dredged from three ports of the Normandy region in France from 2010 to 2017.

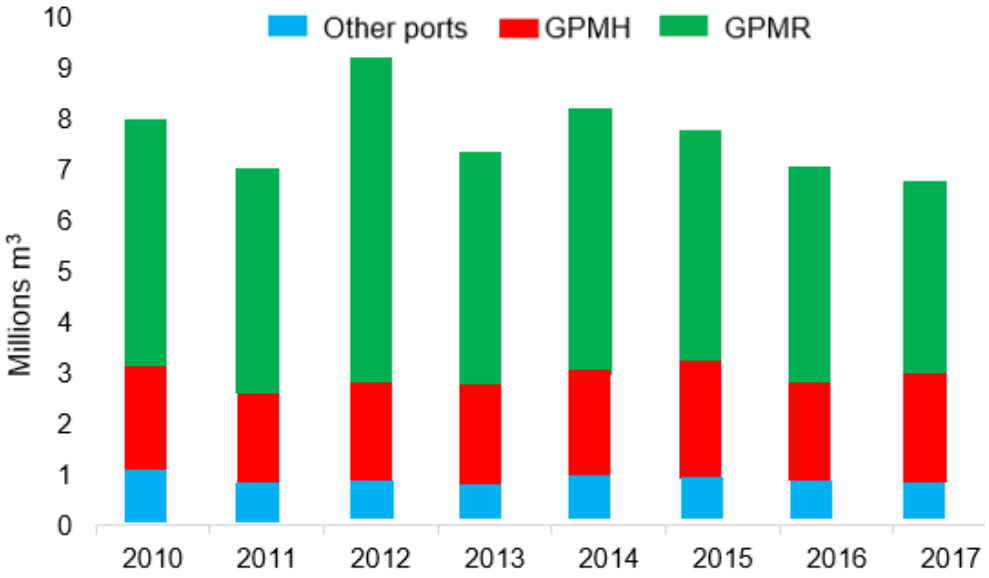

Figure 1. 3. Sediments dredged in Normandy, France (Cerema, 2021).

Figure 1.4 shows the level of contaminants in Normandy sediments

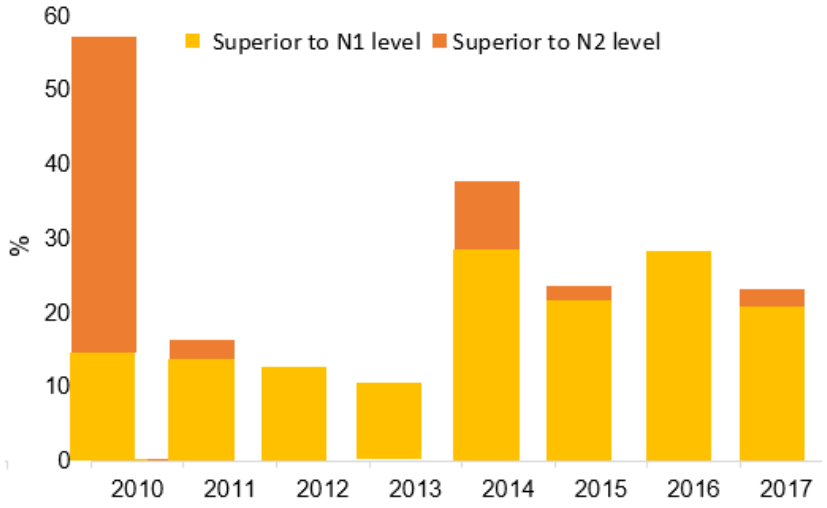

Figure 1. 4. Presence of pollutants in Normandy sediments (Cerema, 2021)

65%-85% of sediments dredged in the Normandy region (France) from 2010 to 2017 have pollutants below the N1 level (Cerema, 2021). 84% of dredged sediments from Normandy region are immersed in the sea, 3% of sediments are used in recharging the beaches and 7% of sediments are stored in land sites. Polluted sediments are stored on land sites, but the cost of land and leaching are key issues of sediments land storage. Therefore, these sediments must be treated to reuse them.

Dredged sediments are used in dykes, riverbanks, roads, agronomy, bricks and concrete applications etc. by partially or fully replacing traditional materials (Sheehan et al., 2009). Dredged sediments use in these applications is limited due to the presence of pollutants, inadequate research, sediments transportation and higher initial water content of sediments.

Dredged sediments stored in sea and land sites can be used in different sectors. The possible sectors for sediment reuse are indicated in Figure 1.5.

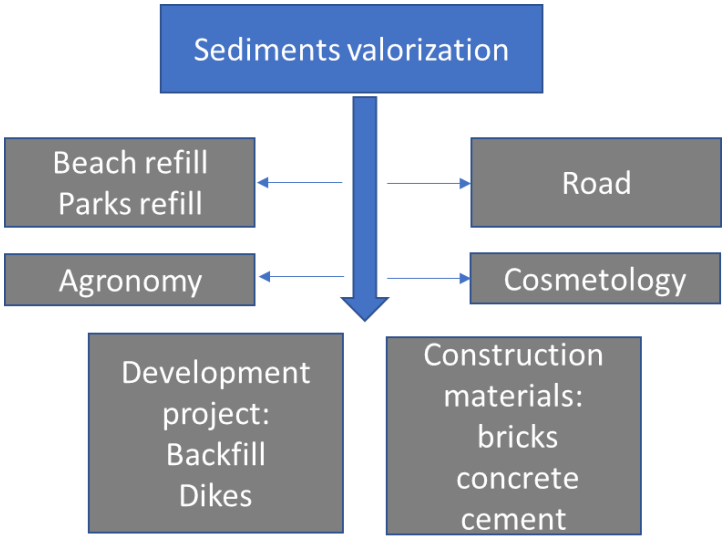

Figure 1. 5. Possible recovery sectors of sediments (Bénédicte, 2017)

Three-million-ton sediments are dredged from Dunkirk port in France. On the other hand, erosion of coastlines in France is damaging the beaches and engulfing coastlines. Recharging of beaches can be accomplished by making artificial aggregates from dredged sediments with the addition of binders (Brakni et al., 2009). In France, dredged sediments are mostly used in roads, cement, concrete and backfill operations (UNICEM, 2021).

Dredged sediments can be used in roads after analyzing their characteristics and the presence of contaminants like arsenic, lead, copper etc. Grain size analysis and leaching tests are essential to use these sediments in road construction. Dredged sediments are used in sub-layers and foundation layers of the road by replacing the sand (Sedilab, 2015). The initial water content of dredged sediments can be reduced by dewatering sediments through decantation to use them in road construction. The mix of fine dredged sediments with dredged sand makes grain size distribution suitable for base course material for roads and increases the bearing capacity. In this way, sediments are be used as base course material in road construction and the amount of binder required is decreased (Dubois et al., 2009).

Dredged sediments reuse in cement mortar for non-structural usages by complete replacement of sand decreases the mechanical strength of mortar and enhances the porosity. For efficient use of sediments in cement mortar, treatment of sediments is done to reducing their size to 80µm which increases the mechanical strength of mortar, reduces its porosity and leads to sediments valorization in cement mortar (Couvidat et al., 2016). In concrete, dredged sediments can be used to partially replace sand and binder.

In ceramics, dredged sediments are used in manufacturing fired bricks and tiles. Dredged sediments can be reused in fired bricks by replacing traditional clayey soils mined from quarries. Dredged sediments can also be used in earth bricks along with natural fibers. Grain

size and Atterberg limits of sediments play an important role for sediment recycling in earth bricks.

1.3.1 Sediments reuse in fired bricks

Dredged sediments have been reused in the ceramic industry to make bricks and tiles. Dredged sediments can be mixed with additives like clay to make them suitable for fired bricks by improving their granulometry and chemical composition (Baksa et al., 2018). The nature of dredged sediments and their proportion in mixture are important factors behind the quality of bricks and their thermal and mechanical characteristics (Slimanouet al., 2020). Mezencevova et al., (2012), used harbor dredged sediments to manufacture bricks by mixing dredged sediments with 50% clay and firing the bricks at 900 °C and 1000 °C. Strength, water absorption and other properties of both dredged sediments and sediments with clay mix were within ASTM standards.

The presence of pollutants is tackled with different techniques for sediments reuse in fired bricks. Contaminants in polluted sediments can diluted with the addition of non-polluted sediments. Moreover, organic pollutants in sediments are decomposed by firing the bricks at high temperatures. Hamer et al., (2002), used partially polluted dredged harbor sediments in making bricks after treatment. Dredged sediments were mixed with natural clay. Wastewater obtained after drying bricks contained many pollutants and pollutants were further removed by burning the bricks at high temperatures. Volatile pollutants in exhaust gas were neutralized by injecting $Ca(OH)_2$, activated carbon and a filter to absorb dust. Resulted bricks fulfilled German standards and were environmentally acceptable. Although bricks from dredged sediments fulfill the strength and environmental considerations, there are social and economic barriers in the market to sell the bricks made from dredged sediments. Consumers are suspicious about brick's quality and the presence of chemical contaminants. Awareness about the environment and the age of customers play a significant role in the marketing of fired bricks from dredged sediments. To make dredged sediments bricks a commercial product and increase their demand, awareness among the public is also important (Cappuyns et al., 2015).

For sediments reuse in fired bricks, their physical, chemical and mineralogical characteristics are important. The strength of bricks varies with the nature of sediments, sand and clay percentage, organic matter, and presence of different minerals.

Granulometry of soil is critical for their reuse in fired bricks. Soil with an intermediate quantity of clay and sand is appropriate for making bricks. Clay particles have a fine size and a specific amount of clay is necessary to make good quality bricks. Sediments used for bricks require certain plasticity which is due to the presence of clay. Soil with high clay content is also undesirable for fired bricks as excessive shrinkage and cracks are common in clayey soils. Clay minerals used for the manufacturing of bricks are kaolinite, illite and montmorillonite. Clay acts as a binder for coarser particles. The soil having a high percentage of kaolinite clay can absorb a higher amount of water and have high plasticity. Therefore, higher kaolinite content is

inappropriate for fired bricks. The higher volume variation in kaolinite produces shrinkage and cracks during the drying and firing process (Koroneos and Dompros, 2007).

Silt particles decrease the shrinkage and fill up the pores between coarse and fine particles. Sand mostly consists of silica and quartz particles. Sandy soils have low plasticity, and it is difficult to use them in bricks, as bricks made from sandy sediments are fragile and induce brittleness in bricks. Sometimes additive like fly ash is used to prevent shrinkage. A specific quantity of sand is important to reduce the high plasticity of clay, shrinkage and cracks (SDC, 2008).

Percentage of carbonate content and organic matter is also very important for fired bricks. The higher percentage of calcium carbonate causes swelling and disintegration in bricks. High amount of organic matter in soil is also undesirable due to the development of voids on burning. On other hand, it requires less energy to burn bricks in which soil has high organic matter. Zhao et al., (2019), found that the strength of bricks decreases with high organic matter and the presence of gravel.

Soil used for fired bricks is primarily composed of silica. Other important component is alumina while the remaining portion consists of calcite and oxides of iron, magnesium, sodium etc. (Fgaier et al., 2015, Kazmi et al., 2017). The chemical composition of sediments used in manufacturing fired bricks by various researchers is presented in Table 1.3.

Table 1. 3. Chemical composition of sediments used in fired bricks

Application	**SiO_2 (%)**	**Al_2O_3 (%)**	**Fe_2O_3 (%)**	**CaO (%)**	**MgO (%)**	**K_2O (%)**	**Na_2O (%)**	**Reference**
Fired bricks	12.50	87.5	7.40	2.03	1.62	1.36	0.61	Mezencevova et al., 2012
Fired bricks	57.48	12.16	4.71	9.25	2.58	2.09	1.96	Kazmi et al., 2017
Fired bricks	59.2	14.90	8.54	2.36	1.64	2.86	0.96	Sutcu, (2014)
Fired bricks	52.36	14.16	6.22	9.45	1.97	1.02	1.85	Baronio and Binda 1997
Fired bricks	62.75	16.41	6.37	3.53	3.90	1.87	1.68	Manoharan et al., 2011
Fired bricks	48.55	16.83	6.80	5.15	6.19	0.94	-	Karaman et al., 2006

Minerals such as silica, alumina, calcium oxide, manganese oxide and organic matter play important role in clay bricks. Silica is useful to harden the bricks and decreases the shrinkage of bricks during the drying process. The fusion temperature of silica is kept small by calcium oxide, so silica particles bind together at low temperatures. Alumina is useful for plasticity in sediment mixtures and helps to mould them into desired shapes.

The presence of a high amount of $CaCO_3$ in brick material can produce a higher amount of CO_2. CO_2 during its emission can increase the porosity of bricks. Porosity of bricks is also induced with burning of organic matter inside the sediment mixture at high temperature. Additives like barium carbonate are mixed with soil to improve the chemical resistance and other properties. Table 1.4 shows the range of different oxides in soils used for ceramics applications in France.

Table 1. 4. Percentage of oxide in ceramic applications in France (Kornmann, 2009)

Range	LOI	SiO_2	Al_2O_3	TiO_2	Fe_2O_3	CaO	MgO	Na_2O	K_2O	S	F
Minimum %	3	35	8	0.3	2	0.5	0	0.1	0.1	0	0
Maximum %	18	80	30	2	10	18	5	1.5	4.5	0.5	0.15

Note : LOI = loss on ignition

The elemental composition of metals found in sediments used for fired bricks by different researchers is shown in Table 1.5. Chromium (Cr), copper (Cu), lead (Pb), zinc (Zn) and titanium (Ti) are impurities in soil.

Table 1. 5. Elemental composition of heavy metals in sediments used for fired bricks

Application	Cr (ppm)	Cu (ppm)	Pb (ppm)	Zn (ppm)	Ti (ppm)	Reference
Fired bricks	61.65	15	21.7	89.4	1.42	Mezencevova et al., 2012
Fired bricks	38	801	104	112	-	Kazmi et al., 2017
Fired bricks	-	0.007	-	-	0.75	Karaman et al., 2006

Physical properties of sediments such as granulometry, Atterberg limits and optimum moisture content used in manufacturing fired bricks by various researchers are shown in Table 1.6.

Table 1. 6. Granulometry and Atterberg limits of sediments used for fired bricks

Application	Clay (%)	Silt (%)	Sand (%)	W_n (%)	LL (%)	PL (%)	Reference
Fired bricks	**47**	38	15	-	99.2	49.5	Mezencevova et al., 2012
Fired bricks	**43.2**	44	12.8	-	33.23	24.65	Karaman et al., 2006
Fired bricks	**16**	37	47	-	63	32	Ismail and Yaacob, 2011
Fired bricks	**5**	80	15	21	24	21	Fgaier et al., 2015
Fired bricks	**6**	89	5	24	100	28	Fgaier et al., 2016

1.3.2 Industrial approaches to manufacture fired bricks

Some important industrial approaches used for manufacturing fired bricks are the Winkler diagram, Augustinik diagram and Casagrande-Gippini diagram. These diagrams help to select the appropriate soil manufacturing fired bricks with sediments granulometry, oxide content and Atterberg limits.

In the Winkler diagram (Winkler 1954) soil suitability for fired bricks and tiles is identified with the clay, silt and sand content of the soil. Augustinik diagram describes soil suitability for fired bricks with oxide content such as silica and alumina (Haurine, 2015). Casagrande-Gippini diagram describes the extrusion characteristic of sediments mixture. It is plotted with the help of Atterberg limits of soil and is show in Figure 1.6.

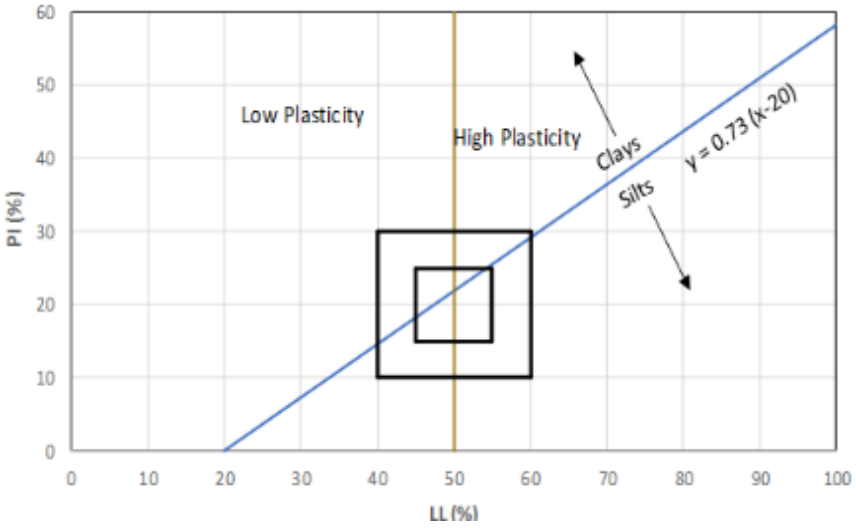

Figure 1. 6. Casagrande–Gippini diagram (Fonseca et al., 2015).

Clay workability chart is also based on Atterberg limits. Soils that lie inside the inner zone in Figure 1.7 have optimum moulding characteristics (Fonseca et al., 2015). Soil in the exterior zone have good moulding characteristics while the soils outside the two rectangular zones do not possess good moulding properties.

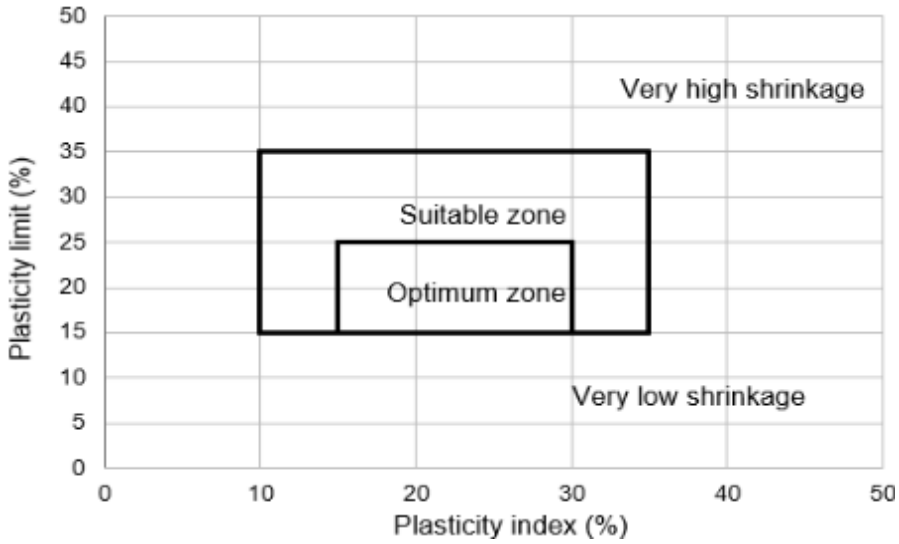

Figure 1. 7. Clay workability chart

1.3.3 Manufacturing of fired bricks

Fired bricks are a very common building material across the world as they are cheap and economical. Due to their high compressive strength and durability, bricks are used in making houses, walls, pavement and other construction activities. The housing needs of rapid urbanization in developing countries are mainly fulfilled by using bricks as construction material. Prismatic, cubic and perforated bricks are some common types of fired bricks.

The manufacturing process of fired bricks consists of material preparation, moulding, drying and firing. Generally, the top layer of soil is used in making clay bricks. The mined soil is

stored, crushed, screened and a glazing agent is added before drying the bricks followed by firing at a high temperature (Brick Industry Association, 2006). With the advancement in technology of mining, transportation, screening, moulding and kiln system, the manufacturing of bricks has become very fast.

1.3.2.1. Material preparation

Material preparation consists of sediments selection, crushing, grinding and mixing with water to make a sediments mixture. Homogeneity of soil mixture is important for good quality bricks. The particle size of soil has a significant impact on making uniform sediments mixture and properties of fired bricks. Particles of 2 mm size are used in manufacturing bricks to make homogenous mixture. Soil is crushed and mixed with water to make a homogenous mixture of sediments and left until the soil becomes soft enough to mould into bricks. Monap et al., (2015), used 15% water by total weight of the sediments to make fired bricks from dredged sediments, and sand soil mixture.

Moulding moisture content of fired bricks is very important. Optimum moulding moisture content is derived with Atterberg limits after Sembenelli interpretation (Sembenelli, 1966) and with optimum water content through the Proctor test. Higher moulding moisture content deforms the bricks during transportation and leads to considerable shrinkage on drying and firing. On the other hand, a low quantity of water makes the moulding of sediments matrix difficult. Therefore, optimum moulding moisture content must be used to mix sediments.

1.3.2.2. Moulding of bricks

Sediments mixture is moulded into wooden and steel moulds of different sizes. Machine moulding and manual moulding of bricks are common. In machines, extrusion and wire cutting are also common. Manual moulding is done with bottomless wooden moulds. The inner surface of mould is oiled so that sediments can be demoulded easily in the form of bricks. Moulds are filled with sediments, leveled and excessive clay on the top of mould is trimmed. Prismatic and cubic moulds are commonly used for manufacturing bricks for compressive and tensile strength test.

1.3.2.3. Compaction of bricks

Compaction of fired bricks is achieved by tamping, vibrations, and dynamic and static loading (Seifi et al., 2018). Compaction of bricks removes the voids, increases the strength of bricks and decreases water absorption of bricks. Hyper-compaction of bricks at 100 MPa allows the manufacturing fired bricks at significantly low temperatures (455 °C to 640 °C) with compressive strength and water absorption similar to the commercial bricks (Bruno et al., 2018).

1.3.2.4. Drying of bricks

After moulding bricks are air-dried, or oven-dried for a specific time interval to preserve their shape and facilitate their transport firing. Drying of bricks prevents the bricks from swelling

and cracking when fired at a high temperature which happens due to moisture entrapped in the bricks. Drying temperature and duration applied by different researchers are given in Table 1.7.

Table 1. 7. Bricks drying time and firing temperature

Application	Drying time	Firing time (hours)	Firing temperature (°C)	Reference
Fired bricks	2 days	36	800	Kazmi et al., 2017
Fired bricks	3 weeks	36	800	Riaz et al., 2019
Fired bricks	105 °C for 24 h		900 - 1000	Mezencevova et al., 2012
Fired bricks	24 h room temperature 24 h 200 °C in the furnace	2,4,6,8	700-1100	Karaman et al., 2006
Fired brick	Open-air for 4 days	12	700	Hakkoum et al., 2017
Fired bricks	3 days room temperature 105 °C for 24 hours	10	950-1050	Esmeray and Atis, 2019
Fired bricks	110 °C for 24 hours	3	950 to 1050	Dai et al., 2019
Fired bricks	24 room temperature 105°C for 3 days		800 to 1250	Johari et al., 2010

1.3.2.5. Firing of bricks

Drying of bricks is followed by the firing of bricks. Usually, bricks are fired at a temperature range of 700°C to 1100 °C in the bricks kiln in industry (Karaman et al., 2006, Johari et al., 2010, Haurine et al., 2015). The firing of brick is one of the important parameters behind the strength and thermal characteristics of bricks. In developing countries, coal is a primary source of firing bricks in the brick manufacturing industry which produces a high amount of carbon dioxide, carbon monoxide, ammonia etc. Outdated brick manufacturing technology and methods in developing countries consume a higher amount of energy and emit a substantial quantity of pollutants. (Greentech knowledge solution, 2015).

Different reactions take place in sediments matrix when fired at high temperature. Evaporation of inherent water takes place at temperature around 200 °C. Evaporation of moisture is followed by dehydration and oxidation due to organic matter and pyrites at a temperature of 300 to 500 °C. At 500 °C, the transition of kaolinite into metakaolin takes place. Clay has different compounds such as kaolinite, illite and montmorillonite etc. During their decomposition, clay compounds release water molecules. The organic matter inside the sediments is also decomposed at 550 °C. Transformation of quartz from alpha quartz to beta quartz takes place at 573 °C. Carbon dioxide is emitted due to chemical reactions associated with carbonates at a temperature of 400 °C to 700 °C. CO_2 and SO_2 are emitted due to the decomposition of calcium carbonate and sulfate at a temperature between 600 °C to 800 °C (JKSPL. 2016). Around 850 °C, reorganization of particles in metakaolin occurs (Fgaier, 2013). Phenomenon of vitrification starts at a temperature of around 950 °C. Finally, glass formation takes place at a temperature from 900 °C to 1000 °C (European commission, 2007). At high temperatures, the components of bricks which have low melting points adopt a liquid phase and fuse together by filling the empty pores inside the bricks.

Calcareous sediments exhibit good compressive strength at low temperatures but their resistance against salt crystallization is poor due to bad pore size distribution. Calcium carbonate near 800 ^{0}C, transforms into CaO which reacts with moisture and converts into $Ca(OH)_2$ due to which volume increases and cracks appear. The formation of $Ca(OH)_2$ can be checked by controlling the carbonate content in sediments. For durable and resistant calcareous and non-calcareous bricks with a uniform pore size distribution, temperature of 1000 ^{0}C and 1100 ^{0}C are recommended (Elert et al., 2003). Different reactions in fired bricks at high temperatures are explained in Figure 1.8.

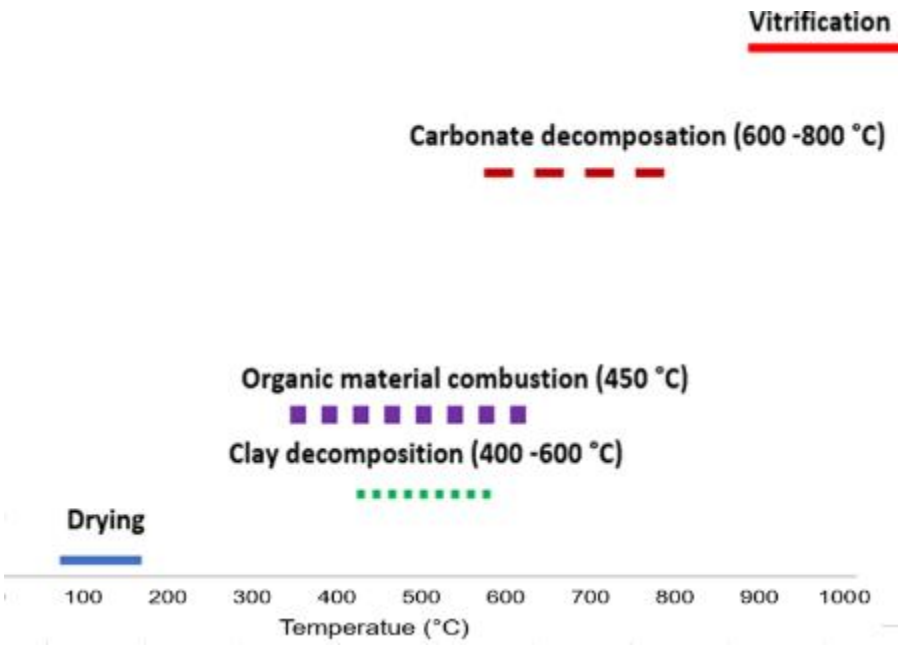

Figure 1. 8. Firing mechanism of bricks

Firing temperature is very important as over and under the burning of bricks significantly decreases the quality of bricks (Slimanouet al., 2020). Over burnt bricks are very hard and irregular in shape. Under burnt bricks have low strength and they have higher water absorption. Firing temperature has a significant impact on the characteristics of fired bricks such as porosity, compressive strength and water absorption capacity. At high firing temperatures porosity of bricks decreases. Length and thickness of bricks decrease on firing due to shrinkage by the firing and drying process. Evaporation of water from sediments decreases the final length of bricks. At high temperatures, carbon and sulfur present in bricks are burnt.

The firing duration of bricks ranges from 4-12 hours in different industries and literature studies. However, the impact of firing duration is not significant on the properties of fired bricks (Karaman et al., 2006). Johari et al., (2010) after manufacturing fired bricks at a temperature range of 800 °C to 1200 °C found that the compressive strength of bricks and other mechanical parameters are better at a firing temperature of 1200 °C. Therefore, firing temperature must be optimized with careful consideration of sediment characteristics.

As fired bricks consume higher energy, use of energy makes these bricks costly and the emission of greenhouse gases during the firing process pollutes the environment. (Reddy and Jagadish et al., 2003).

1.3.4 Properties of fired bricks

Strength and properties of fired bricks vary nature of soil, firing temperature and method of manufacturing. Bodian et al., (2018), mixed laterite with soil mixture and found that 30 % of laterite in the mixture gives ideal physical, thermal and mechanical properties to the bricks. These properties include water absorption, compressive strength, tensile strength, the color of bricks, density, thermal conductivity, resistance against weathering, reaction with salt and chemical composition. Water absorption test, bulk density and compressive strength tests are widely used to observe the quality of bricks (Al-Fakih et al., 2019). Mineralogical analysis of bricks is conducted to see the percentage of different oxides (Arce et al., 2003).

Mechanical properties of bricks include compressive strength, modulus of elasticity and tensile strength. Fired bricks have usually high compressive and tensile strength. The compressive strength of bricks depends on the characteristics of sediments, the procedure adopted to manufacture bricks, porosity and the minerals present in the bricks. Modulus of elasticity of bricks has larger variability.

(a) Color

Presence of different minerals such as iron oxide, calcium oxide, magnesium oxide and chemical reactions give different colors to fired bricks such as red, white and dark. Color of bricks vary and depends on the calcium, iron and magnesium content inside the sediments. Mainly iron oxide is responsible for the dark red color of bricks at high temperatures. At high-temperature iron minerals transform into hematite which gives bricks a reddish and reddish-brown color. Color of bricks after firing in the case of kolanitic clays depends on Fe_2O_3 content and impurities. The yellow color of bricks indicates that sediments are mainly composed of quartz and kaolinite and the presence of CaO is less. In Cao rich sediments where CaO and MgO content is more than 10%, pyroxene is formed and light brown color in bricks appears (Kreimeyer, 1986).

The firing temperature of bricks plays a significant role in bricks colors. Karaman et al., (2006) observed that the color of bricks starts to become dark when the temperature is increased above 875 ^{0}C. Yellow color in bricks is dominated due to minerals such as quartz, diopside and a small quantity of feldspar while red color bricks are dominant due to presence of quartz, hematite and feldspar minerals (Cultrone et al., 2005).

(b) Porosity

Uniform pore size distribution and less porosity make bricks durable and resistant. Porosity of bricks increases with increasing organic matter. Kim et al., (2018), used gold tailings and red mud mixture (bauxite residue) in manufacturing bricks. It was observed that a higher amount of gold tailings gives high thermal conductivity and increases the porosity of bricks.

(c) Thermal conductivity

Thermal conductivity of bricks significantly influences the heat losses in any brick structure. Thermal conductivity of good quality bricks is kept minimum to keep the temperature stable inside the buildings in summer and winter. Kazmi et al., (2017) used agricultural waste (sugarcane bagasse ash and rice husk ash) in manufacturing bricks and it was observed that thermal conductivity of bricks decreases with the addition of agricultural waste. Reduction in density and compressive strength of bricks was also observed but the compressive strength of bricks was within standards. Burning of organic matter and agricultural waste in sediments at high temperatures produce micro pores. These pores play an important role to increase the thermal efficiency of bricks (Kazmi et al., 2017).

(d) Water absorption

Water absorption of bricks has a significant influence on durability of bricks. Firing temperature greatly influences the water absorption of bricks. Water absorption of bricks decreases with increasing firing temperature (Karaman et al., 2006). At high temperatures, sediments are transformed into a liquid state due to which pores are filled and isolated (Manoharan et al., 2011). Water absorption of good quality bricks is below 15% according to ASTM standards. Water absorption of bricks should be similar to the water absorption capacity of mortar, otherwise, the bond between the bricks and mortar can fail.

(e) Durability of bricks

Bricks durability is their resistance against snow, water and salt attacks. Durability of bricks is substantially influenced by the presence of soluble salts, impurities and organic matter.

(f) Compressive strength of bricks

Compressive strength of bricks depends on the raw material and manufacturing process of bricks. Generally, fired bricks have good compressive strength. Compressive strength of bricks increases with increasing temperature (Tsega, et al. 2017). Karaman et al., (2006) found a polynomial relationship between the firing temperature and compressive strength of bricks as shown in Figure 1.9.

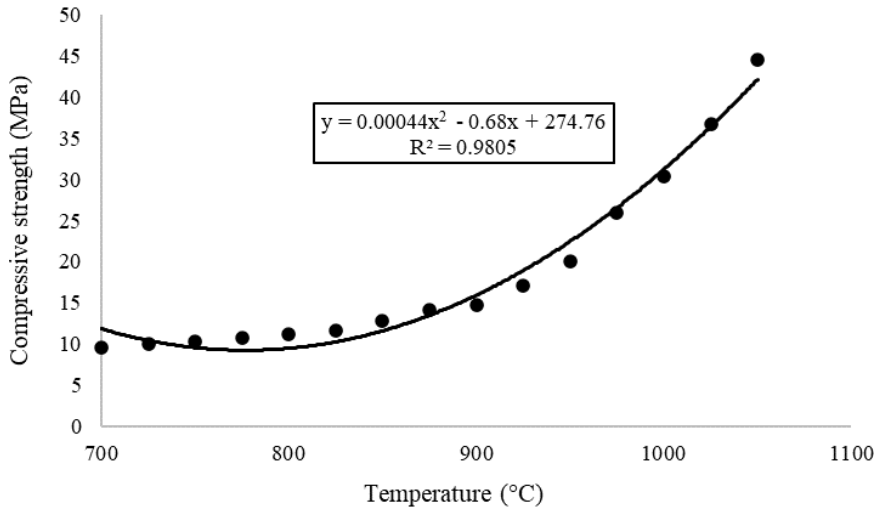

Figure 1. 9. Compressive strength variation with temperature (Karaman et al., 2006)

Following equation shows the relationship between compressive strength and temperature at 700 °C to 1050 °C (Karaman et al., 2006).

$$UCS = 274.76 - 0.68\,T + 0.00044\,T^2 \quad (1.1)$$

In this equation, UCS stands for compressive strength and T for temperature.

Compressive strength of bricks is measured with a universal testing machine. However, compressive strength of fired bricks can also be found by indirect methods such as ultrasonic pulse velocity (UPV). Recommended minimum compressive strength in ASTM standards depends on the application of bricks and weathering conditions. It ranges from 8.6 MPa to 17.2 MPa (ASTM C62-17, 2017).

Average compressive strength, porosity, water absorption and ultrasonic pulse velocities of fired bricks found by different researchers are shown in Table 1.8.

Table 1. 8. Properties of fired bricks

Sediments origin	Porosity (%)	WA (%)	UCS (MPa)	UPV (m/s)	Density (kg/m^3)	Reference
Clay bricks from ancient buildings	33	21.3	8.5		1742	Lourenço et al., 2010
Fresh clay from dam premises	35.53	21.95	9.1	1934	-	Riaz et al., 2019
Clayey soil	22.8	-	-	-	1792	Kadir and Maasom 2013

Note: UCS= compressive strength and UPV = ultrasonic pulse velocity, WA = water absorption

(g) Loss on ignition

Loss on ignition is the mass loss of fired bricks that occurs due to the firing of bricks at a high temperature. Sediments mass loss is associated with burning of organic matter and decomposition of carbonate content. Mass loss on ignition of fired bricks increases linearly with

increasing organic matter (Ukwatta and Mohajerani, 2017). Loss on ignition of sediments to be used in bricks found by different researchers is given in Table 1.9.

Table 1. 9. Loss on ignition of fired bricks

Soil origin	LOI (%)	Reference
River sediments	12.81	Mezencevova et al., 2012
Local clay industry	8.47	Kazmi et al., 2017
Soil quarry	12.15	Baronio and Binda, 1997
Soil quarry	6.03	Fgaier et al., 2015
Local raw material	6.27	Millogo et al., 2008
Alluvial deposits	3.39	Manoharan et al., 2011

(h) Efflorescence

Efflorescence is a thin salt layer on the surface of bricks. Efflorescence starts to appear when a structure becomes dry and salt dissolved in pores gathers near the surface. Major sources of efflorescence in bricks are sulphates of sodium, potassium and calcium which are formed during the firing of bricks at high temperatures (Brocken and Nijland, 2004).

(i) Hardness of bricks

Mohs scale of hardness on a scale of 1 to 10 is used to check the hardness of bricks. Hardness of bricks is directly linked with compressive strength of bricks. Hardness of good quality bricks is more than the hardness of fingernails (2.5) on Mohs scale of hardness.

(j) Lime pitting of bricks

Lime pitting of bricks happens on the surface of bricks by the expansion of calcium carbonate particles with moisture content. This phenomenon makes small pits on the surface of the bricks. In calcareous clays at firing temperature around 800 ^{0}C, calcite is altered into calcium oxide. Calcium oxide when interact with moisture, it forms calcium hydroxide due to which the volume of bricks is increased and cracks in bricks are developed. Controlling the carbonate percentage in sediments and firing the bricks higher temperature around 1100 °C prevents this phenomenon (Elert et al., 2003).

(k) Morphology of bricks

Scanning electron microscopy (SEM) is done to observe the microstructure of bricks. SEM of bricks is helpful to understand the morphology and nature of different particles present in their structure. Different features present in the structure can be distinguished by using high resolutions.

(l) Chemical composition of bricks

Chemical composition of fired bricks is found by X-ray fluorescence spectrometry. Major chemical components of bricks are (SiO_2, TiO_2, Al_2O_3, Fe_2O_3, MnO, MgO, CaO, Na_2O, K_2O,

P_2O_5 while trace chemical components include Ni, Cr, V, La, Ce, Co, Ba, Nb, Y, Sr, Zr, Rb. (Taranto et al., 2019).

Structural and chemical composition is modified when clay minerals are subjected to high temperature in ceramics (Ouahabi et al., 2015).

1.3.5 Waste material reuse in fired bricks

Raw material needed for bricks is non-renewable. Due to the higher demands of bricks, soil deposits used for brick construction are also exploited on large scale (Riaz et al., 2019). To preserve these non-renewable resources and their minimum use, numerous studies have been conducted to use waste material in bricks. Some waste materials used in fired bricks by different researchers are given in Table 1.10.

Table 1. 10. Waste material used in bricks

Application	Waste	Percentage	Reference
Fired bricks	Sewage sludge	5-15	Esmeray and Atis, 2019
Fired bricks	Electroplating Sludge	0-20	Dai et al., 2019
Fired bricks	Brick kiln dust	0-25	Riaz et al., 2019
Fired bricks	Foundry sand	Up to 50%	Hossiney et al., 2018
Fired bricks	Sugar can bagasse	Up to 3%	Kadir and Maasom, 2013
Fired bricks	Straw	0.5-3.5	Yousif, 2007
Fired bricks	Mine tailings	-	Kim et al., 2018

As dredged sediments are also a waste material, they can be used in bricks by fully or partially replacing traditional clay materials.

1.3. Earth bricks

Building sector is responsible for a huge amount of greenhouse gases emission and consumption of the higher amount of energy. Building sector in France consumes 44% energy (Ministère de la Transition Ecologique, 2021). Earth bricks are traditional environment-friendly building materials used from centuries. Nearly one-third world's population lives in adobe houses in developing countries. Earth bricks are green products made with minimum energy consumption and CO_2 emissions. Earth bricks are made with soil and natural fibers. Dredged sediments can also be used in earth bricks. Sediment's suitability for earth bricks is decided on the base of their granulometry, organic matter and Atterberg limits. Sediments are used with natural fibers to manufacture earth bricks. Natural fibers are byproduct of agriculture crops and easily available material. Their reuse in earth bricks as reinforcement increases the strength and durability of bricks.

1.3.1 Waste material reuse in earth bricks

Globally, 1.3 billion tons of waste is produced every year and it is expected to increase up to 2.2 billion tons per year in 2025 (Al-Fakih et al., 2019). The share of waste production by different regions of the world is shown in Figure 1.10.

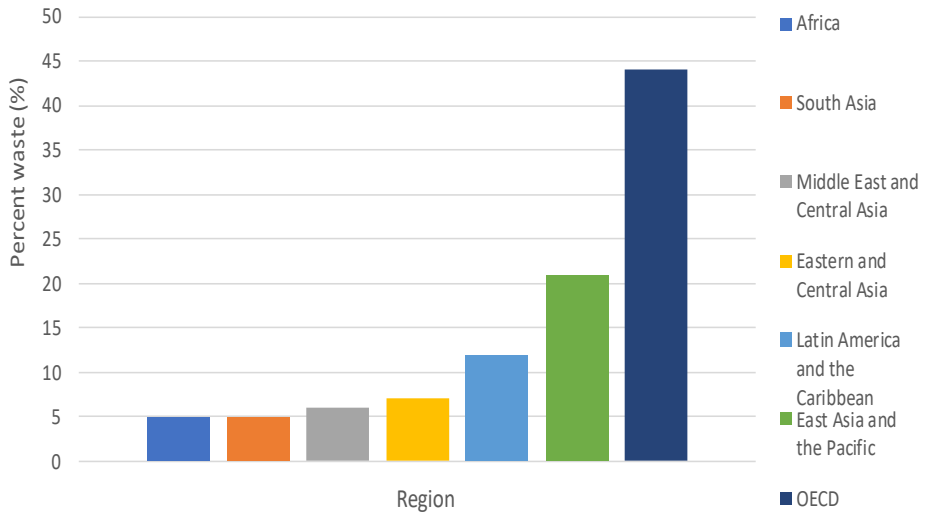

Note: OECD = Organisation for economic cooperation and development

Figure 1. 10. Global waste production (Al-Fakih et al., 2019)

Due to the increasing demand for bricks and depleting clay resources and agricultural lands, different waste materials are used in manufacturing earth bricks. Some of these wastes are rice husk ash, sugarcane bagasse, plastic fibers etc.

1.3.2 Natural fibers

Natural fibers are low cost, environment friendly, biodegradable and renewable material generated from agriculture. Common plant fibers are jute, palm fibers (OPF), banana spine fibers (Bs), sugar cane fibers (Sc), coconut fibers (Cn) and hemp (Salih et al., 2018). Fiber extraction is done by mechanical processing and retting. Due to humidity and microorganism activity, changes in pectin and hemi-cellulose occurs which makes fibers extraction much easier. After extraction, fibers are cleaned and dried to remove impurities and moisture content. Mechanical extraction of fibers is done with milling action by using sieves of different sizes.

Natural fibers are used in earth bricks as reinforcement. Addition of natural fibers improves mechanical and thermal properties of adobe bricks. Fibers are mixed with sediments to increase the binding of sediments. Fibers are strong in tension and increase the resistance of earth bricks against cracking and shear strength. Presence of fibers in the longitudinal and transversal direction of bricks increases the compressive and tensile strength of mud bricks and prevents the development of cracks. Earth bricks manufacturing using dredged sediments and fibers valorize both waste materials in an eco-friendly and green product. Natural fibers increase the cohesion of sediments and the strength of earth bricks (UN habitat, 2009).

1.3.3 Tropical fibers

Tropical natural fibers commonly found in Mexico are palm oil fibers, coconut shell fibers, banana spine fibers and sugarcane bagasse fibers. Palm is amply cultivated in tropical regions of the world and fibers are extracted from palm fruit, empty fruit bunches, trunk and leaf of the palm tree. Characteristics of palm fibers from different parts of palm tree varies. Another type

of tropical fibers are coconut fibers, extracted from coconut coir. Mexico is one of the major coconut producers in the world and its coconut annual production is around 1.06 million tons (Montfort et al., 2021). The length of coconut fibers ranges from 1 cm to 5 cm.

Banana spine fibers are available on large scale in tropical regions as banana is one of the important crops. The diameter of banana spine fibers ranges from 80 μm to 250 μm and their tensile strength of banana fibers is ranges from 523 MPa to 914 MPa (Bhatnagar et al., 2015). Sugarcane bagasse is another tropical fiber. Mexico is the fifth-largest sugarcane producer in the world with sugarcane fields covering the area of 770000 hectares (Aguilar-Rivera et al., 2012).

Global production of banana spine, coconut, palm oil and sugarcane bagasse fibers are presented in the Table 1.11.

Table 1. 11. Global tropical natural fibers production in million tons (FAO, 2021).

Year	**Tropical natural fibers**			
	Banana	**Coconut**	**Palm oil fruit**	**Sugar cane**
2009	103	61	216	1673
2019	116	62.4	411	1950

1.3.4 Characteristics of fibers

Some important properties of fibers include length, diameter, density, thermal conductivity, water absorption, elongation to break, tensile strength, modulus of elasticity and chemical composition. Natural length of fibers is very important for their use in composite materials. Recommended length of fibers for concrete applications is 2.5 cm (ASTM D7357-07, 2012). For adobe bricks, fibers length ranges from 1 cm to 10 cm (Araya-Letelier et al., 2021, Bakhaled et al., 2019, Kumar and Barbato, 2022).

Natural fibers have a good affinity with water which can change the strength of fibers. Mercerization, saline treatment, coating of latex and different other techniques are used to reduce hydrophilic nature of natural fibers as fibers are susceptible to increase the water absorption capacity of composite materials (Sreekala and Thomas, 2003). Water absorption of plant fibers and tropical fibers is summarized in Table 1.12.

Morphology and texture of fibers is important for the adhesion between the fibers and sediments matrix. Morphology of fibers is observed with scanning electron microscopy (SEM). Flatness, unevenness, pores and silica bodies are observed with SEM. Plant fibers usually consist of tubular structures which increase surface roughness. Surface roughness is very important for bonding between sediments and fibers. However, with a higher percentage of porous structures, tensile strength of fibers decreases which has a negative impact on the tensile strength of earth bricks.

Thermal stability of fibers is their resistance against extreme temperatures. Thermal stability of different materials is observed by thermogravimetry and differential thermal analysis.

Different physico-chemical characteristics of natural and tropical fibers are shown in Table 1.12.

1.3.5 Mechanical properties of fibers

Mechanical properties of fibers include tensile strength, tensile strain, young modulus, and elongation to break etc. Plant fibers exhibit very high tensile strength which makes them suitable additives in earth bricks. Deformation modulus of fibers is found from the stress-strain curve obtained with a tensile strength test. Fibers usually exhibit elasto plastic behavior with hardening under tensile load. The load-deflection behavior of fibers is shown in Figure 1.11.

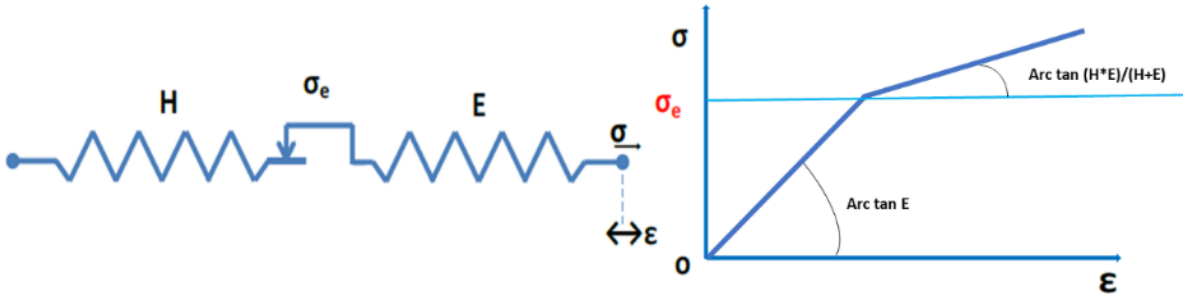

Figure 1. 11 . Elasto plastic behavior of fibers under tensile load (Saouti et al., 2019).

Mechanical properties of palm oil fiber (empty bunches), coconut fiber, sugarcane bagasse and date palm fibers used in manufacturing mud bricks by different researchers are summarized in Table 1.12.

Table 1. 12. Review of physical and mechanical properties of natural fibers (Bui et al., 2022).

Type of fiber	Density (g/cm^3)	Absorption coefficient (%)	Elasticity modulus (GPa)	Tensile strength (MPa)
Temprerature climate and subtropical fibers				
Bamboo	0.45-1.3	40-145	2.82-54	39.5-1000
Cotton	1.21-1.6	-	1.1-13	265-800
Flax	1.19-1.55	63-330	4.4-110	93-2000
Hemp	1.07-1.50	85-415	10-90	159-1264
Jute	1.23-1.50	84-281	2.5-78	300-800
Palm date	0.902	133-140	1.9-85	58-678
Ramie	1-1.58	-	23-128	400-1620
Reed	0.54-0.94	-	35.9	112-503
Rice straw	0.86-1.11	52-84	3.3-26.3	435-450
Sisal	1.2-1.50	110-230	1.46-38	80-1002.3
Wheet straw	1.14-2.05	96-320	1.4-4.8	3.45-140
Tropical fibers				
Banana spine	0.31-1.36	134-282	3-32	49.3-914
Coconut-coir	0.67-0.52	63-180	0.628-28	15-593
Palm oil*	0.1-1.55	54-120	0.5-25	147-400
Sugar cane	0.31-1.31	102-219	15-27.1	20-290.5

*Note: *Palm oil flowers and fruit fibers are all considered.*

1.3.6 Biochemical composition of fibers

Chemical composition of fibers plays an essential role in the decomposition of fibers and their shelf life. It has a significant influence on the tensile strength of fibers. Chemical components of fibers include cellulose, lignin, hemi-cellulose, ligno-cellulose, pectin, protein and ash. Cellulose is basic fiber content and it comprises 50%-90% of fiber (Pradeep et al., 2016). Tensile strength of fibers increases with cellulose content. Therefore, higher cellulose content is important for earth bricks as tensile strength of earth bricks increases with tensile strength of fibers (Bordoloi et al 2018). Pectin normally acts as a binder between fibers and straws of plants. Chemical composition of some natural fibers used in composite materials is shown in Table 1.13.

Table 1. 13. Chemical composition of fibers

Type of fiber	Cellulose (%)	Hemi-cellulose (%)	Lignin (%)	Ash (%)	Reference
Straw	40.8	31.7	10		Azhary et al., 2017
Banana	60-65	6-19	5-10	1-3	Bhatnagar et al., 2015
Bagasse	42	28	20	2.4	Barrera et al., 2016
OPEFB	59	2.1	25	3.2	Chaib et al., 2015

Note: OPEFB = Oil palm empty fruit bunches

1.3.7 Treatment of fibers

Strength, performance and life of natural fibers decrease with time due to bacterial and fungus actions. Degradation of fibers is rapid in alkaline environments associated in concrete structures (Bergström and Gramt, 1984). Chemical treatment of fibers is done to reduce the biodegradability of fibers and increase their shelf life. Chemical treatment of fibers increases the roughness of fiber surface, its strength, durability, and thermal stability. As fibers are hydrophilic, treatment of fibers decreases their affinity to water. Fibers are treated with sodium hydro oxide (NaOH) solution followed by washing with clean water and drying (Mostafa and Uddin, 2015).

Variations in tensile strength of bagasse and coir fibers before and after alkali treatment are shown in Table 1.14.

Table 1. 14. Alkali treatment of bagasse and coir fibers

Fibers	Tensile strength (MPa)	Average diameter (mm)	Reference
Untreated bagasse	70.9	0.49	Bergström and Gramt, 1984
Alkali treated bagasse	83.4	0.39	Bergström and Gramt, 1984
Untreated coir	123.6 ± 37.6	-	Bui, 2021
Alkali treated coir	111.2 ± 16.3	-	Bui, 2021

1.3.8 Types of earth bricks

Earth bricks have different types which depend on the specific requirement, moulding techniques and compaction method. Some common types are adobe bricks, compressed earth blocks, and rammed earth.

(a) Adobe bricks

Adobe bricks are common bricks all over the world and are sometimes named earth bricks. They are prepared by mixing soil and fibers with a suitable quantity of water. Soil is moulded without compression and air dried.

(b) Rammed earth blocks

Rammed earth blocks are traditional construction materials. They are composed of soil and fibers. Soil is poured in a wooden framework and compacted. The framework is removed after compaction. Usually, soil is compacted in different layers to construct walls. Water content needed to be mixed is important in the case of rammed earth. Optimum water content from the Proctor test can be used as moulding moisture content to have maximum strength (Simenson, 2013).

(c) Compressed earth blocks (CEB)

Compressed earth blocks are modern forms of adobe bricks and manufactured by applying compression on soil which significantly reduces soil volume. Sometimes additives like cement are also used to stabilize the compressed earth blocks. The use of compressing earth blocks is increasing due to improvement in machinery. Tensile strength of CEB is increased with the addition of fibers which addition increases their tensile strength and hinder the propagation of cracks (Mesbah et al., 2004).

1.3.9 Soil suitability for earth bricks

Soil suitability for earth bricks is decided after investigating sediments characteristics such as Atterberg limits, mineralogy and moisture content etc. The top layer of soil has sometimes higher organic matter which makes the soil undesirable for bricks. Top layer of soil is removed, and subsoil is used for making bricks (Little and Morton, 2001). Good quality soils for making bricks and earth structures have a specific range of plasticity. The liquidity limit of sediments used for earth bricks ranges from 32% to 46% while the plasticity index ranges from 16%-18%. Good quality soil for earth bricks lies in the regions prescribed for different types of earth bricks in Figure 1.12 (Delgado and Guerrero, 2007).

Figure 1.12 shows the suitability of soil for compressed earth blocks, adobe bricks and rammed earth blocks.

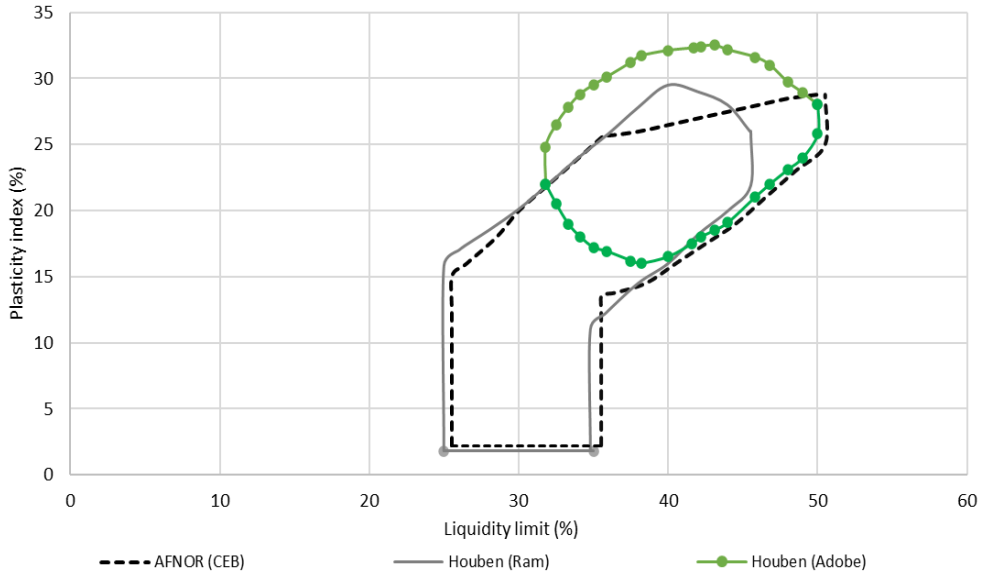

Figure 1. 12. Soil suitability for earth bricks with Atterberg limits

Grain size analysis is very important to make durable earth bricks. Minimum percentage of clay recommended in earth bricks is 5% and silt content varies from 10% to 25% (Delgado and Guerrero, 2007). Particle size for adobe bricks compressed earth blocks (CEB) and rammed earth is given in Figure 1.13 which is a logarithmic graph between grain size and percentage of passing sediments. The different limits are recommended by French and Spanish standards for earth bricks (Delgado and Guerrero, 2007). Suitable soil for mud bricks lies in the prescribed upper and lower limits of the adobe line shown in Figure 1.13.

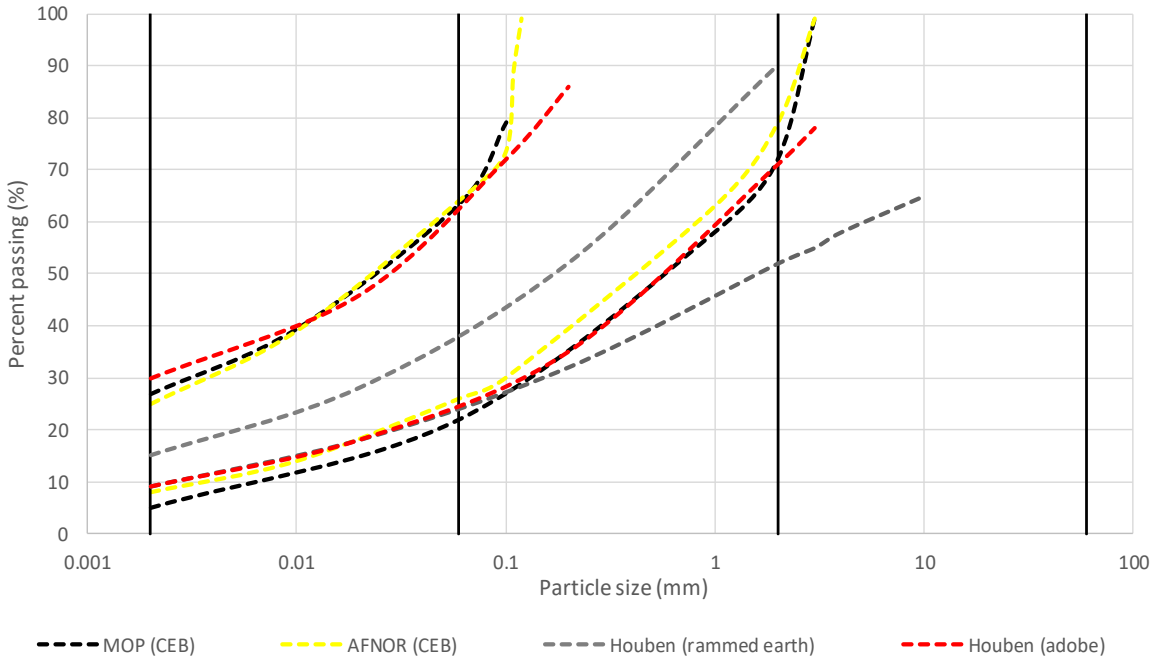

Note: CEB = compressed earth block, Ram = rammed earth, Adobe = adobe bricks, MOPT = Ministerio de Obras Públicas y Transportes, AFNOR = Association Française de Normalisation, Houben = Houben and Guillaud, (1994)

Figure 1. 13. Particle size for earth bricks (After Delgado and Guerrero, 2007).

1.3.10 Earth bricks manufacturing

Earth bricks are manufactured by mixing sediments and plant fibers. Characteristics of both sediments and fibers are studied before their reuse in bricks. Manufacturing process of earth bricks consist of material preparation, moulding and drying the bricks.

Material preparation is the first stage of manufacturing earth bricks. In this step, sediments are mixed with water and fibers. Mixing of sediments can be done by machine mixing or hand mixing. Machine mixing is preferred due to homogeneous mixture. For this purpose, electric mixers are commonly used at laboratory scale. (Salih et al., 2018). Two approaches are suggested by different researchers to mix sediments, water and fiber. Fibers are mixed with respect to the mass or volume of sediments. Quantity of water and fibers to mixed with sediments is very important to make good quality bricks. Higher percentage of fibers decreases the weight, density and strength of bricks. Compressive strength of bricks decreases as bonding between fibers and sediments becomes weak with higher fiber content. Clustering of fibers in sediments matrix is another problem associated with higher fibers percentage. Therefore, the optimum quantity of fibers should be mixed with sediments to reduce bricks density and increase their strength. The suitable quantity of fibers mixed with sediments for manufacturing earth bricks varies for different natural fibers and usually ranges from 1% to 7% by mass (Azhary et al., 2017, Danso, 2016).

Percentage of fibers used for earth bricks by different researchers are given in Table 1.15.

Table 1. 15. Quantity of fibers added in earth bricks

Fibers	Mass (%)	Volume (%)	Reference
OPEFB	1-5	-	Ismail and Yaccob, 2011
Plastics	0.1-0.2	-	Prasad et al., 2012
Coconut	3-7	-	Heru et al., 2013
Straw	0-3	30-40	Calatan et al., 2016
Plastic fiber	0.125	-	Binici et al., 2005
polystyrene fabric	2.5	-	Binici et al., 2005

Note: OPEFB = Oil Palm Empty Fruit Bunches

Moulding moisture content is also very important for the strength of earth bricks. Higher moisture content decreases the density of sediment solution and compressive strength of mud bricks considerably (Fgaier et al., 2016). For the earth bricks, suggested moulding moisture content range from 5% to 40% (Delgado and Guerrero, 2007). Moulding moisture content varies for clay and sandy soils and it can be derived from Atterberg limits and optimum moisture content with Proctor test (Ramakrishnan et al., 2021; Piani et al., 2020).

Sediments mixture is used in manufacturing bricks with moulding and extrusion. Extruded bricks are manufactured by passing paste through steel plates and cut by a wire. In moulding, bricks are moulded manually and with machines. At laboratory scale manufacturing, sediments can be moulded manually while in industry, machine moulding is practical. Special moulds

with varying dimensions are used to make earth bricks. Prismatic moulds of size 4*4*16 cm^3 are commonly used for mortar and composite materials laboratory manufacturing for flexural strength test (AFNOR EN196-1., 2016).

1.3.11 Compaction of bricks

Compaction of bricks removes the air inside the small pores in sediments matrix and improves the bonding. Compaction of sediments matrix can be done by tamping, vibration, static and dynamic compaction (Seifi et al., 2018). Compaction of bricks is optimal with dynamic compaction (Bahar et al., 2004; Dormohamadi and Rahimnia, 2020). Compaction of bricks densifies the bricks which increases their shear strength, durability and resistance against water absorption. Compressive strength and tensile strength of bricks increase with increasing compaction and densification.

Homogenous mixture of sediments and fibers is essential to get the maximum strength of bricks. Similarly, position and placement of fibers in bricks is also very important. However intense compaction of bricks disrupts the homogeneity of sediments matrix by displacing fibers. Accumulation of fibers at the top surface of bricks occurs with dynamic compaction and by tamping of bricks due to upward movement of water which leads to the formation of fibers clusters near the top surface of bricks and affects the uniformity and homogeneousness of fibers in the sediment matrix. Fibers upward movement in static loading is minimum. Therefore, compaction method has also a significant impact on the movement and distribution of the fiber.

Finally earth bricks are dried after compaction in open air under the sun or in the oven at low temperature up to 105 °C. Piani et al., (2020) found that water content in oven drying and air drying in the lab after 28 days was similar for both bricks but a difference in density of both sorts of dried bricks was observed. Air drying depends on the weathering conditions and in some cases lasted from 14 days to a month (Ismail and Yaacob, 2011; Heru et al., 2013).

Natural fibers have high water absorption tendency which is associated with presence of a hydroxyl group in cellulose and lignin content. Fibers water absorption affects the behavior of sediments matrix and the performance of earth bricks. Water absorption and drying of natural fibers lead to swelling and shrinkage of fibers which produce cracks in the sediments matrix and affect the bonding between two materials. Figure 1.14 shows the behavior of fibers with their interaction with water (Hejazi et al., 2012). Fibers swell when they interaction with water. During the drying of composite materials, fibers shrink due to water evaporation which induces microcracks in composite materials. The strength and performance of bricks are affected by the presence of pores as they decrease bonding between the sediments and fibers. With higher fiber content, bridging of microcracks sometimes leads to macrocracks which decrease the strength of bricks considerably (Piani et al., 2020). Therefore, moulding moisture content and quantity of fibers should be optimized to manufacture earth bricks.

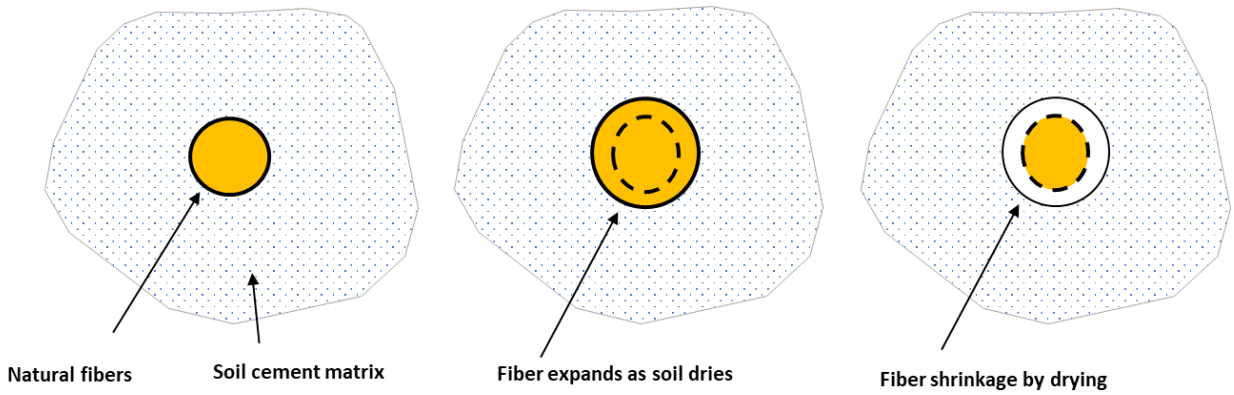

Figure 1. 14. Swelling and shrinkage of fibers with water absorption and removal (Hejazi et al., 2012).

Although fibers addition induces small cracks on drying, it also prevents the shrinkage in earth bricks and excessive cracking on drying.

1.3.12 Soil stabilization

Stabilization in sediment's matrix is achieved through the addition of binders and by compaction. Common binders are cement, gypsum and lime (Adam and Agib, 2001). Stabilization of bricks decreases the water absorption capacity of earth bricks. Water absorption of lime-based bricks ranges from 6% to 16% by weight (Jackson and Dhir, 1996). Microstructural analysis of lime-based bricks shows that with addition of lime in the sediments, calcite and calcium silicate hydrates are developed. Calcium silica hydrates is produced by reaction between lime and silica. Creation of these two substances increases the compaction and strength of mud bricks. However higher quantity of stabilizers has negative impact on physical characteristics of earth bricks (Millogo et al., 2008) and increases the cost.

1.3.13 Impact of fibers addition

Addition of fibers increases the plastic deformation in earth bricks and resists against brittle failure of earth bricks. Natural fibers control the shrinkage on drying of bricks (Quagliarini and Lenci, 2010) and regulate the absorption and evaporation of humidity and thus improve the hygroscopic properties of adobe bricks.

Characteristics of fibers such as diameter, length and water absorption have also a significant influence on the strength and properties of earth bricks. Tensile strength of earth bricks increases with long fibers. However, the impact of higher fibers length on compressive strength is negative.

The strength and behavior of bricks change with the percentage of fibers in the mixture. Calatan et al., (2016), made adobe bricks with different percentages of hemp fibers and straw and described the relationship between the brick strength and fiber content. By the comparison of strength and density of earth bricks, it was observed that bricks with 40% addition of straw by volume of sediments develop good compressive strength and density. On the other hand, bricks have optimum strength at 10% addition of hemp fibers by volume of sediments.

Tensile strength of adobe bricks observed by using different natural fibers is summarized in Table 1.16.

Table 1. 16. Natural fibers impact on tensile strength of earth bricks

Fibers	Fiber content (wt.%)	Tensile strength (MPa)	Reference
Jute	0.5-2	0.55-0.66	Araya-Letelier et al., 2021
Seagrass	0.5-3	0.4-0.6	Olacia et al., 2020
Straw	0.5	0.71	Abdulla et al., 2020
Sugarcane bagasse	0-1	0.29-0.89	Kumar and Barbato 2022
Date palm waste	0-10	0.29-2.26	Khoudja et al., 2021

1.1.13.1. Fiber's adhesion

Plant fibers have tubular structures which increase their surface roughness. Fibers surface roughness and fibers embedded length in sediment matrix play an important role in bonding between natural fibers and sediment matrix. Fiber's failure mechanism inside the composite material is also important for their strength. Insufficient fibers length leads to sliding of fibers and the contribution of fibers in tensile strength of composite material is minimized. Pull out test mechanism used to define the critical length of fibers is shown in Figure 1.15.

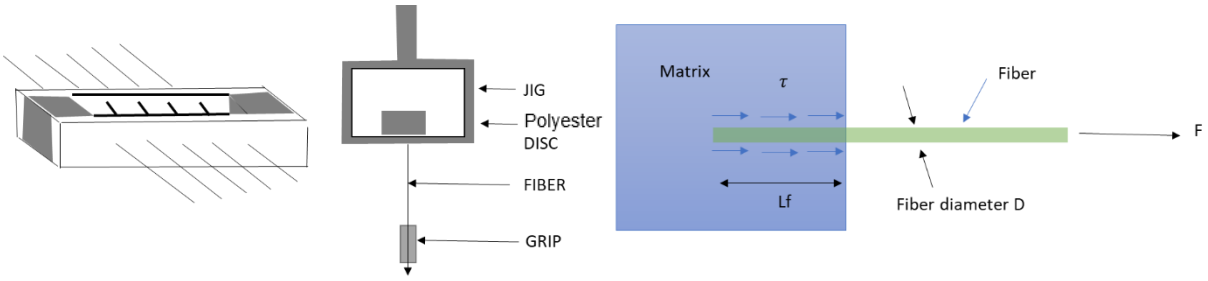

Figure 1. 15. Pull out test mould (a) and mechanism for pull-out force and shear stress (Bui et al., 2022)

1.1.13.2. Distribution and orientation of fibers

Uniform distribution, orientation and alignment of fibers have a substantial influence on the tensile strength and performance of earth bricks. However, fibers are randomly distributed in longitudinal and transverse directions. The longitudinal distribution of fibers along the axis of earth bricks increases their tensile strength and prevents the deformation in bricks. The orientation of short fibers is usually better in composite materials, but it is difficult to control fibers orientation in bricks (Alberti et al., 2018). Orientation and distribution of fibers are also associated with the length of fibers, moulding and compaction procedure.

The shape of fibers varies with plants. However, elliptical and circular shapes are common in natural fibers. Figures 1.16a and 1.16b describe the position of fibers with angles θ and φ in composite materials (Fu et al., 2009).

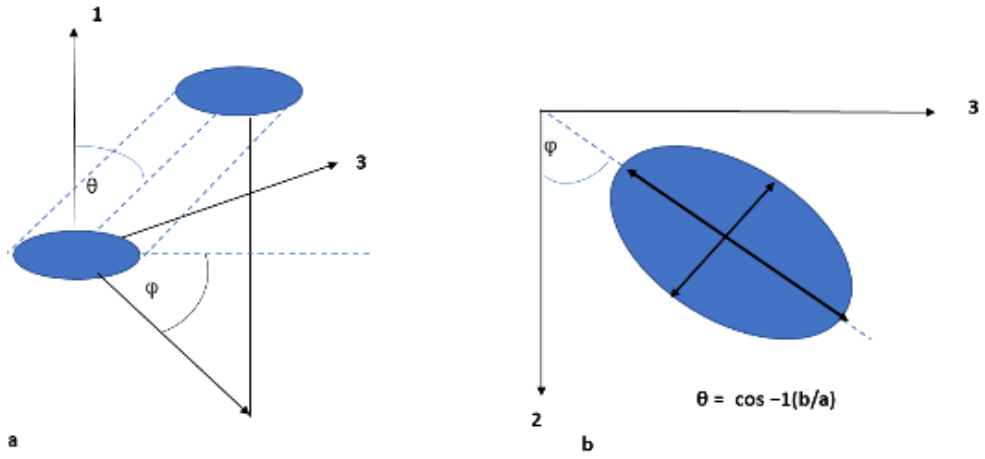

Figure 1. 16. Natural fibers orientation estimation (Fu et al., 2009).

The orientation factor of fibers in composite materials in case of elliptical shape fibers is calculated by the following formula (Hine et al., 1996).

$$\theta = arc.\cos\frac{b}{a} \quad (1.2)$$

θ = angle created by fiber axis and Y-axis ($0 \leq \theta \leq 90°$), a and b are major and minor axis of the ellipse. $\theta = 90°$ if fibers is perpendicular to the cutting plane and 0° if it is parallel

$$\eta_\theta = \frac{1}{N_f}\sum_{i=1}^{N_f}\cos(\theta) \quad (1.3)$$

N_f = total number of fibers in a cross section.

Alignment of fibers at different microfibers angles is very important for tensile strength of earth bricks. Perfectly aligned fibers with complete overlapping of elementary fibers increase the tensile strength of technical fibers and the tensile strength of earth bricks increases with increasing strength of fibers.

1.3.14 Characteristics of earth bricks

(a) Tensile strength of earth bricks

Earth bricks are weak in tension and their tensile strength is low compared to their compressive strength (Olacia et al., 2020). Indirect tensile strength of earth bricks is usually found with three-point bending test (ASTM D790-03, 2003). The failure in unreinforced earth bricks is similar to composite materials such as plain concrete (Mostafa and Uddin, 2015). Tensile load after initial cracking is supported by fibers which transfer the load to bond stresses and the propagation of cracks continues. The fibers hold the blocks pieces and prevent spalling. Earth bricks failure occurs at failure or sliding of fibers. Sliding of fibers occurs due to insufficient fibers depth and weak adhesion (Mehta and Monteiro, 2001).

Failure mechanism of reinforced mortar sample is described in Figure 1.17 where point A show the evolution of load and displacement in nonlinear elastic region. Point B shows the evolution in linear elastic zone. Point C shows the peak of load where specimen fails partially and reaches

at C' due to residual forces. At this step, some fibers fail and others slip inside the matrix. From D to E the load is nearly constant and supported by fibers (Bui, 2021).

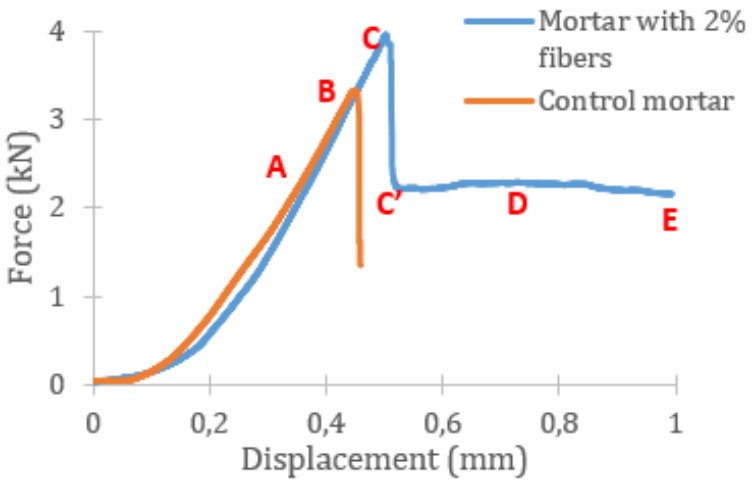

Figure 1. 17. Flexural load deflection of behavior of reinforced mortar (Bui, 2021)

Figure 1.18 shows the increase in toughness of fiber reinforced composite materials. The failure in unreinforced earth bricks occurs at point A at which Toughness is zero. With the addition of fiber, but the bricks continue to support the load after point A. Toughness index increases with fibers addition up to optimum fiber content (ASTM C 1018, 1998).

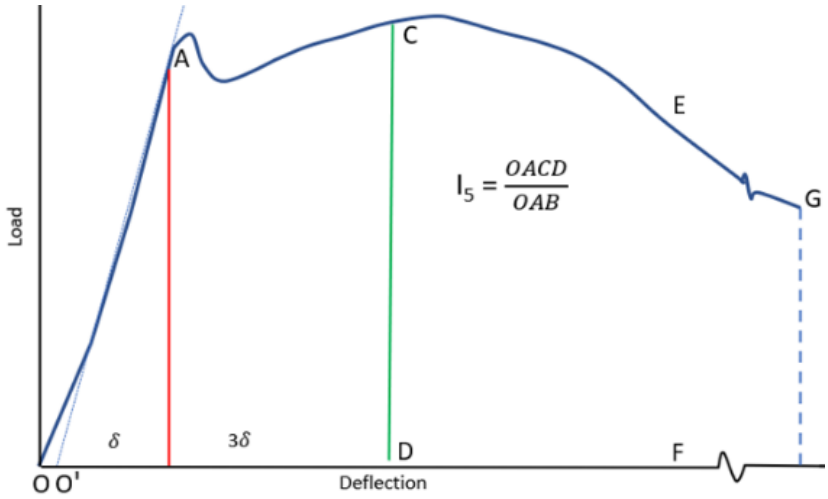

Figure 1. 18. Toughness index calculation (ASTM C 1018 – 1998).

Tensile strength of earth bricks varies greatly and depends on number of factors such as fiber content, mineralogy of sediments, moulding moisture content and compaction method etc. For the strength and quality of bricks, there is a lack of standardization. Recommended tensile strength of earth bricks fluctuates between 0.012 and 0.25 MPa in international standards such as New Zealand and Mexican standards (NZS 4298, 1998, NORMA E.080, 2017).

(b) Compressive strength of earth bricks

Compressive strength of earth bricks is important for structures. French and Mexican standards have a threshold value of 1 MPa for adobe bricks (AFNOR XP, P13-901, NORMA E.080, 2017).

(c) Density of earth bricks

Natural fibers have low density which makes them suitable additives for building composite. Density of adobe bricks decreases with increasing fibers content as fibers are lightweight and induce pores in earth bricks which helps to reduce the density of construction composites materials. Density of earth bricks ranges from 1260 kg/m^3 to 1950 kg/m^3 (Illampas et al. 2011, Salih, et al. 2019).

(d) Thermal conductivity

Earth bricks have a low thermal conductivity which is important for construction materials. Lower thermal conductivity of plant fibers makes them suitable additives for earth bricks. Thermal conductivity of earth bricks decreases with fibers addition (Chaib et al., 2015) and ranges from 0.18 to 1.13 W/m-K (Revuelta-Acosta et al., 2010, Calatan et al., 2016).

1.4 Conclusion

This chapter presents overview of the dredged sediments management, recovery, disposal and environmental regulation for dredged sediments. Dredged sediments disposal and reuse in different sectors are defined after analyzing their physical, chemical, geotechnical and mineralogical characteristics. Non-polluted sediments are usually immersed in the sea. However, land storage of sediments is costly and requires treatment. These sediments can be reused in roads, construction materials, embankments and dikes, depending on local requirements.

Sediments are heterogeneous and most of the research on dredged sediments is concerned only with specific applications. In this study, sediments characteristics were reviewed and their suitability for fired and earth bricks is investigated. In the case of fired bricks, sediments mineralogy and Atterberg limits play an important role. Fired bricks manufacturing is done at a temperature range of 700 °C to 1100 °C. Important fired bricks characteristics include tensile strength, compressive strength, water absorption, mass loss and shrinkage etc.

Sediments reuse in earth bricks is strengthened with the addition of natural fibers. Fiber's tensile strength, morphology, water absorption, density and thermal conductivity are key factors that contribute to the higher tensile strength of earth bricks. Tensile load deflection behavior of most of the plant fibers is elastoplastic with hardening and they are hydrophilic materials. Length of fibers ranges from 1-10 cm in earth bricks. Fibers acts are reinforcement and increase the tensile strength of bricks. Sediments and fibers are mixed with moulding moisture content derived from Atterberg limits and Proctor test. Sediments fibers matrix is compacted to remove the voids and increase the strength. Tensile strength, compressive strength, water absorption, density and thermal conductivity are some important characteristics of earth bricks. Earth

bricks are green products with minimum environmental consequences. However, earth bricks have strength limitations and are sensitive to weathering.

References

Abdulla, K.F., Cunningham, L.S., Gillie, M. (2020). Experimental sttudy on the mechanical properties of straw fiber–reinforced adobe masonry. J. Mater. Civ. Eng., 32(11): 04020322. DOI: 10.1061/(ASCE)MT.1943-5533.0003410

Adam, E.A., Agib, A.R.A. (2001). Compressed stabilised earth block manufacture in Sudan; United Nations Educational, Scientific and Cultural Organization, UNESCO, Paris, 11: 2001.
AFNOR EN196-1. (2016). Méthodes d'essais des ciments - Partie 1 : détermination des résistances.

AFNOR XP P13-901 (2001): Compressed earth blocks for walls and partitions: definitions– specifications – test methods.

Agostini, F., Skoczylas, Z., Lafhaj, Z. (2007). About a possible valorisation in cementitious materials of polluted sediments after treatment. Cement & Concrete Composites 29, 270–278. https://doi.org/10.1016/j.cemconcomp.2006.11.012

Aguilar-Rivera, N., Rodriguez, L. D. A., Enriquez, R. V. Castillo M. A., Herrera, A. S. (2012). The Mexican Sugarcane Industry: Overview, Constraints, Current Status and Long-Term Trends. Sugar Tech 14(3): 207–222. DOI 10.1007/s12355-012-0151-3

Alberti, M.G., Enfedaque, A., Gálvez, J.C., (2018). A review on the assessment and prediction of the orientation and distribution of fibres for concrete, Composites Part B: Engineering, Volume 151, 2018, 274-290, https://doi.org/10.1016/j.compositesb.

Al-Fakih, A.A., Mohammed, B.S., Liew, M.S., Nikbakht, E. (2019). Incorporation of waste materials in the manufacture of masonry bricks: An update review. Journal of Building Engineering 21: 37–54. https://doi.org/10.1016/j.jobe.2018.09.023

Arce, P. L., Guinea, J.G., Gracia, M., Obis, J. (2003). Bricks in historical buildings of Toledo City: characterization and restoration. Materials Characterization 50:59–68. https://doi.org/10.1016/S1044-5803(03)00101-3

Araya-Letelier, G., Antico, F.C., Burbano-Garcia, C., Concha-Riedel, J., Norambuena-Contreras, J., Concha. J., Flores, E.I. S. (2021). Experimental evaluation of adobe mixtures reinforced with jute fibers.Construction and building materials, volume 276, 122127

ASTM C62-17. (2017). Standard Specification for Building Brick. Solid Masonry Units Made From Clay or Shale.

ASTM C1018 (1998). Standard Test Method for Flexural Toughness and First-Crack Strength of Fiber-Reinforced Concrete (Using Beam With Third-Point Loading)

ASTM D790 (2003). Standard Test Methods for Flexural Properties of Unreinforced and Reinforced Plastics and Electrical Insulating Materials

ASTM D7357-07. (2012). Standard specification for cellulose fibers for fiber- reinforced concrete, ASTM International, West Conshohocken, PA.
Augustinik, A.I. (1957). Ceramic Leningrad.

Azhary, E., Chihaba, Y., Mansourb, M., Laaroussia, N. Garoum, M. (2017). Energy Efficiency and thermal properties of composite material clay-straw. Energy Procedia 141,160–164. https://doi.org/10.1016/j.egypro.2017.11.030

Bahar, R., Benazzoug, M., Kenai, S., 2004. Performance of compacted cement-stabilised soil. Cem. Concr. Compos. 26 (2004), 811–820. https://doi.org/10.1016/j.cemconcomp.2004.01.003.

Bakhaled, M.L., Bentchikou M., Ferroukhi, M.Y., Belarbi, R. (2019). Properties of extruded clay bricks reinforced by date palm fibers following the same industrial production steps. Academic Journal of Civil Engineering. DOI: https://doi.org/10.26168/ajce.36.1.64

Baksa, P., Cepak, F., Lukman, R.K., Ducman, V. (2018). An Evaluation of Marine Sediments in Terms of their usability in the Brick Industry: Case Study Port of Koper. J. sustainable development energy water environmental. system., 6(1), pp 78-88, DOI: https://doi.org/10.13044/j.sdewes.d5.0183

Baronio, G., Binda. L. (1997). Study of the Pozzolanicity of some bricks and clays. Construction and Building Materials, Vol. 11, No. 1, pp. 41-46. https://doi.org/10.1016/S0950-0618(96)00032-3

Barrera, I., Myriam, A., Allierib, L., Estupinanb, T., Martínez, T. (2016). Technical and economical evaluation of bioethanol production from lignocellulosic residues in Mexico: Case of sugarcane and blue agave bagasse. Chemical Engineering Research and Design. 1 0 7: 91–101. https://doi.org/10.1016/j.cherd.2015.10.015

Bénédicte, D. (2017). La faisabilité de la valorisation des sédiments de dragage de l'estuaire de la Vilaine, une démarche territoriale. PhD thesis, Institution d'Aménagement de la Vilaine, France.

Bergström, S.G., Gramt H. E. (1984). Durability of alkali-sensitive fibres in concrete". The International Journal of Cement Composites and Lightweight Concrete, Volume 6, Number 2. https://doi.org/10.1016/0262-5075(84)90036-8

Bhatnagar, J. M., Goel, R. K., Gupta, R. G. (1994). Brick-making characteristics of river sediments of the South West Bengal region of India. Construction and Building Materials, 8(3): 177-183. Number 3. https://doi.org/10.1016/S0950-0618(09)90032-0

Bhatnagar, R., Gupta, G., Yadav, S., (2015). A review on composition and properties of banana fibers. International Journal of Scientific & Engineering Research, Volume 6. DOI: 10.22214/ijraset.2017.10120

Binici, H., Aksogan, O., Shah, T. (2005). Investigation of fibre reinforced mud brick as a building material. Construction and Building Materials 19: 313–318. doi:10.1016/j.conbuildmat.2004.07.013

Bodian, S., Faye, M., Sene, N.A., Sambou, V., Limam, O., Thiam, A. (2018). Thermo-mechanical behavior of unfired bricks and fired bricks made from a mixture of clay soil and laterite. Journal of building engineering, 18:172-179. https://doi.org/10.1016/j.jobe.2018.03.014

Bordoloi, S., Kashyap, V., Garg, A., Sreedeep, S., Wei, L., Andriyas, S. (2018). Measurement of mechanical characteristics of fiber from a novel invasive weed: A comprehensive comparison with fibers from agricultural crops.

Brakni, S., Abriak, N. E., Hequette A. (2009). Formulation of artificial aggregates from dredged harbour sediments for coastline stabilization. Environmental Technology Vol. 30, No. 8: 849–854 DOI: 10.1080/09593330902990154

Brick Industry Association, Reston, Virginia (2006). Manufacturing of brick. Technical notes on brick construction.

Brocken, H., Nijland, T. G. (2004). White efflorescence on brick masonry and concrete masonry blocks, with special emphasis on sulfate efflorescence on concrete blocks. Construction and Building Materials, vol. 18, no. 5, pp. 315–323

Bruno, A.W., Gallipoli, D., Perlot, C., Mendes, J. (2018). Optimization of bricks production by earth hypercompaction prior to firing. Journal of Cleaner Production 214: 475:482. https://doi.org/10.1016/j.jclepro.2018.12.302

Bui, H. (2021). Study on performance enhancement of coconut fibres reinforced cementitious composites. PhD thesis. Caen Normandie University, France

Bui, H, Hussain, M., Levacher, D. (2022). Recycling of tropical natural fibers in building materials. Natural fibers, Intechopen book. DOI: 10.5772/intechopen.102999.

Calatan, G., Hegyi, A., Dico, C., Mircea, C. (2016). Determining the optimum addition of vegetable materials in adobe bricks. Procedia Technology 22: 259 – 265. https://doi.org/10.1016/j.protcy.2016.01.077

Cappuyns, V., Deweirt, V., Rousseau, S. (2015). Dredged sediments as a resource for brick production: Possibilities and barriers from a consumers' perspective. Waste Management 38: 372–380. https://doi.org/10.1016/j.wasman.2014.12.025

Cerema (2021). Les sédiments de dragage en Normandie au cœur de l'économie circulaire des matériaux du BTP – Colloque (visio) régional du 25 mai 2021, Région Normandie.

Chaib, H., Kriker, A., Mekhermeche, A. (2015). Thermal study of earth bricks reinforced by date palm fibers. Energy Procedia 74: 919 – 925. International Conference on Technologies and Materials for Renewable Energy, Environment and Sustainability, https://doi.org/10.1016/j.egypro.2015.07.827

Couvidat, J., Benzaazoua, M., Chatain, V., Bouamrane, A., Hzah, H. B. (2016). Feasibility of the reuse of total and processed contaminated marine sediments as fine aggregates in cemented

mortars. Construction and Building Materials 112: 892–902. https://doi.org/10.1016/j.conbuildmat.2016.02.186

Cultrone, G., Sidrab, I., Sebastian, E. (2005). Mineralogical and physical characterization of the bricks used in the construction of the Triangul Bastion, Riga (Latvia). Applied Clay Science 28, 297 – 308. https://doi.org/10.1016/j.clay.2004.02.005

Dai, Z., Zhou, H., Zhang, W., Hu, L., Huang, Q., Mao, L. (2019). The improvement in properties and environmental safety of fired clay bricks containing hazardous waste electroplating sludge: The role of Na2SiO3. Journal of Cleaner Production, 228: 1455-1463. https://doi.org/10.1016/j.jclepro.2019.04.274

Danso, H. (2016). Use of agricultural waste fibres as enhancement of soil blocks for low-cost housing in Ghana. PhD thesis, University of Portsmouth, UK. https://www.researchgate.net/publication/320739325

Delgado, M. C.J., Guerrero, I. C. (2007). The selection of soils for unstabilised earth building: A normative review. Construction and Building Materials 21, 237–251. https://doi.org/10.1016/j.conbuildmat.2005.08.006

Dormohamadi, M.; Rahimnia, R. Combined effect of compaction and clay content on the mechanical properties of adobe brick. Case Studies in Construction Materials, Volume 13, 2020, e00402. https://doi.org/10.1016/j.cscm.2020.e00402

Dubois, V., Abriak, N.E., Zentar, R., Ballivy. G. (2009). The use of marine sediments as a pavement base material. Waste Management 29, 774–782. https://doi.org/10.1016/j.wasman.2008.05.004

Elert, K., Cultrone, G., Navarro, C. R., Pardo, E.S. (2003). Durability of bricks used in the conservation of historic buildings—influence of composition and microstructure. Journal of Cultural Heritage,4:91–99. https://doi.org/10.1016/S1296-2074(03)00020-7

Esmeray, E., Atıs, M. (2019). Utilization of sewage sludge, oven slag and fly ash in clay brick production. Construction and Building Materials 194: 110–121 https://doi.org/10.1016/j.conbuildmat.2018.10.231

European Commission (2007). Reference document on best available techniques in the ceramic manufacturing industry.

FAO. (2021). Statistic of crop production in the world - Crops and livestock products (Production). Food and Agriculture Organization. Rome. [Internet]. 2021. Available on https://www.fao.org/faostat/en/#data [Accessed: 2021-11-22]

Fgaier, F.E. (2013). Conception, production et qualification des briques en terre cuite et en terre crue. PhD thesis, Ecole Centrale de Lille, 2013.

Fgaier, F.E., Lafhaj, Z., Brachelet, F., Antczak, E., Chapiseau, C. (2015). Thermal performance of unfired clay bricks used in construction in the north of France: Case study. Case Studies in Construction Materials 3, 102–11. https://doi.org/10.1016/j.cscm.2015.09.001

Fgaier, F.E., Lafhaj, Z., Chapiseau, C., Antczak, E. (2016). Effect of sorption capacity on thermo-mechanical properties of unfired clay bricks. Journal of Building Engineering, Doi: http://dx.doi.org/10.1016/j.jobe.2016.02.011

Fonseca, B.S., Galhano, C. D. Seixas, D. (2015). Technical feasibility of reusing coal combustion by-products from a thermoelectric power plant in the manufacture of fired clay bricks. Applied Clay Sci., 104 (2015) 189–195. http://dx.doi.org/10.1016/j.clay.2014.11.030

Fu, S.Y., Lauke, B., Mai, Y.W. (2009). Science and engineering of short fibre reinforced polymer composites. 1st edit. CRC Press. eBook ISBN: 9781845696498

Greentech knowledge solution (2015). Case studies on cleaner brick production, case study No.2. Production of bricks through natural draft Zigzag Kiln. Greentech Knowledge Solutions, New Delhi, India

Hakkoum, S., Kriker, A, Mekhermeche, A. (2017). Thermal characteristics of model houses manufactured by date palm fiber reinforced earth bricks in desert regions of Ouargla Algeria. Energy Procedia 119 662–669. https://doi.org/10.1016/j.egypro.2017.07.093

Hamer, K., Karius, V. (2002). Brick production with dredged harbour sediments. An industrial-scale experiment. Waste Management 22: 521–530. https://doi.org/10.1016/S0956-053X(01)00048-4

Haurine, F. (2015). Caractérisation d'atterrissements d'argiles récents sur le territoire français, en vue de leur valorisation dans l'industrie des matériaux de construction en terre cuite. Sciences de la Terre. PhD thesis, Ecole Nationale Supérieure des Mines de Paris, Français.

Hayet, A., Deram, A., Bohain, D. (2017). Contexte et cadre réglementaire de la gestion des sédiments de dragage. Etude n°14-1023/1B, 2017. Premier chapitre de l'étude impacts écologiques de sédiments pollués extraits et déposés en milieux terrestres. Ilis - Université de Lille 2

Heru, P., Dedi, P., Riana, L. H. (2013). Strength improvement of early age unfired soil lime bricks. Advanced Materials Research Vol 689 pp 299-303. doi:10.4028/www.scientific.net/AMR.689.299

Hejazi, S.M., Sheikhzadeh, M., Abtahi, S.M., Zadhoush, A. (2012). A simple review of soil reinforcement by using natural and synthetic fibers. Construction and Building Materials. 2012; 30: 100-116. DOI:10.1016/j.conbuildmat.2011.11.045

Hine, P.J., Duckett, R.A., Ward, I.M., Allan, P.S., Bevis, M.J. (1996). A comparison of short glass fiber reinforced polypropylene plates made by conventional injection molding and using shear controlled injection molding. Polymer Composites;17 (3):400-407. DOI:10.1002/pc.10627

Hossiney, N., Das. P., Krishna, M., George, M.J. (2018). In-plant production of bricks containing waste foundry sand—A study with Belgaum foundry industry. Case studies in construction materials. https://doi.org/10.1016/j.cscm.2018.e00170

Houben, H., Guillaud, H. (1994). Earth construction: A comprehensive guide. Intermediate Technology Publications, London.

Illampas, R., Ioannou, I., Charmpis, D.C. (2011). A study of the mechanical behaviour of adobe masonry. Structural Repairs and Maintenance of Heritage Architecture XII 485. WIT Transactions on The Built Environment, Vol 118. doi:10.2495/STR110401

Ismail, S., Yaacob, Z. (2011). Properties of laterite brick reinforced with oil palm empty fruit bunch fibres. Pertanika J. Sci. & Technol. 19 (1): 33 – 43.

Jackson, N.L., Dhir, R.V.K. (1996). Civil Engineering Materials. Fifth edition

Johari, I., Said, S., Hisham, B., Bakar, A., Ahmad, Z. (2010). A. Effect of the Change of Firing Temperature on Microstructure and Physical Properties of Clay Bricks from Beruas (Malaysia. Science of Sintering, 42: 245-254. doi: 10.2298/SOS1002245J

JKSPL (2106). Introduction to Brick Kilns & Specific Energy Consumption Protocol for Brick Kilns, India.

Kadir, A.A., Maasom, N. (2013). Recycling sugarcane bagasse waste into fired clay brick. International Journal of Zero Waste Generation. Vol.1, No.1, 2013; ISSN 2289 4497.

Karaman, S., Ersahin, S., Guna. H., (2006). Firing temperature and firing time influence on mechanical and physical properties of clay bricks. Journal of Scientific and Industrial Research, Vol 65, pp. 153-15.

Kazmi, M.S., Munir, M.J, Patnaikuni, I., Wu, Y. F., Fawad, U. (2017). Thermal performance enhancement of eco-friendly bricks incorporating agro-wastes. 158: 1117–1129 Energy and Buildings. https://doi.org/10.1016/j.enbuild.2017.10.056

Khoudja, D., Taallah, B., Izemmouren, O., Aggoun, O., Herihiri, O., Guettala, A., (2021). Mechanical and thermophysical properties of raw earth bricks incorporating date palm waste. Construction and Building materials, 270, 121824.

Kim, Y., Lee, Y., Kim, M., Park. H. (2018). Preparation of high porosity bricks by utilizing red mud and mine tailing. Journal of Cleaner Production, 207: 490-497 https://doi.org/10.1016/j.jclepro.2018.10.044

Kornmann, M. (2009). Matériaux de terre cuite - Matières de base et fabrication.Techniques de l'ingénieur (ref C905): 26.

Koroneos, C., Dompros, A. (2007). Environmental assessment of brick production in Greece. Building and Environment 42, 2114–2123. https://doi.org/10.1016/j.buildenv.2006.03.006

Kreimeyer, R. (1986). Some notes on the firing colour of clay bricks. Applied Clay Science, 2, 175-183. https://doi.org/10.1016/0169-1317(87)90007-X

Kumar, N., Barbato, M. (2022). Effects of sugarcane bagasse fibers on the properties of compressed and stabilized earth blocks. Construction and building materials, 315, 125552.

Little, B., Morton, T. (2001). Building with earth in Scotland: innovative design and sustainability. Scottish Executive Central Research Unit.

Lourenço, P. B., Fernandes, F. M., Castro, F. (2010). Handmade Clay Bricks: Chemical, Physical and Mechanical Properties. International Journal of Architectural Heritage: Conservation, Analysis, and Restoration, 4:1, 38-58. DOI: 10.1080/15583050902871092

Manoharan, C., Sutharsan, P., Dhanapandian, S., Venkatachalapathy, R., Asanulla, R. M. (2011). Analysis of temperature effect on ceramic brick production from alluvial deposits, Tamilnadu, India. Applied Clay Science 54: 20–25. https://doi.org/10.1016/j.clay.2011.07.002

MEDD (2020). Ministère de l'Ecologie et du Développement Durable. Gestion des sediments extraits de cours d'eau et des canaux. Direction de l'eau et direction de la prevention des pollutions et des risques.

Mehta, P.K., Monteiro, P.J.M. (2001). Concrete microstructure, properties and materials. McGraw-Hill, New Jersey, 2006.

Mesbah, A., Morel, J. C., Walker, P., Ghavami, K. (2004). Development of a direct tensile test for compacted earth blocks reinforced with natural fibers. Journal of Materials in Civil Engineering. DOI: 10.1061/~ASCE!0899-1561~2004!16:1~95!

Mezencevova, A., Yeboah, N., Susan, E. B., Kahn, L. F., Kurtis, K.E. (2012). Utilization of Savannah Harbor river sediment as the primary raw material in production of fired brick. Journal of Environmental Management 113, 128-136. https://doi.org/10.1016/j.jenvman.2012.08.030

Millogo, Y., Hajjaji, M., Ouedraogo, R. (2008). Microstructure and physical properties of lime-clayey adobe bricks. Construction and Building Materials 22, 2386–2392. https://doi.org/10.1016/j.conbuildmat.2007.09.002

Ministère de la Transition Ecologique, (2021). Energie dans les Bâtiments. Available online: https://www.ecologie.gouv.fr/energie-dans-batiments (accessed on 13 December 2021).

Monap, N., Bedali, R., Sandirasegaran, K., Masrom, N., Yahya, Y. (2015). Strength of brick made from dredged sediments. Jurnal Teknologi (Sciences & Engineering) Vol 78, No 7-3,page 87–92 DOI: https://doi.org/10.11113/jt.v78.9490

Montfort, G.R.C, Santana, T.J.M., Barrera, M.A.F., Valencia, R.A.S., (2021). Prospectiva de la producción de coco en Yucatán, México. región Y Sociedad, 33, e1467. DOI: 10.22198/rys2021/33/1467

MOPT (1992). Bases Para el Diseño Y Construcción Tapial. Madrid, Spain: Centro de Publicaciones, Secretaría General Técnica, Ministerio de Obras Públicas y Transportes.

Mostafa, M., Uddin, N. (2015). Effect of banana fibers on the compressive and flexural strength of compressed earth blocks. Buildings, 5: 282-296. doi:10.3390/buildings5010282

NORMA E.080 (2017). Diseño y Construcción Con Tierra Reforzada. Ministerio de Vivienda, Construcción y Saneamiento. Anexo-Resolución Ministerial N° 121-2017-Vivienda. Available online: https://procurement-notices.undp.org/view_file.cfm?doc_id=109376 (accessed on 12 December, 2021).

NZS 4298 (1998). Materials and Workmanship for Earth Buildings. [Building Code Compliance Document E2 (AS2)]; Standards New Zealand, 1998, Wellington, New Zealand.

Olacia, E., Pisello, A.L., Chiodo, V., Maisano, S., Frazzica, A., Cabeza, L.F. (2020). Sustainable adobe bricks with seagrass fibres. Mechanical and thermal properties characterization. Construction and building materials, 239, 117699. https://doi.org/10.1016/j.conbuildmat.2019.117669

Ouahabi, M.E., Daoudi, L., Hatert, F., Fagel, N. (2015). Modified mineral phases during clay ceramic firing. Clays and clay minerals, Vol. 63, No. 5, 404–413. https://doi.org/10.1346/CCMN.2015.0630506

Piani, T. L., Weerheijm, J., Peroni, M., Koene, L., Krabbenborg, D., Solomos, G., Sluys, L.J. (2020). Dynamic behaviour of adobe bricks in compression: The role of fibres and water content at various loading rates. Construction and Building Materials 230:

Pradeep, P., Dhas, J.E.R., Suthan R., Vijayarangam, J. (2016). Characterization of palm fibers for reinforcement in polymer matrix. ARPN Journal of Engineering and Applied Sciences. vol. 11, no. 12. ISSN 1819-6608.

Prasad, C. K. S., Nambiar, E. K., Abraham, B.M. (2012). Plastic fibre reinforced soil blocks as a sustainable building material. International Journal of Advancements in Research & Technology, volume 1, Issue 5, ISSN 2278-7763.

Quagliarini, E., Lenci, S. (2010). The influence of natural stabilizers and natural fibers on the mechanical properties of ancient Roman adobe bricks. Journal of Cultural Heritage 11: 309–314.

Riaz, M.H., Khitab, A., Ahmed, S. (2019). Evaluation of sustainable clay bricks incorporating brick kiln dust. Journal of Building Engineering, 24: 100725 https://doi.org/10.1016/j.jobe.2019.02.017

Rakshith, S., Singh. D. N. (2016). Utilization of dredged sediments: contemporary issues. American Society of Civil Engineers. DOI: 10.1061/(ASCE)WW.1943-5460.0000376.

Ramakrishnan, S., Loganayagan, S., Kowshika, G., Ramprakash, C., Aruneshwaran, M. (2021). Adobe blocks reinforced with natural fibres: A review. Mater. Today Proc. 2021, 45, 6493–6499.

Reddy, B. V., Jagadish, K. (2003). Embodied Energy of common and alternative Building materials and Technologies. Energy and Buildings 35, 129-137. DOI: 10.1016/S0378-7788(01)00141-4

Revuelta- Acosta, J.D., Garcia- Diaz, A., Soto- Zarazua, G.M. Rico- Garcia, E. (2010). Adobe as a Sustainable Material: A Thermal Performance. Journal of applied sciences, Vol: 10 (19): 2211-2216. DOI: 10.3923/jas.2010.2211.2216

Sahfi, A.M. (2020). Valorisation des sédiments de dragages dans des bétons autoplaçants : Optimisation de la formulation et étude de la durabilité. PhD thesis, Ecole nationale supérieure Mines-Télécom Lille Douai ; Université de Sherbrooke (Québec, Canada).

Salih, M.M., Osofero, A. I., Imbabi, M. S. (2018). Mechanical properties of fibre-reinforced mud bricks. 2nd Conference of Civil Engineering Sudan, 2018. https://www.researchgate.net/publication/329786369

Salih, M.M., Osofero, A.I., Imbabi, M.S. (2019). Critical review of recent development in fiber reinforced adobe bricks for sustainable construction. Front. Struct. Civ. Eng., 14(4): 839–854 https://doi.org/10.1007/s11709-020-0630-7

Samara, M. (2007). Valorisation des sédiments fluviaux pollués apres inertage dans la brique cuite. PhD thesis. Ecole Centrale de Lille, 2007

Samara, M., Lafhaj, Z., Chapiseau, C. (2009). Valorization of stabilized river sediments in fired clay bricks: Factory scale experiment. Journal of Hazardous Materials 163: 701–710. https://doi.org/10.1016/j.jhazmat.2008.07.153

Saouti, L. (2019). Etudes des propriétés de fibres naturelles mexicaines. Master thesis report, Caen university, France

Sedilab (2015). Beneficial use of dredged sediments in road engineering. Sédimatériaux approach, sedilab, Mines Douai, France

Seifi, S., Sebaibi, N., Levacher, D., Boutouil, M. (2018). Mechanical performance of a dry mortar without cement, based on paper fly ash and blast furnace slag. Journal of Building Engineering, 22: 113-121. DOI: https://doi.org/10.1016/j.jobe.2018.11.004

Sembenelli, P. (1966). Los limites de Atterberg y su significando en la industria ceramica y ládrillera. American society of civil engineers.

Sheehan, C., Harrington, J., Murphy. J.D. (2009). Dredging and dredged material beneficial reuse in Ireland. Terra et Aqua, Number 115.

Simenson, E. W. (2013). Rammed earth: fiber-reinforced, cement-stabilized. Master thesis. B.S., University of Colorado Denver.

Slimanou, H., Eliche-Quesada, D., Kherbache, S., Bouzidi, N., Tahakourt, K. (2020). Harbor dredged sediment as raw material in fired clay brick production: Characterization and properties. Journal of Building Engineering.

Sreekala, M.S., Thomas, S. (2003). Effect of fibre surface modification on water-sorption characteristics of oil palm fibres. Composites Science and Technology 63, 861–869. https://doi.org/10.1016/S0266-3538(02)00270-1

Sutcu, M., (2014). Influence of expanded vermiculite on physical properties and thermal conductivity of clay bricks. Ceramics International 41:2819–2827. https://doi.org/10.1016/j.ceramint.2014.10.102

Taranto, M., Barba, L., Blancas, J., Bloise, A., Cappa, M., Chiaravalloti, F., Crisci, G.M., Cura, M., Angelis, D. D., Luca, R.D., Lezzerini, M., Pecci, A., Miriell, D. (2019). The bricks of Hagia Sophia (Istanbul, Turkey): a new hypothesis to explain their compositional difference. Journal of Cultural Heritage, 38, 136–146. https://doi.org/10.1016/j.culher.2019.02.009

Tsega, E., Mosisa, A., Fufa, F. (2017). Effects of firing time and temperature on physical properties of fired clay bricks. American Journal of Civil Engineering, 5(1): 21-26. doi: 10.11648/j.ajce.20170501.14.

UN habitat (2009). Interlocking stabilized soil blocks, appropriate earth technologies in Uganda. United nations human settlement programs.

UNICEM (2021). L'industrie française des granulats en 2019. https://www.unicem.fr/wp-content/uploads/2021/12/unpg-chiffres-2019-web.pdf.

Ukwatta, A., Mohajerani, A. (2017). Effect of organic content in biosolids on the properties of fired-clay bricks Incorporated with biosolids. American Society of Civil Engineers. DOI: 10.1061/ (ASCE) MT.1943-5533.0001865.

SDC, Swiss Agency for Development and Cooperation (2008). Vertical shaft brick kiln project clean building technologies for Nepal. Green bricks making manual.

Winkler, H.G.F., (1954). Bedeutung der Korngrössenverteilung und des Mineral-bestandes von Tonen fürdie Herstellung grobkeramischer erzeugnisse. Ber. DKG, v. 31, p. 337-343.

Xu, Y., Yan, C., Xu, B., Ruan, X., Wei. Z. (2014). The use of urban river sediments as a primary raw material in the production of highly insulating brick. Ceramics International 40, 8833–8840. https://doi.org/10.1016/j.ceramint.2014.01.105

Yousif, I.M. (2007). Straw stabilized local clay bricks. Journal of Pure and Applied Science, Vol. 19, No.2.

Zhao, P., Zhang, X., Qin, L., Zhang, Y., Zhou, L., (2019). Conservation of disappearing traditional manufacturing process for Chinese grey brick: Field survey and laboratory study. Construction and Building Materials, vol. 212, pp. 531–540, Jul. 2019.

Chapter 2. Characteristics of Usumacinta River sediments

For sustainable and ecological recovery of dredged sediments, investigation of their physico-chemical, mineralogical, hydrological and environmental characteristics is essential to select the potential recovery application. In this chapter, characteristics of Usumacinta River sediments were examined for their reuse in building materials such as fired bricks and earth bricks and agronomy. Presence of contaminants in Usumacinta River sediments was observed as it is essential for prospective recycling of sediments in any application. In case of fired and earth bricks, Usumacinta River sediments granulometry, chemical composition, consistency limits, organic matter and carbonate content were investigated to observe the sediment's suitability for fired and earth bricks. Usumacinta River sediments agronomic characteristics were also determined for their reuse in agronomy. These characteristics include sodium absorption ratio (SAR), electrical conductivity (EC), organic matter, nutrients and minerals.

2.1. Origin of sediments

Sediments were dredged from the banks of the Usumacinta River in the Tabasco state of Mexico. Sediments were dredged from Tenosique (T) and Jonuta (J) towns. Sediment's dredging region can be seen in the map of the Gulf of Mexico in Figure 2.1. According to the geologic time scale of sediment deposition, Tenosique sediments are Oligocene-Miocene while the sediments at Jonuta are clastic-sediment.

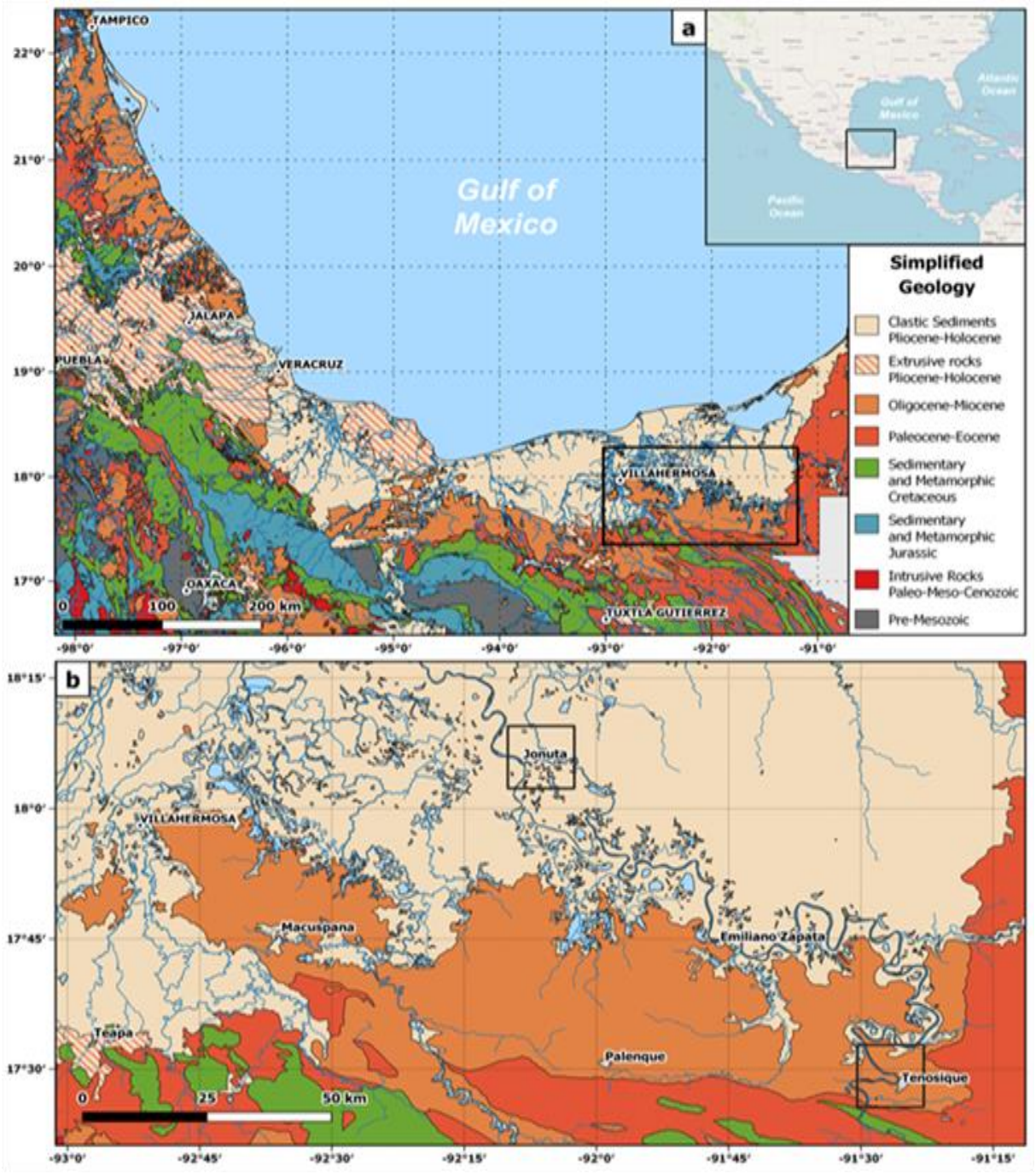

Figure 2. 1. Map of Gulf of Mexico

From Figure 2.2, the different sampling locations near Jonuta and Tenosique towns can be seen.

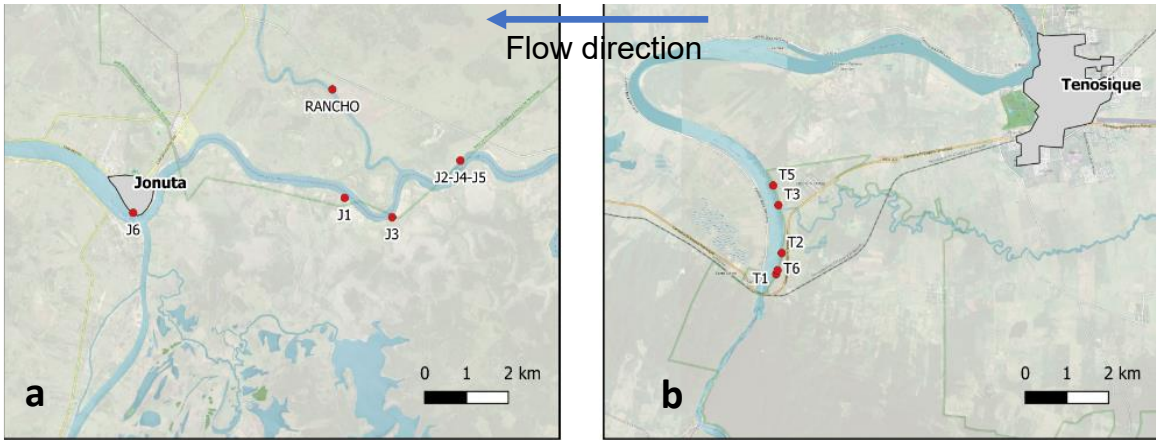

Figure 2. 2. Sampling sites in Jonuta (a) and Tenosique (b)

Dredged sediments were transported to France in hermetic and sealed barrels to preserve the sampling conditions. The samples were referenced according to their sampling sites and represented by the letters T and J respectively. The sediments in M2C laboratory (Caen) are labeled as T1, T2, T5, T6, J3 and J4 where T and J stand for Tenosique and Jonuta sites while the numerical digit shows the site number. The sediment barrels transported to M2C lab are shown in Figure 2.3.

Figure 2. 3. Sediments barrels in M2C lab.

2.2. Characterization methodology

Physico-chemical, mineralogical, environmental and hydromechanical characteristics of Usumacinta River sediments were investigated through laboratory tests to observe the suitability of these sediments in different applications such as fired bricks, earth bricks and agronomy. Sediments are divided into coarse (≥ 2mm) and fine (≤ 2mm) particles and the size of particles recommended for each test varies. Sediments were dried and subjected to crushing, grinding and sieving to meet the specific requirements of each test.

2.2.1 Physico-chemical parameters

Physical and chemical characteristics of sediments have a huge influence on the characteristics of bricks and the quality of bricks. These characteristics include initial water content, solid particle density, grain size distribution, Atterberg limits, methylene blue value, organic matter and carbonate content. Investigation of physico-chemical characteristics of Usumacinta River sediments was done for their reuse in manufacturing bricks at laboratory scale experiments.

(a) Initial water content (Wi)

Usumacinta River sediments were transported in hermetic and sealed barrels which keeps the sediments moisture content similar to the dredging conditions. Higher moisture content of sediments is one of the biggest hurdles for their valorization in different applications. Dewatering of sediments can be done with sun drying or oven drying. In this study, Usumacinta River sediments were dried in the oven at 60 °C for two days to determine their initial water content and use for different tests.

(b) Solid particle density (ρ_s)

Solid particle density of Usumacinta River sediments was measured with a water and helium pycnometer. Density test was repeated three times to get an average value. For density with helium pycnometer, model AccuPyc 1330 Pycnometer from Micromeritics was used. In case of water pycnometer density is calculated from the following formula:

$$\rho_s = \frac{m_1 * \rho_w}{m_0 - m_3} \quad (2.1)$$

m_0 is the mass of fluid in g, m_1 is the mass of sediments in g, and m_2 is the sum of mass fluid and mass of sediments while $m_3 = m_2 - m_1$.

(c) Grain size distribution

Particle size of sediments was found with laser granulometry, and sediments were classified according to French standards (AFNOR NF X31-107, 2003). Laser granulometry test is performed on sediments which are passed through a sieve of size 2 mm. The laser is diffracted at different angles after interaction with sediments. With the help of the diffraction angle, size of particles is determined. Beckman Coulter LS 13320 model was used for grain size analysis of Usumacinta River sediments. Test was repeated twice to get an average value. The setup of the laser granulometry apparatus is shown in Figure 2.4.

Figure 2. 4. Laser granulometry setup in M2C lab

Different coefficients are used to describe the grading, uniformity and nature of sediments. Some of these coefficients are uniformity coefficient, grading coefficient and sorting coefficient etc. Grading coefficient is calculated by the formula given with equation 2.2.

$$C_C = \frac{(d_{30})^2}{d_{10} * d_{60}} \tag{2.2}$$

where d_{60} = diameter corresponding to 60% passing sediments, d_{10} = diameter corresponding to 10% passing sediments and d_{30} = diameter corresponding to 30% passing sediments.

Uniformity coefficient describes the uniformity of sediment particles. it is calculated with the following formula:

$$C_U = \frac{d_{60}}{d_{10}} \tag{2.3}$$

Sorting coefficient is calculated with the following formula:

$$S_0 = \sqrt{\frac{d_{75}}{d_{25}}} \tag{2.4}$$

where d_{75} = diameter corresponding to 75% passing sediments, d_{25} = diameter corresponding to 10% passing sediments

(d) Argilosity parameters

(d1) Atterberg limits

Consistency limits of sediments were determined through liquidity and plasticity measurements according to French standards (AFNOR NF EN ISO 17892-12, 2018). Liquidity limit of Tenosique and Jonuta sediments was found with Casagrande and fall cone test. In Casagrande test, sediments were dried, crushed and passed through a 400 µm sieve (AFNOR NF P 94-051, 1993).

Casagrande test was performed 4 times on each sediments sample. Flow curve is obtained by plotting a semi-logarithm graph between the number of blows on X-axis and water content on the Y-axis. The value of water content at 25 numbers of blows gives the liquidity limit of sediments. Casagrande apparatus is shown in Figure 2.5.

Figure 2. 5. Casagrande apparatus for liquidity test

In fall cone test the homogenous mixture of sediment particles having a diameter less than 400μm is subjected to the falling cone. Graph between the water content and penetration depth gives liquidity limit of sediments at 17mm depth according to French standard (AFNOR NF EN ISO 17892-12, 2018).

Plasticity limit of Usumacinta River sediments was measured by making a cylindrical roll of 3 mm diameter and 10cm length. The water content at which cracks start to appear in the sediments roll gives the value of plasticity of the sediments.

Figure 2. 6. Sediment mixture and rolls to observe plasticity limit

Plasticity index of soil is calculated with the difference between liquidity limit and plasticity limit. It is calculated with following equation:

$$PI = LL - PL \tag{2.5}$$

where LL is the liquidity limit and PL is the plasticity limit of sediments.

Based on plasticity index of Usumacinta River sediments, activity of clay was calculated with following formula.

$$\text{Activity of clay (A)} = \frac{PI}{C_2} \quad (2.6)$$

where C_2 is the percentage of fine particles below 2 mm.

(d2) Methylene blue value (MBV)

Methylene blue value of sediments was found to observe the presence of clay in sediments according to the standard (AFNOR NF P 94-068,1998). A homogenous mixture of Jonuta and Tenosique sediments having grain size below 2mm was prepared and the solution of methylene blue was poured into the sediment mixture. The value of methylene blue was observed when the test results were positive.

MBV value is calculated with the following formula:

$$MBV = \frac{n^*}{M} \quad (2.7)$$

n*= Methylene blue solution in ml added to the sediment solution.

M= mass of sediment in g added to prepare the solution of sediment and water.

The setup to perform the methylene blue test is shown in Figure 2.7.

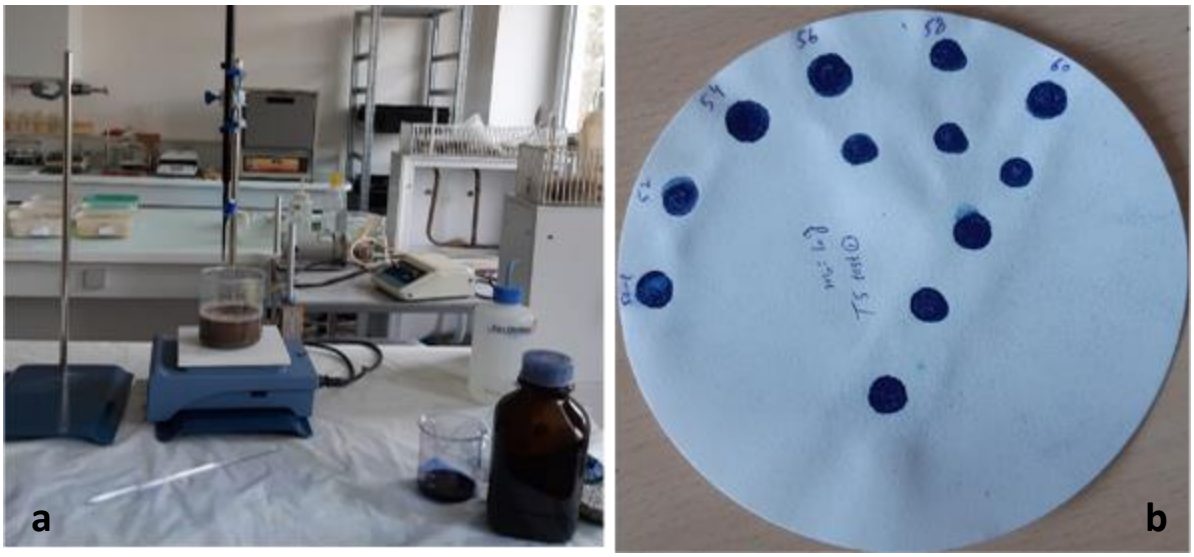

Figure 2. 7. Methylene blue test apparatus (a) and filter paper to observe positive test (b)

Sediment categories on the base of MBV value can be derived from the technical guide GTR (Guide technique, 2000). Figure 2.8 is used to classify the sediment on the base of their MBV value.

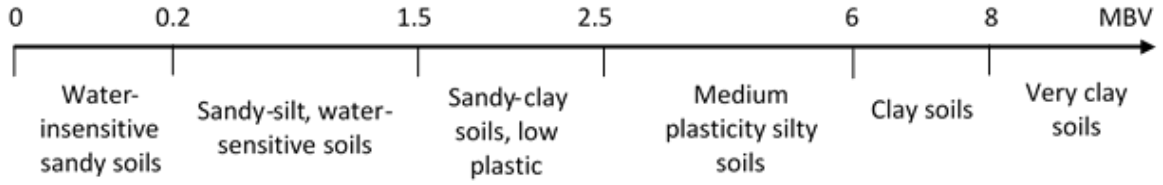

Figure 2. 8. Sediment categories as function of MBV value (GTR, 2000).

Based on MBV values of Usumacinta River sediments, activity of clay was found with French standard (AFNOR XP P94-011, 1999) by using following equation.

$$A_{CB} = \frac{MBV}{C_2} \quad (2.8)$$

where C_2 is the percentage of fine particles of size below 2 µm.

(e) Organic and carbonate content

(e1) Organic matter (OM)

Organic matter in sediments is due to the decomposition of plants and animals. Organic matter in Usumacinta River sediments was calculated by burning the sediments at 550 ^{0}C (AFNOR XP P 94-047, 2007). At this temperature, organic matter is combusted and its percentage is deduced from the following formula:

$$\text{Organic matter (\%)} = \frac{M_1 - M_2}{M_1 - M_0} * 100 \quad (2.9)$$

with M_0 = mass of empty crucible and M_1 = mass of crucible and sediments before calcination.

M_2= mass of crucible and sediments after calcination.

(e2) Carbonate content ($CaCO_3$)

Carbonates are generally accumulated by sedimentation in the marine atmosphere and erosion of lime. Carbonate content of sediments was found with Bernard calcimeter method (AFNOR NF ISO 10694, 1995) which is a precise method to find the carbonate content of sediments (Tiessen et al, 1983). The Bernard calcimeter apparatus is shown in Figure 2.9.

Figure 2. 9. Bernard calcimeter set up in M2C lab

The concentration of $CaCO_3$ is observed by mixing the sediment with HCl. The chemical reaction of $CaCO_3$ with hydrochloric acid (HCl) is as follows.

$$CaCO_3 + HCl \rightarrow CaCl_2 + CO_2 + H_2O \quad (2.10)$$

The chemical reaction between calcium carbonate and HCL produces CO_2 which is emitted in the form of bubbles. Percentage of $CaCO_3$ is determined by the discharged volume of CO_2.

$$\text{Percentage of } CaCO_3 = V * \frac{k}{m} \quad (2.11)$$

V is the volume of gas released in ml, and m is the mass of sediments. k is calculated from equation 3.

$$k = \frac{(0.154 * P)}{273 + t} \quad (2.12)$$

where P is atmospheric pressure in mm Hg and t is the temperature in ^{0}C.

2.2.2 Environmental characterization

(a) pH value of sediments

Seepage of industrial waste containing heavy metals and other impurities changes the pH of river sediments. The acidic and alkaline nature of sediments is observed with pH value. pH value of Usumacinta River sediments was determined with pH meter according to French standard (AFNOR NF ISO 10390, 2005) and with pH paper. pH meter in M2C lab is shown in Figure 2.10 (a). In pH paper test, pH paper was dipped into the sediment's solution. With the color of the pH paper, pH values of different sediment samples are deduced. pH paper test is shown in Figure 2.10 (b).

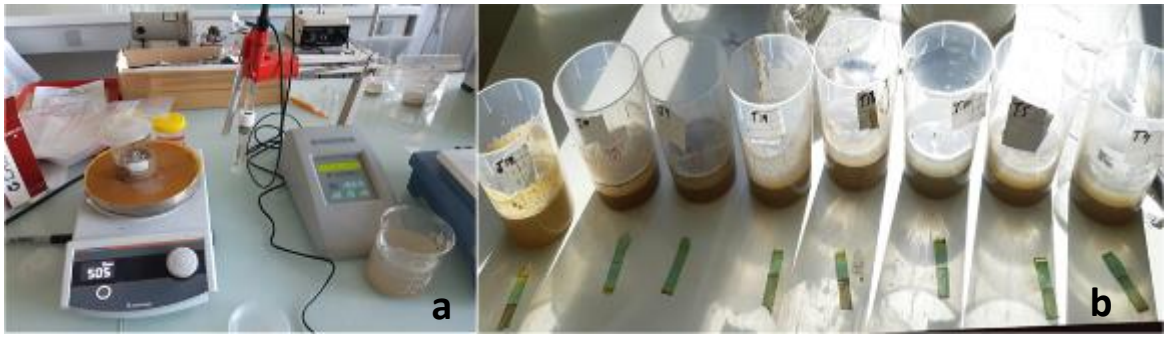

Figure 2. 10. pH measurement by pH meter (a) and pH paper (b)

(b) Heavy metals and chemical analysis

Heavy metals are found in river sediments due to human industrial activities. Heavy metals in Usumacinta River sediments were observed with x-ray diffraction (XRD) and scanning electron microscopy (SEM).

Chemical analysis of Usumacinta River sediments was also conducted to evaluate the composition of sediments *i.e.* major chemical elements, heavy metals, organic matter,

carbonates, oxides, pH measurement and other pollutants if necessary. Organic (PCBs, PAHs, TBT, dioxins) and inorganic (As, Pb, Cu, Zn, Cr etc.) pollutants in sediments were observed according to French standards (AFNOR NF EN ISO 11885, 2016). These pollutants come from industrial effluents, hydrocarbons and agricultural waste from fertilizers and pesticides. Polycyclic Aromatic Hydrocarbons (PAHs) and Polychlorinated Biphenyl (PCBs) pollutants were found with gas chromatography by using the French standard (AFNOR XP X33-012, 2000).

(c) Cation exchange capacity (CEC)

CEC is an important property of sediments which indicates the cation retaining capacity of soil. CEC value indicates the presence of minerals in sediments such as kaolinite, illite and montmorillonite. Following formula is used to calculate CEC value with methylene blue value of sediments (Abayazeed and El-Hinnawi, 2011).

$$CEC = (100/D) * C * NMB \quad (2.13)$$

where NMB is the normality of blue methylene blue solution equal to A/319.9 knowing that A is the mass of dry methylene blue which is dissolved in 1 liter of water = 10 g and 319.9 is the molecular mass of methylene blue.

C is the weight of methylene blue solution added to endpoint and D is the weight of dry sediments sample.

2.2.3 Hydromechanical characteristics

Hydromechanical characteristics of sediments suitable for bricks are optimum moisture content and shear strength.

(a) Compaction test (Optimum moisture content)

Optimum water content (W_{opt}) and maximum dry density of sediments were determined with Proctor miniature test (ASTM D689- 12e2, 2007). Soil was compacted in two layers by falling mass with 42 strokes in each layer. The falling mass removes the air inside the voids and increases the density of the soil. Mini Proctor apparatus is shown in Figure 2.11.

Figure 2. 11. Proctor miniature test apparatus

Soil compaction changes with variation in the water content of sediments. Optimum compaction is achieved at maximum dry density and the water content at maximum density corresponds to the optimum water content of the soil. Optimum water content is deduced from Proctor curve. Following formula is used to find the dry density of sediments.

$$\rho_d = \frac{M/V}{1+W} \tag{2.14}$$

where ρ_d stands for a dry density of soil, M is the total mass, V is volume and w is the water content of soil.

(b) Shear strength of sediments

Direct shear test is used to find the shear strength of cohesive and non-cohesive soils. Metallic shear box of 6 cm diameter was used to find the shear strength of Usumacinta River sediments with direct shear test. Direct shear strength test apparatus used is shown in the following Figure 2.12.

Figure 2. 12. Direct shear test apparatus

Sediments specimens were prepared by adding optimum water content (w_{opt}) obtained from Proctor test. Sediments samples were compacted with optimum proctor energy. Shear stress of soil sample is calculated with the following formula:

$$\tau = \frac{F}{A} \tag{2.15}$$

where F is shear force and A is the area of the ring. Area of ring used is 0.0028 m^2. No correction of area during the shearing was considered for the stress calculations. Normal stress was calculated by the following formula:

$$\sigma = \frac{F_n}{A} \tag{2.16}$$

where F is the normal force perpendicular to the shearing plane.

Shear strength of soil depends on cohesion and friction angle of soil. Mohr-Coulomb relationship between normal stress and shear stress is prescribed in equation 2.17.

$$\tau = c + \sigma \tan \varphi \tag{2.17}$$

where c is the cohesion of soil, expressed in kPa and φ, the internal friction angle in degrees.

2.2.4 Mineralogy and microstructure

(a) Mineralogy of sediments

Mineralogical analysis of sediments was done to investigate the presence of minerals in sediments such as quartz, kaolinite, muscovite, illite and montmorillonite. Mineralogical analysis of Usumacinta River sediments was done with x-ray diffraction (XRD) and scanning electron microscopy (SEM).

(b) Microstructural analysis

Microstructural analysis of sediments includes specific surface area and pore size distribution. Specific surface area (SSA) of sediment is the ratio of the surface area of sediment solid particles and corresponding mass. Its unit is m^2/kg. SSA was determined with MBV values and by BET method.

Specific surface area of sediments with MBV value is calculated equation 2.18 (Abayazeed, and El-Hinnawi, 2011).

$$\text{SSA } (m^2/g) = \frac{\text{mass of MBV added}}{319.9} * \text{Avogadro number} * A_{mb} * \left(\frac{1}{A}\right) \tag{2.18}$$

In this equation value of Avogadro number is $6.02*10^{23}$/mol. A_{mb} is the area covered by one methylene blue molecule and its value is $130*10^{-20}$ mol. A is the mass of dry methylene blue dissolved in one liter of water = 10 g.

(c) Thermogravimetric analysis of Usumacinta River sediments

Thermogravimetric analysis was performed to observe the mass loss of sediments by burning them at a temperature range from 0 °C to 800 °C. Evaporation of moisture content and decomposition of organic matter occurs at different temperatures. Sediment samples in the ATG apparatus are shown in Figure 2.13.

Figure 2. 13. Sediments samples for ATG analysis

2.3. Results and discussion

2.3.1 Physico chemical characteristics of Usumacinta River sediments

(a) Initial water content

Usumacinta River sediments were collected near the riverbanks and were settled in barrels for six months. Most of the sediments in barrels have water content between 20% to 30% which is water content between their liquidity and plasticity limits. Initial water content of Usumacinta River sediments was found by oven drying of sediments and the results are shown in Table 2.1.

Table 2. 1. Initial water content of Usumacinta River sediments

Sediments	**T1**	**T2**	**T5**	**T6**	**J3**	**J4**
Wi (%)	38.82	25.72	29.57	30.08	11.34	21.82

Water content in Usumacinta sediments ranges from 21% to 38% and it is highest in T1 sediments and lowest in J3 sediments. Initial water content of sediments is not very high. In some cases, initial water content of dredged sediments might go up to 300% (Sahfi, 2020). Dehydration of sediments is necessary to use them in any application. As Usumacinta River sediments initial water content is low, natural dehydration can be good choice.

(b) Dry density of Usumacinta River sediments

Particle density of Usumacinta River sediments was determined with water and helium pycnometer. The results are summarized in Table 2.2.

Table 2. 2. Solid particles density of Usumacinta River sediments

Sediments	*ρsed-water* (g/cm^3)	*ρsed-helium* (g/cm^3)
T1	2.42	2.7
T2	2.5	2.71
T5	2.6	2.61
T6	2.52	2.67
J3	2.41	2.66
J4	2.33	2.53

Density is lowest for J4 sediments which have higher clay content while for T2 sediments density is highest and these sediments have higher sand content. Except J4 sediments, density of remaining sediments is within the range of 2.61 to 2.71 which is density range of soft clays. Solid particles density values are more precise with helium pycnometer as in case of water pycnometer, it is difficult to remove air bubbles and impurities at the top of the water surface which influences the density of sediments.

(c) Grain size analysis of Usumacinta River sediments

Grain size of Usumacinta River sediments was found with laser granulometry. Median diameter (d_{50}) of Usumacinta River sediments is shown in Table 2.3. Median diameter of T5 and J4 sediments is very low.

Table 2. 3. Typical grain size diameters

Sediments	**T1**	**T2**	**T5**	**T6**	**J3**	**J4**
d_{50} (µm)	53.28	87.33	24.57	53.66	52.62	14.12

The grading coefficient (C_c), uniformity coefficient (C_u) and sorting coefficient (S_0) of Usumacinta River sediments were calculated with equations 16,17 and 18. Results are presented in Table 2.4.

Table 2. 4. Granulometry coefficients

Sediments	**C_u**	**C_c**	**S_0**	**Sediment type**
T1	23.91	1.87	2.84	Well graded
T2	19.07	1.07	3.22	Well graded
T5	30.58	0.62	4.57	Poorly graded
T6	21.66	1.58	2.8	Well graded
J3	18.49	2	8.39	Well graded
J4	17.15	0.8	3.48	Poorly graded

Usumacinta sediments have extended granulometry. C_c value is ranged between 1 and 3 for most of the sediments which shows that sediments are well graded. C_c value is below 1 for T5 and J4 sediments which means they are poorly graded according to unified soil classification system (Casagrande, 1948). The clay content of T5 and J4 sediments is high which affects the grading of sediments.

Sand, silt and clay content were determined with laser granulometry with French standard (AFNOR NF X31-107, 2003). Clay, silt and sand content of sediments was determined after Table 2.5.

Table 2. 5. Granulometric classification according to AFNOR NF X31-107 (2003).

Classification	**Clay**	**Fine silt**	**Coarse silt**	**Fine sand**	**Coarse sand**	**Gravel**
Particle size	< 2μm	2μm-20μm	20μm – 50μm	50μm– 200μm	200μm -2mm	>2mm

The percentage of silt, sand and clay in Usumacinta River sediments is shown in Table 2.6.

Table 2. 6. Percentage of clay, silt and sand in Usumacinta River sediments

Sediments	**Clay (%)**	**Silt (%)**	**Sand (%)**
T1	6.90	40.20	52.90
T2	3.57	31.08	65.35
T5	8.75	45.90	45.00
T6	6.09	40.70	53.20
J3	4.66	36.30	59.00
J4	13.40	62.50	24.10

Grading curves for Tenosique and Jonuta sediments are shown in Figure 2.14.

Clay content of sediments ranges from 3.5% to 13.4%. T2 sediments have higher sand content. Plasticity in sediments is mainly induced with clay. However higher clay content leads to shrinkage in bricks and developments of cracks (Koroneos and Dompros, 2007). On other hand it is difficult to mould sandy sediments. Therefore, specific quantity of sand and clay is necessary to make fired and crude bricks (AFNOR XP P13-901).

Tenosique and Jonuta sediments have similar grading curves. T1, T2, T6 and J3 have uniform and well-graded curves while T5 and J4 curves are poorly graded. Grading curves of J4 and T2 sediments are away from other curves due to higher fine and coarse particles respectively.

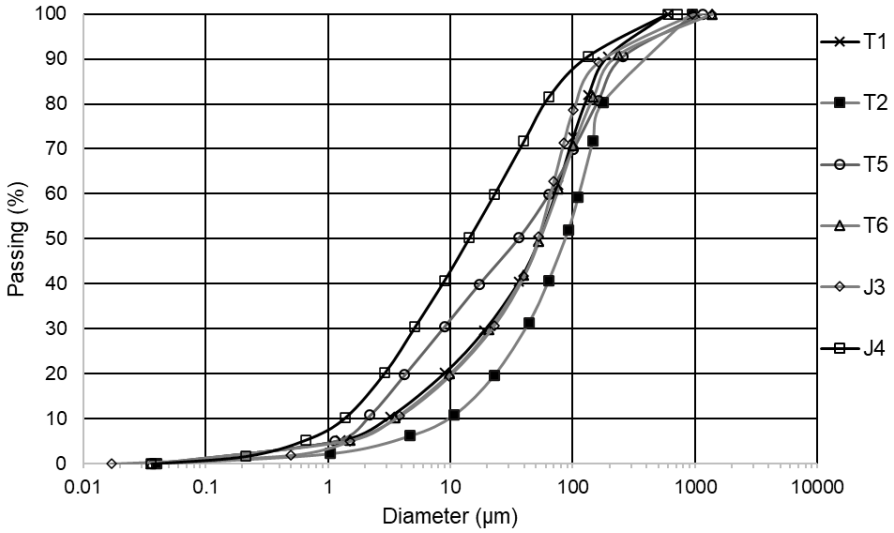

Figure 2. 14. Grading curves of Usumacinta River sediments

Sediment texture ternary diagram describes the type of sediment based on its grain size. (USDA, 1951). Sediment texture consists of the size and shape of sediments. Soil texture ternary diagram of Usumacinta River sediments based on clay, silt and sand content in Table 2.6 is shown in Figure 2.15.

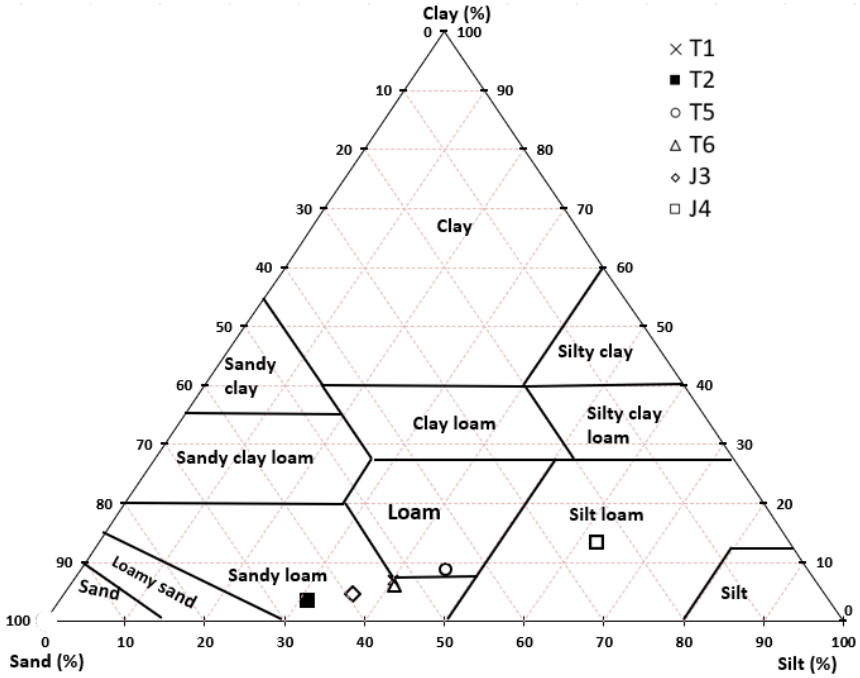

Figure 2. 15. Soil texture ternary diagram

Sediment texture based on Figure 2.15 is described in Table 2.7. We can observe from Table 2.7 that T2 and J4 sediments are silt loam. T5 is loam and the rest of the sediments are sandy loam.

Table 2. 7. Percentage of clay, silt and sand

Sediments	T1	T2	T5	T6	J3	J4
USDA texture	Sandy loam	Sandy loam	Loam	Sandy loam	Sandy loam	Silt loam

For sediments reuse in agronomy mostly loam soils are ideal (USDA NRCS 1999). Granulometry of soil can also be correlated with porosity and permeability. Ternary diagram in Figure 2.16 shows Usumacinta sediment's correlation with permeability and porosity. The different zones such as WS, MWS and PS stand for well sorted, moderately well sorted and poorly sorted respectively. Porosity is high in the top WS section, low in the middle zones (PS and MWS) and moderate-high in the bottom zones (WS, MWS and WS). Permeability is very low in top WS zone, low in the middle zones (PS and MWS) and moderate-high in the bottom MWS zone. In the bottom WS zone permeability is high and moderate in bottom WS zone. (McManus, J. 1998).

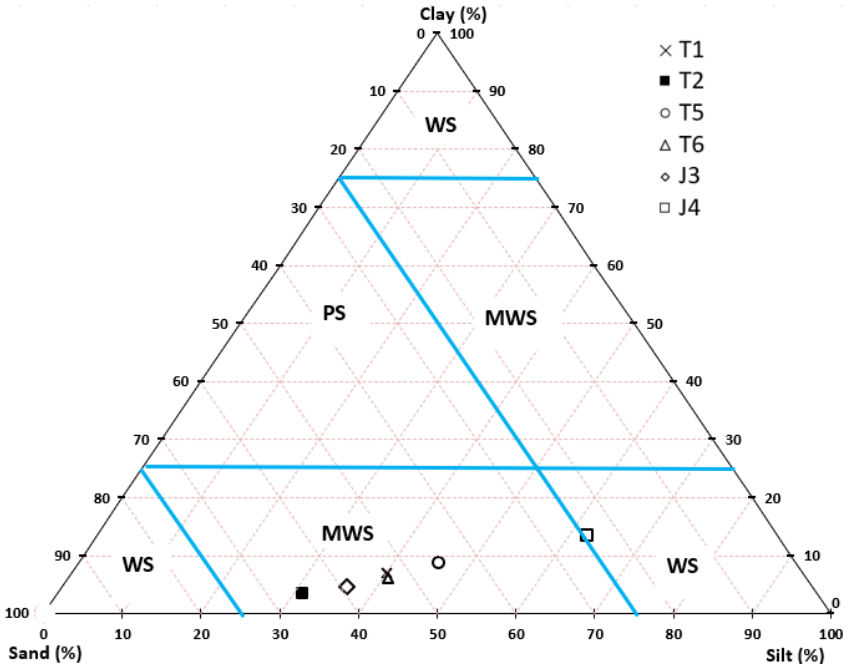

Note: WS = well-sorted, MWS = moderately well sorted, PS = poorly sorted

Figure 2. 16. Permeability variation with granulometry

It can be observed in Figure 2.16 that J4 sediments are in the zone of moderate permeability. These sediments have higher clay content compared to other Usumacinta River sediments. The remaining Usumacinta River sediments are in the zone of moderately high permeability. Permeability of soil is important for sediments reuse in agronomy as in low permeability soils, provision of water, air and nutrients is disrupted.

(d) Argilosity parameters of Usumacinta River sediments

d1. Atterberg limits of Usumacinta River sediments

Liquidity limit of sediments was determined with Casagrande and fall cone test. Liquidity limits by Casagrande and fall cone test are shown in Table 2.8.

Table 2. 8. Liquidity limits by Casagrande and fall cone test

Sediments	$LL_{Casagrande}$ (%)	$LL_{Fall\ cone}$ (%)
T1	35.04	35.13
T2	25.20	30.88
T5	38.73	36.56
T6	28.10	29.88
J3	34.86	34.67
J4	53.97	51.15

Liquidity limits of Usumacinta River sediments range from 25.20% to 53.97%. Liquidity limit of sandy sediments (T2) is lowest and for clayey sediments (J4) its value is maximum. Liquidity limits of sediments are very important for moulding of sediments in fired and crude bricks. It is difficult to mould sandy sediments. While the sediments with very high liquidity limits are also unsuitable for bricks. Clay workability chart is used to see the sediments suitability for fired bricks (Fonseca et al., 2015). Sediments suitability for earth bricks is also found with Atterberg limits (AFNOR XP P13-901, 200).

Comparison of liquidity limits obtained by Casagrande and fall cone test reveals that the liquidity limit values obtained by the fall cone test are slightly higher. Figure 2.17 and 2.18 shows the histograms of liquidity limits with standard deviation in error bars.

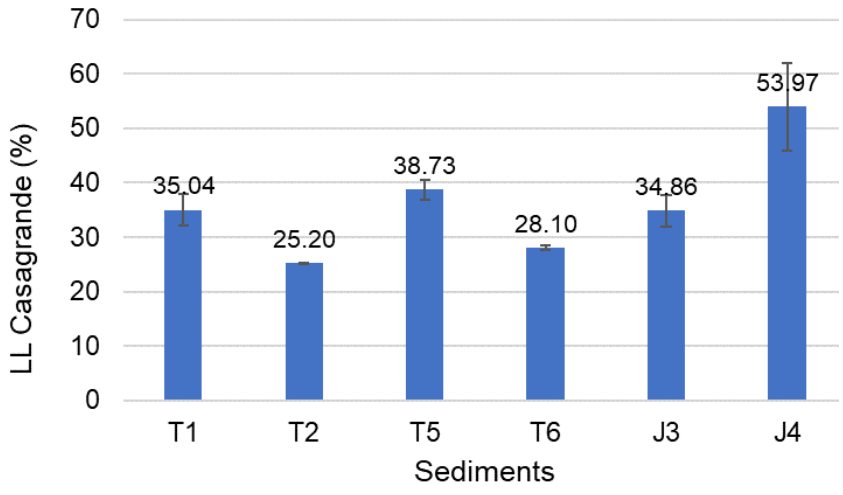

Figure 2. 17. Liquidity limits of Usumacinta River sediments with Casagrande method

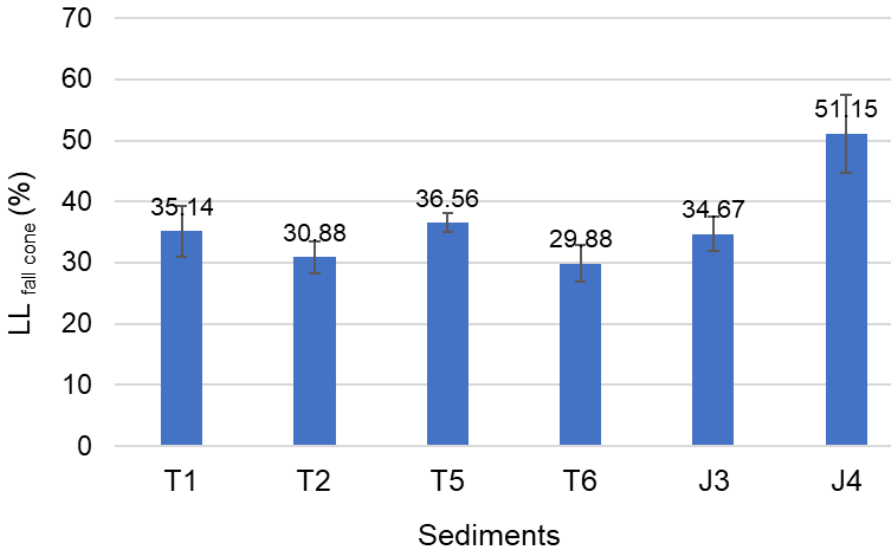

Figure 2. 18. Liquidity limits of Usumacinta River sediments with fall cone method

The graph in Figure 2.19 is plotted between the liquidity limit with Casagrande method and liquidity limit with fall cone method.

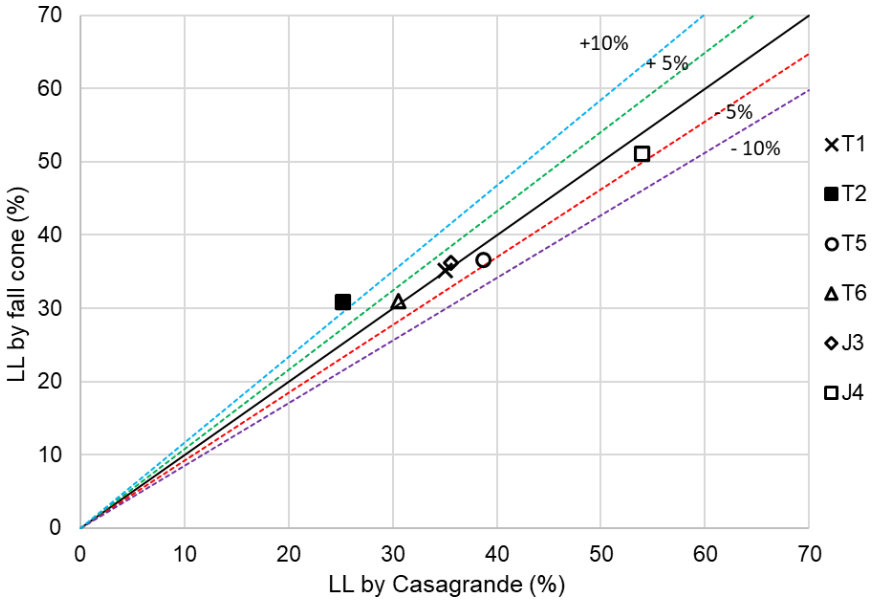

Figure 2. 19. LL by fall cone vs LL by Casagrande method

Most of the liquidity limit values lie on bisector lines which shows that values from both Casagrande test and fall cone test are similar. The remaining sediments are within 5% deviation from bisector line. However, T2 sediments have higher liquidity limits with fall cone test. These sediments have higher sand content and it is difficult to find their liquidity and plasticity limits precisely.

GTR (2000) soil classification classifies the soils on the base plasticity index into soils shown in Table 2.9.

Table 2. 9. Soil classification on the base of plasticity index

Plasticity index (%)	Sediments nature
PI ≤12	Less plastic silts, low plastic fine sand
12<PI≤25	Fine clayey sands, low plasticity
25<PI≤40	Clays, clayey marls, very plastic
P I>40	Clays, clayey marls, very plastic

Plasticity of clay particles is usually high while in sandy sediments plasticity is very low.

Average liquidity and plasticity results of Usumacinta River sediments are summarized in Table 2.10. Plasticity index values for Usumacinta River sediments are also given in Table 2.10.

Table 2. 10. Atterberg limits calculation

Sediments	T1	T2	T5	T6	J3	J4
LL	35.50	28.04	37.65	28.98	34.76	52.55
PL (%)	18.61	14.56	17.84	16.58	19.34	27.73
PI (%)	16.92	12.92	19.81	14.21	16.57	24.82

It can be observed that J4 sediments have higher liquidity and plasticity limits while T2 sediments have low plasticity. Based on GTR soil classification, Usumacinta River sediments have low plasticity. Plasticity index of soils used for fired bricks ranges from 10% to 35% and plasticity limits of soil ranges from 15% to 35% (Fonseca et al., 2015). Most of the Usumacinta River sediments are within this range.

Graph between plasticity index and liquidity limit helps to determine the nature of sediments. The A-line at the slope of 0.73 separates the silts and clays. The clay and silt are further classified into high plasticity, medium plasticity and low plasticity clays and silts on the base of liquidity limit. From the graph in Figure 2.20, plotted between average liquidity limit and plasticity index, we can observe that J4 is high plasticity clay. T2 and T6 are low plasticity clays, while the rest of the samples are medium plasticity clays.

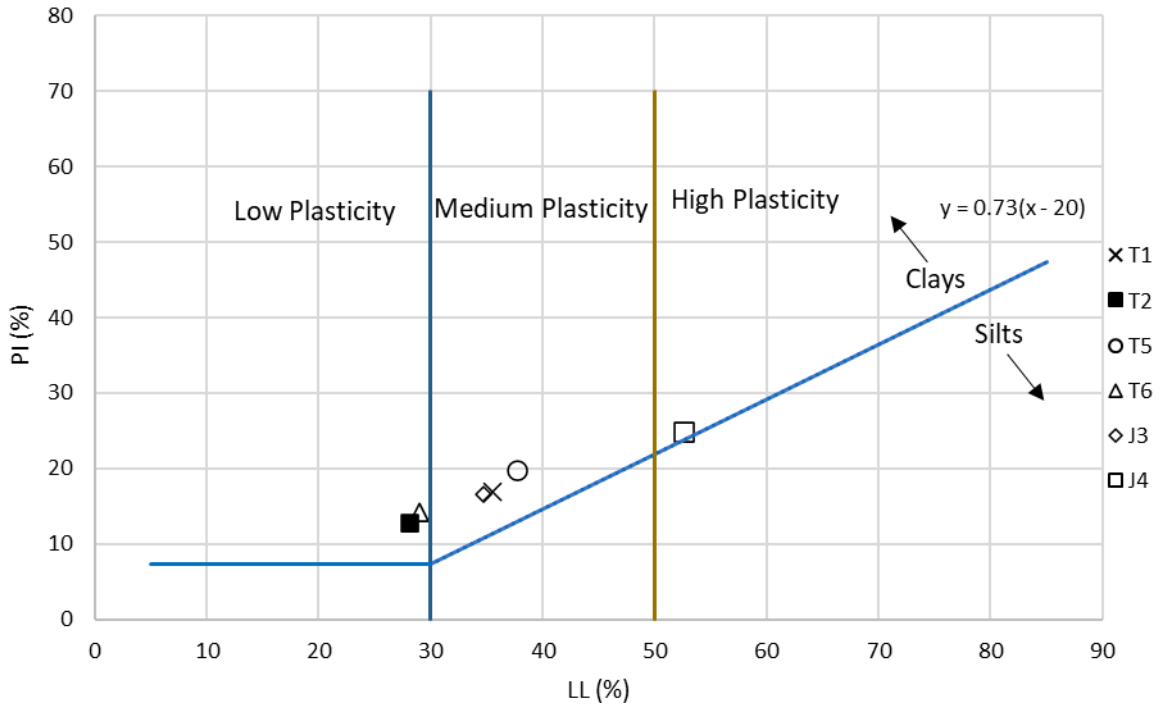

Figure 2. 20. Plasticity chart of Usumacinta River sediments

d2. Methylene blue value (MBV) of Usumacinta River sediments

Methylene blue values (MBV) of Usumacinta River sediments were determined with Methylene blue test. Methylene blue values (MBV), Activity of clay (A_{CB}) and Specific surface area (SSA) of Usumacinta River sediments are presented in Table 2.11.

Table 2. 11. Methylene blue values of Usumacinta River sediments

Soil type	**MBV** (g/ 100 g)	**SSA_{MBV}** (m^2/g)	**A_{CB}**	**Sediment category**
T1	2.53	18.6	0.37	Silt, average plasticity
T2	2.00	14.7	0.22	Sandy clay, less plastic
T5	5.90	43.3	0.67	Silt, average plasticity
T6	2.86	14.2	0.45	Silt, average plasticity
J3	2.73	20.1	0.52	Silt, average plasticity
J4	8.00	58.7	0.60	Very clayey sediment

MBV values increases with increasing percentage of fine particles. It can be observed from Table 2.11 that J4 and T5 sediments have highest MBV values. This is because these sediments have a higher percentage of fine particles. Higher clay content exhibit higher activity which leads to swelling of composite materials. Therefore, very high quantity of clay is undesirable (Türköz and Tosun, 2011). T5 sediments have low plasticity while the remaining sediments have average plasticity.

Specific surface area was also found with MBV values. From Table 2.11, it can be observed that J4 and T5 sediments have the highest specific area. This is common for clayey soils as SSA

area of fine particles is more than the coarse particles. The specific surface area of T2 sediments is low.

French standards classify soil on the base of the activity of clay as shown in Table 2.12.

Table 2. 12. Soil classification based on the activity of clay

Clay activity of clay fraction	Activity
$0 < A_{CB} < 3$	Inactive
$3 < A_{CB} < 5$	Low active
$5 < A_{CB} < 13$	Medium active
$13 < A_{CB} < 18$	Active
$18 < A_{CB}$	Very active

Activity of clay based from MBV is below 3 for Usumacinta River sediemnts and they can be classified as inactive sediments.

(e) Organic matter and carbonate contents of Usumacinta River sediments

e1. Organic matter (OM)

Organic matter of sediments was found by burning sediments at 550 °C. Table 2.13 shows the organic matter of the Usumacinta River sediments.

Table 2. 13. Percentage of organic matter in sediments

Sediments	T1	T2	T5	T6	J3	J4
OM (%)	3.77	3.50	3.46	4.90	4.48	5.72

Note: OM = organic matter

Table 2.13 shows that Usumacinta River sediments have low organic matter and it ranges from 3.5 to 5%. Table 2.14 defines the sediment's nature with the presence of organic matter in sediments (AFNOR XP P 94-011, 1999).

Table 2. 14. Sediments nature on the base of organic matter

Organic matter (%)	Classification
OM (%) ≤ 3	inorganic
3 < OM (%) ≤ 10	Low organic
10 < OM (%) ≤ 30	Medium organic
OM (%) < 30	Very organic

Note: OM = organic matter

Table 2.14 classifies Usumacinta River sediments into low organic matter soils. Low organic matter is good for fired and earth bricks as higher organic matter decreases the compressive strength and density of bricks (Ukwatta & Mohajerani, 2017). Higher organic matter in sediments increases the porosity and water absorption of bricks. Moreover, the water retention of soil with high organic matter is higher which leads to swelling and shrinkage which changes the behavior of soil and decreases the strength of bricks (Farouk et al. 2014).

e2. Carbonate content of Usumacinta River sediments ($CaCO_3$)

Carbonate content of sediments was determined with Bernard calcimetry method. Average values of carbonate content of Usumacinta River sediments are shown in Table 2.15.

Table 2. 15. Carbonate content of sediments

Sediments	T1	T2	T5	T6	J3	J4
$CaCO_3$ (%)	8.21	7.19	1.90	8.73	7.84	8.49

Table 2.15 shows that the Usumacinta River sediments have low carbonate content. Table 2.16 defines the nature of the soil based on carbonate content based in French standards (AFNOR NF94-048, 2002).

Table 2. 16. Sediments classification based on carbonate content

Carbonate content (%)	Classification
0 < $CaCO_3$ (%) < 10	Non marly
10 < $CaCO_3$ (%) < 29	Low marly
30 < $CaCO_3$ (%) < 69	Marlstone soil
70 < $CaCO_3$ (%) < 89	Marly-calcareous
90 < $CaCO_3$ (%) < 100	Chalky, calcareous

As the carbonate content of Usumacinta River sediments is below 10%, we can deduct from Table 2.16 that Usumacinta River sediments have non marly nature which is common for clay and silica sand. Carbonate content of T5 sediment is very low. Calcium carbonate keeps in control of the acidity of sediment and sticks the sediment particles together, but clay is usually stable without calcium carbonate. Higher carbonate content in sediments causes swelling and disintegration in bricks as it transforms into CO_2 at high temperatures and emits in the form of bubbles.

2.3.2 Environmental characterization of Usumacinta River sediments

(a) pH value of sediments

pH value of sediments was determined with pH paper and pH meter. The results are shown in Table 2.17.

Table 2. 17. Values of pH for different sediments

Sediments	T1	T2	T5	T6	J3	J4
pH value by pH meter	8.04	8.21	8.17	8.40	7.91	8.51
pH value by pH paper	8.00	8.00	7.50	7.50	7.50	7.00

From Table 2.17, it can be observed that Usumacinta River sediments are slightly alkaline as their pH value is above 7. Carbonate minerals are mainly responsible for alkalinity of sediments. Alkaline soils have usually higher percentage of salts and are unsuitable for agronomy to grow crops. Literature studies show that pH values of sediments used in agronomy varies from 7 to 9.9 (Fourvel, 2018).

pH values by pH meter are more precise than from pH paper, it is difficult to distinguish the exact region of sediments on pH paper.

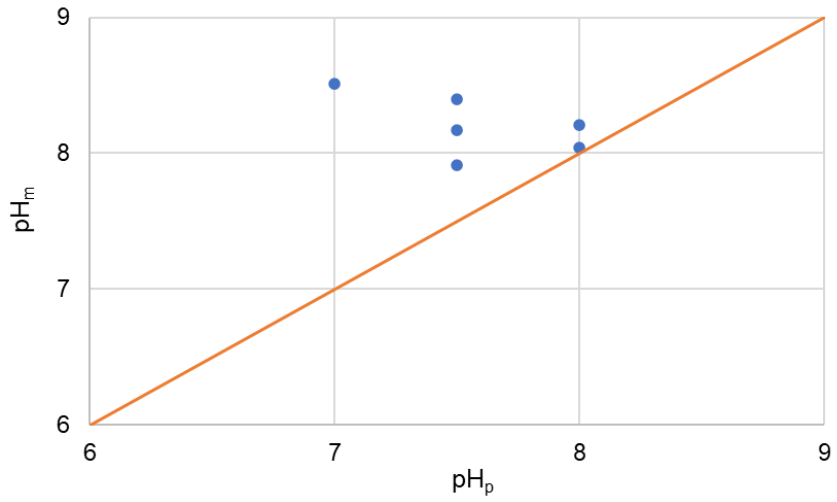

Figure 2. 21. pH values comparison

In Figure 2.21 pH values are away from bisector line and are lying above this line which indicates the higher pH values with pH meter.

(b) Heavy metals and chemical analysis

Chemical analysis of sediments was carried out with XRF, XRD and SEM analysis. The elemental composition of Usumacinta River sediments was found by XRF and SEM to observe the presence of heavy metals and contaminants in sediments. Elemental composition by XRF is presented in Table 2.18.

Table 2. 18. Chemical composition of Usumacinta River sediments (Del Negro, 2019)

Elements (mg/kg)	Level S1	T1	T2	T5	T6	J3	J4
Arsenic (As)	30.00	2.73	2.31	3.02	2.75	2.71	5.19
Cadmium (Cd)	2.00	0.4	0.4	0.4	0.4	<0.4	<0.4
Chromium (Cr)	150	108	76.1	98.6	96.3	99.8	131
Copper (Cu)	100	17.2	10.8	15.4	14.5	15.8	20.5
Mercury (Hg)	1	<0.1	<0.1	<0.1	<0.1	<0.1	<0.1
Nickel (Ni)	50	164	107	147	141	157	256
Lead (Pb)	100	9.49	6.53	9.97	7.78	9.2	11.3
Zinc (Zn)	300	46.6	36.8	42.4	40.8	45.9	40.2
PCB total	0.68	<0.001	<0.001	<0.001	<0.001	<0.001	<0.001
HAP total	22.8	0.11	0.012	0.049	0.025	0.12	0.014

Heavy metals presence in Usumacinta River sediments is below S1 level which is recommended thresholds in French standards. However, the quantity of Nickel (Ni) surpasses the recommended limits. Nickel mining in the catchment area of Usumacinta River in Guatemala is a possible source of a higher quantity of Ni. In case of earth and fired bricks, Ni

can be neutralized with addition of lime. As contaminants in Usumacinta River sediments are low, their reuse in bricks, roads, and other applications does not require additional treatment to remove contaminants.

Organic impurities such as PAHs and PCBs are resulted from industrial activities and by use of fertilizers. Presence of PAHs contaminants in Usumacinta River sediments and their threshold limits with French recommendations (JORF, 2013) are shown in Table 2.19.

Table 2. 19. PAHs values (mg/kg) of Usumacinta River sediments (Del Negro, 2019)

PAHs (mg/kg)	N1	N2	T1	T2	T5	T6	J3	J4
Naphtalene	0.16	1.13	0.064	0.0031	0.0043	0.0048	0.01	0.0024
Acenaphtylene	0.015	0.26	<0.0022	<0.0023	0.0087	<0.0021	<0.0023	<0.0023
Acenaphtene	0.04	0.34	0.0031	<0.0023	0.0029	<0.0021	<0.0023	<0.0023
Fluorene	0.02	0.28	0.0082	<0.0023	0.0056	0.0022	0.0038	<0.0023
Phenanthene	0.085	0.59	0.014	0.0054	0.013	0.0072	0.012	0.0031
Anthracene	0.24	0.87	0.0024	<0.0023	0.0049	0.0065	0.011	0.0043
Fluoranthene	0.6	2.85	0.0038	<0.0023	<0.0024	<0.0021	0.0052	<0.0023
Pyrene	0.5	1.5	0.0067	0.0038	0.0063	0.0038	0.0066	0.0042
Benzo anthracene	0.26	0.93	0.0034	<0.0023	0.0028	<0.0021	0.0037	<0.0023
Chrysene	0.38	1.59	0.0041	<0.0023	<0.0024	<0.0021	<0.0023	<0.0024
Benzo pirene	0.43	1.01	<0.0022	<0.0023	<0.0024	<0.0021	0.0025	<0.0027
Dibenzo anthracene	0.06	0.16	<0.0022	<0.0023	<0.0024	<0.0021	<0.0023	<0.0028
Benzo perylene	1.7	5.56	<0.0022	<0.0023	<0.0024	<0.0021	<0.0023	<0.0029
Indono pyrene	1.7	5.56	0.0023	<0.0023	<0.0024	<0.0021	0.0058	<0.0030

Note: N1 = level 1 and N2 = level 2

PAHs values of Usumacinta River sediments are considerably lower than the recommended level 1. Similarly, PCBs in Usumacinta River sediments were also measured and it was observed that PCBs: 28, 52, 101, 118, 138, 153 and 180 are negligible in these sediments and the sum of PCBs values is below 0.001 mg/kg which is considerably lower than the recommended value of 0.02 mg/kg (VROM, 2000).

2.3.3 Hydromechanical characteristics of Usumacinta River sediments

(a) Compaction test (Optimum moisture content)

Optimum moisture content of sediments was found with Proctor normal test. Proctor curves of Usumacinta River sediments between dry density and water content are shown in Figure 2.22.

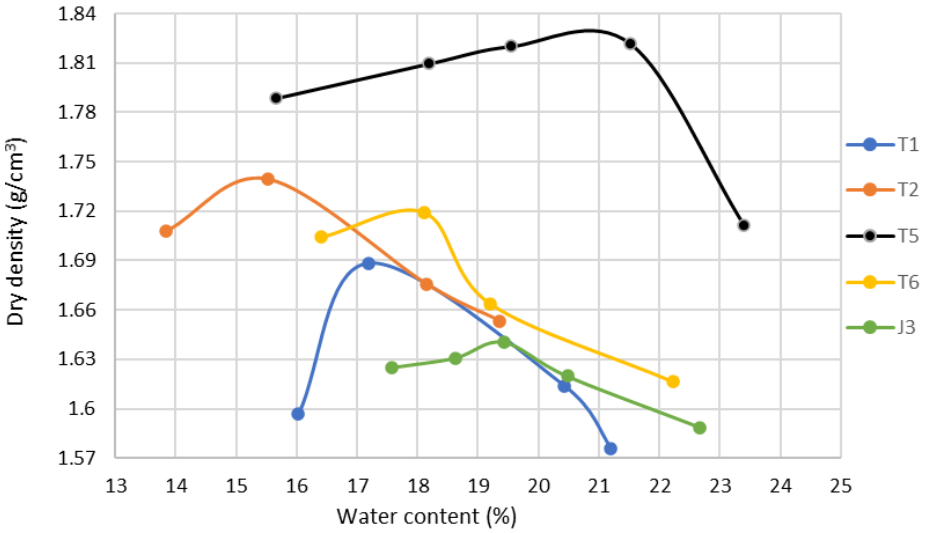

Figure 2. 22. Proctor curves for Usumacinta River sediments

Proctor curve of T5 sediments in Figure 2.22 is above all other curves due to the clayey nature of these sediments. Moisture content of T2 sediments is low. T2 sediments have very high percentage of sand. Optimum moisture content of sediments increases with increasing clay content and organic matter.

Table 2.20 shows the optimum moisture content and dry density of Usumacinta River sediments.

Table 2. 20. Optimum moisture content of Usumacinta River sediments

Sediments	**T1**	**T2**	**T5**	**T6**	**J3**
W_{opt} (%)	17.3	15.5	20.8	17.9	19.4
Dry density (g/cm^3)	1.69	1.74	1.82	1.72	1.64

Optimum moisture content of the soil is important as it is commonly used as moulding moisture content in bricks (Bruno et al., 2018). Soil has maximum density and shear strength at optimum moisture content.

(b) Shear strength of sediments

Shear strength of Usumacinta River sediments was determined with direct shear test. Water content used to make sediments samples is shown in Table 2.21. Dry density of soil specimens is also given in Table 2.21.

Table 2. 21. Water content and dry density of samples

Sed	**T1**	**T2**	**T5**	**T6**	**J3**	**J4**
W_{opt} (%)	17.3	15.5	20.8	17.9	19.4	21
Dry density (kg/m^3)	1831.5	1894.7	1638.7	1831.2	1754.3	1667

Soil samples were tested with direct shear apparatus. Soil samples before and after shear strength test are shown in Figure 2.23.

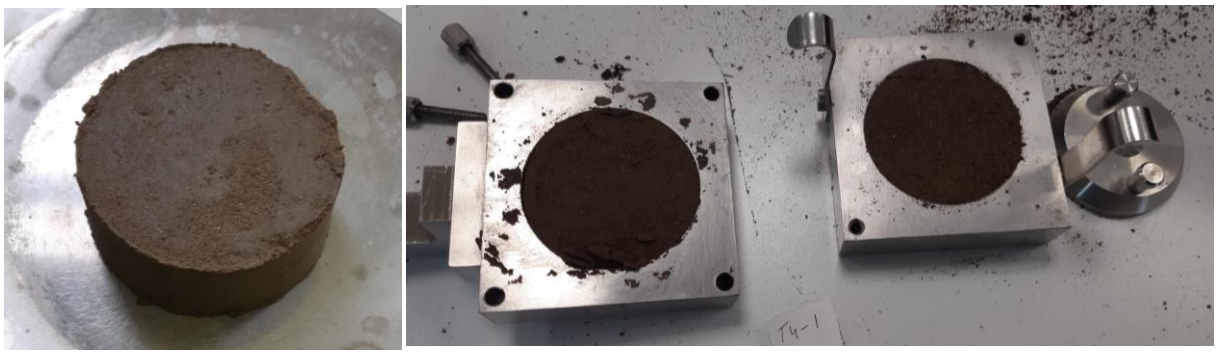

Figure 2. 23. Soil sample before (a) and after shear strength test (b)

Shear stress and displacement curves of Jonuta and Tenosique sediments are shown in Figures 2.24 and 2.25. Shear force for J4 is comparatively lower than other sediments.

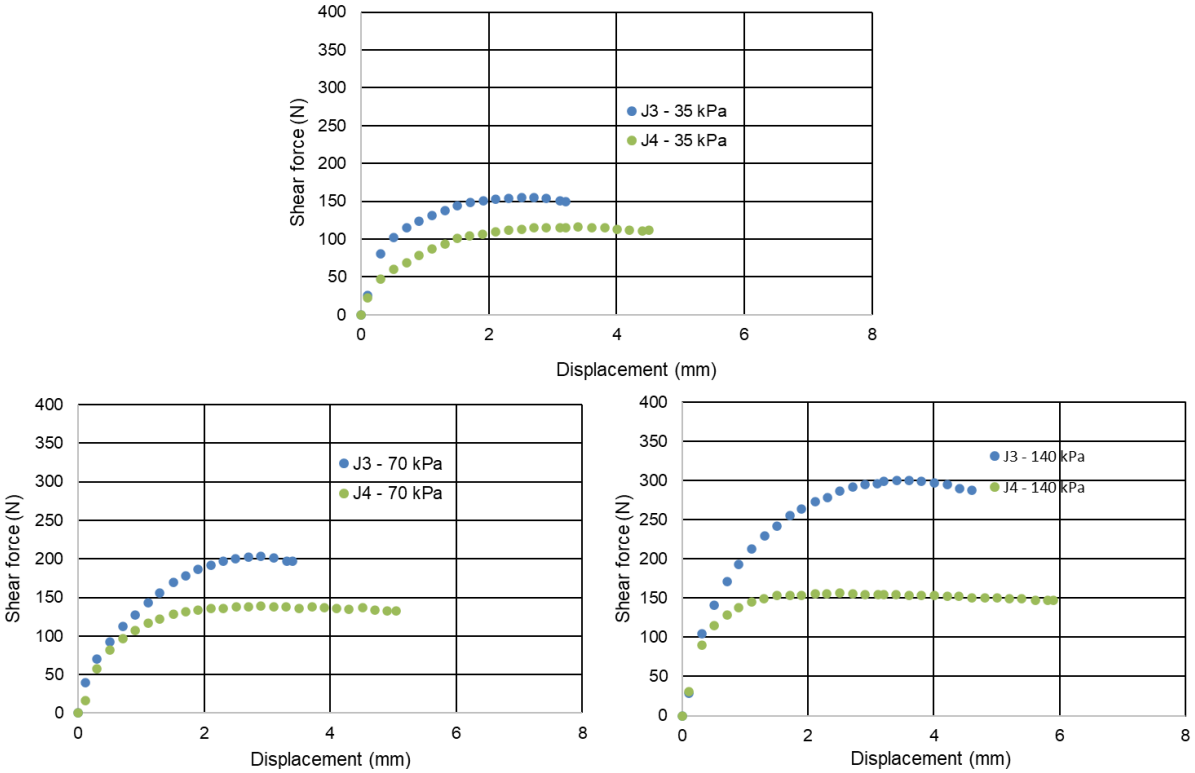

Figure 2. 24. Shear force vs displacement curve for Jonuta sediments (σ = 35, 70 and 140 kPa)

Shear force increase with displacement is gradual and becomes flat after observing maximum shear force (N)

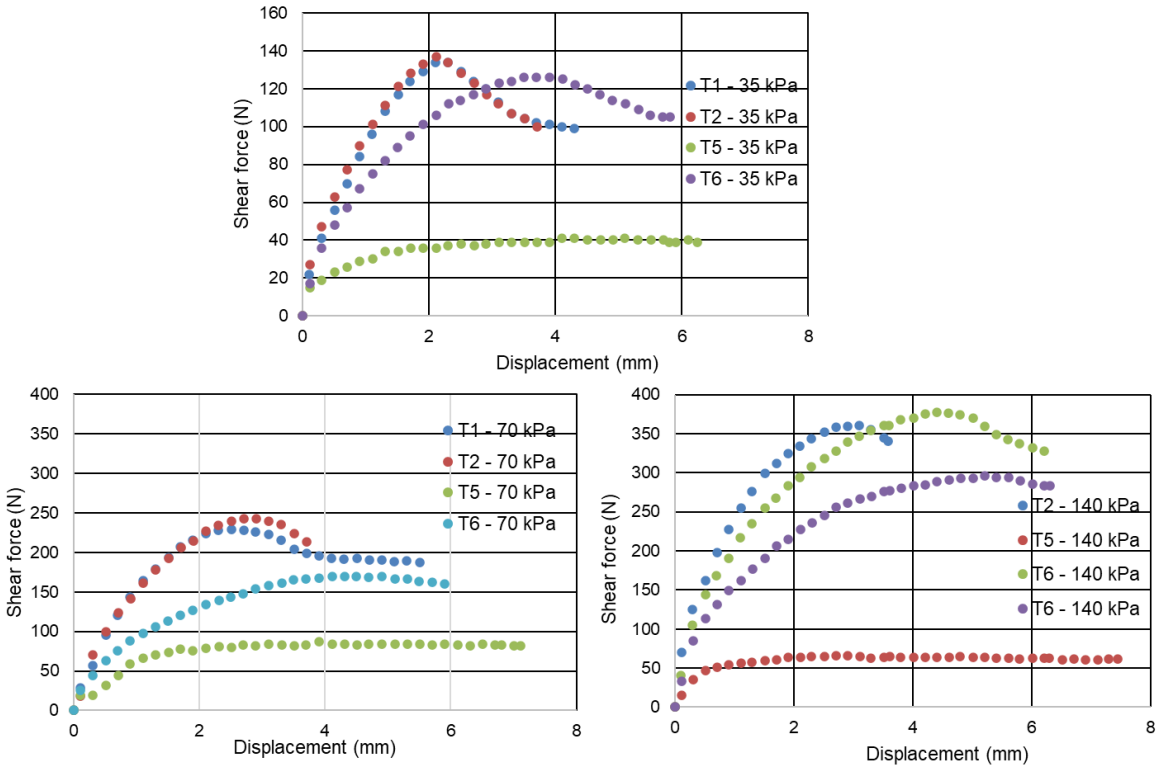

Figure 2. 25. Shear force vs displacement curve for Tenosique sediments (σ = 35, 70 and 140 kPa)

From the peak values of shear stress, normal and shear stress relationships for Jonuta and Tenosique sediments are deduced and shown in Figure 2.26.

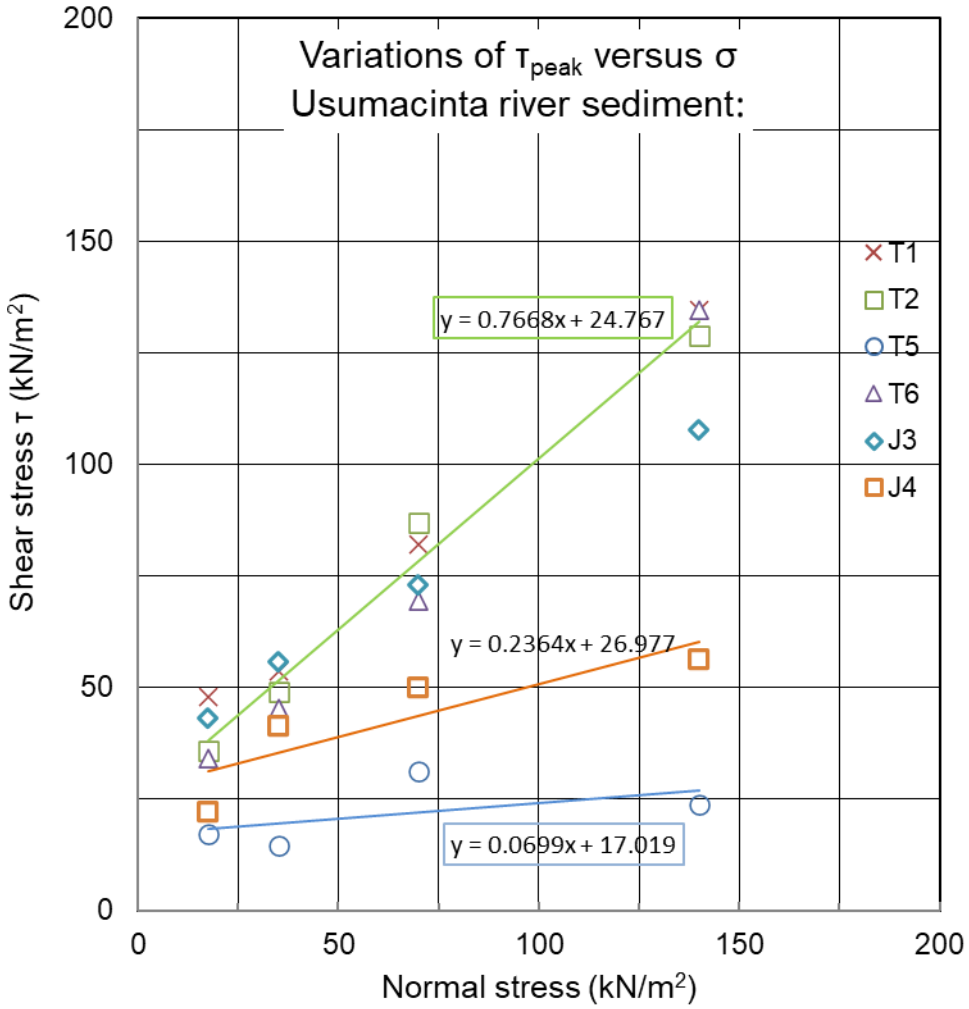

Figure 2. 26. Shear stress vs normal stress of Usumacinta River sediments

Figure 2.26 shows the linear correlation between normal and shear stress. Shear stress is maximum for sandy sediments (T1, T2 and T6) and lowest for clayey sediments (T5, J4) and the slope is nearly flat for clayey sediment (T5). Shear stress is maximum for T1, T2 and T6 sediments and its value is nearly 0.13 MPa at normal stress of 140 kN/m^2. J3 sediment have value around 0.1 MPa while for T5 and J4 this value is 0.02 and 0.05 MPa. Wu et al. (2011), founds the shear strength of adobe masonry around 0.105 MPa. T1, T2, T6 and J3 sediments have similar shear strength to the shear strength of adobe masonry.

The internal friction angle and cohesion for Jonuta and Tenosique sediments are summarized in Table 2.22.

Table 2. 22. Friction angle and cohesion for Usumacinta River sediments

Sediments	**T1**	**T2**	**T5**	**T6**	**J3**	**J4**
Tan ϕ	0.73	0.77	0.07	0.83	0.52	0.24
Friction angle ϕ (degree)	36.13	37.47	3.95	39.62	27.34	13.30
Cohesion C (kPa)	31.63	24.76	17.02	16.42	38.21	26.97

Friction angle of Jonuta sediments is low and their clay content is relatively higher than Tenosique sediments. Most of the Tenosique sediments have higher friction angles which show higher sand content in this soil except for T5 sediments. J4 and T5 are clayey soils and their friction angle is also small.

2.3.4 Minerology and microstructure of Usumacinta River sediments

(a) Mineralogy by XRD

Mineralogy of Usumacinta River sediments was studied with XRD analysis. XRD spectrum of Tenosique (T1) and Jonuta (J3) sediments is shown in Figures 2.27 and 2.28.

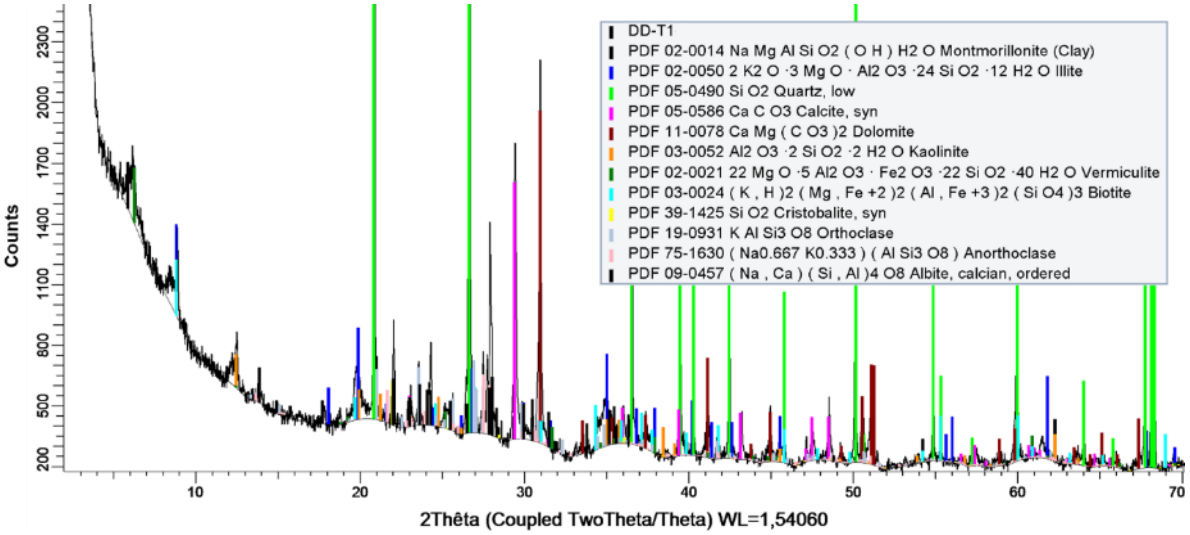

Figure 2. 27. XRD spectrum of Tenosique sediments (T1) (Del Negro, 2019)

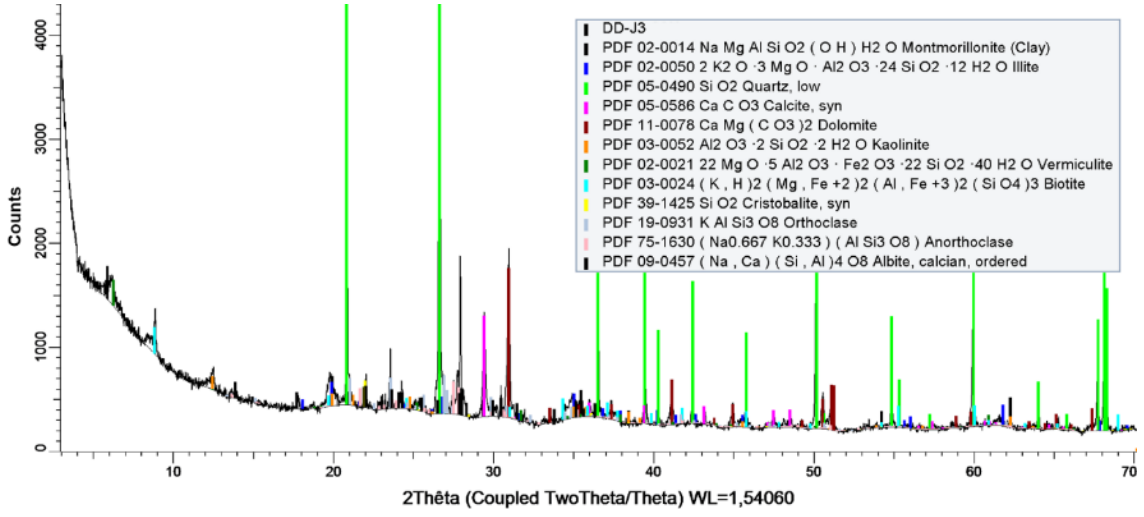

Figure 2. 28. XRD spectrum of Jonuta sediments (J3) (Del Negro, 2019)

XRD spectrum of remaining sediments are attached in annex.

Different minerals in Usumacinta River sediments found with XRD analysis are shown in Table 2.23.

Table 2. 23. Dominant clay minerals in Usumacinta River sediments

	Mnt (%)	Ilt (%)	Vrm (%)	Bt (%)	Qz (%)	Cal (%)	Dol (%)	Crs (%)	Or (%)	Ano (%)	Ab (%)	NIM (%)
T1	2.6	5.1	3.1	3.1	43.7	7.1	18.4	2.5	4.0	5.3	3.2	1.9
T2	4.0	2.2	2.2	2.7	52.0	4.8	14.1	3.2	3.8	5.9	3.9	1.2
T5	5.1	5.4	3.0	2.6	50.5	3.0	9.7	1.7	3.1	5.4	3.2	7.3
T6	3.4	2.3	3.1	2.8	48.7	3.9	14.7	2.6	4.0	9.2	3.8	1.5
J3	3.6	2.6	2.9	2.9	48.4	5.6	16.5	2.9	4.2	5.9	3.0	1.5
J4	10.0	6.4	17.1	7.0	21.4	2.2	10.1	1.6	5.3	9.6	4.3	5

** Mnt= montmorillonite, Ilt = illite, Qz = quartz, Cal= calcite, Dol= Dolomite, Vrm= vermiculite, Bt= biotite, Crs= cristobalite, Or = orthoclase, Ano = anorthoclase, Ab =albite, NIM = non identified minerals*

Table 2.23 shows the main mineral in Usumacinta River sediments is quartz which is nearly 50% of all the sediments except J4. Calcite content varies from 2.2 to 7.9 but these values are slightly lower than the carbonate content found with Bernard calcimeter test in which results are deduced from experimental work by reaction of carbonate with acid. Clay in Usumacinta River sediments is present in the form of montmorillonite, illite, bentonite and vermiculite. Minerology of sediments play an important role for their reuse in bricks and agronomy.

(b) Microstructure analysis

Specific surface area (SSA) of Usumacinta River sediments was found with BET method (Dogan et al., 2006) and pore size distribution was determined with BHJ method. Pores in sediments are separated into micropores (< 2nm), mesopores (2 to 50nm) and macro pores (>50nm) (Dogan et al. 2006). Pore size distribution of Usumacinta River sediments is shown in Figure 2.29.

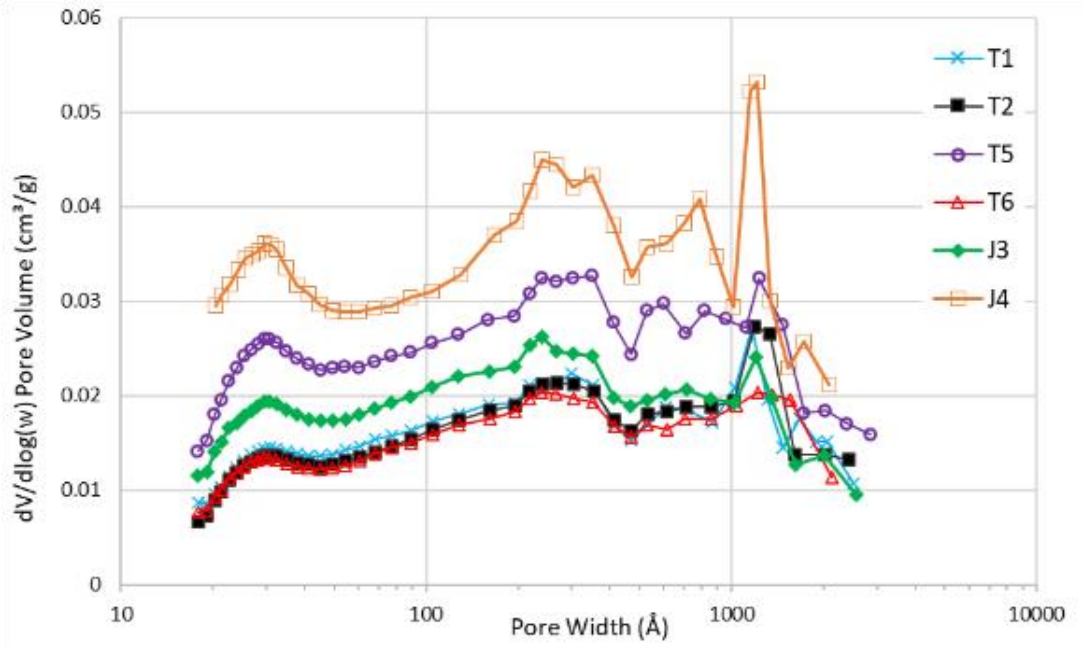

Figure 2. 29. Pore size distribution of Usumacinta River sediments

Figure 2.29 shows the peaks at pore widths of 30Å, 300Å and 1300Å. Pore volume of J4 and T5 sediments is considerably higher. T6, T2 and T1 have lower pore volumes due to a higher percentage of coarse-size particles.

Pore size distribution of sediments is shown in Figure 2.30. 70-80% of Usumacinta River sediments consist of micropores of size below 25Å. 7-8% have pore widths between 25Å to 100Å, pores while the greater pores occupy 0.14 to 0.19% of sediments.

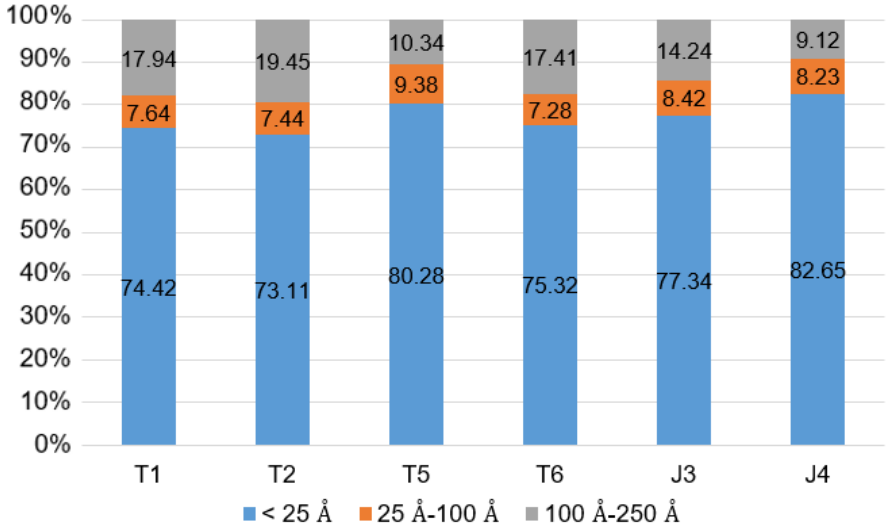

Figure 2. 30. Pore size distribution of Usumacinta River sediments

Adsorption isotherm of Usumacinta River sediments is shown in Figure 2.31. The width of hysteresis in isotherm curves indicates the sediment's affinity for water and specific surface area. Water affinity and SSA increase with increasing hysteresis.

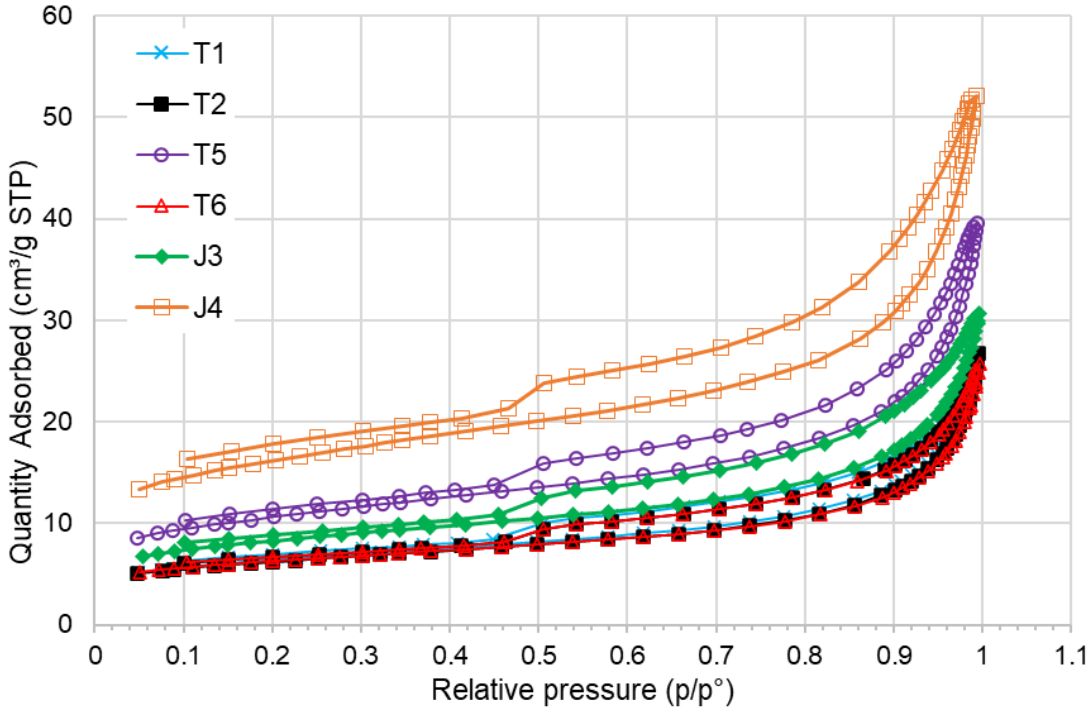

Figure 2. 31. Adsorption isotherm of Usumacinta River sediments

Hysteresis and specific surface of Usumacinta River sediments are given in Table 2.24.

Table 2. 24. SSA of Usumacinta River sediments by BET method

Sediments	**T1**	**T2**	**T5**	**T6**	**J3**	**J4**
Hysteresis (cm^3/g)	2.26	1.93	2.75	1.94	2.73	3.98
SSA_{N2} (m^2/g)	21.9	21.14	36.20	21.30	28.20	54.50

Specific surface area of J4 and T5 sediments is high as these sediments have higher clay content. Affinity to water of sediments increases with higher hysteresis and specific surface area.

Linear relation between SSA values obtained from methylene blue values and BET method is shown in Figure 2.32. There is a good correlation between SSA from MBV and BET method.

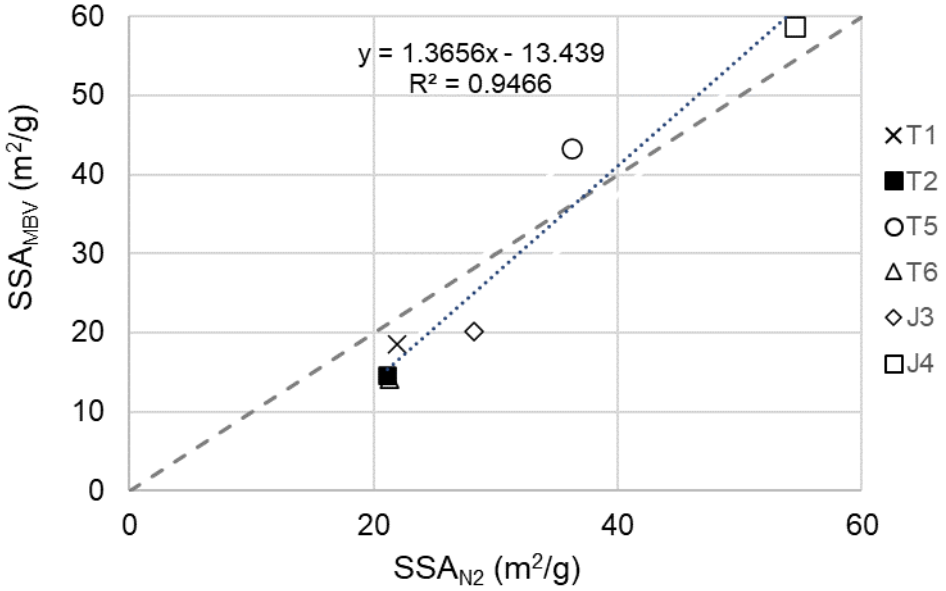

Figure 2. 32. Correlation between specific surface area (SSA) from MBV and BET method

Specific surface area (SSA) from MBV and BET method show linear correlation. However, values are slightly away from bisector line. Specific surface area with methylene blue value is higher for clayey sediments such as T5 and J4.

Clay minerals in Usumacinta sediments are determined with XRD analysis. However, clay minerals can also be assessed through SSA by using correlation developed by Yukselen and Kaya, 2006.

Table 2. 25. Relationship between SSA and clay minerals (Yukselen and Kaya, 2006)

Minerals	**Range of SSA**
Kaolinite	6,9-56,4
Halloysite	93,5
Zeolite	32,0-34,3
Chlorite	5,3
Illite	15,5
Montmorillonite	11,2-56,7

Table 2.26 shows the dominant clay minerals in Usumacinta River sediments on the base of correlation in Table 2.25.

Table 2. 26. Dominant clay minerals in Usumacinta River sediments

Soil sample	SSA (m^2/g)	Dominant clay mineral
T1	21.9	K, M, I
T2	21.14	K, M, I
T6	21.30	K, M, I
T3	19.1	K, M, I
T5	36.20	K, M, Z
J1	28.20	K, M, I
J3	54.50	K, M, Z

Table 2.26 shows that kaolinite, montmorillonite, illite and zeolite are some common clay minerals in Usumacinta River sediments. Higher percentage of kaolinite is undesired for fired and earth bricks as it is very plastic and absorb higher quantity of water. Volume variation on drying and firing of bricks in kaolinitic sediments produce shrinkage and cracks (Koroneos and Dompros, 2007).

(c) Porosity and void ratio (n)

Porosity and void ratio of Usumacinta River sediments are given in Table 2.27.

Table 2. 27. Porosity of Tenosique and Jonuta sediments

Sediments	T1	T2	T5	T6	J3	J4
Porosity	0.7	0.62	0.57	0.61	0.61	0.5
Void ratio	2.41	1.65	1.31	1.58	1.57	0.99

Porosity of sediments is linked with grain size. Porosity of T1 sediments is the highest while porosity of J4 sediments is low. Permeability of soil is directly linked with porosity. As J4 sediments have higher percentage of fine particles, therefore, they have comparatively low porosity and moderated permeability when compared with other Usumacinta River sediments whose porosity is higher with moderately high permeability as shown in Figure 2.16.

In case of bricks, porosity of bricks has a significant influence on durability of bricks as porous bricks have higher water absorption. In case of fired bricks, porosity of bricks is decreased due to fusion at high temperatures. Presence of pores in soils is also essential for sediments reuse in agronomy as it helps to circulate water and air.

(d) Chemical composition of Usumacinta River sediments

Elemental composition of Usumacinta River sediments was determined with SEM analysis and XRD. SEM image of T2 sediments and spectrum of elements is shown in Figure 2.33.

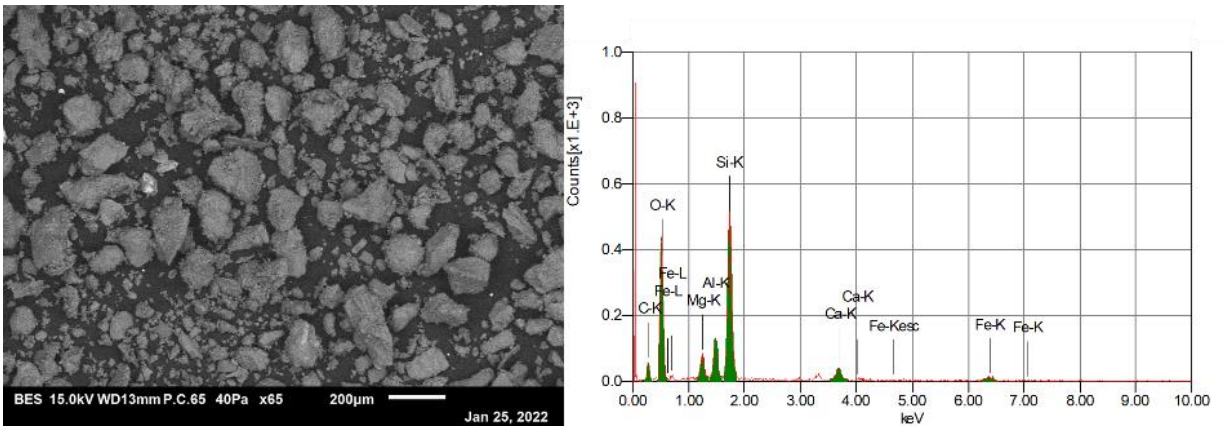

Figure 2. 33. SEM image of T2 sediments (a) and sediments spectrum (b)

The shape of sediments can be observed with SEM image. The shape of sediments can be rounded, angular and sub-angular. Most of the sediments in Figure 2.33a are angular in shape. Shape and morphology of sediments have considerable influence on the porosity and permeability of sediments, and it is important for modification of agronomic soils with sediments for sediments recovery.

Elemental composition of Usumacinta River sediments with SEM is shown in Table 2.28.

Table 2. 28. Elemental composition of Usumacinta River sediments

Sediments	**O (%)**	**Al (%)**	**Si (%)**	**Ca (%)**	**Mg (%)**	**Fe (%)**	**K (%)**	**Na (%)**	**P (%)**
T1	51.98	7.51	38.47	1.43	0.61	-	-	-	-
T2	57.77	9.04	22.28	2.01	2.57	3.89	1.31	1.12	0
T5	59.74	9.60	30.36	0	0.29	-	-	-	-
T6	50.69	8.54	36.99	3.25	0.52	-	-	-	-
J3	54.88	8.66	22.42	3.75	1.52	4.66	2.88	0.34	0.90
J4	56.44	11.98	25.90	5.21	0.30	-	-	0.18	-

Oxygen is primary element in Usumacinta River sediments followed by Si and AL. Si and Al are mainly due to presence of sand and clay and most important elements for fired bricks. Presence of different minerals such as iron is important as iron oxide helps to fuse silica at high temperatures and is responsible for the reddish color in bricks. Ca and Mg elements are associated with calcium and magnesium oxides and their carbonates. Furthermore, potassium (K) and phosphorus (P) are primary nutrients in sediments from the perspective of agronomy while Fe, S, Mn, Mg and B are secondary nutrients and essential for sediments recovery in agronomy.

Analysis of oxide in sediments is essential to observe the sediment's suitability for fired bricks and to anticipate different reactions inside the bricks when fired at high temperature. Oxides such as SiO_2, TiO_2, Al_2O_3, Fe_2O_3, MnO, MgO, CaO, Na_2O, K_2O, P_2O_5 are major oxides in soil used for manufacturing bricks (Taranto et al. 2019).

Oxide composition of Usumacinta River sediments was found with SEM and XRD method and presence of oxide in these sediments with SEM and XRD method is shown in Tables 2.29 and 2.30 respectively.

Table 2. 29. Oxide composition of Usumacinta River sediments with SEM

Sediments	**SiO_2 (%)**	**Al_2O_3 (%)**	**CaO (%)**	**MgO (%)**	**FeO (%)**	**K_2O (%)**	**Na_2O (%)**	**P_2O_5 (%)**
T1	80.21	15.5	2.925	1.369	-	-	-	-
T2	59.42	21.37	3.63	5.28	6.45	2.04	1.81	-
T5	77.68	21.76	-	0.56	-	-	-	-
T6	68.39	22.62	9.00	-	-	-	-	-
J3	62.58	19.35	2.68	3.21	6.99	4.02	1.18	-
J4	65.43	23.63	10.11	0.59	-	-	0.30	-

Oxide of silicon, aluminum and calcium are dominant in Usumacinta River sediments. Percentage of SiO_2 ranges from 59.42% to 80.21% while quantity of Al_2O_3 ranges 15% to 23%. Oxide of iron, potassium, sodium and potassium have a lower percentage. Ferrous oxide (FeO) is an important oxide in bricks, and it has black appearance contrary to ferric oxide (Fe_2O_3) which has a reddish appearance and is responsible for the red color of bricks. In Cao and MgO rich soils, development of pyroxene takes place light brown appearance of bricks (Kreimeyer, 1986). Percentage of different oxides in sediments is useful to decide the sediments reuse in different types of fired bricks in Augustinik diagram widely used in industry for sediments selection (Hussain et al. 2020).

Table 2. 30. Oxide composition of Usumacinta River sediments with XRD (Yamaguchi, 2018).

Sediments	**SiO_2 (%)**	**Al_2O_3 (%)**	**CaO (%)**	**TiO_2 (%)**	**Fe_2O_3 (%)**	**K_2O (%)**
T1	55.4	12.2	16	1.2	10.9	3.6
T2	55.4	11.7	11.2	1.2	8.5	3.7
T5	62.8	14.7	8.3	1	9.1	3.2
T6	59.6	12.2	12.1	1.1	9.8	4.2
J3	59.3	14.6	11.2	1	9.7	3.5
J4	56.3	16.1	6.4	1.9	16.1	2.6

From XRD, SiO_2 value range from 55.4% to 62.8%. Results of oxide from XRD show less variation in SiO_2 and Al_2O_3 content of different sediments. Percentage of SiO_2 and Al_2O_3 is higher with SEM calculation. Precision of results from XRD is better as calibration of SEM apparatus is difficult and results are influenced by the thickness of sediments sample as the electron beams penetrate deeply by crossing the sediments further into recipients which influence the results.

(e) Thermogravimetric analysis of Usumacinta River sediments

Mass loss of Usumacinta River sediments with temperatures due to different reactions inside sediments was observed with ATG test. Thermogravimetric analysis of Usumacinta River sediment is shown in Figure 2.34.

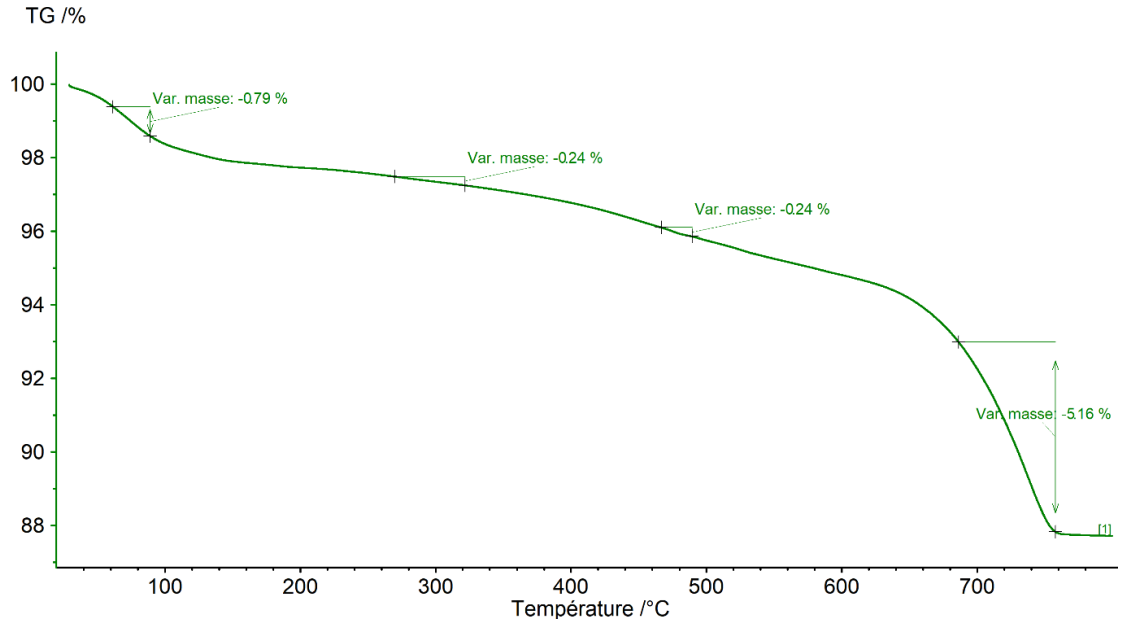

Figure 2. 34. Thermogravimetric analysis of Usumacinta River sediments

Graphs in Figure 2.35 show mass loss for Tenosique and Jonuta sediments with increasing temperature.

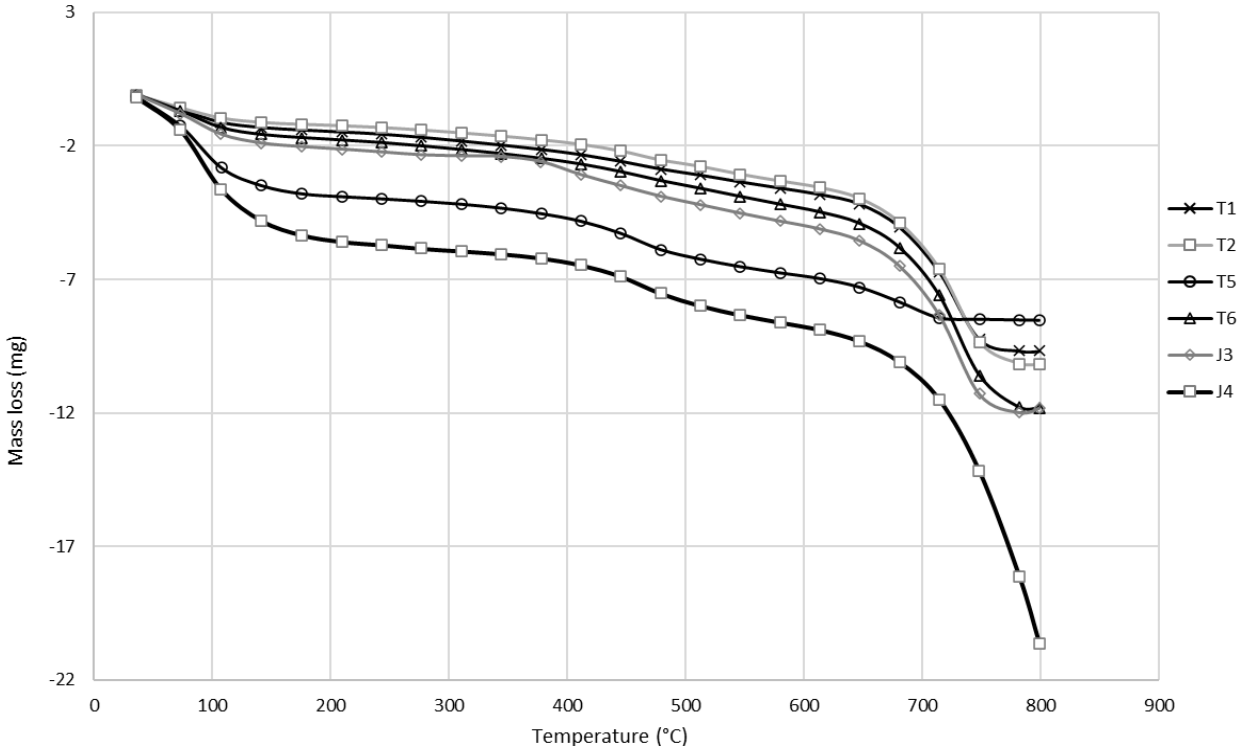

Figure 2. 35. Mass loss with temperature

Column chart in Figure 2.36 explains the mass loss in percentage with temperature. Mass loss was determined at a temperature from 0 to 200, 200 to 500 and 500 to 800. At this temperature inherent water evaporation, burning of organic matter and emission of CO_2 associated with chemical reaction of $CaCO_3$ are responsible for mass loss. Mass loss in J4 is higher and for T2 sediments mass loss is low. As T5 has low carbonate content and mass loss in T5 is also lowest at a temperature range of 500-800 °C.

Degradation of sediments with temperature is shown in Table 2.31.

Table 2. 31. Mass loss in percentage at different temperature

Sediments	200 °C	300-550 °C	550-800 °C	Total loss
T1	1.65 %	2.14 %	7.08 %	10.86 %
T2	1.21 %	1.82 %	6.95 %	10.60 %
T5	3.65 %	2.53 %	1.87 %	8.04 %
T6	1.93 %	2.25 %	7.68 %	11.86 %
J3	2.38 %	2.54 %	7.78 %	12.69 %
J4	4.18 %	2.15 %	9.28 %	15.60 %

Figure 2.36 shows the mass loss of sediments with different reactions.

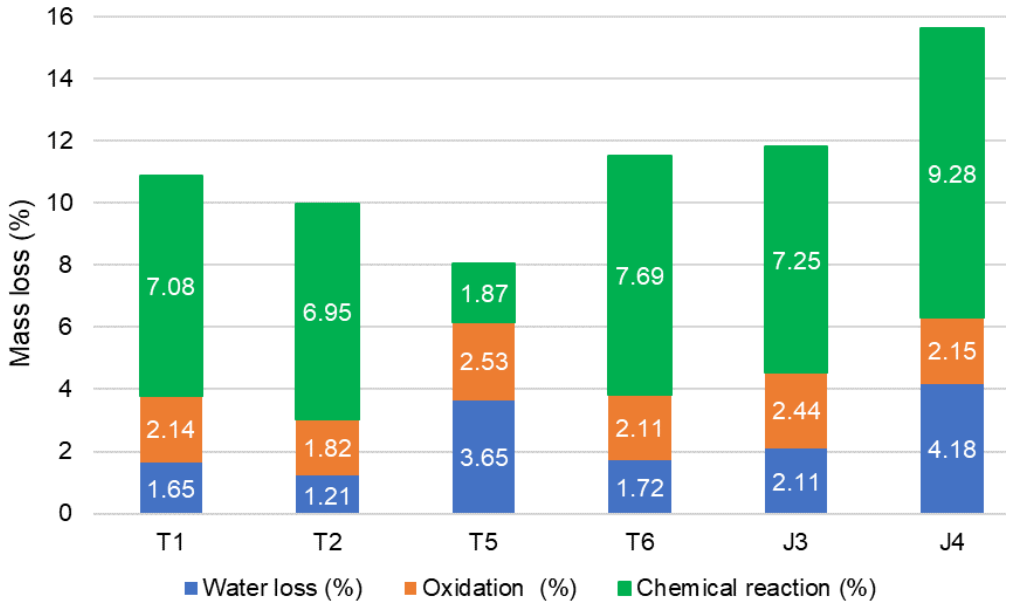

Figure 2. 36. Mass loss associated with different reactions in percentage

In case of fired bricks, similar reactions take place when bricks are fired at a high temperature. Loss on ignition, burning of organic matter and decomposition of carbonate content occurs at same temperature in ATG test and firing of bricks.

2.4. Conclusion

In this chapter, physical, chemical and hydromechanical and geotechnical characteristics of Usumacinta River sediments were determined by different tests. Presences of contaminants in sediments and regulations for pollutants were examined. It is observed that heavy metals concentration in Usumacinta River sediments is considerably lower than the recommended thresholds. However, only Ni is higher than the recommended limits. PAHs and PCBs concentrations are also lower than the recommended limits. Granulometry of sediments shows that most of the sediments have low clay content except for J4 and T5 sediments. T2 sediments have higher sand content. Usumacinta River sediments are low organic sediments as organic matter of sediments is below 6%. Carbonate content ranges from 1.9 to 8.21%. Higher carbonate creates pores in bricks when fired at high temperatures.

pH values of sediments are nearly 8 which means the sediments are slightly alkaline. Optimum moisture content of most of the sediments is below 20. Optimum moisture content is important for molding and compaction of bricks. MBV values for J4 sediments are highest and lowest for T2 sediments. Specific surface area of J4 sediments is highest due to higher percentage of fine particles.

Chemical composition of sediments shows that SiO_2 and Al_2O_3 are the main components in Usumacinta River sediments and their percentage varies from 50% to 80%. Mineralogical analysis shows that quartz is the most important mineral in Usumacinta River sediments. Other minerals include montmorillonite, illite etc. Microstructural analysis of sediments shows that hysteresis width and specific surface area of J4 sediments are considerably higher and 70-80% of pores in sediments are micropores. Shear strength test shows that J4 and T5 sediment lowest friction angle. TGA analysis of sediments shows that mass loss in Usumacinta River sediments ranges from 8%-15.8%. Mass loss of sediments increases with increasing moisture content, carbonate content and organic matter.

Physico-chemical and mineralogical characteristics of Usumacinta River sediments are similar to characteristics of soils used for manufacturing fired and earth bricks. Presence of nutrients such as potassium and iron highlight their potential for agronomic applications.

References

Abayazeed, S.D., and El-Hinnawi, E. (2011). Characterization of Egyptian Smectitic Clay deposits by methylene blue adsorption. American Journal of Applied Sciences 8 (12): 1282-1286.

AFNOR NF P 94-051. (1993). Détermination des limites d'Atterberg.

AFNOR NF ISO 10694, (1995). Qualité du sol–dosage du carbone organique et du carbone total apres combustion seche (Analyse Elementaire).

AFNOR NF P 94-068 (1998). Sols reconnaissance et essais - Mesure de la capacité d'adsorption de bleu de méthylène d'un sol ou d'un matériau rocheux - Détermination de la valeur de bleu de méthylène d'un sol ou d'un matériau rocheux par l'essai à la tache.

AFNOR XP P94-011 (1999). Sols : reconnaissance et essais, description - identification - dénomination des sols. Terminologie - eléments de classification.

AFNRO XP X33-012 (2000). Characterisation of sludges – Determination of polynuclear aromatic hydrocarbons (PAH) and polychlorinated biphenyls (PCB).

AFNOR XP P13-901 (2001): Compressed earth blocks for walls and partitions: definitions– specifications – test methods.

AFNOR NF P 94-048 (2002). Sols : Reconnaissance et essais. Détermination de la teneur en carbonate. Méthode du calcimètre.

AFNOR NF X31-107 (2003). Qualité du sol - Détermination de la distribution granulométrique des particules du sol - Méthode à la pipette, 2003.

AFNOR NF ISO 10390 (2005). Qualité du sol - Détermination du pH. Norme française.

AFNOR XP P 94-047 (2007). Sols: Reconnaissance et essais. Détermination de la teneur pondérale en matières organiques d'un matériau.

AFNRO NF EN ISO 11885, 2016. Water quality — Determination of selected elements by inductively coupled plasma optical emission spectrometry (ICP-OES)

AFNOR NF EN ISO 17892-12 (2018). Reconnaissance et essais geotechniques-essais de laboratoire sur les sols-partie 12: Détermination des limites de liquidité et de plasticité.

ASTM D689- 12e2 (2007). Standard Test Methods for Laboratory Compaction Characteristics of Soil Using Standard Effort (12 400 ft-lbf/ft3 (600 kN-m/m3).

Bruno, A.W., Gallipoli, D., Perlot, C., Mendes, J. (2018). Optimization of bricks production by earth hypercompaction prior to firing. Journal of Cleaner Production 214: 475:482. https://doi.org/10.1016/j.jclepro.2018.12.302

Casagrande (1948). Classification and identification of soils. Trans. ASCE, 113 (1948), pp. 901-991. https://doi.org/10.1061/TACEAT.0006109

Del Negro, R. (2019). Characterization of Usumacinta River's sediments, Master thesis, Université de Nantes-IFSTTAR Nantes, 18p.

Dogan, A. U., Dogan, M., Onal, M., Sarikaya, Y., Aburub, A., Wurster, D. E. (2006). Baseline studies of the clay minerals society source clays: specific surface area by the Brunauer Emmett Teller (BET) method. Clays and Clay Minerals 54.1 62-66

Farouk, B.A, Walid, M., Mohamed, B. (2014). Caractérisation géotechnique des sédiments de dragage marins en vue de leur valorisation en techniques routières. Déchets Sciences et Techniques - N°66 - Mars 2014.

Fonseca, B.S., Galhano, C. D. Seixas, D. (2015). Technical feasibility of reusing coal combustion by-products from a thermoelectric power plant in the manufacture of fired clay bricks. Applied Clay Sci., 104 (2015) 189–195. http://dx.doi.org/10.1016/j.clay.2014.11.030

Fourvel G. (2018). Valorisation agronomique des sédiments fins de retenues hydroélectriques en construction d'anthroposols fertiles. Thèse de doctorat Agrocampus Ouest, 2018. 397p. https://tel.archives-ouvertes.fr/tel-02136422

GTR (2000). Réalisation des remblais et des couches de forme. Guide technique Paris, LCPC, SETRA. 2ème édition, 211 p.

Hussain, M., Levacher, D., Leblanc, M., Zmamou, H., Djeran-Maigre, I., Razakamanantsoa, A., (2020). Sediments-based fired brick strength optimisation A discussion on different approaches. XVIèmes Journées Nationales Génie Côtier – Génie Civil Le Havre, 2020 DOI:10.5150/jngcgc.2020.072.

JORF (2013). Arrêté du 8 février 2013 complémentaire à l'arrêté du 9 août 2006 relatif aux niveaux à prendre en compte lors d'une analyse de rejets dans les eaux de surface ou de sédiments marins, estuariens ou extraits de cours d'eau ou canaux relevant respectivement des rubriques 2.2.3.0, 3.2.1.0 et 4.1.3.0 de la nomenclature annexée à l'article R. 214-1 du code de l'environnement. Journal Officiel de la République Française

Kreimeyer, R. (1986). Some notes on the firing colour of clay bricks. Applied Clay Science, 2, 175-183. https://doi.org/10.1016/0169-1317(87)90007-X

Koroneos, C., Dompros, A. (2007) Environmental assessment of brick production in Greece. Build. & Env. 42, 2114–2123. https://doi.org/10.1016/j.buildenv.2006.03.006

McManus, J. 1988. Grain size distribution and interpretation, in M.E. Tucker (Ed.), Techniques in Sedimentology, pp. 63–85.

Sahfi, A.M. (2020). Valorisation des sédiments de dragages dans des bétons autoplaçants : Optimisation de la formulation et étude de la durabilité. PhD thesis, Ecole nationale supérieure Mines-Télécom Lille Douai ; Université de Sherbrooke (Québec, Canada).

Taranto, M., Barba, L., Blancas, J., Bloise, A., Cappa, M., Chiaravalloti, F., Crisci, G.M., Cura, M., Angelis, D. D., Luca, R.D., Lezzerini, M., Pecci, A., Miriell, D. (2019). The bricks of Hagia

Sophia (Istanbul, Turkey): a new hypothesis to explain their compositional difference. Journal of Cultural Heritage, 38, 136–146. https://doi.org/10.1016/j.culher.2019.02.009

Tiessen, H., Roberts, T. L., Stewart, J. W. B. (1983). Carbonate analysis in sediments and minerals by acid digestion and two-endpoint titration. S7N 0W0. Commun. in Sediment Sci. Plant Anal., 14(2), 161-166.

Türköz, M, Tosun, T. (2011). The use of methylene blue test for predicting swellparameters of natural clay soils. Scientific Research and Essays Vol. 6(8), pp. 1780-1792, 1. DOI: 10.5897/SRE10.629

USDA-NRCS (1999). U.S. Department of Agriculture, National Resources and Conservation Service). 1999. Guide to Texture by Feel. www.nrcs.usda.gov/wps/portal/nrcs/ detail/soils/edu/?cid=nrcs142p2_054311.

USDA (1951). Soil survey manual. USDA Handbook No. 18, U.S. Department of Agriculture Washington, DC, 503 p.

Ukwatta, A., and Mohajerani, A. (2017). Effect of organic content in biosolids on the properties of fired-clay bricks incorporated with biosolids. Journal of materials in civil engineering, vol. 29 (7), https://doi.org/10.1061/(ASCE)MT.1943-5533.0001865

VROM. (2000). Circular on target values and intervention values for soil remediation. Ministry of Housing, spatial Planning and Environment DBO/1999226863.

Wu, F., Li, G., Jia, J., Li, H. (2011). Mechanical properties of Adobe masonry in shear test. Applied Mechanics and Materials Vols. 71-78 (2011) pp 3691-3694. doi:10.4028/www.scientific.net/AMM.71-78.3691.

Yamaguchi K. (2018). Consideration of the sustainable utilization of the sediments in Usumacinta River. Master thesis report, Kyoto University-IFSTTAR-Université de Caen-Normandie, 20p.

Yukselen, Y. and Kaya A. (2006). “Comparison of Methods for determining Specific Surface Area of Soils.” J. Geothch. Geoenviron. Eng., 132(7), 931-936

Chapter 3. Fired bricks

Fired bricks are important construction material and commonly used all over the world as they are low cost, durable and have good strength. In this study, characteristics of Usumacinta River sediments were investigated for their use in fired bricks. Characteristics of sediments such as granulometry, chemical composition, mineralogy and consistency limits show that Usumacinta River sediments can be used in manufacturing bricks.

Prismatic and cubic brick specimens were manufactured with Usumacinta River sediments with the addition of moulding moisture content. Bricks specimens were dried and fired at a temperature range of 700 °C to 1100 °C. The impact of firing temperature and moulding moisture content on the strength of bricks was observed. Furthermore, bricks were manufactured with different approaches to optimize their strength. Along with compressive and tensile strength, bricks physical characteristics such as water absorption, density, linear shrinkage, etc. were determined.

3.1. Introduction

Fired bricks have been used for construction activities for centuries. Due to rapid urbanization and construction activities, the demand for bricks is increasing which is exhausting non-renewable soil resources. Mining of soil has a devastating impact on agricultural lands due to the overconsumption of clay by the ceramic industry. On other hand, every year millions of tons of sediments are dredged and immersed in the sea. Dredged sediments are renewable waste materials. The use of dredged sediments in fired bricks can reduce the burden on soil resources by fully or partially replacing soil. Rouen and Le Havre region of France consumes 0.85 million m^3 of soil in fired bricks annually while 6-7 million m^3 of dredged sediments from this region are submerged in the sea (AMI, 2018). Dredged sediments contain a huge amount of water. Dewatering of sediments increases the cost of sediments for their recycling. However natural dehydration of sediments allows the recovery of sediments with minimum cost.

Dredged sediments are heterogeneous and characterization is important to recycle them in ceramics applications. The strength of fired bricks depends on the nature of the soil, percentage of clay, silt, sand, organic matter and firing temperature. Common oxides in soil used for bricks are silica, alumina, calcium oxide, manganese oxide and organic matter etc. Specific quantity of sand and clay is essential for fired bricks as higher clay content induces cracks and shrinkage in bricks. Sandy soils are also not suitable for bricks as their plasticity is low. Figure 3.1 shows the recycling mechanism of dredged sediments in fired bricks.

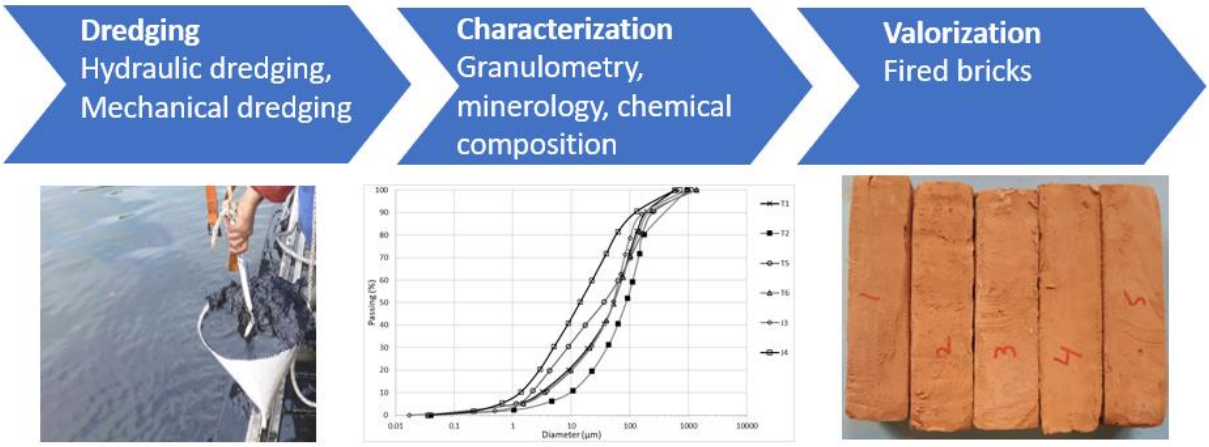

Figure 3. 1. Dredged sediments valorization in fired bricks

The objective of this study is the recovery of Usumacinta River sediments in fired bricks. For this purpose, characteristics of Usumacinta River sediments are to be analyzed and strength of bricks will be optimized with moulding moisture content and firing temperature.

3.2. Materials and methods

In this study, Usumacinta River sediments were used to manufacture fired bricks. Selection of suitable sediments to make fired bricks is very important. Usumacinta River sediment's suitability for fired bricks was observed with industrial approaches. Grain size, chemical composition, Atterberg limits, percentage of clay minerals, carbonates, quartz and feldspars have a significant influence on the strength and quality of bricks.

Usumacinta sediment's physico-chemical, mineralogical and geotechnical characteristics were determined as they are critical for their use in fired bricks. Figure 3.2 indicates with red arrows, the essential characteristics of sediments for their use in fired bricks. Environmental assessment is suggested in areas with higher industrial activities.

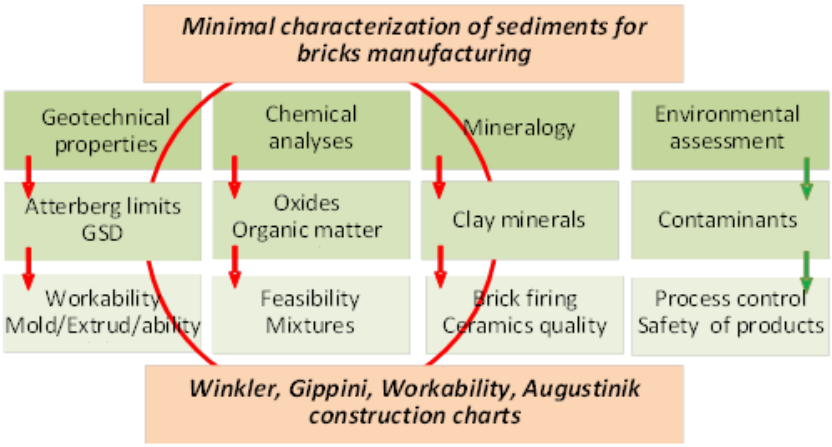

Figure 3. 2. Sediment characterization for the feasibility of fired bricks

Different approaches are followed in the fired bricks industry to observe soil suitability. Some common techniques are the Winkler diagram, Casagrande-Gippini diagram, clay workability chart and Augustinik diagram etc.

3.3.1 Sediments suitability for fired bricks with granulometry

Winkler diagram describes soil suitability for fired bricks and tiles on the base of clay, silt and sand content of sediments (Winkler, 1954). Different zones highlighted in soil texture ternary diagram in Figure 3.3 are based on the percentage of silt, sand and clay (Haurine, 2015). Silt, sand and clay percentages can be modified to shift the placement of sediments in Winkler diagram by changing the composition of the sediment with the addition of missing components.

Usumacinta River sediments placement in the Winkler diagram can be seen in Figure 3.3

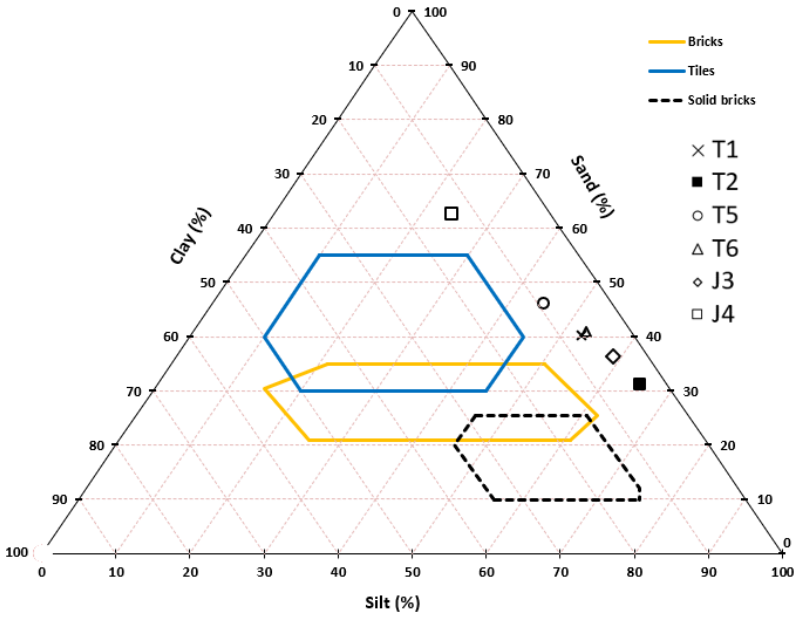

Figure 3. 3. Sediments suitability for fired bricks on the base of granulometry

Figure 3.3 shows that Usumacinta River sediments are located outside the zone recommended for fired bricks due to low clay content. Sediments can be relocated into the proposed zone for fired bricks with the addition of other sediments and missing components (clay). Figure 3.4 shows the possible solution of sediments mixing which shifts sediments into suitable zones.

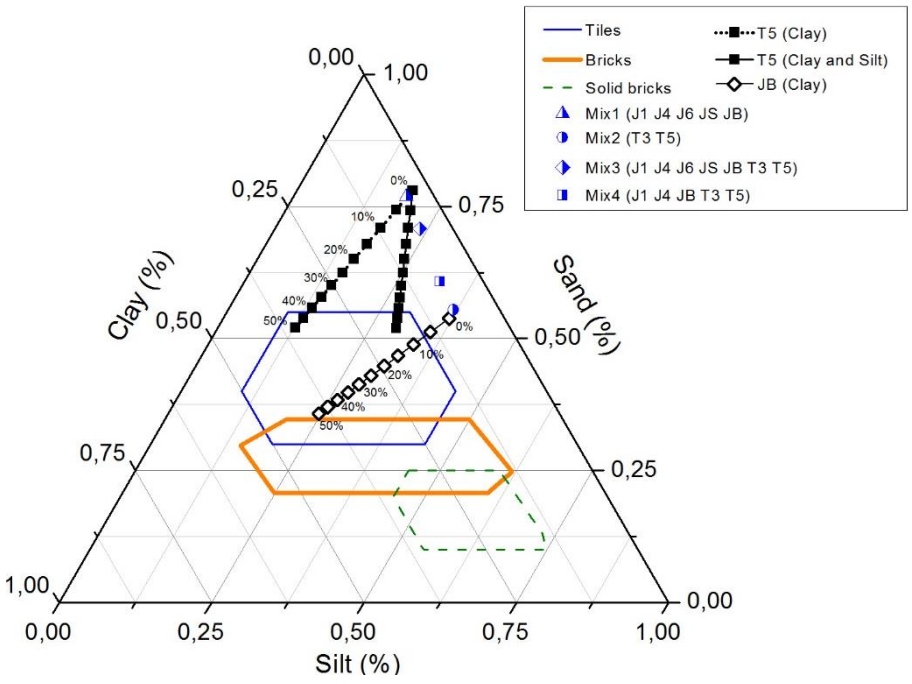

Figure 3. 4. Sediments shifting into suitable zones for bricks (Yamaguchi, 2019).

McNally diagram in Figure 3.5 also helps to select sediments for ceramics applications based on the grain size of sediments. McNally diagram seems more practical as it separates fine silt particles from coarse silt particles. Usumacinta sediment's location in McNally diagram is shown in Figure 3.5.

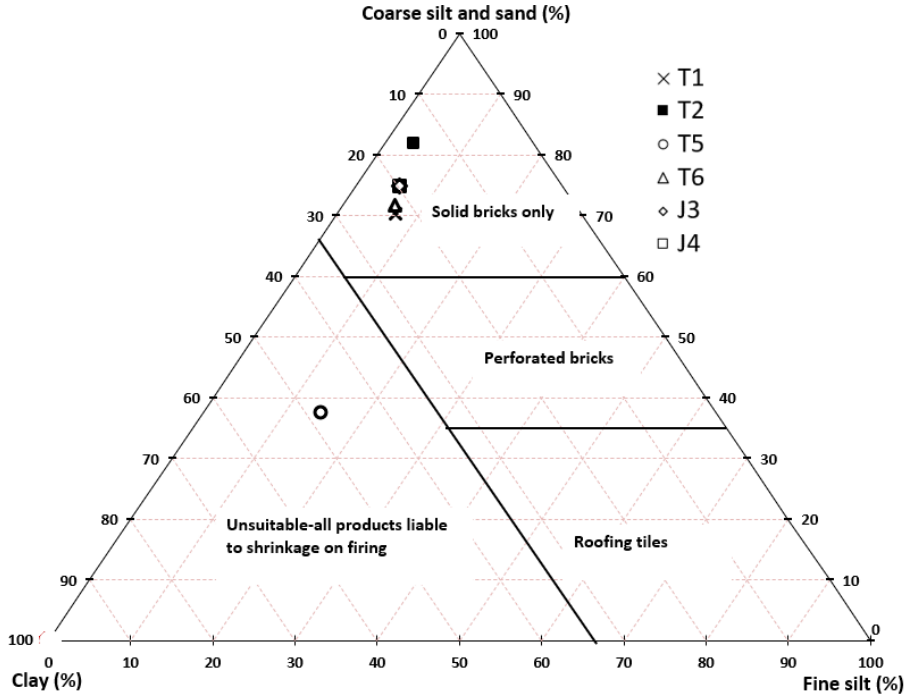

Figure 3. 5. McNally diagram based on soil granulometry

Figure 3.5 shows that most of the sediments are suitable for solid bricks. However, T5 is outside the zones suitable for bricks as these sediments have high clay and fine silt content which leads to higher shrinkage in bricks. Winkler diagram in Figure 3.3 shows Usumacinta River sediments lying outside the zone recommended for fired bricks. This contrast is because industrial approaches mainly focus on the soil mined from quarries and do not address the dredged sediments. Moreover, the soil is heterogeneous material, and its characteristics vary from region to region

3.3.2 Sediments suitability for fired bricks with oxides

Chemical analysis of sediments helps to determine the presence of oxides such as silica, alumina, calcium, iron oxide and magnesia etc. Silica and alumina are two important oxides in soil used for fired bricks. In France, soil used for fired bricks has usually silica content between 35% to 80% and alumina content between 8% to 30% (Kornmann, 2009). Percentage of SiO_2 and Al_2O_3 in Usumacinta River sediments ranges from 50% to 80%. Usumacinta sediment's suitability for fired bricks with their oxide content is shown in Figures 3.6 and 3.7.

Augustinik diagram in Figure 3.6, describes soil suitability for fired bricks based on the oxide content of sediments. It is plotted between the ratio of Al_2O_3 and SiO_2 on Y-axis and $R_2O+RO+Fe_2O_3$ on X-axis, where $R_2O = K_2O+Na_2O$ and $RO = CaO+MgO+NaO$ (Augustinik, 1957). Augustinik diagram to observe Usumacinta River sediments suitability is shown in Figure 3.6.

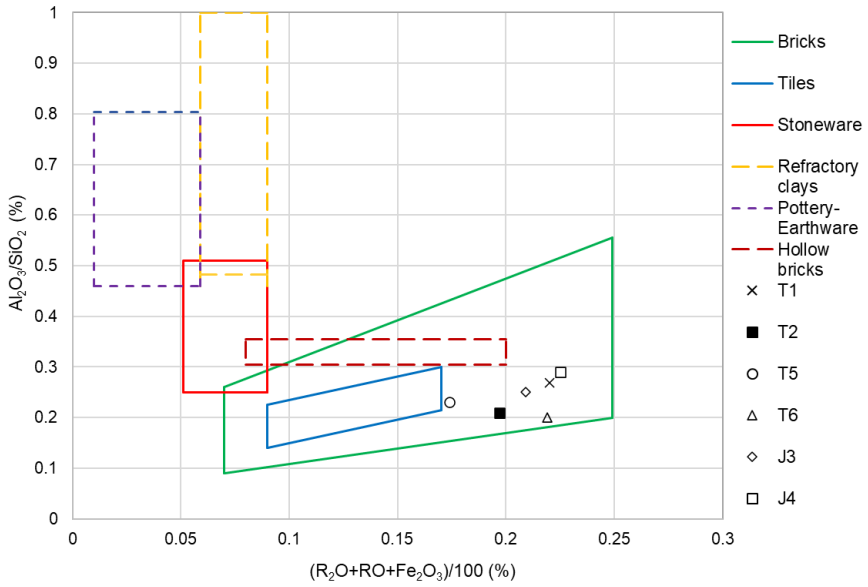

Note: R_2O = K_2O+Na_2O and RO = CaO+MgO+NaO

Figure 3. 6. Sediments suitability for fired bricks on the base of oxide content

Figure 3.6 shows that chemical composition of sediments is suitable for their use in bricks as all the sediments lie in zones suitable for bricks. Sediments outside the recommended zones for bricks can be shifted into the suitable zone with the help of additives. Figure 3.7 shows the mixture of sediments and their position in Augustinik diagram.

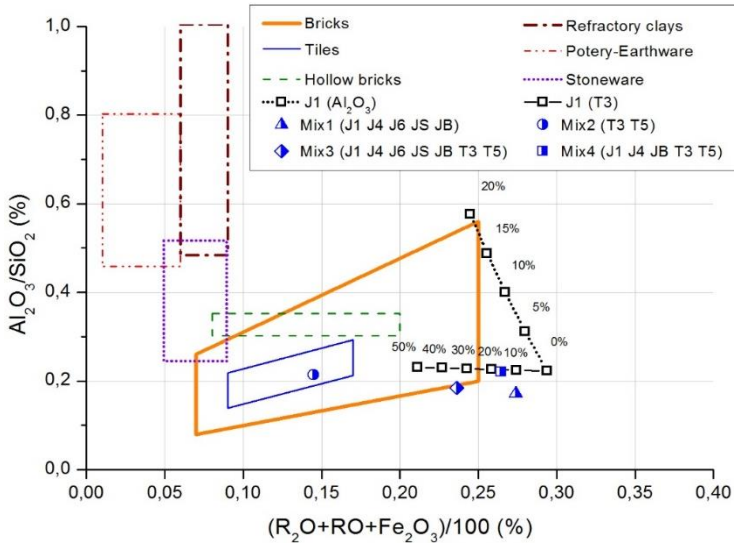

Figure 3. 7. Sediments shifting into fired bricks zones with oxides (Yamaguchi, 2019)

Figure 3.8 is a ternary diagram based on the oxide content of the soil that shows the suitable zone for fired bricks. Usumacinta River sediment's suitability for fired bricks based on their oxide content is shown in Figure 3.8 (Taha, 2017).

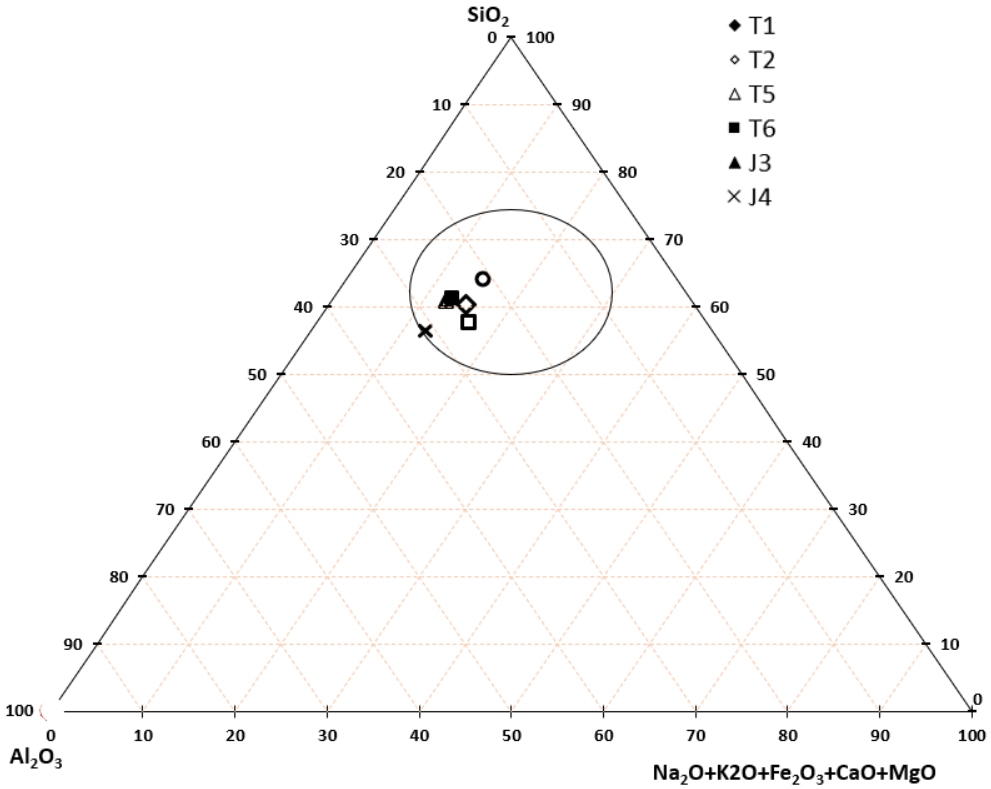

Figure 3. 8. Ternary diagram based on oxides content of sediments

It can be seen from Figure 3.8 that all the Usumacinta River sediments are within the zone recommended for fired bricks represented by a black circle.

3.3.3 Sediments suitability for fired bricks with Atterberg limits

Clay workability chart defines moulding characteristics of sediments with different zones based on Atterberg limits of sediments. In Figure 3.9, sediments have optimum moulding characteristics inside zone C, good moulding characteristics in zone B and high shrinkage in the zone (Fonseca et al., 2015). Usumacinta River sediment's suitability for moulding is shown in the clay workability chart in Figure 3.9.

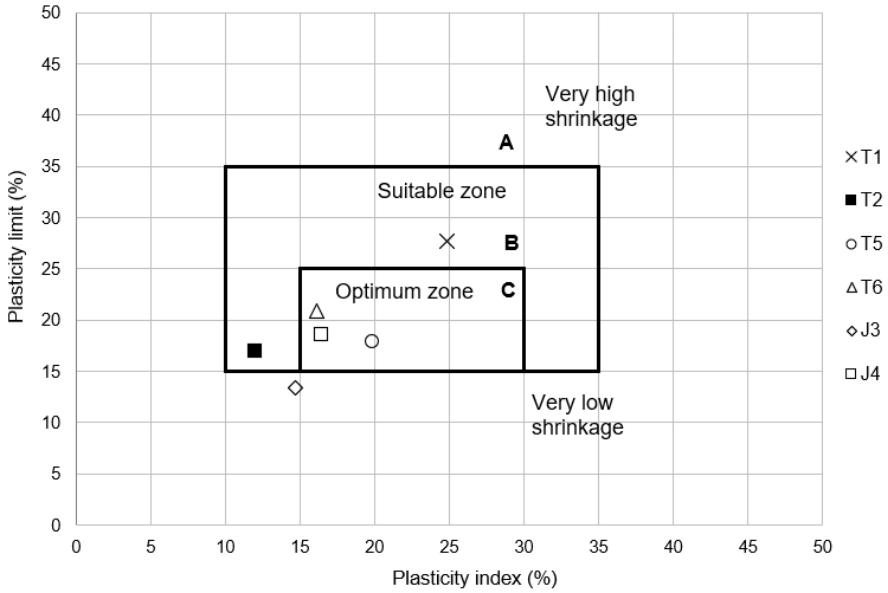

Figure 3. 9. Clay workability chart

It can be seen from Figure 3.9 that most of the sediments have optimum moulding characteristics. T1 and T2 sediments are within the zone having good moulding characteristics while J3 sediments are outside the recommended zones. Moulding characteristics vary with Atterberg limits, sand content and clay content of sediments.

3.3.4 Presence of pollutants

Presence of pollutants in Usumacinta River sediments is negligible (discussed in chapter 2) and their level is below the thresholds recommended by French authorities. Therefore, Usumacinta River sediments can be used in bricks without any additional treatment. Presence of pollutants in dredged sediments has social and economic barriers to the marketing of bricks as consumers are susceptible to the quality of bricks and presence of chemical contaminants (Cappuyns et al., 2015).

3.3.5 Manufacturing of bricks

Fired brick manufacturing consists of four steps which are material preparation, moulding or extrusion, drying and firing. In material preparation, sediments and moulding moisture content are mixed followed by moulding of bricks. Moulded bricks samples are compacted to remove the voids and dried in the oven. Dried brick specimens are fired at high temperatures in oven or kilns (Brick industry association, 2006). Fired brick manufacturing and testing steps are shown in Figure 3.10.

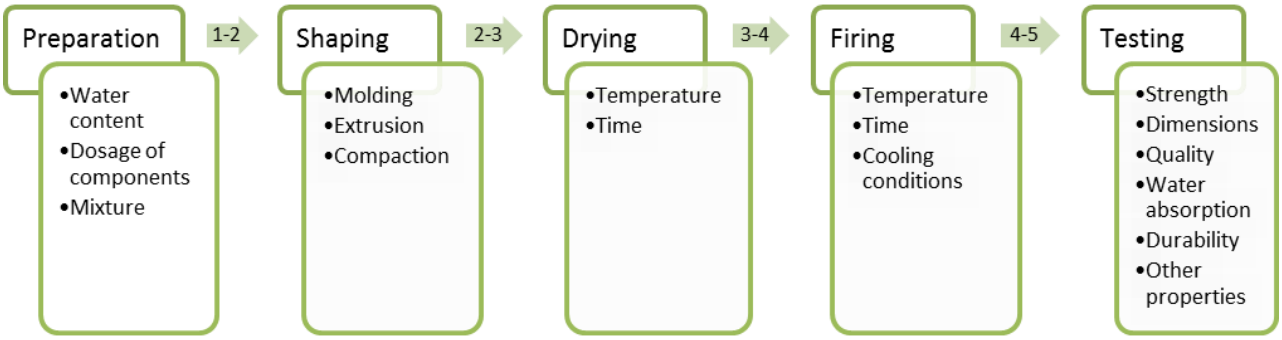

Figure 3. 10. Steps for manufacturing and controlling sediment-based fired brick samples

Manufacturing process of Usumacinta River sediments-based bricks is shown in Figure 3.11.

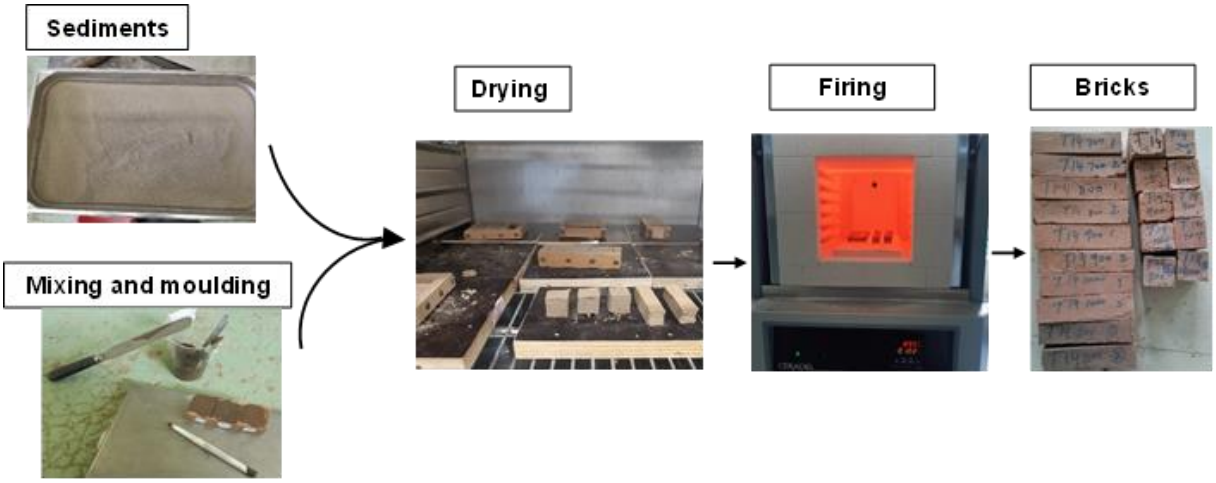

Figure 3. 11. Manufacturing process of fired bricks

(a) Material preparation

In material preparation, soil is mixed with to make a homogenous mixture. Usumacinta River sediments were dried, crushed, grinded and passed through a 2 mm sieve. Sediments mixture for fired bricks was prepared with the addition of moulding moisture content found with the Sembenelli diagram which is commonly used in bricks industry. Moisture content was taken at the midpoint between the liquidity and plasticity limit, shown in 3.10. In the plasticity chart, a new line crossing through the sediment location and parallel to the A line is drawn. The water content where this new parallel line passes through X-axis gives the value of the shrinkage limit. A vertical line is drawn from the sediment and the point where this line passes through X-axis is named D. Water content needed to mix with sediments ranges between points C and D and is named point E. Sembenelli plot for T2 sediment is given in Figure 3.12.

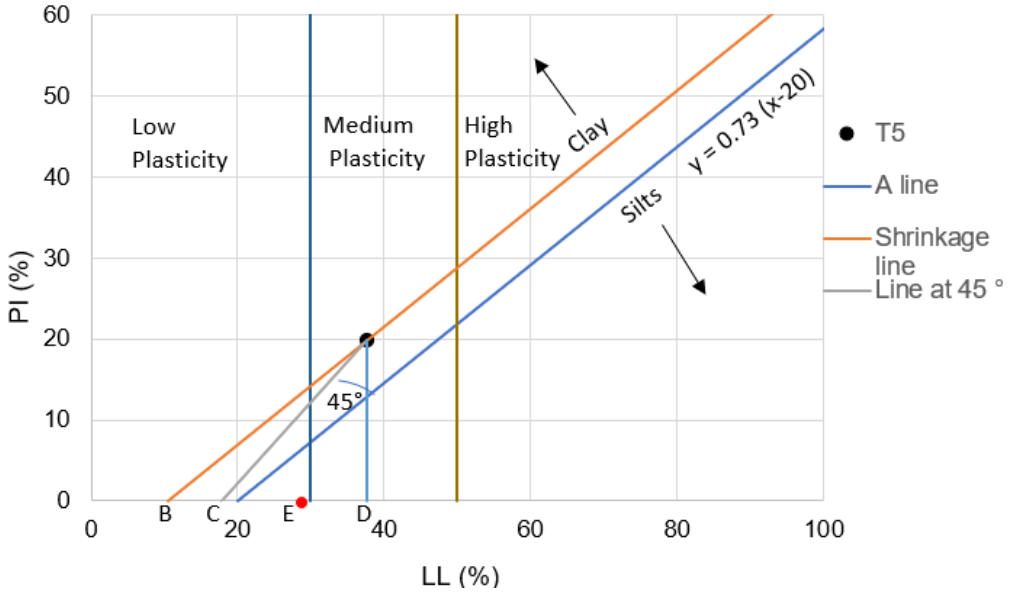

Figure 3. 12. Sembenelli graphical representation for T5 Usumacinta River sediment

The quantity of water added with sediments to prepare the sediments mixture is given in Table 3.1.

Table 3. 1. Water content used to mix sediments

Sediments	**T1**	**T2**	**T5**	**T6**	**J3**	**J4**
W (%)- E	29.83	23.44	26.4	25.125	29.625	42.93*

*Note: *for J4 sediments, plasticity limit of sediments was used as moulding moisture content*

J4 sediments have fine particle size and their clay content is highest among Usumacinta River sediments and its value is 13.4%. Furthermore, the organic matter of J4 sediments is also high among Usumacinta sediments and it is 5.72%. Due to higher clay content and organic matter, their liquidity and plasticity limits are high. Moulding moisture content from Figure 3.12 at point E for J4 is also very high and the solution at this moisture content shows liquid behavior. Therefore, the plasticity limit of J4 sediments was used as moulding moisture content for these sediments.

(b) Moulding

Usumacinta River sediments mixture was moulded into cubic and prismatic brick specimens of sizes 20*20*20 mm^3 and 15*15*60 mm^3 to observe the compressive and tensile strength of bricks. Bricks were manually moulded in bottomless wooden moulds. Moulds were filled with sediments, leveled and excessive clay on the top of moulds was removed by trimming. Furthermore, the inner surface of mould was oiled so that bricks can be removed easily from the moulds. Prismatic and cubic moulds are shown in Figure 3.13.

Figure 3. 13. Prismatic and cubic moulds

(c) Drying of bricks

Usumacinta bricks samples were dried in the oven at 60 °C for 4-12 hours. Drying of bricks removes the moisture, preserves the shape and prevents crack development during firing. Furthermore, drying of bricks prevents the bricks from swelling at a high temperature which happens due to moisture entrapped in the bricks. Usumacinta bricks drying in the oven is shown in Figure 3.11. Dried Usumacinta bricks samples are shown in Figure 3.14.

Figure 3. 14. Dried Usumacinta bricks

Shrinkage in Usumacinta bricks occurs during the drying of bricks due to the evaporation of water. Shrinkage of bricks is considerably high in clayey sediments such as T5 and J4.

(d) Firing of bricks

Dried Usumacinta bricks were fired in an oven for six hours at a temperature range of 700 °C to 1100 °C which is a common temperature range for firing bricks in brick kilns and literature studies (Karaman et al., 2006; Johari et al., 2010; Ettoumi et al., 2020; Wei et al., 2021). The firing of Usumacinta bricks in the oven is shown in Figure 3.15a. Figure 3.15b shows the firing program of the oven.

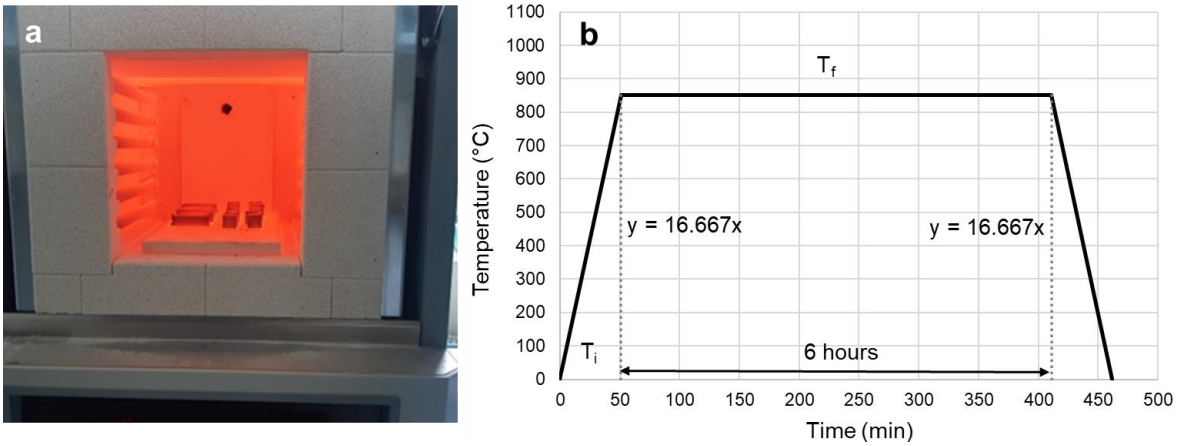

Figure 3. 15. Firing of Usumacinta bricks (a) and firing program of the oven (b)

In Figure 3.15b, initial temperature (T_i) starts from zero and gradually rises to the final temperature (T_f) which is the final value of temperature set to burn the bricks *i.e.* 700°C to 1100 °C and kept constant for 6 hours. After 6 hours, the temperature gradually becomes zero. Bricks were cooled after firing to transport. Cubic and prismatic brick specimens after firing are shown in Figure 3.16.

Figure 3. 16. Usumacinta bricks cubic (a) and prismatic specimens (b)

Several reactions take place in bricks during firing at different temperatures such as moisture evaporation, burning of organic matter and oxidation. During burning, dehydration and oxidation start at a temperature around 450 °C. While the phenomenon of vitrification starts at a temperature around 950 °C. At high temperatures, the components of bricks having low melting points adopt the liquid phase and fill the empty pores inside the bricks. Figure 3.17 shows the reactions in fired bricks at high temperatures.

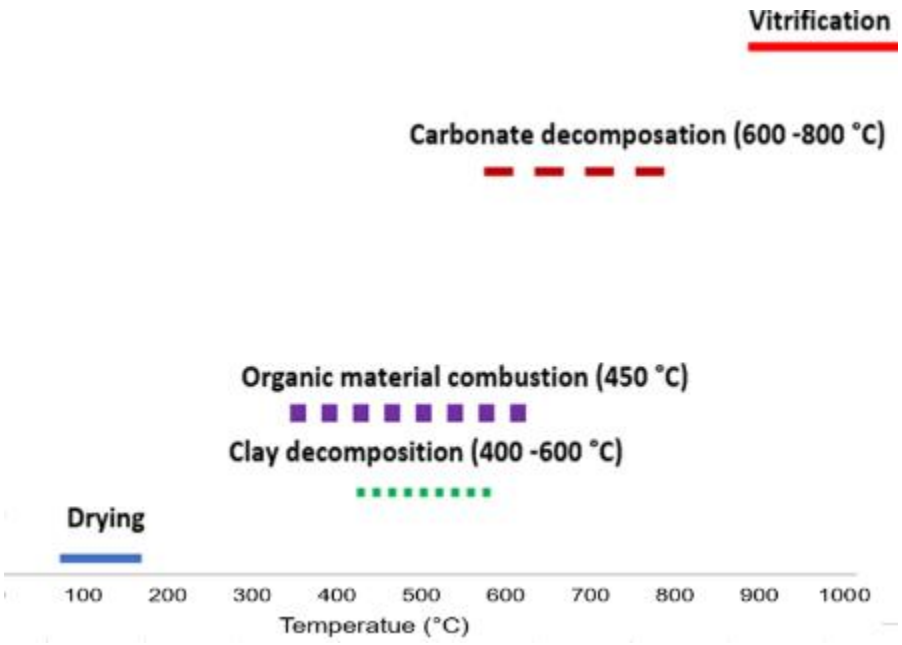

Figure 3. 17. Reactions during brick firing

During the firing of bricks, organic matter inside the brick is combusted which creates pores. Presence of small pores leads to density reduction and higher thermal resistance of bricks. Organic matter of Usumacinta River sediments is below 6% which is considered the low organic matter.

Lime pitting of bricks happens at the surface of bricks by the expansion of calcium carbonate with moisture content. Excessive carbonate content causes swelling and disintegration of bricks. Evaporation of gases such as CO_2 during firing leads to the popping phenomenon in which brick parts split with gas emissions. It may damage the kiln. Popping in Usumacinta bricks is shown in Figure 3.18.

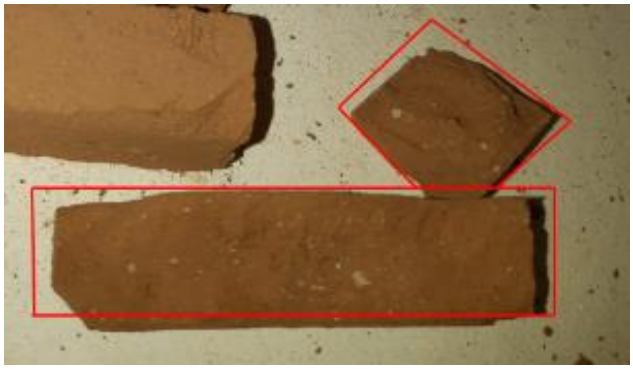

Figure 3. 18. Damaged J4 prismatic and cubic bricks in the oven

Bricks offer different colors which depend on different minerals present inside the sediments. Color of bricks changes with increasing temperature. Usumacinta brick's color variation at different firing temperatures is shown in Figure 3.19.

Figure 3. 19. Color variation with firing temperature in Usumacinta bricks

Usumacinta bricks exhibit dark color at high temperatures. Important oxides in Usumacinta River sediments are alumina, silica, iron, calcium and magnesium. Iron, calcium and magnesium oxide give bricks red, white and dark colors respectively on firing. Kaolinite and quartz are responsible for the yellow color of bricks (Kreimeyer, 1986).

3.3.6 Strength optimization of fired bricks

Sediment suitability for fired bricks can be improved by mixing different sediments. Figure 3.2 describes the approaches to define sediments mixture based on their dredging sites, mineralogy, granulometry, specific surface area and chemical composition to optimize the strength of bricks.

Usumacinta river sediment-based fired bricks experimentation methodology

Firing temperature T_f =750°C – Water content of manufacturing (Use of Sembenelli diagram, 1966) $W_{cm} = (W_L+W_P)/2$

Methodology process	Approach methodology	Sediment type or mix of sediments	Diagram of reference	Papers of reference	Unicaen references	Common references	Type of testing
From case-by-case	Ad hoc approach	Sediment by sediment from each barrel	---	Hussain et al. 2020	T1-4C; T5-10C; T6-14C;T6-18C; J3-09C;J3-10C; J4-13C;J6-C	T1;T5;T6 J3;J4;J6	UCS,ITS, WAT
	Site approach	Mix of sediments from each site J or T	---	Hussain et al. 2020	T1-4C+T5-10C+ T6-14C+T6-18C; J3-09C+J3-10C+ J4-13C+J6-C	T1+T5+T6=T J3+J4+J6=J[4]	UCS,ITS, WAT
	Global approach	Mix of all sediments J+T	---	Hussain et al. 2020	T1-4C+T5-10C+ T6-14C+T6-18C+ J3-09C+J3-10C+ J4-13C+J6-C	T+J=JT	UCS,ITS, WAT
Industrial approach - CTMNC	Plasticity approach		Gippini (1969)	Anger (2014)			UCS,ITS, WAT
	Particle size approach		Winkler (1954)	Anger (2014), Yamaguchi (2019)			UCS,ITS, WAT
	Chemical approach		Rankin-Wright (1915), Agustinik (1957)	A. Faure (2017), Yamaguchi (2019)			UCS,ITS, WAT
	Mineralogical approach		MIF - Haurine (2016)	Haurine (2015), Del Negro (2019)			UCS,ITS, WAT
	Statistical approach		Dendogram	Del Negro (2019)			UCS,ITS, WAT
to optimization	Optimization		700°C<T_f<1100°C W_P<W_{cm}<W_L				UCS,ITS, WAT

Figure 3. 20. Methodology and approaches used for optimization (Levacher, 2020).

Note: UCS = unconfined compressive strength; ITS = indirect tensile strength; WAT=water absorption test; J=Jonuta – T=Tenosique

Different Usumacinta River sediments mixtures based on approaches described in Figure 3.20 are shown in Table 3.2.

Table 3. 2. Sediments mixtures suggested with different approaches

Approaches	**Oxides**	**SSA**	**Winkler**	**Augustinik**
Mixtures	T1T2T6, J3T5, J1J5, J4, T3	T2T6, T1J3	J5, J1, J1J5, T3, J3T5, T1T2T6	J5, T3, J3T5, J1J5, T1T2T6, J1

Note: J1, J3, J5, T3 sediments are Mexican sediments stored at UGA (University of Gustave Eiffel)

Usumacinta bricks were manufactured with individual sediments from Jonuta and Tenosique sites. In the site-based approach, sediments of Jonuta (J3 and J4) were mixed to make fired bricks and named J. Similarly, Tenosique site sediments (T1, T2, T5, T6) were mixed and named T. Finally, both Tenosique and Jonuta sediments were mixed in the global approach to manufacture bricks.

3.3.7 Scale effect of brick dimensions

Different cubic and prismatic size specimens were manufactured to observe the influence of scale on the mechanical characteristics of fired bricks. For this purpose, cubic bricks of size 2*2*2 cm^3, 3*3*3 cm^3 and prismatic bricks of size 1.5*1.5*6 cm^3, 2*2*8 cm^3, 3*3*12 cm^3 and 4*4*16 cm^3 were manufactured. Compressive strength, flexural strength, density and shrinkage limit of these brick samples were determined to observe the influence of bricks size on these characteristics. Bricks specimens of J4 (J4-13C) and T5 (T5-10C) sediments are shown in Figure 3.21.

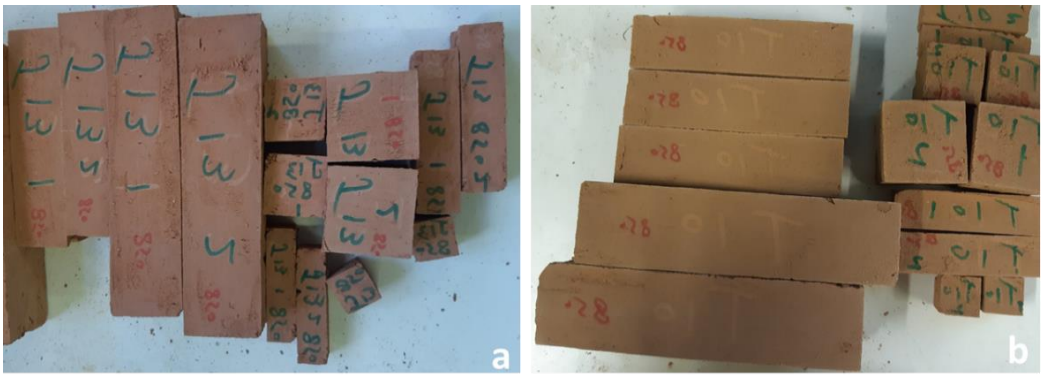

Figure 3. 21. Fired bricks samples of J4-13C (a) and T5-10C (b)

3.3.8 Temperature and moulding moisture content variation

Compressive and tensile strength of bricks strength changes with firing temperature and moulding moisture content. Prismatic and cubic brick samples were manufactured at firing temperature of 700°C to1100 °C at the different moulding moisture content (PL, 0.25PI, 0.5PI, 0.75PI and LL) for optimization of tensile and compressive strength of bricks.

3.3.9 Fired bricks for wall construction

Fired bricks of size 4*4*16 cm^3 were manufactured with T5-10C sediments for building fired bricks wall to observe their behavior under horizontal loading and their durability. The brick samples were dried at 60 °C and fired at 850 °C. Bricks samples drying, and firing is shown in Figures 3.22a and 3.22b.

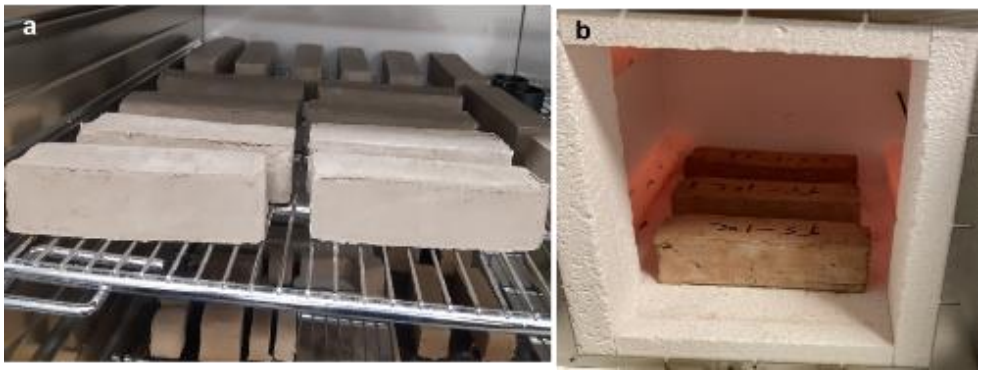

Figure 3. 22. Drying and firing of bricks

Fired bricks used for the construction of fired bricks wall are shown in Figure 3.23a and fired bricks wall to test its behavior under horizontal loading is shown in Figure 3.23b.

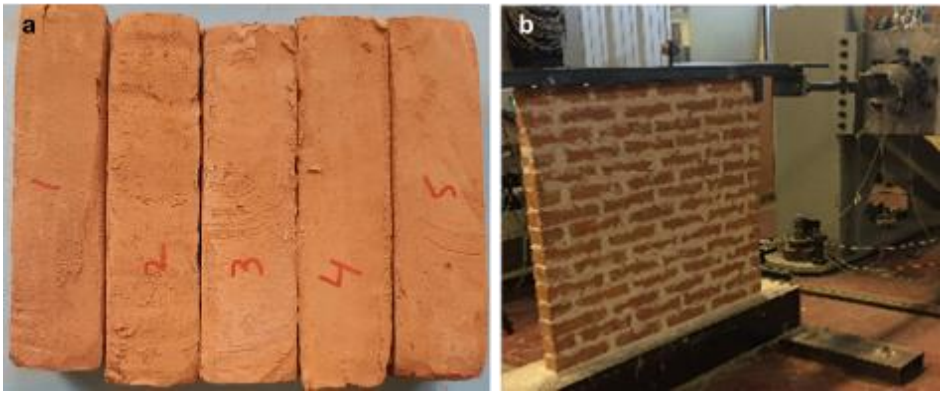

Figure 3. 23. Fired bricks samples (a) and horizontal loading of fired bricks wall

Physical characteristics of bricks such as density, linear shrinkage (LS) and loss on ignition (LOI) were determined and are shown in Table 3.3.

Table 3. 3. Characteristics of fired bricks

Bricks	LOI (%)	LS (%)	Density (kg/m^3)
T5	9.54	0.35	1731.1

Bricks from T5 sediments show a 9.54% loss on ignition when fired at 850 °C. ATG analysis of T5 sediments was performed at a temperature range of 0°C to 800 °C. Figure 3.24 shows the mass loss of Usumacinta River sediments (T5) at a temperature range of 0 °C to 800 °C. At this temperature range, inherent water evaporation takes place at a temperature of 0°C to 200 °C, burning of organic matter at 200 °C to 500 °C and emission of CO_2 associated with chemical

reaction of $CaCO_3$ at 500 to 800 °C. These reactions are responsible for mass loss in sediments. Similar reactions take place during firing of bricks and ATG test on sediments.

Mass loss of T5 sediments associated with different reactions with increasing temperature from 0°C to 800 °C in ATG test is shown in Figure 3.24.

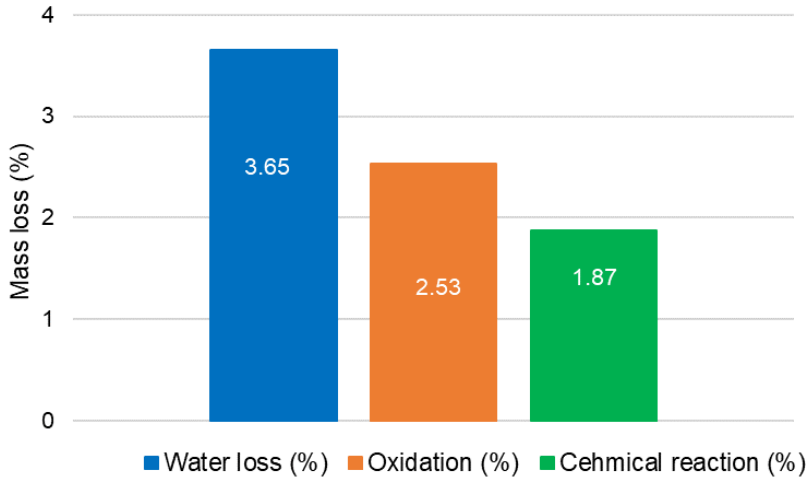

Figure 3. 24. Mass loss at different temperatures

Overall, 8.04 % mass loss occurs in T5 sediments when fired at a temperature range of 0°C to 800 °C during the ATG test while the loss on ignition of fired bricks from T5 sediments in the oven is around 9.54%.

3.3. Testing of bricks

3.3.1 Physical characteristics

Physical characteristics of fired bricks include linear shrinkage, loss on ignition, water absorption, and density etc.

(a) Linear shrinkage (LS)

The length of bricks decreases by burning the bricks at a high temperature. Linear shrinkage in Usumacinta bricks was calculated with equation 3.1.

$$Linear\ shrinkage(\%) = \frac{Length\ before\ drying - Length\ after\ drying}{Lenght\ before\ drying} * 100 \qquad (3.1)$$

(b) Loss on ignition (LOI)

Loss on ignition of bricks occurs due to evaporation of inherent moisture, clay decomposition, burning of organic matter and carbonate decompositions when bricks are fired at high temperatures. Percentage of organic matter and carbonate content have a significant influence on LOI. Loss on ignition of Usumacinta bricks was observed by their mass difference before and after firing.

(c) Water absorption (WA)

Water absorption of Usumacinta bricks was found by immersing the bricks in water for 24 hours as shown in Figure 3.25a. Equation 3.2 was used to calculate water absorption of Usumacinta bricks.

$$\text{Water absorption } (\%) = \frac{\text{Saturated weight} - \text{Dry weight}}{\text{Dry weight}} * 100 \quad (3.2)$$

In this equation, saturated weight is the weight of brick after keeping in water for 24 hours and dry weight is the weight of the dry brick.

Efflorescence of bricks was also observed by immersing bricks in water for one week. Efflorescence is negligible in Usumacinta bricks as only a few bricks show slight salt deposition. Salt accumulation on Usumacinta bricks is shown in Figure 3.25b.

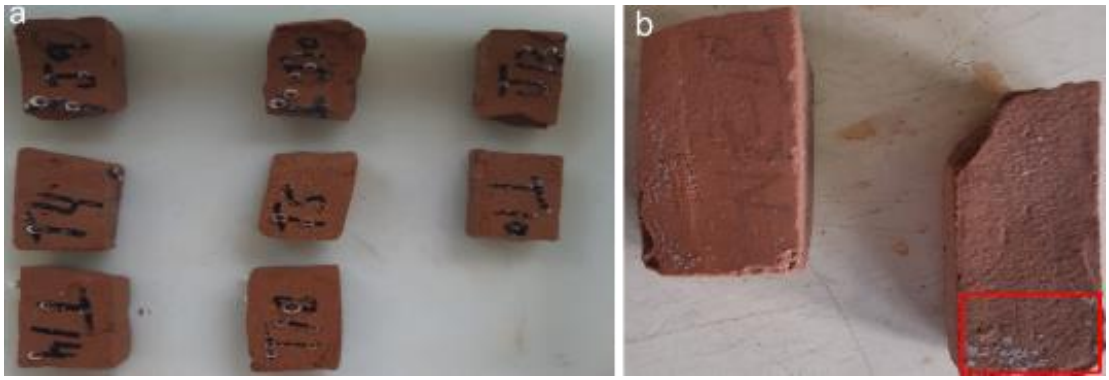

Figure 3. 25. Water absorption testing (a) and salt accumulation on Usumacinta bricks (b)

(d) Bulk density

Bulk density of Usumacinta bricks was calculated with their mass and volume by using equation 3.3.

$$Bulk\ density\ \left(\frac{g}{cm^3}\right) = \frac{Dry\ weight}{Volume} \quad (3.3)$$

3.3.2 Mechanical characteristics

Mechanical properties of bricks include compressive strength, modulus of elasticity and tensile strength. Fired bricks have usually high compressive strength and tensile strength. Strength of bricks depends on the grain size of sediments, oxide content, moulding moisture content, compaction procedure adopted, presence of minerals and firing temperature.

(a) Compressive strength of bricks

Compressive and tensile strength of Usumacinta bricks was found with Shimadzu AGS-X model machine by using 200 N and 50 KN sensors. Compressive strength testing of a Usumacinta brick sample and failure mode is shown in Figures 3.26a. A typical compressive load-deflection curve for Usumacinta bricks is shown in Figure 3.26b.

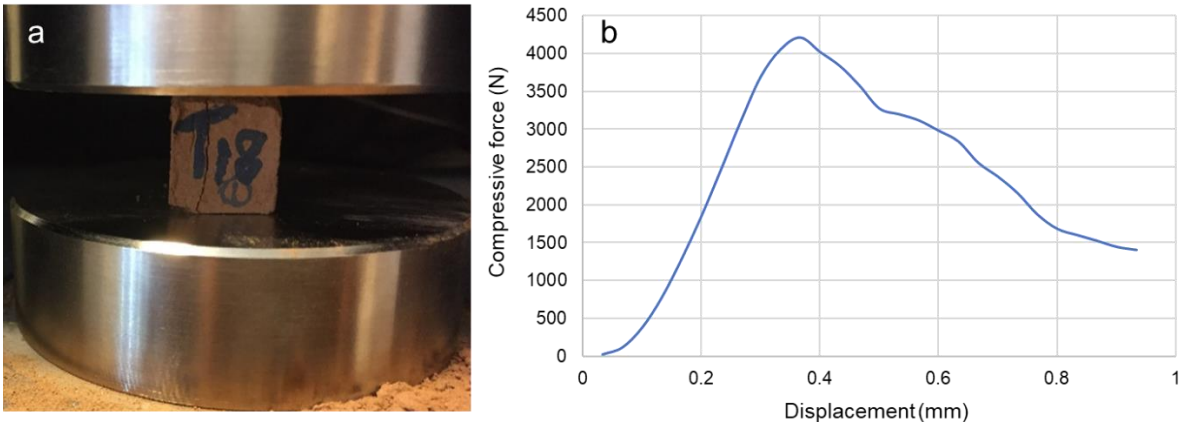

Figure 3. 26. Compressive strength test (a) and load deflection curve (b)

Compression load-deflection curve in Figure 3.26b shows that compressive load increases linearly up to the failure point.

Compressive strength of Usumacinta bricks was determined with compressive load by using equation 3.4.

$$\text{Compressive strength} = \frac{Compressive\ force}{Area\ of\ brick} \qquad (3.4)$$

Modulus of elasticity of Usumacinta bricks was determined from stress-strain curves of Usumacinta bricks.

(b) Flexural strength of bricks

Flexural strength (indirect tensile strength) of Usumacinta bricks was found by three-point bending test. Flexural strength testing of the prismatic brick sample is shown in Figure 3.27a and a typical flexural load deflection curve for fired bricks is presented in Figure 3.27b.

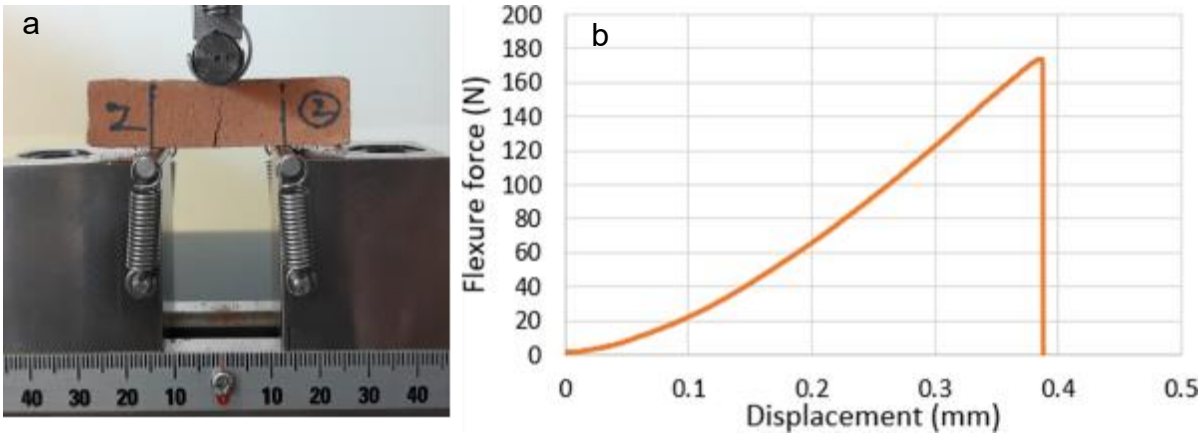

Figure 3. 27. Flexural strength test and failure (a) and load deflection curve (b)

Load deflection curve in Figure 3.27b shows that the flexural load of bricks increases linearly and after initial cracking, a sudden drop in flexural force is observed with zero deflection.

Flexural strength of fired Usumacinta bricks was calculated with the following formula.

$$Flexural\ strength = \frac{1.5*F*l}{bd^2} \quad (3.5)$$

where F= flexural force, l= length of supported span, b= width of brick and d= height of brick.

3.4. Results and analysis

3.4.1 Physical characteristics of bricks

Physical characteristics of fired bricks such as linear shrinkage, density, loss on ignition and water absorption of bricks depend on the raw material used in manufacturing bricks and the firing temperature of bricks.

(a) Linear shrinkage (LS)

Usumacinta bricks manufactured at a temperature range of 700 °C to 1100 °C exhibit shrinkage on drying and firing. Linear shrinkage in Usumacinta bricks is shown in Table 3.4.

Table 3. 4. Linear shrinkage in bricks

Sediments	**LS (%)** 700 °C	**LS (%)** 800 °C	**LS (%)** 900 °C	**LS (%)** 1000 °C	**LS (%)** 1100 °C
T1	0.56	0.9	1.62	0.72	1.75
T2	-	-	-	-	-
T5	10.77	10.25	12.82	11.1	13.25
T6	1.255	2.155	2.35	3.42	3.405
J3	4.95	4.655	4.58	5.66	6.865
J4	12.72	13.91	12.96	12.15	13.5

Shrinkage in bricks increases with increasing clay content, moulding moisture content and firing temperature. J4 and T5 sediments have the highest clay content in Usumacinta and linear shrinkage in bricks for these sediments is also very high and ranges from 10.77 % to 13.5 %. Higher percentage of fine particles, organic matter and higher moulding moisture content has a significant influence on their linear shrinkage. In sandy sediments such as T1, shrinkage is very low even at a high temperature of 1100 °C. T2 sediments have high sand content and shrinkage in bricks from T2 sediments bricks is negligible. Linear shrinkage of fired bricks varies with soil characteristics and in some literature studies its value varies from 4.5% to 7.62% (Diao et al., 2021; Srisuwan and Phonphuak, 2020).

Graph in Figure 3.28 shows the variation in linear shrinkage with temperature. Linear shrinkage in this graph is increasing with temperature.

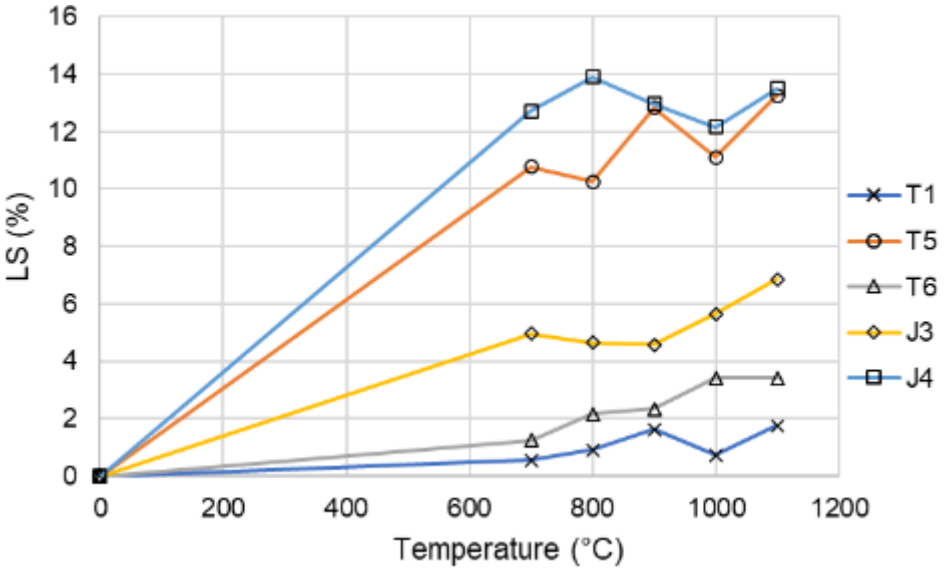

Figure 3. 28. Linear shrinkage variation in Usumacinta River

(b) Density of bricks

Density of Usumacinta bricks was found with their mass and volume before performing different tests. Density variation of Usumacinta bricks with temperature is shown in Table 3.5.

Table 3. 5. Density variation with temperature

Sediments	**ρ (kg/m^3)** 700 °C	**ρ (kg/m^3)** 800 °C	**ρ (kg/m^3)** 900 °C	**ρ (kg/m^3)** 1000 °C	**ρ (kg/m^3)** 1100 °C
T1	994.39	1268.93	1303.56	1188.95	1244.42
T2	1146.27	1155.02	1148.73	-	1320.68
T5	1683.36	1606.64	1724.42	1672.16	1818.39
T6	1321.23	1337.40	1277.17	1358.05	1432.05
J3	1330.98	1281.02	1226.13	1302.10	1401.40
J4	1702.64	1588.79	1554.62	1666.29	1637.80

Density of bricks increases with increasing temperature and it is maximum at 1100 °C. This is due to the elimination of pores with vitrification. Sandy sediments such as T1 and T2 have the lowest density. Clayey sediments (J4 and T5) have maximum density due to higher shrinkage associated with higher fine particles, higher moulding moisture content and higher organic matter in J4 sediments.

Density increase with temperature for Usumacinta River sediments in graphical form is shown in Figure 3.29.

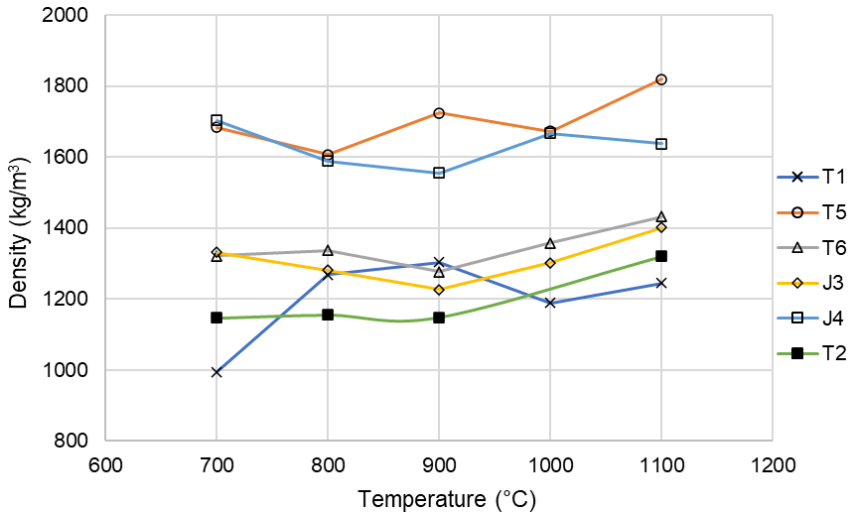

Figure 3. 29. Density variation with temperature

(c) Loss on ignition (LOI)

Loss on ignition of fired bricks was determined with mass loss of bricks after burning at high temperature. Loss on ignition of Usumacinta bricks is shown in Table 3.6.

Table 3. 6. Loss on ignition of Usumacinta bricks

Sediments	**LOI (%)** 700 °C	**LOI (%)** 800 °C	**LOI (%)** 900 °C	**LOI (%)** 1000 °C	**LOI (%)** 1100 °C
T1	0.56	0.91	1.625	0.72	1.75
T2	-	-	-	-	-
T5	10.7	10.26	12.82	11.1	13.26
T6	1.255	2.16	2.35	3.42	3.36
J3	4.95	4.66	4.59	5.66	6.86
J4	12.72	13.92	12.96	12.16	13.51

Loss on ignition of J4 and T5 sediments is high, and its value is more than 10%. Both sediments have higher clay content. T2 sediments have higher sand content and their loss on ignition is negligible. Overall loss on ignition of bricks increases with increasing temperature as with increasing temperature, emission of gases occurs due to burning of organic matter and decomposition of carbonates. Voids in bricks are also removed at higher temperatures due to vitrification. All these phenomena contribute to increasing LOI. Furthermore, organic matter in J4 sediments is highest which also contributes to the loss on ignition of these bricks.

Loss on ignition of Usumacinta sediments at 850 °C with ATG test is shown in Table 3.7.

Table 3. 7. Loss on ignition (LOI) of sediments in ATG and oven firing of bricks

Sediments	LOI oven (%)	LOI ATG (%)
T1	0.91	10.86
T5	10.28	8.04
T6	2.16	11.86
J3	4.66	12.69
J4	13.92	15.6

Figure 3.30 show the relationship between loss on ignition between the two methods.

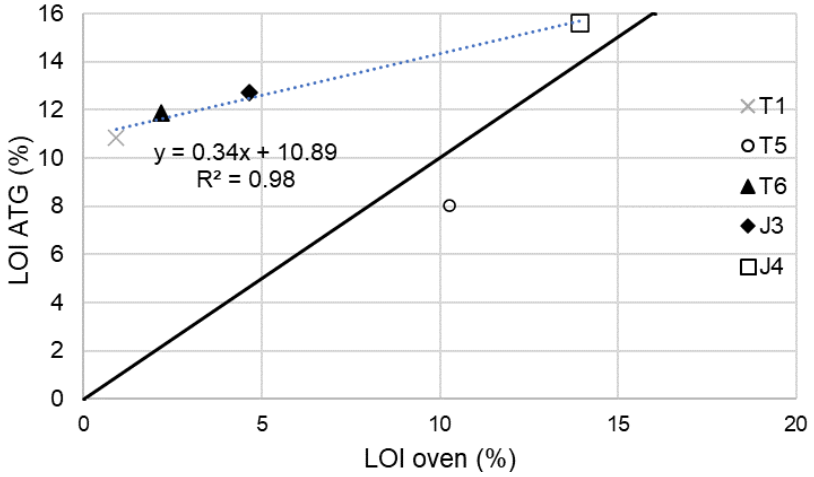

Figure 3. 30. Loss on ignition with ATG and oven burning

Table 3.8 and Figure 3.30 show that most of the values of LOI with ATG test are overestimated except for T5 sediments which lie close to the bisector line in Figure 3.30. Overestimation of results by ATG is because only a few grams sediments are used in ATG test while in the firing of bricks in the oven, the sediments quantity used is higher. It can be seen in Figure 3.30 that, there exists a correlation between LOI from ATG and LOI from the oven by excluding T5 values. LOI of sediments from ATG test is around 34% of LOI from firing bricks in the oven.

Loss on ignition of fired bricks depends on the characteristics of soil and its value in fired bricks varies from 3% to 18% in fired bricks used in France (Kornmann, 2009). Table 3.8 shows the LOI of fired bricks in different studies.

Table 3. 8. Loss on ignition of fired bricks

Soil origin	LOI (%)	Reference
River sediments	12.81	Mezencevova et al., 2012
Local clay industry	8.47	Kazmi et al., 2017
Soil quarry	12.15	Baronio and Binda, 1997
Soil quarry	6.03	Fgaier et al., 2015
Local raw material	6.27	Millogo et al., 2008
Alluvial deposits	3.39	Manoharan et al., 2011

Note: Reference for this Table are given in chapter 1.

Table 3.9 shows that loss on ignition values of Usumacinta River sediments are similar to LOI values reported in literature.

(d) Water absorption (WA)

Water absorption of Usumacinta bricks fired at 850 °C was determined by immersing the bricks for 24 hours. Results are shown in Table 3.9.

Table 3. 9. Water absorption of bricks fired at 850 °C

Sediments	T1	T2	T5	T6	J3	J4
WA (%)	22.39	17.56	10.71	19.31	21.53	16.16

Water absorption of Usumacinta bricks varies between 10.71% to 22.39%. T5 and J4 are clayey sediments and they have the lowest water absorption due to higher shrinkage which decreases the pores and water absorption of bricks. Water absorption of Usumacinta River sediments is similar to the recommended water absorption limits for good quality bricks in ASTM standards (ASTM C62-17, 2017) which is 15%-22% of bricks mass after immersion of 24 hours.

Firing temperature and porosity of bricks significantly influence on the water absorption of bricks. Water absorption capacity of fired bricks decreases with increasing temperature. Vitrification of bricks at high temperature decreases the pores in bricks which reduces the water absorption capacity of bricks. Bricks expand and contract with a change in moisture content. Higher water absorption of bricks reduces the durability of bricks. However, a small quantity of pores is essential for the absorption of a certain quantity of water. Figure 3.31 shows the increase in bricks absorption of water with temperature. Most of the mass gain takes place during the first hour of immersion.

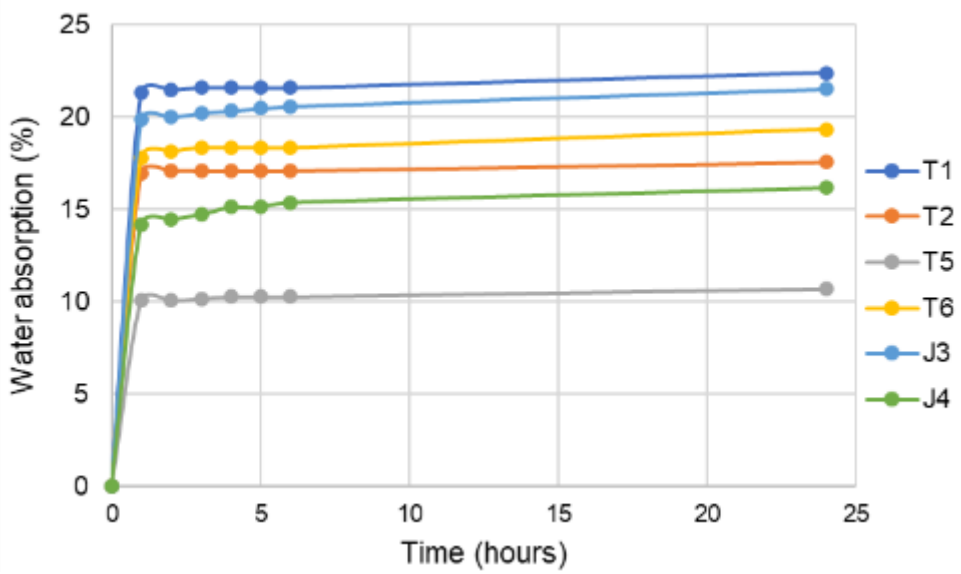

Figure 3. 31. Water absorption of bricks fired at 850 °C with time

Table 3.10 show the absorption during the first hours and 24 hours of immersion. The percentage of water absorption with respect to final absorption is also shown.

Table 3. 10. Water absorption after 1 hour and 24 hours immersion of bricks fired at 850 °C

Time	1-hour (%)	24-hours (%)	Initial immersion (%)
T1	21.33	22.39	95.27
T2	16.98	17.56	96.70
T5	10.06	10.71	93.96
T6	17.81	19.31	92.23
J3	19.87	21.53	92.29
J4	14.20	16.16	87.89

Most of the water absorption in bricks takes place during the first one hour of immersion. Immersion in the first hours is maximum in bricks with sandy sediments (T2) which is 96.70% while for clay sediments, initial absorption in the first one hour is lowest and its value is 87.89%.

Water absorption of bricks decreases with increasing firing temperature. The relationship between the water absorption coefficient and temperature for Usumacinta bricks does not follow a linear trend for bricks in sediments with low percentage of fine particles and low strength. However, there exists a strong linear correlation between water absorption and firing temperature of bricks manufactured with clayey sediments such as T5 and J4. Figure 3.32 shows the relationship between water absorption and bricks firing temperature.

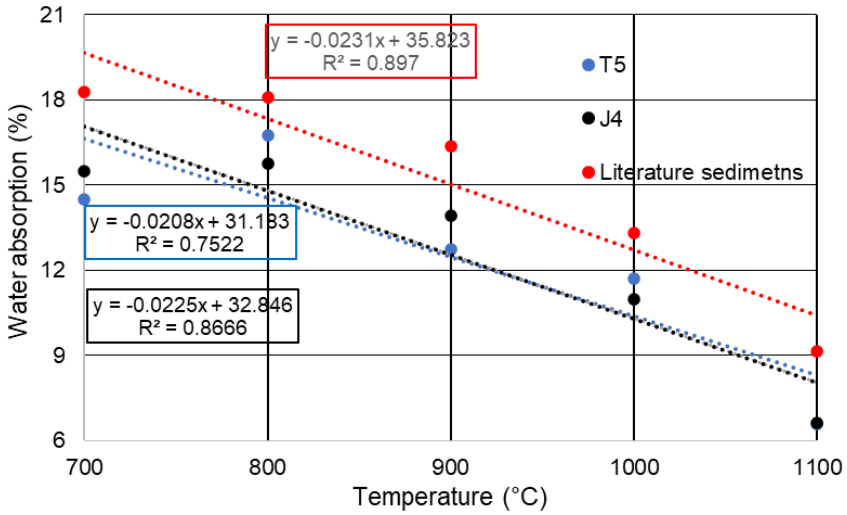

Figure 3. 32. Water absorption variation with bricks firing temperature

Figure 3.32 shows that water absorption of fired bricks decreases with increasing temperature. Karaman et al., (2005) studied bricks made with clay soil which have higher compressive strength. The following relation between firing temperature and water content was observed by

$$WA = -0.023T + 35.82 \quad (3.6)$$

Where WA = water absorption (%) and T= temperature (°C).

Relationship in equation 6 is similar to the relationship found for J4 and T5 sediments in Figure 3.32.

3.4.2 Mechanical characteristics of fired bricks

Important mechanical characteristics of bricks include compressive and tensile strength, elasticity modulus and flexion stiffness.

(a) Compressive strength of Usumacinta bricks

Compressive strength of Usumacinta bricks was determined at different firing temperatures and moulding moisture contents. Table 3.11 shows the compressive strength of Usumacinta bricks at different firing temperatures.

Table 3. 11. Compressive strength (MPa) of fired bricks with firing temperature variation

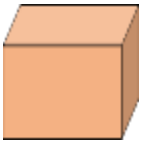

Specimen size = 20x20x20mm^3

Temperature variation				Water content = PL + (LL-PL) /2			
Approach	Sediments	700 °C	800 °C	850 °C	900 °C	1000 °C	1100 °C
Per site sampling	T1	0.40	0.57	0.53	1.84	0.68	2.69
	T2	0.10	0.12	0.94	0.83	0.67	2.00
	T5	15.51	7.59	4.92	13.15	9.04	16.67
	T6	1.98	3.17	3.18	4.37	1.93	6.75
	J3	4.08	5.23	4.10	6.25	5.57	13.11
	J4	17.04	19.00	19.15	15.57	15.65	19.38
Mixture by site	J	0.60	1.85	5.33	5.01	6.31	3.87
	T	0.255	0.39	2.42	0.28	1.98	2.88
Global mix	JT	0.525	1.24	1.68	2.25	2.56	4.4

Note: PL = plasticity limit and LL = liquidity limit; water content used is equal to PL as sediment mixture is very liquid at midpoint between LL and PL.

It can be observed from Table 3.11 that, at a moderate temperature of 850 °C, compressive strength for T5, J4 and mixture of Jonuta site sediments is greater than 3.5 MPa. Furthermore, T5, J3 and J4 sediments exhibit good compressive strength at all temperatures. The mixture of Jonuta sediments and the mixture of Tenosique and Jonuta sites also show good compressive strength at a temperature range of 700 °C to 1100 °C.

Compressive strength of fired bricks varies in different standards and depends on the type of application. Generally, its values vary from 3-15 MPa (IS 1077,1992; ASTM C62-17, 2017). Maximum compressive strength is observed with T5 sediments and J4 sediments. These sediments have higher clay content and suitable Atterberg limits for moulding. Moreover, their

chemical composition also lies in a zone suitable for fired bricks. T2 sediments have the lowest strength and are unsuitable for bricks due to high sand content and lower liquidity and plasticity limits. The strength of T1 sediments is also less due to a higher percentage of coarse particles. Higher sand content makes the bricks brittle and decreases their compressive strength.

Compressive strength of fired bricks increases with increasing temperature (Johari et al., 2010). Table 3.11 show that Usumacinta bricks have maximum compressive strength at 1100 °C which is above 5 MPa except for T1 and T2 sediments. At high temperatures, the fusion of sediments fills the pores and makes the bricks hard and strong. However, the high consumption of energy makes bricks costly.

Graph in Figure 3.33 shows the trends between temperature and compressive strength for Usumacinta River bricks. Trends show an increase in strength, but it is difficult to fit the data as a linear or polynomial trend.

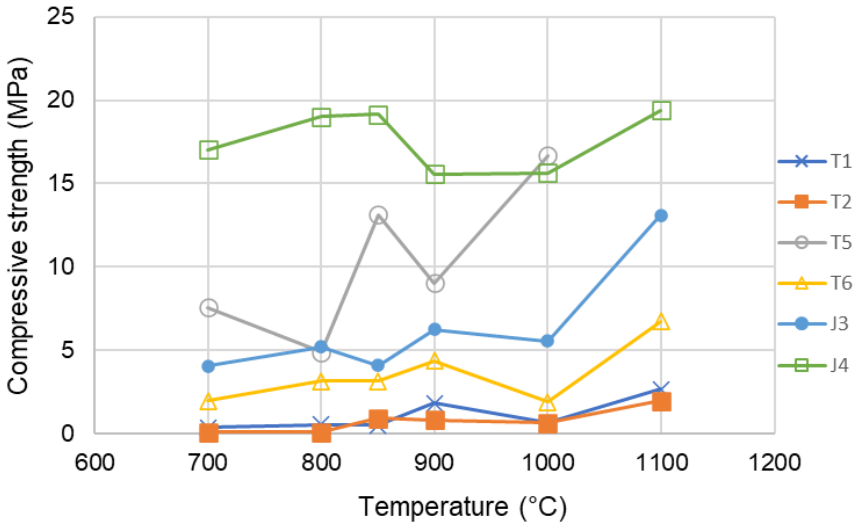

Figure 3. 33. Compressive strength variation with temperature

Fired bricks in literature have wide range of compressive strength. Table 3.21 shows that bricks compressive strength ranges from 1.9 to 29.4 MPa.

Moulding moisture content has a significant impact on compressive strength of fired bricks. Table 3.12 shows fired brick's compressive strength variation with moulding moisture content.

Table 3. 12. Compressive strength (MPa) of fired bricks with workability water content

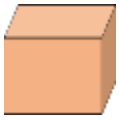

Specimen size = 20x20x20mm^3

Water content variation				Firing temperature = 1100°C		
Approach	Sediments	PL	PL + 0.25PI	PL + 0.5PI	PL + 0.75PI	LL
Per site sampling	T1	0.92	1.48	2.69	1.00	-
	T5	5.97	4.05	16.67	4.02	-
	T6	6.18	10.10	6.75	6.52	-
	J3	4.27	6.62	13.11	3.91	-
	J4	19.38	-	-	-	-
Mixture by site	J	-	9.03	3.87	4.72	-
	T	-	5.96	2.88	4.09	-
Global mix.	JT	-	10.04	4.4	3.51	-

Note: PL = plasticity limit, LL = liquidity limit and PI = plasticity index

It can be seen from Table 3.12 that bricks have maximum strength at moulding moisture content of PL+0.25PI and PL+0.5PI. Overall compressive strength of fired bricks is good at 1100 °C at all moulding moisture contents except T1 sediments. Highest strength is shown by J4 and T5 sediments. At 0.75PI, the strength of bricks is low due to the liquid nature of the mixture. T2 sediments bricks are very fragile. Therefore, additional bricks samples were not made from this sediment. J4 sediments have very high liquidity and plasticity limits, so bricks were made only at plasticity limits. Low and high moulding moisture contents affect the compaction, density and decrease the compressive strength of bricks. At liquidity limits, mixture tends to be too liquid and at the plasticity limit, it is difficult to mould the sediments. Therefore, intermediate moulding moisture content gives better results.

Compressive strength of bricks made with sediments mixtures suggested with specific surface area (SSA) approach, mineralogical approach, Winkler diagram and Augustinik diagram at a temperature range of 700 °C and 1100 °C is shown in Table 3.13.

Table 3. 13. Compressive strength (MPa) of different bricks mixes with temperature variation

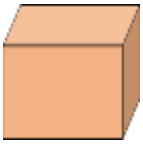

Specimen size = 20x20x20mm^3

Temperature variation				Water content = PL + (LL-PL) /2			
Approach	Sediments	700 °C	800 °C	850 °C	900 °C	1000 °C	1100 °C
Specific surface area (SSA)	J3T1	1.75	2.30	-	-	2.17	6.94
	T2T6		1.23	1.18	1.35	0.28	3.43
HCA-dendogram without mineralogy	T1T2T6			0.38	0.84		
	J3T5			1.23			1.99
	J1J5			1.20			
	J4						
	T3						
Winkler diagram	J5			3.71			
	J1			3.74			
	T3						

Note: HCA = Hierarchical classification analysis

Table 3.13 shows that mixture with specific surface area approach (J3T1 and T2T6) and with mineralogy approach (T1T2T6, J3T5and J1J5) have very low strength. Sediments suggested with the Winkler diagram (J5, J1) show good strength.

Compressive strength of Usumacinta bricks with varying dimensions is shown in Table 3.14.

Table 3. 14. Compressive strength of fired bricks with dimension variation

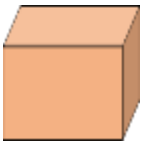

Specimen size = 20x20x20mm^3; 30*30*30 mm^3; 40*40*40 mm^3

Temperature = 850 °C			Water content = PL + (LL-PL) /2	
Approach	Sediments	20*20*20 mm^3	30*30*30 mm^3	40*40*40 mm^3
Per site of sampling	T1	0.52	3.91	0.69
	T5	4.92	25.03	10.51
	T6	3.18	3.94	1.43
	J3	4.10	10.24	1.71
	J4*	19.15	28.35	6.48

*Note: PL = plasticity limit and LL = liquidity limit; * water content used is equal to PL as sediment mixture is very liquid at midpoint between LL and PL.*

Table 3.15 shows that intermediate-size bricks have good compressive strength. Change in the dimension of bricks influences the compressive failure mode of bricks. Furthermore, due to the absence of compaction, there is a huge variation in compressive strength of brick specimens.

(b) Modulus of elasticity

Modulus of elasticity of fired bricks was calculated from compressive stress-strain curves. The values of modulus of elasticity are shown in Table 3.15.

Table 3. 15. Modulus of elasticity (MPa) variation with temperature

Sediments	**700 °C**	**800 °C**	**900 °C**	**1000 °C**	**1100 °C**
T1	13	22	114	37	159
T5	567	145	334	985	-
T6	58	99	225	96	274
J3	172	238	278	279	719
J4	1018	756	550	494	690
J	110	209	-	318	406
T	25	101	34	98	272
JT	58	178	-	228	457

Modulus of elasticity of Usumacinta bricks varies from 13 to 1018 MPa for Usumacinta bricks and it shows increases with increasing temperature. This is because modulus of elasticity of bricks increases with increasing compressive strength which increases with temperature. The

relationship between the modulus of elasticity and compressive strength for fired bricks manufactured with Usumacinta River sediments is presented in the shown in Figure 3.34.

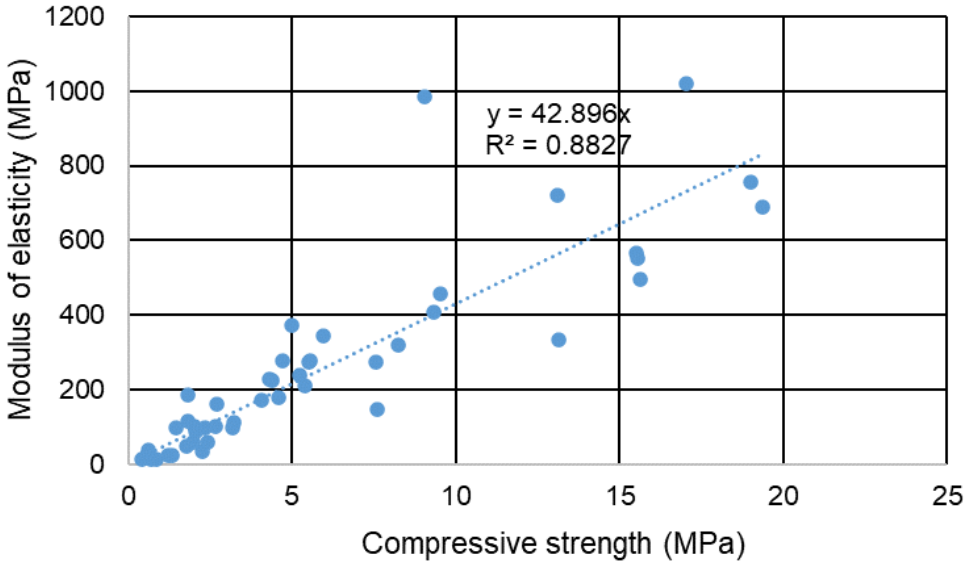

Figure 3. 34. Relationship between compressive strength and modulus of elasticity

Figure 3.34 shows that the modulus of elasticity of Usumacinta bricks is 42 to 43 times of compressive strength (UCS) for fired bricks at different temperatures.

(c) Flexural strength of Usumacinta bricks

The results of flexural strength testing of Usumacinta bricks at different temperatures are shown in Table 3.16.

Table 3. 16. Flexural strength (MPa) for fired bricks with firing temperature variation

Specimen size = 15x15x60mm^3

Temperature = 850 °C				Water content = PL + (LL-PL) /2			
Approach	Sediments	700 °C	800 °C	850 °C	900 °C	1000 °C	1100 °C
Per site sampling	T1	0.17	0.275	0.45	0.43	0.64	1.23
	T2	0.19	-	0.63	-	0.31	0.90
	T5	3.55	2.31	2.23	4.57	4.17	6.60
	T6	0.35	1.63	1.22	1.84	1.78	3.00
	J3	0.92	1.37	1.92	3.84	2.15	4.86
	J4*	6.35	9.01	7.66	7.30	12.82	8.68
Mixture by site	J	0.60	1.85	5.33	5.01	6.32	3.88
	T	0.26	0.39	2.42	0.29	1.99	2.88
Global mix.	JT	0.53	1.24	1.68	2.25	2.56	4.40

*Note: PL = plasticity limit and LL = liquidity limit; * water content used is equal to PL as sediment mixture is very liquid at the midpoint between LL and PL.*

Usumacinta bricks have a maximum tensile strength at 1100 °C. Table 3.16 shows that J4 (12.82 MPa at 1000 °C) and T5 (6.60 MPa at 1100 °C) sediments have maximum tensile strength due to a higher percentage of fine particles and suitable oxide composition. Tensile strength of T2 sediments is low due to higher sand content. MBV values of sediments indicate that T2 sediments have low plasticity while J4 sediments have highest plasticity. Organic matter, carbonate content and percentage of fine particles have a substantial impact on strength.

Relationship between flexural strength and temperature for individual sediments is shown in Figure 3.35.

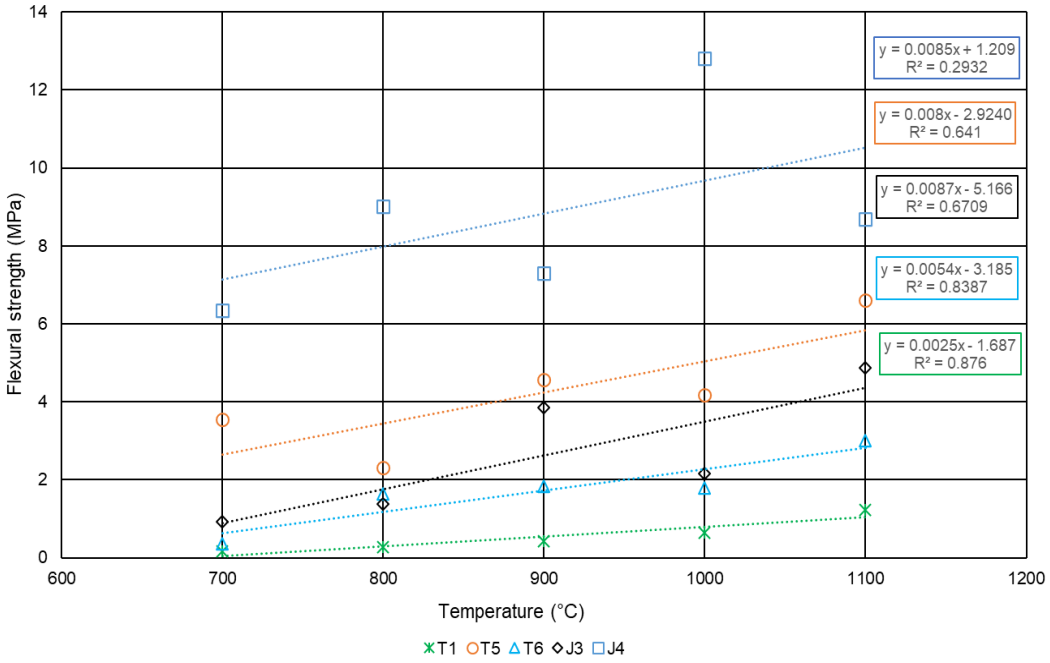

Figure 3. 35. Individual sediments brick flexural strength variation with temperature

Flexural strength of fired bricks increases with increasing temperature. Figure 3.35 shows flexural strength increases linearly for bricks with low strength (T1 and T6). However, for bricks with higher strength (J4 and T5) flexural strength increases with temperature but the increase is not linear. Karaman et al., 2006 observed the following relation between temperature and flexural strength for higher strength clay-based fired bricks, fired at a temperature range of 700 °C to 1100 °C.

$$\text{Flexural strength (MPa)} = 17.43 - 0.045T + 0.0036T^2 \text{ with } R^2 = 0.96 \quad (3.7)$$

where the temperature is in °C.

Most of Usumacinta bricks do not follow the polynomial trend. Usumacinta bricks are sediments based while traditional bricks are made with soil from quarries. Furthermore, variations in sediment characteristics and moulding moisture significantly influence the results. Therefore, it is difficult to find a universal approach.

Fired bricks were made at different moulding moisture content (PL, PL+0.25PI, PL+0.5PI, 0.75PI). Flexural strength variation with moulding moisture content is shown in Table 3.17.

Table 3. 17. Flexural strength (MPa) for fired bricks with workability water content variation

Specimen size = 15x15x60mm^3

Water content variation				Firing temperature = 1100°C		
Approach	Sediments	PL	PL + 0.25PI	PL + 0.5PI	PL + 0.75PI	LL
Per site sampling	T1	-	-	-	-	-
	T2	-	-	-	-	-
	T5	2.1	3.34	-	4.28	-
	T6	2.365	4.79	-	4.19	-
	J3	11.61	12.18	-	6.13	-
	J4	-	-	-	-	-
Mixture by site	J	4.49	8.32	-	5.04	-
	T		5.17	-	2.25	-
Global mix.	JT	0.92	6.98	-	2.82	-

*Note: PL = plasticity limit, LL = liquidity limit and PI = plasticity index; * sandy sediments, from previous observations bricks were not manufactured with these sediments.*

Table 3.18 shows that bricks Usumacinta bricks have maximum flexural strength at moulding moisture content of 0.25PI and 0.5PI. Similar observations were observed for compressive strength of Usumacinta bricks.

Different mixtures were suggested on the base of sediments characteristics and industrial approaches. Flexural strength of bricks based on recommended sediments mixtures is shown in Table 3.18.

Table 3. 18. Flexural strength (MPa) for fired bricks with different mixtures and firing temperature variation

Specimen size = 15x15x60mm^3

Temperature variation				Water content = PL + (LL-PL) /2			
Approach	Sediments	700 °C	800 °C	850 °C	900 °C	1000 °C	1100 °C
Specific surface area (SSA)	J3T1	0.285	0.52	0.42	1.51	0.75	4
	T2T6	0.12	0.25	0.20	0.09	0.6	3.04
HCA- dendogram Without mineralogy	T1T2T6			0.07			
	J3T5			0.89			
	J1J5			1.02			
	J4						
	T3						
Winkler diagram	J5			3.82			
	J1			2.63			
	T3						

Note: HCA = Hierarchical classification analysis

Flexural strength of fired bricks manufactured with a specific surface area approach and mineralogy approach is low. Similar observations for compressive strength of Usumacinta bricks have been observed in Table 3.13.

Flexural strength of Usumacinta bricks with varying dimensions is shown in Table 3.19.

Table 3. 19. Flexural strength (MPa) for fired bricks with dimension variation

Specimen size =15*15*60 mm^3; 20*20*80 mm^3; 30*30*120 mm^3; 40*40*160 mm^3

Temperature = 1100 °C			Water content = PL + (LL-PL) /2		
Approach	Sediments	15*15*60 mm^3	20*20*80 mm^3	30*30*120 mm^3	40*40*160 mm^3
Per site sampling	T1	0.45	0.71	0.30	0.10
	T5	2.83	13.45	4.33	3.16
	T6	1.27	1.73	0.98	1.64
	J3	2.1	3.57	1.16	1.03
	J4*	4.14	11.09	5.64	3.90

*Note: PL = plasticity limit and LL = liquidity limit; *water content used is equal to PL as sediment mixture is very liquid at midpoint between LL and PL.*

Table 3.19 shows that intermediate-size bricks (20*20*80 mm^3) have good flexural strength. Similar observations for compressive strength of Usumacinta bricks are discussed in Table 3.14. Compaction of bricks is influenced with specimen size which affects the final strength. In literature, some studies have reported decreases in flexural strength of bricks with increasing height and dimensions of bricks specimens (Fódi, 2011).

(d) Flexion stiffness

Flexion stiffness of fired bricks was calculated from flexural load deflection curves at different temperatures. Results are shown in Table 3.20.

Table 3. 20. Flexion stiffness (N/mm) variation with bricks firing temperature

Sediments	**700 °C**	**800 °C**	**900 °C**	**1000 °C**	**1100 °C**
T1	53	60	683	76	332
T5	1516	1038	1798	2109	4178
T6	178	524	568	413	1023
J3	476	611	552	1329	2206
J4	1698	2096	3159	2909	5343
J	248	528	510	546	1045
T	141	184	110	362	1504
JT	171	355	1369	1128	1763

Flexion stiffness of fired bricks increases with increasing temperatures. This is because the flexural strength of bricks also increases with increasing temperature and bricks have higher flexion stiffness with increasing flexural strength. Graph in Figure 3.36 shows the relation between flexion stiffness and temperature for Usumacinta bricks with individual sediments. Sandy sediments such as T1, T6 have low strength and correlation of their flexion stiffness with temperature is weak.

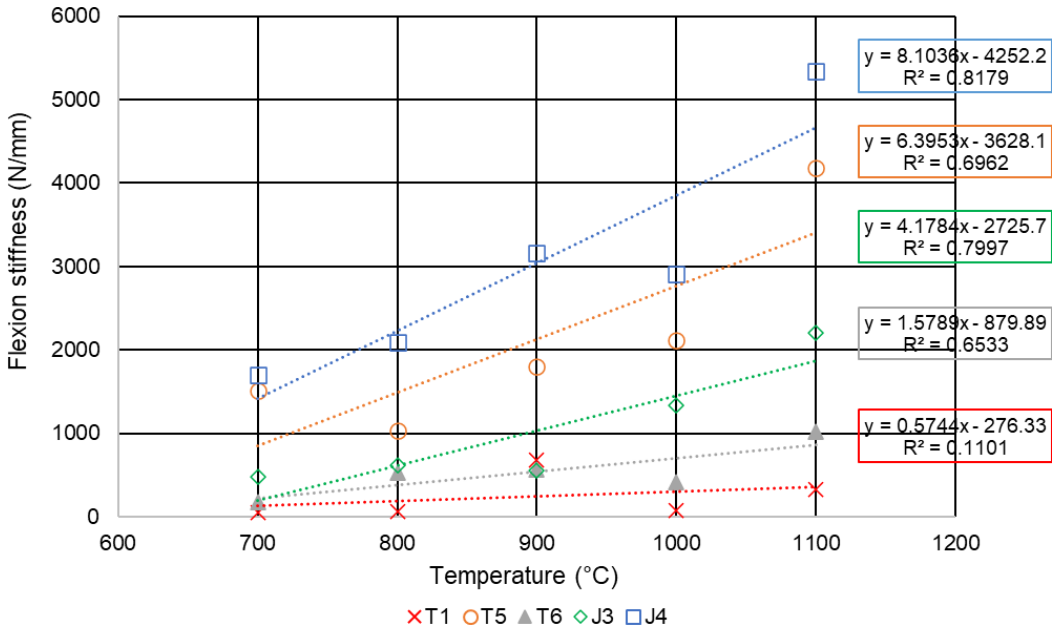

Figure 3. 36. Flexion stiffness variation with temperature relative to individual sediments

Flextion stiffness of fired bricks increases with increasing temperature. Linear trend between the flexion stiffness of Usumacinta bricks is weak for low strength sediments (T1, T6) and good for higher strength sediments. T2 sediments bricks are not shown in the graph as they have very low strength and T2 sediments are unsuitable for fired bricks. Characteristics of all Usumacinta River sediments are not same due to which characteristics of bricks also vary.

(e) Flexural strength relation with compressive strength

Relationship between flexural strength and compressive strength of Usumacinta bricks is shown in Figure 3.37.

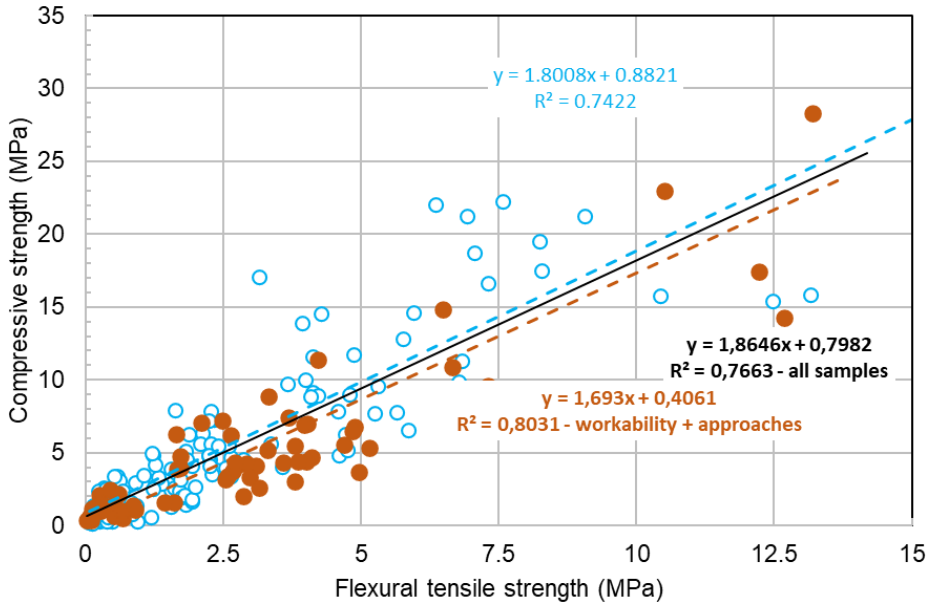

Figure 3. 37. Compressive strength relationship with flexural strength

Compressive strength relation to flexural tensile strength shows that compressive strength is around 1.80 times of flexural strength for Usumacinta bricks fired at a temperature range of 700 °C to 1100 °C. Similarly, this value for workability and approaches samples is around 1.69. Global value of Usumacinta River sediments is 1.86. Theoretically compressive strength of concrete is 10 times of tensile strength. Due to the low strength of Usumacinta bricks, this value is around 1.86 times of flexural strength. Compressive and flexural strength for individual sediments and site-based mixtures is plotted in Figure 3.38.

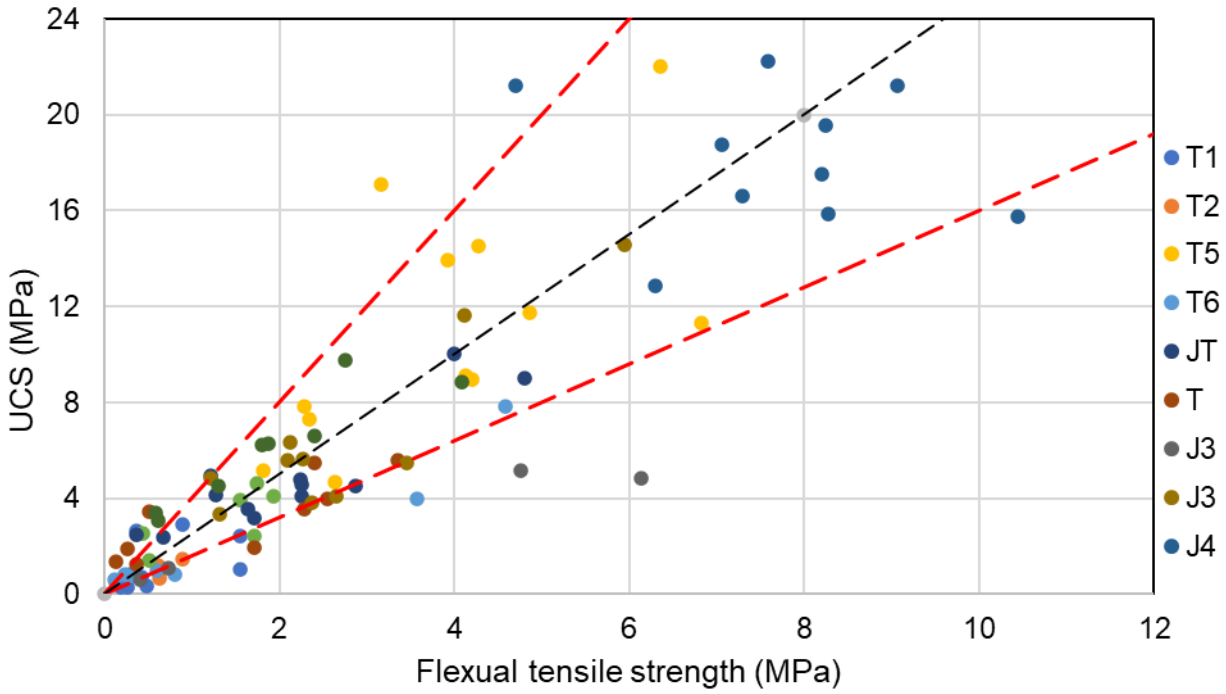

Figure 3. 38. Compressive strength vs flexural strength of all sediments

Most of the sediments surround the central line drawn at a slope of 2.5. However, sediments such as T5, T and sediments have higher slopes and J3 sediments have low slopes and these sediments tend to go beyond the zones where most of the sediments lie.

Physico-chemical and mechanical characteristics of fired bricks described in literature are summarized in Table 3.21.

Table 3. 21. Studies on production of bricks made from non and low-contaminated sediments (Hussain et al., 2020).

References	Sediment origin	Sediment rate (%)	Others (%)	Firing temp. (°C)	UCS (MPa)	WSC (%)	Porosity (%)	Bulk density (g/cm^3)
Anger (2014)	Dam sediments, (France)	80-100	Kaolinite	800-880-1100-1150	7.5-10	20-31	41-51	1.36-1.52
Baruzzo et al (2006)	Marine sediment							
Bathnagar & Goel (2002)	Alluvial deposits, Indo-Gange (India)			700-1100				
Ben Allal et al (2011); Frar et al (2014)	Port sediment, Larache & Tanger, Morroco	0-70	Clay	920	33-6.8	10-33	18-45	1.81-1.37
Benkadja et al (2013)	Dam sediment, K'sob, Algeria	0-65	Dune sand	800		55		
Boulingui et al (2015)	Mined clay			900 - 1150				
Chiang et al (2008)	Dam sediment, Shi-Men (Taiwan)	80-100	Clay	1050-1100-1150				
Haurine (2015)	Dam sediments (France)	70-100	Fine sand, crushed tiles	950-1100	5-50			
Labiod et al (2004)	Bouhanifa dam sediment, (Algeria)	100	-		5-9			
Liang &Li (2015)	Dam sediment		Gypsum	1100				
Marouf et al (2018)	Bouhanifa dam sediment, (Algeria)			850-1050	21	30-40		
Nedloussi et al (2019)	Gargar dam sediment, (Algeria)	80-100	Sand	600-900	28-46			
Remini (2006)	Dam sediments, (Algeria)	0-100	Yellow clay	900	10-40	6-20	12-24	1.4-1.9
Romero et al (2009)	Santander Harbour (Spain)	100	-	900-1200	34	4-22	12-38	1.60-2.45
Samara et al (2009)	Dampremy River, Charleroi, (Belgium)	100	Low PI	1000	36	7.5	15.4	-
Tangprasert et al (2015)	Lumsai River, Bangkok (Thailand)	80- 100	Rice husks	700	1.9-9	17.8-29	-	1.13-1.57
Torres et al (2009)	Ria de Aveiro River, (Portugal)	5-10	Low to plastic clays	950-1100	7.5-35	3.5-15.5	-	-
Wei et al (2014)	Harbour sediment		Steel slag	950-1100				
Xu et al (2014)	River sediment	50-80		1100				
Yeboah et al (2011); Mezencevova et al (2012)	Savannah Harbour, (USA)	100 50	- Clay (50)	900-1100 900-1000	8.3-11.7 29.4		-	-
Zhang et al (2016)	Lake sediment, Nanjing, (China)		Cinder, sewage sludge					

Note: Sediment rate: Sediment proportion in mixture; Others: other components in mixture; UCS: Unconfined compressive strength; WSC: Water sorption capacity (24h); PI: Plasticity Index. Firing temp.: firing temperature; 880-1100: optimal values of temperature.

Table 3.21 demonstrates that fired bricks can be made with partially or fully replacing conventional materials with dredged sediments from dams, rivers and ports. Sediment replacement can be 5 to 10% and as high as 100% along with materials such as clay, sand, kaolinite, and other waste materials. Strength and physico-chemical characteristics of fired bricks depend on the nature and properties of sediments. Table 3.21 shows that sediments based fired bricks have been fired at a temperature range of 600 °C to 1200 °C while the common firing temperature ranges from 800 °C to 1100 °C. Compressive strength of sediments-based bricks ranges from 1.9 MPa to 50 MPa and it is influenced by the clay content of sediments, organic matter, moulding moisture content and firing temperature. Water sorption capacity of sediments-based bricks varies from 3.5 to 55% and it depends on porosity of the bricks. Bulk density of these bricks ranges from 1.13 g/cm^3 to 2.45 g/cm^3. huge variation in the characteristics of fired bricks made from dredged sediments is attributed to the heterogeneous nature of sediments and different manufacturing conditions of bricks.

3.5. Limitations of bricks

In developing countries, coal is a primary source of heat in the brick manufacturing industry which produces a high amount of carbon dioxide, carbon monoxide, ammonia etc. and pollutes the environment. Another problem associated with fired bricks is that the raw material needed for bricks is non-renewable. Due to higher demands for bricks, soil deposits used for brick construction are also exploited on large scale. Many countries are facing an acute burden on agricultural lands due to the utilization of topsoil surfaces in the brick industry.

3.6. Conclusion

In this chapter, Usumacinta sediment's physico-chemical, geotechnical, hydro-mechanical and mineralogical characteristics were investigated for their reuse in fired bricks. Winkler diagram based on sediment granulometry indicates the low clay content in Usumacinta sediments. However, Augustinik diagram based on the oxide content of sediments and clay workability chart shows the suitability of Usumacinta sediments for fired bricks. In addition, Presence of pollutants such as heavy metals, PAHs and PCBs is negligible in Usumacinta River sediments.

Cubic and prismatic bricks specimens of sizes 20*20*20 mm^3 and 15*15*60 mm^3 were manufactured for compressive and tensile strength tests. Sediment moulding moisture content was found with the Sembenelli diagram. Bricks were dried at 60 °C and fired at a temperature range of 700 °C to 1100 °C for 6 hours to optimize the strength and energy. Bricks were made with individual sediments and different sediments mixtures based on-site, mineralogy, oxides and specific surface area approach. Physical and mechanical characteristics of bricks such as linear shrinkage, loss on ignition, water absorption, density, compressive and tensile strength were investigated.

Linear shrinkage in Usumacinta bricks ranges from 0.56 to 13.5%. Shrinkage is highest in clayey sediments such as J4 and T5 and low in sandy sediments such as T1. Density of Usumacinta bricks ranges from 994 kg/m^3 to 1888 kg/m^3. Density of bricks increases with

increasing temperature, and it is lowest for sandy sediments (T1 and T2) and highest for clayey sediments (J4 and T5). Loss on ignition (LOI) of fired bricks ranges from 0.56% to 13.51% and it is highest for clayey sediments such as T5 and J4. Decomposition of clay and carbonates and organic matter combustion contributes to higher LOI. Water absorption of bricks ranges from 10.71% to 22.39%. Water absorption is highest in T1 sediments and lowest in T5 sediments. Higher shrinkage in T5 and J4 sediments removes pores which reduces the absorption capacity of bricks. Water absorption of bricks increases with increasing temperature.

Mechanical testing of bricks shows an increase in compressive and tensile strength of bricks with increasing temperature and strength is maximum at 1100 °C. T5, J3, J4, mixes suggested with Winkler diagram and site-based approach have good compressive strength. Compressive strength of T5 and J4 sediments is 15.51 MPa and 17.04 MPa at a moderate temperature of 700 °C and satisfies the compressive strength requirement of fired bricks. Moulding moisture content variation shows that bricks have maximum compressive strength at moulding moisture content of 0.25PI and 0.5PI in the Sembenelli diagram. Scale effect shows that bricks have good compressive strength with intermediate dimensions of cubes (30*30*30 mm^3). Sediments mixtures with specific surface area approach (J3T1 and T2T6) and mineralogy approach (T1T2T6, J3T5 and J1J5) have low compressive strength while mixture suggested with Winkler diagram have good compressive strength at a moderate temperature of 850 °C. Modulus of elasticity of Usumacinta bricks ranges from 13 MPa to 985 MPa and increases with increasing compressive strength and increasing temperature.

Flexural strength of J4 (12.82 MPa at 1000 °C) and T5 (6.60 MPa at 1100 °C) sediments is the highest and it increases with increasing temperature. Flexural strength of bricks is maximum at moulding moisture content of 0.25PI and 0.5PI in Sembenelli diagram and bricks have maximum flexural strength for bricks of intermediate dimensions (20*20*80 mm^3). Compressive strength relation with flexural tensile strength shows that compressive strength is around 1.80 times of flexural strength for Usumacinta bricks fired at a temperature range of 700 °C to 1100 °C

References

AMI (2018). SEDIBRIC, Valorisation de sédiments en briques et tuiles. Transition Ecologique et Valorisation Economique. CPIER Vallée de la Seine

Anger, B. (2014). Caractérisation des sédiments fins des retenues hydroélectriques en vue d'une orientation vers des filières de valorisation matière. PhD thesis, Unicaen, France.

ASTM C62-17 (2017). Standard Specification for Building Brick (solid masonry units made from clay or shale)

Augustinik, A.I., 1957. Ceramic Leningrad.

Baruzzo, D., Minichelli, D., Bruckner, S., Fedrizzi, L., Bachiorrini, A. and Maschio, S., 2006. Possible production of ceramic tiles from marine dredging spoils alone and mixed with other waste materials. Journal of Hazardous Materials, B134, pp. 202-210.

Ben Allal, L., Ammari, M., Azmani, A., Lamrani, S., Frar, I. (2011). Valorisation des sédiments de dragage portuaire du nord du Maroc dans des matériaux de construction en terre cuite. Conférence Méditerranéenne Côtière et Maritime edition 2, Tanger, Maroc.

Benkadja, R., Benhadouga, M., Benkadja, A. (2013). Quantification des matie`res en suspension et valorisation des se´diments de dragage a` l'e´chelle d'un bassin semi-aride: Cas du barrage du K'sob (Algérie). Bull Eng Geol Environ (2013) 72:523–531. DOI 10.1007/s10064-013-0516-1.

Boulingui, J.E., Nkoumbou, C., Njoya, D., Thomas, F., Yvon, J. (2015). Characterization of clays from Mezafe and Mengono (Ne-Libreville, Gabon) for potential uses in fired products. Applied Clay Science, Volume 115, Pages 132-144.

Brick Industry Association, Reston, Virginia (2006). Manufacturing of brick. Technical notes on brick construction.

Cappuyns, V., Deweirt, V., Rousseau, S. (2015). Dredged sediments as a resource for brick production: Possibilities and barriers from a consumers' perspective. Waste Management 38: 372–380. https://doi.org/10.1016/j.wasman.2014.12.025

Chiang, K.Y., Chien, K.L., Hwang, S.J. (2008). Study on the characteristics of building bricks produced from reservoir sediment. Journal of Hazardous Materials 159 (2008) 499–504. doi:10.1016/j.jhazmat.2008.02.046

Del Negro, R. (2019). Characterization of Usumacinta River's sediments, Master thesis, Université de Nantes-IFSTTAR Nantes, 18p.

Diao, I., Diagne, M., Dia, I. (2021). Characterization of fired clay bricks for an economic contribution of the exploitation of thicky clay deposit. Materials Sciences and Applications, Vol.12 No.9. DOI: 10.4236/msa.2021.129027

Ettoumi, M., Jouini, M., Neculita, C.M., Bouhlel, S., Coudert, L., Taha, Y., Benzaazoua, M., 2020. Characterization of phosphate processing sludge from Tunisian mining basin and its potential valorization in fired bricks making. Journal of Cleaner Production, Vol. 284, 124750.https://doi.org/10.1016/j.jclepro.2020.124750

Fódi, A. (2011). Effects influencing the compressive strength of a solid, fired clay brick. Civil Engineering 55/2 (2011) 117–128, periodica polytechnica, doi: 10.3311/pp.ci.2011-2.0

Fonseca, B.S., Galhano, C.D., Seixas, D. (2015). Technical feasibility of reusing coal combustion by-products from a thermoelectric power plant in the manufacture of fired clay bricks. Applied Clay Sci., 104 (2015) 189–195. http://dx.doi.org/10.1016/j.clay.2014.11.030

Frar, I., Ben Allal, L., Ammari, M., Azmani, A. (2014). Utilisation des sédiments de dragage portuaire comme matière première dans la fabrication des briques en terre cuite (Utilization of dredged port sediments as raw material in production of fired brick). J. Mater. Environ. Sci. 5 (2) (2014) 390-399. ISSN : 2028-2508

Gippini, E (1969). Contribution à l'étude des propriétés de moulage des argiles et des mélanges optimaux de matières premières. L'Industrie Céramique 619, 423–435.

Haurine, F. (2015) Caractérisation d'atterrissements d'argiles récents sur le territoire français, en vue de leur valorisation dans l'industrie des matériaux de construction en terre cuite. Sciences de la Terre. Ecole Nationale Supérieure des Mines de Paris, HAL Id: tel-01423865, https://pastel.archives-ouvertes.fr/tel-014238652015.

Hussain, M., Levacher, D., Leblanc, D., Zmamou, H., Djeran-Maigre, I., Razakamanantsoa, A. (2020). Sediment-based fired brick strength optimization, A discussion on different approaches. XVIèmes Journées Nationales Génie Côtier – Génie Civil Le Havre, DOI:10.5150/jngcgc.2020.072

IS 1077 (1992). Common Burnt Clay Building Bricks -Specification.

Johari, I., Said, S., Hisham, B., Bakar, A., Ahmad, Z.A. (2010) Effect of the change of firing temperature on microstructure and physical properties of clay bricks from Beruas (Malaysia). Science of Sintering, 42: 245-254. doi: 10.2298/SOS1002245J

Karaman, S., Ersahin, S., Guna, H. (2006). Firing temperature and firing time influence on mechanical and physical properties of clay bricks. Journal of Scientific and Industrial Research, Vol 65, pp. 153-15.

Kornmann M (2009) Matériaux de terre cuite - Matières de base et fabrication." Techniques de l'ingénieur (ref C905): 26.

Kreimeyer, R. (1986). Some notes on the firing colour of clay bricks. Applied Clay Science, 2, pp.175-183. https://doi.org/10.1016/0169-1317(87)90007-X.

Labiod, Z., Remini, B., Belaredj, M.: Treatment of the vase of the bouhanifia dam in view of its valorization. Larhyss J. 03, 7–12.

Levacher, D. (2020). Val-uses project report.

Liang, H.H., Li, J.L. (2015). The influence of hydration and swelling properties of gypsum on the preparation of lightweight brick using water supply reservoir sediment. Construction and Building Materials, Volume 94, 30 September 2015, Pages 691-700. https://doi.org/10.1016/j.conbuildmat.2015.07.111

Marouf, H., Semcha, A., Mahmoudi, N., Bouhamou, N., Benzerzour, M., Maherzi, M., (2018). Experimental study on the reuse of a dredging sludge from west of Algeria in brick fabrication. Journal Of Materials And Engineering Structures 5 (2018) 163–172.

Mezencevova, A., Yeboah, N., Susan, E. B., Kahn, L. F., Kurtis, K.E. (2012). Utilization of Savannah Harbor river sediment as the primary raw material in production of fired brick. Journal of Environmental Management 113, 128-136. https://doi.org/10.1016/j.jenvman.2012.08.030

Nedloussi, F., Benamara, L., Ouhba, K. (2019). Utilisation des sédiments d'envasement de barrages comme matières premières locales dans la production des briques. Matériaux & Techniques, Vol. 107, No. 3. https://doi.org/10.1051/mattech/2019009

Rankin, G. A., Wright, F. E., (1915). The Ternary System Lime-Alumina-Silica. The American Journal of Science, Volume 39, pp. 1-79. doi: 10.2475/ajs.s4-39.229.1.

Remini, B. (2006). Valorisation de la vase des barrages - Ouelques exemples Algeriens. Larhyss Journal, ISSN 1112-3680, nÄ 05, Juin 2006, pp.75-89.

Romero, M., Andrés, A., Alonso, R., Viguri, J., Rincón, ., J.M. (2009). Phase evolution and microstructural characterization of sintered ceramic bodies from contaminated marine sediments. Journal of the European Ceramic Society, Volume 29, Issue 1, January 2009, Pages 15-22. https://doi.org/10.1016/j.jeurceramsoc.2008.04.038

Samara, M., Lafhaj, Z., Chapiseau, C. (2009). Valorization of stabilized river sediments in fired clay bricks: Factory scale experiment. Journal of Hazardous Materials 163 (2009) 701–710. doi:10.1016/j.jhazmat.2008.07.153

Srisuwan, A., Phonphuak, N. (2020). Physical property and compressive strength of fired clay bricks incorporated with paper waste. Journal of Metals, Materials and Minerals, Vol. 30, No. 1, pp. 103-108

Taha, Y. (2017). Valorisation des rejets miniers dans la fabrication de briques cuites: Évaluations technique et environnementale. Ph.D. Thesis, Université du Québec en Abitibi-Témiscamingue, Rouyn-Noranda, QC, Canada.

Tangprasert, W., Jaikaew, S., Supakata, N. (2015). Utilization of dredged sediments from Lumsai Canal with rice husks to produce bricks. International Journal of Environmental Science and Development, Vol. 6, No. 3. DOI: 10.7763/IJESD.2015.V6.593

Torres, P., Fernandes, H., Olhero, S.M., Ferreira, J.M.F. (2009). Incorporation of river silt in ceramic tiles and bricks. Industrial Ceramic, Vol.29(1), 1-8.

Wei, Z., Zhao, J., Wang, W., Yang, Y., Zhuang, S., Lu, T., Hou, Z. (2021). Utilizing gold mine tailings to produce sintered bricks. Construction and Building Materials, Vol. 282, 122655. https://doi.org/10.1016/j.conbuildmat.2021.122655

Wei, Y.L., Lina, C.Y., Chenga, S.H, Wang, H.P. (2014). Recycling steel-manufacturing slag and harbor sediment into construction materials. Journal of Hazardous Materials 265 (2014) 253–260. https://doi.org/10.1016/j.jhazmat.2013.11.049

Winkler, H.G.F, (1954). Bedeutung der Korngrössenverteilung und des Mineral-bestandes von Tonen fürdie Herstellung grobkeramischer erzeugnisse. Ber. DKG, v. 31, p. 337-343.

Xu, Y., Yan, C., Xu, B., Ruan, X., Wei. Z. (2014). The use of urban river sediments as a primary raw material in the production of highly insulating brick. Ceramics International 40, 8833–8840. https://doi.org/10.1016/j.ceramint.2014.01.105

Yamaguchi, K. (2019). Consideration of the sustainable utilization of the sediments in Usumacinta River. Master thesis, Kyoto University, Japan.

Yeboah, N. N., Mezencevova, A., Phillips, J. S., Burns, S. E., Kurtis, K.E. (2011). Investigating the potential for producing fired bricks from Savannah Harbor dredged sediment. Geo-Frontiers 2011 © ASCE.

Zhang, Y.M., Jia, L.T., Mei, H., Cui, Q., Zhang, P.G., Sun, Z.M., (2016). Fabrication, microstructure and properties of bricks fired from lake sediment, cinder and sewage sludge. Construction and Building Materials, Vol.121, Pages 154-160. https://doi.org/10.1016/j.conbuildmat.2016.05.155

Chapter 4. Earth bricks

Earth bricks are eco-friendly and the oldest building material. These bricks are manufactured by mixing soil and natural fibers. Manufacturing process of earth bricks includes the mixing of sediments, moulding and drying. This chapter investigates the characteristics of Usumacinta River sediments and tropical fibers for their reuse in earth bricks. Characteristics of Usumacinta River sediments were investigated to observe the suitability of sediments for earth bricks. Similarly, tropical fibers, especially palm oil fibers were analyzed thoroughly. Characteristics of fibers such as fiber length, diameter, tensile strength and fiber content are important parameters that affect the strength and quality of bricks.

Finally, earth bricks were made with Usumacinta River sediments and palm oil flower fibers at different fiber percentages. Tensile strength, compressive strength and distribution of fibers in bricks were investigated. Mechanical testing of earth bricks shows that the strength of Usumacinta bricks satisfies the compressive and tensile strength requirement of French and Mexican standards. However, durability of bricks needs further consideration.

4.1 Introduction

Earth bricks have been used in construction since antiquity. Modern construction materials such as concrete and cement have replaced earth bricks in developed societies. However, carbon and greenhouse gas emissions from concrete and cement are very high. Each ton of clinker emits nearly 1 ton of CO_2 (Aoual-Benslafa et al. 2014). Higher emissions of CO_2 from concrete and cement encouraged the use of low carbon construction materials and earth bricks are one of the most environment-friendly building materials.

Earth bricks are manufactured with soil and natural fibers as reinforcement. Dredged sediments from rivers and ports can also be used to manufacture earth bricks after analyzing their characteristics. Sediment's physico-chemical, mineralogical and environmental characteristics are important as the strength of earth bricks is heavily influenced by the nature of sediments (Hussain et al., 2020).

Natural fiber morphology, mechanical characteristics and quantity used with sediments have also a significant influence on the strength and durability of earth bricks. Natural fibers are common agriculture waste and some common natural fibers used in building composites are jute, palm fibers (OPF), banana spine fibers (Bs), sugar cane fibers (Sc) and coconut fibers (Cn) and hemp. Earth bricks are manufactured with different fiber content which normally ranges from 0% to 5% (Salih et al., 2018). Natural fibers act as reinforcement in earth bricks and increase the tensile strength of earth bricks. Earth bricks manufacturing method, moulding moisture content and compaction techniques are also important. Compaction of earth bricks increases their strength and reduce their water absorption capacity. Dynamic compaction and static compaction are commonly used to density the building composites (Seifi et al. 2018).

Objective of this research is to investigate Usumacinta River sediments and palm oil flower fibers characteristics for their sustainable recovery in earth bricks. Usumacinta River sediments suitability for earth bricks will be observed with French standards and earth bricks will be manufactured at different fiber dosages to optimize the strength and durability of bricks. Finally, physical and mechanical characteristics of earth bricks will be investigated and compared with the strength requirements of different standards.

4.2 Materials and methods

4.2.1 Usumacinta River sediments

Usumacinta sediment's physical, chemical and mineralogical characteristics were examined to reuse these sediments in manufacturing earth bricks. Important sediments properties for their reuse in earth bricks include grain size, consistency limits, chemical composition and optimum water content.

The suitability of Usumacinta River sediments for earth bricks was investigated with granulometry and Atterberg limits. Granulometry of sediments was found with laser granulometry. Granulometry of sediments recommended for earth bricks in French and Spanish standards is shown in Figure 4.1 (AFNOR XP P13-901, 2001, MOPT, 1992, Houben and

Guillaud,1994). Grading curves of Usumacinta River sediments are also displayed in Figure 4.1.

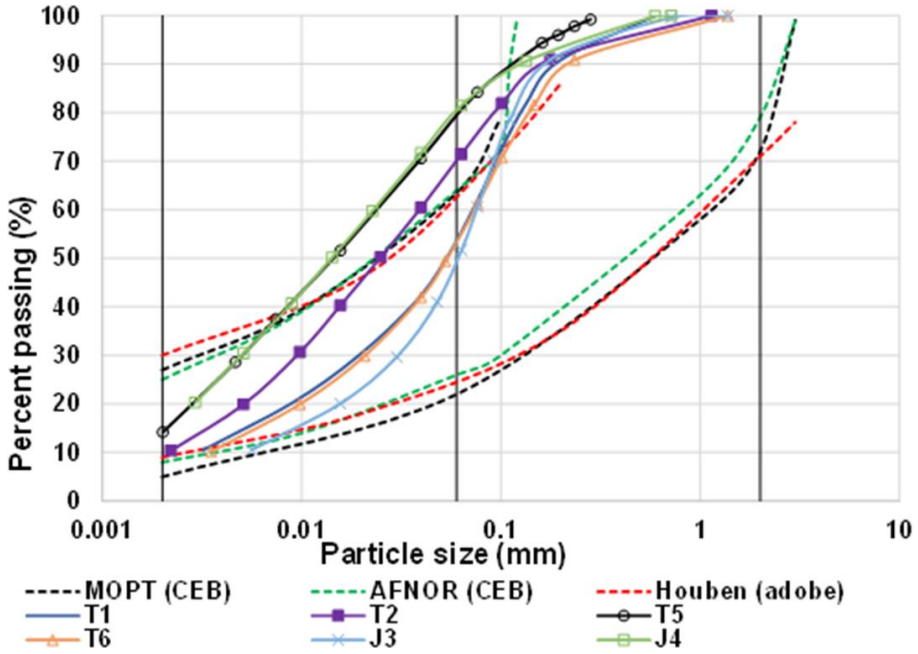

Note: CEB = compressed earth blocks*

Figure 4. 1. Suitability of sediments for earth bricks on the base of granulometry

It can be seen from Figure 4.1 that most of the Usumacinta River sediments lie in the recommended zones for bricks. However, T5 and J4 sediments are outside the zone suitable for bricks due to the presence of higher fine particles.

Furthermore, appropriate soil for manufacturing bricks has specific liquidity and plasticity limits. Figure 4.2 describes different zones suitable for earth bricks based on sediment consistency limits (AFNOR XP P13-901, 2001, Houben and Guillaud, 1994).

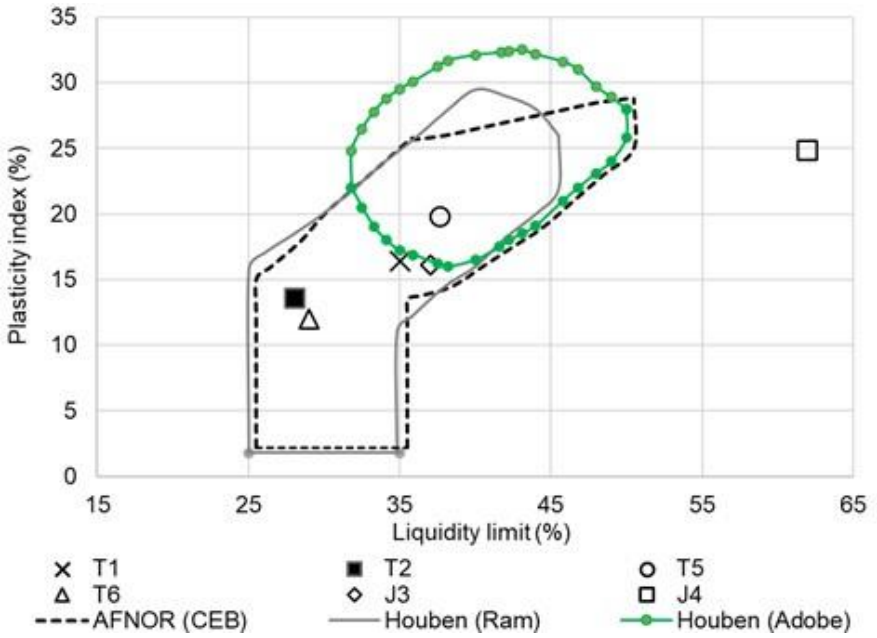

Note: CEB = compressed earth blocks

Figure 4. 2. Suitability of sediments for earth bricks with consistency limits

Figure 4.2 shows that J4 sediment is outside the zones defined for earth bricks as the liquidity limit of sediments is very high. Liquidity limit of sediments is linked with clay content and organic matter and J4 sediments have a comparatively higher percentage of clay and organic matter. T2 and T6 sediments are away from other sediments due to low liquidity limit and plasticity index. Higher sand content is one of the important reasons for this behavior.

4.2.2 Tropical fibers

Natural fibers are waste materials produced by the agriculture industry. For recycling natural fibers in building materials as reinforcement, physical and mechanical characteristics of fibers play an important role. These characteristics include tensile strength, length, diameter, density, morphology and chemical composition.

Common tropical natural fibers in Mexico include coconut coir fibers (Cn), banana spine (Bs), palm oil flower fibers (POFL), palm oil fruit fibers (POFR) and sugar cane bagasse (Sc). These fibers are available in large volumes in the form of agri-waste in Mexico. Mexico is the fifth biggest sugarcane producer in the world with sugarcane fields covering an area of 770000 hectares (Aguilar-Rivera, 2012) and the 9th largest producer of coconut in the world with a production of 1.06 million tons in 2018 (Montfort et al., 2021). Tabasco state of Mexico produced 10749.51 tons of copra in 2017 (Lagunes-Fortiz et al., 2021).

Figure 4.3 shows the source materials of Mexican tropical natural fibers.

Figure 4. 3. Tropical fibers source material

In this study, palm oil flower fibers were used as reinforcement in earth bricks. Palm oil fibers were chosen among other fibers due to their industrial-scale availability, easier extraction, good strength and wide range of length distribution. Palm oil fibers are further divided into palm oil flower fibers (POFL) and palm oil fruit fibers (POFR).

As fibers are strong in tension and their addition to earth bricks increases the tensile strength of bricks and minimizes the growth of the cracks. Physical and mechanical properties of palm oil fibers were investigated for their recycling in raw earth bricks.

Tensile strength of fibers was measured with Universal testing machine with ASTM standard (ASTM C1557-2003). Load deflection behavior, ultimate tensile strength, initial elastic modulus (E_{t1}) and elongation of fibers at failure were also determined. POFL and POFR technical fibers were used for tensile strength testing. Fibers of a gauge length of 2cm were protected with a cardboard frame of 4cm*4cm to perform the tensile strength test. Shimadzu AGS-X model machine was fixed at displacement rate of 0.5 mm/min and sensors of 200N and 50 kN were used. Testing of fibers is shown in Figure 4.4.

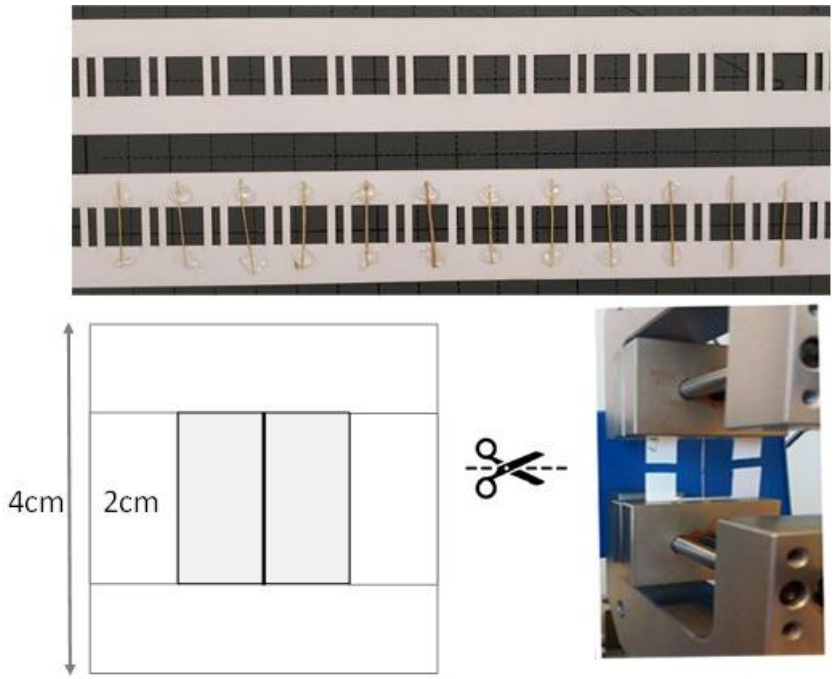

Figure 4. 4. Tensile strength testing of fibers

Tensile strength of POFL and POFR fibers was determined with tensile load and cross section of fibers tested. Figures 4.5 and 4.6 show the stress-strain curves of POFL and POFR fibers.

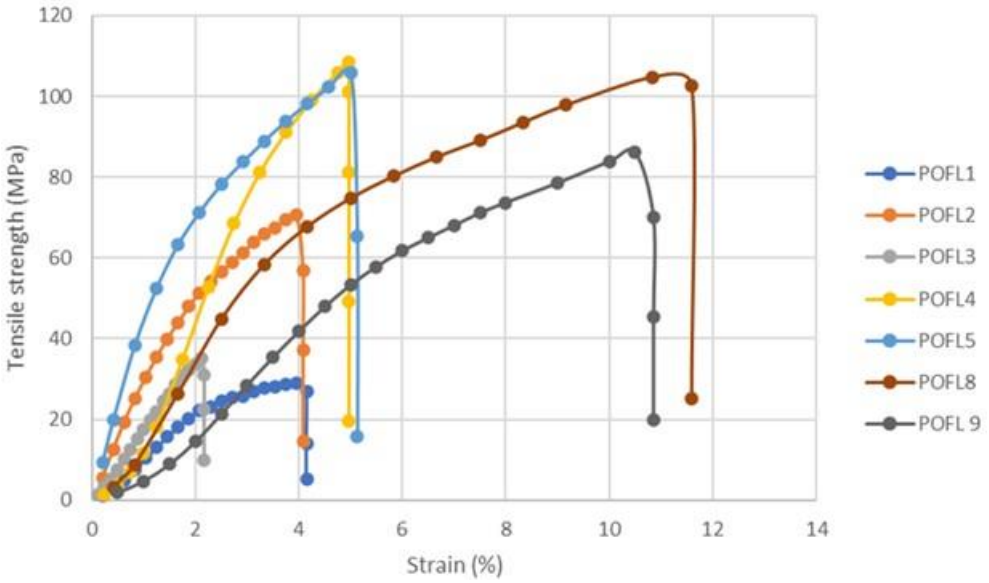

Figure 4. 5. Load deflection curves of POFL fibers

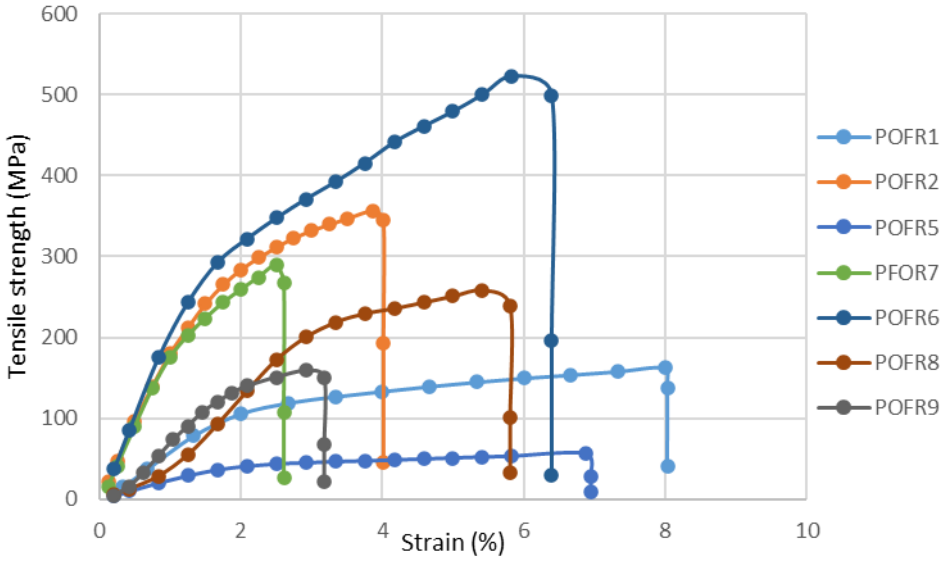

Figure 4. 6. Load deflection curves of POFR fibers

It can be seen in Figures 4.5 and 4.6 that tensile load behavior of both POFL and POFR fibers is elasto-plastic which is very common in natural fibers. Elasto-plastic behavior is associated with the cellulose content of fibers which align itself with the axis of natural fibers during tensile strength test and the fiber's behavior becomes elastic. However, after continuous loading, behavior of fibers changes into plastic deformation.

Figure 4.5 and 4.6 shows the higher variation in tensile strength of fibers which is related to variation in the number of elementary fibers, their orientation, fibers morphology and cross section of fibers. Average tensile strength and initial elasticity modulus of 10 POFL and POFR fibers are shown in Table 4.1.

Table 4. 1. Mechanical characteristics of POFL and POFR fibers

Fibers	**POFL**	**POFR**
Tensile strength (MPa)	119±95	327±192
Strain at failure (%)	7.36	5.70
Et_1 (GPa)	2.91±2.79	12.28±7.70

Tensile strength of POFR fibers (327 MPa) is considerably higher than POFL fibers (119 MPa). POFL fibers are long fibers and usually, presence of knots in long fibers decreases the tensile strength of natural fibers (Defoirdt et al., 2010). Tensile strength of natural fibers have huge variation due to heterogeneous natura of natural fibers and it ranges from 3.45 MPa to 2000 MPa as shown in Table 4.7. Initial elasticity modulus of POFL and POFR fibers is 2.91 and 12.28 GPa. Table 4.7 shows that modulus of elasticity of natural fibers ranges from 0.62 to 128 GPa.

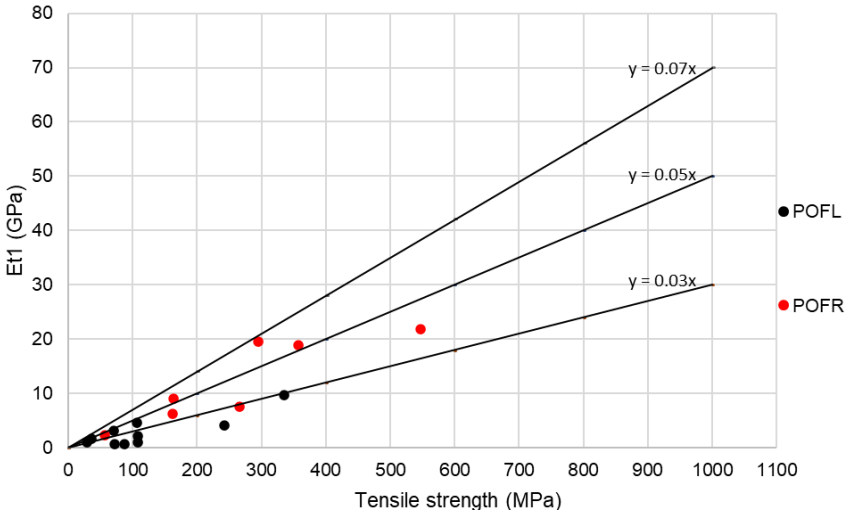

Figure 4. 7. Modulus of elasticity vs tensile strength of POFL and POFR fibers

Modulus of elasticity increases with increasing tensile strength. Figure 4.7 shows that modulus of elasticity (GPa) of POFR fibers is between 0.3 to 0.7 times tensile strength (MPa) while modulus of elasticity (GPa) of POFL fibers is below 0.3 times their tensile strength due to low strength of POFL fibers.

The area of POFL and POFR fibers was found with scanning electron microscopy. Figures 4.8a and 4.8b show the section estimation of POFL fibers with electron microscope.

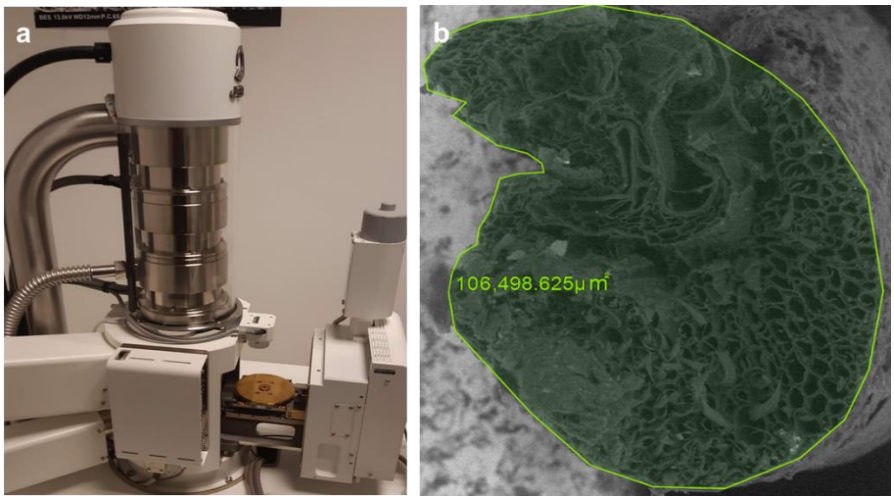

Figure 4. 8. Section estimation of tropical fibers

Area of POFL and POFR fibers is shown in Table 4.2.

Table 4. 2. Area of tropical natural fibers

Fibers	**POFL**	**POFR**
Area (mm^2)	0.07±0.04	0.03±0.01

The average area of POFL fibers is higher than POFR fibers which shows the presence of a higher number of elementary fibers in the fibers bundle.

Morphology of POFR and POFL fibers was also observed with SEM as it plays an important role in adhesion with sediments. POFL and POFR fibers have high morphological heterogeneity which is important for bricks as the presence of trough and irregular fiber structure increase the roughness of the fiber's surface which is essential for bonding between fibers and sediments and increasing the reinforcement of earth bricks. Scanning electron microscopic (SEM) images of POFL and POFR fibers are shown in Figure 4.9. Figures 4.9A and 4.9B show the irregular structure of POFL and POFR fibers because of the existence of non-cellulosic elements such as lignin, pectin etc. Figure 4.9D shows a cross-section of elementary POFR fiber in which fibers are aligned like a honeycomb structure. Tubular structures in the honeycomb of fibers come in different shapes such as circular and cylindrical. Figure 4.9C shows that there is significant variation in the morphology of tubular structure. Tubular structures of small diameter are concentrated at the corners while the coarse tubular structures are concentrated at the center of

fiber bundle. Presence of a hollow structure increases the roughness of fiber's surface and increase adhesion of fibers with matrix.

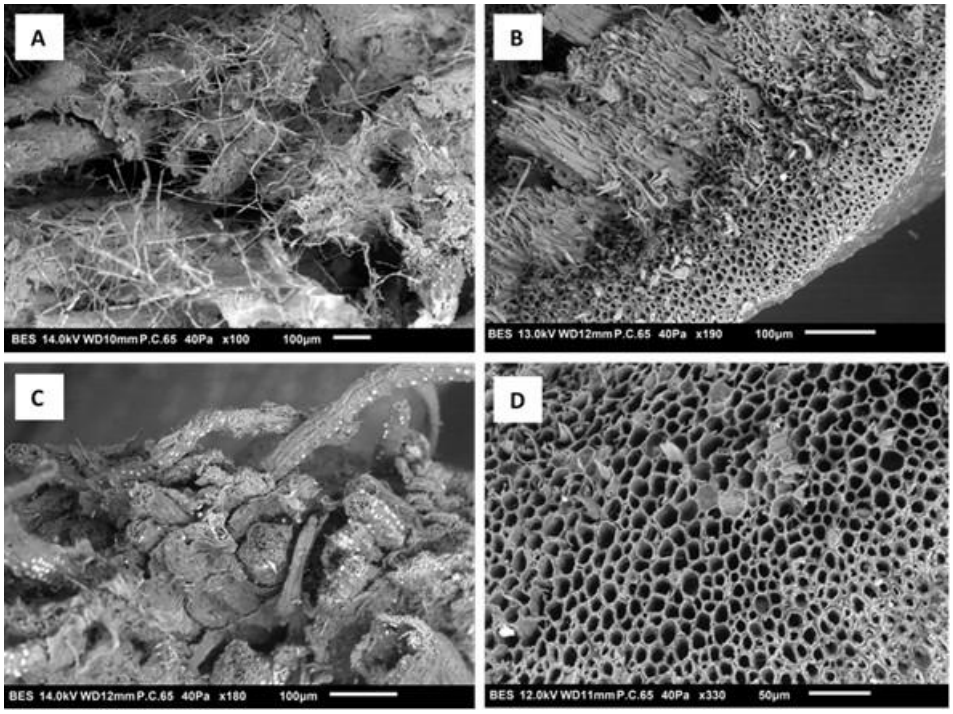

Figure 4. 9. Scanning electron microscopic images of POFL (A and B) and POFR (C and D)

Natural fibers have low density and their use in building composite is helpful to make lightweight construction materials. Absolute density of POFL and POFR fibers was determined with helium pycnometer model AccuPyc 1330. Density of each fiber was determined three times to get an average value. Results of absolute density are shown in Table 4.3.

Table 4. 3. Absolute density of tropical natural fibers

Fibers	**POFL**	**POFR**
Density (g/cm^3)	1.36±0.006	1.371.37±0.021

Density of both POFL and POFR fibers is nearly similar and its value is around 1.36 g/cm^3. Table 4.7 shows that density of natural fibers ranges from 0.1 g/cm^3 to 2.05 g/cm^3.

Water absorption of natural fibers has a substantial influence on the strength and durability of earth bricks as it affects the moulding of sediments mixture and wet fibers produce cracks in bricks on drying. Water absorption coefficient of POFL and POFR fibers was determined by immersing fibers in water. One-gram POFL fibers were soaked in water for 48 hours. After 48 hours, fibers were removed from the water and excessive water from the surface of the fiber was removed with vacuum filtration by using filter paper (Picandet, 2017). Average water absorption of two samples of POFL and POFR fibers is shown in Table 4.4.

Table 4. 4. Water absorption of tropical fibers

Fibers	POFL	POFR
WA (%)	175.9	103.5

Note: WA = water absorption coefficient

Table 4.7 shows that water absorption of natural fibers ranges from 40% to 415%. High variation in water absorption is due to heterogenous nature of natural fibers.

Thermal characteristics of fibers are important for building as they have low thermal conductivity. Thermal behavior of POFL and POFR fibers was investigated with increasing temperatures. Thermogravimetric analysis of palm oil fibers was performed with TGA 295 F1 Libra thermogravimetric analyzer (Netzsch) to see fibers degradation with a gradual rise in temperature up to 800 °C (Khennache et al., 2019). Mass loss variation of POFL and POFR with temperature is shown in figure 4.10.

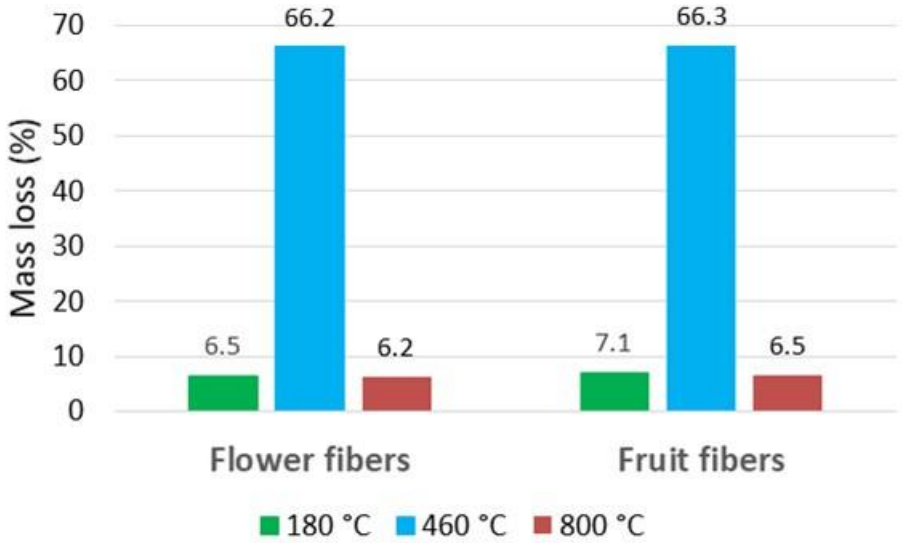

Figure 4. 10. POFL and POFR fiber degradation at different temperatures

Mass loss of both POFL and POFR fibers is similar as both fibers are coming from the same plant. Average mass loss of POFL fibers is nearly 79 % and POFR fibers is nearly 80% at a temperature of 800 °C. The residual mass is around 20% which is due to remaining ash, chemical components and impurities.

Biochemical composition of fibers has a significant impact on the tensile strength of fibers which is an important parameter for strength of building composites. Chemical components of palm oil fiber include cellulose, hemi-cellulose and lignin etc. (Pradeep et al., 2016). Biochemical composition of POFL and POFR fibers was found with the Van Soest method by using Fibertec TM 8000 semiautomatic machine (Van Soest et al., 1991). Figure 4.11 shows the chemical composition of POFL and POFR fibers.

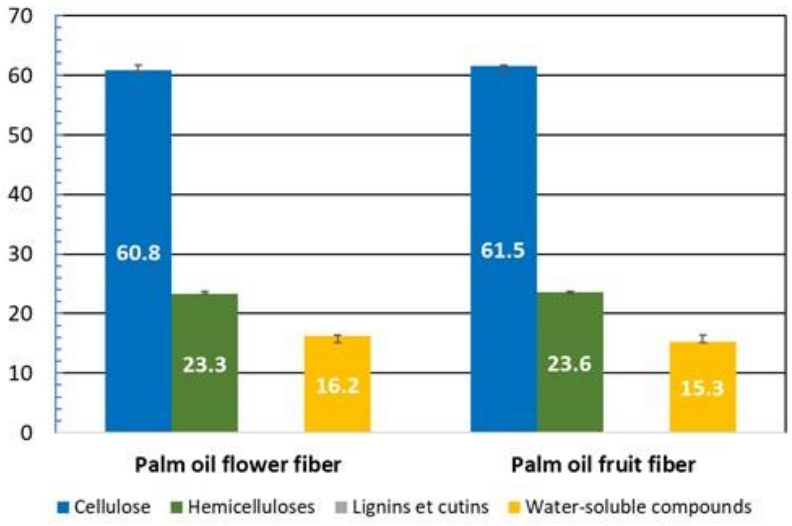

Figure 4. 11. Biochemical composition of tropical fibers

Figure 4.11 shows that cellulose and hemicellulose are the two main components of POFL and POFR fibers.

Tensile strength, suitable fiber length, easier extraction and industrial-scale availability near sediments dredging sites makes POFL fibers ideal for their use in earth bricks. Therefore, POFL fibers were used for manufacturing adobe bricks.

Length of fibers is important to use in bricks. Length of fibers used in earth bricks usually varies from 2cm to 10cm (Hakkoum et al., 2017; Ghavami et al., 1999). In building composites such as concrete, recommended length of natural fibers in ASTM standard is 2.5 cm (ASTM D7357-07, 2012). Therefore, POFL fibers were cut with 2cm and 3cm grids.

Extraction of POFL fibers from the palm oil empty fruit bunches and palm oil fruits was done with a knife mill of model Retsch-SM100 by using grids of 2cm and 3cm length. Figure 4.12 shows the knife mill used and the grids of different sizes.

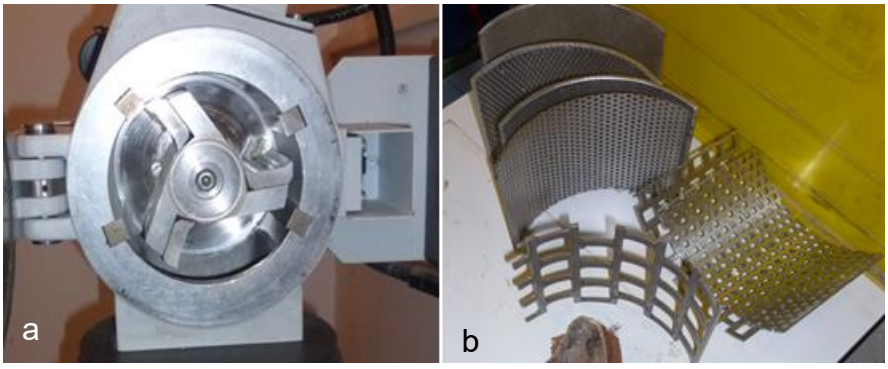

Figure 4. 12. Fiber's extraction with a knife mill

Figure 4.13 shows POFL fibers of lengths G-2cm and G-3cm after extraction from knife mill.

Figure 4. 13. POLF fiber of lengths G-2cm and G-3cm

Length distribution of POFL fibers was observed with ImageJ software. 100 fibers were distributed on the plan sheet. These fibers were treated with ImageJ software to get the length and thickness of fibers. Three measurements were taken by repeating the test to get the average value of length distribution. Length distribution of POFL fibers is shown in Figure 4.14.

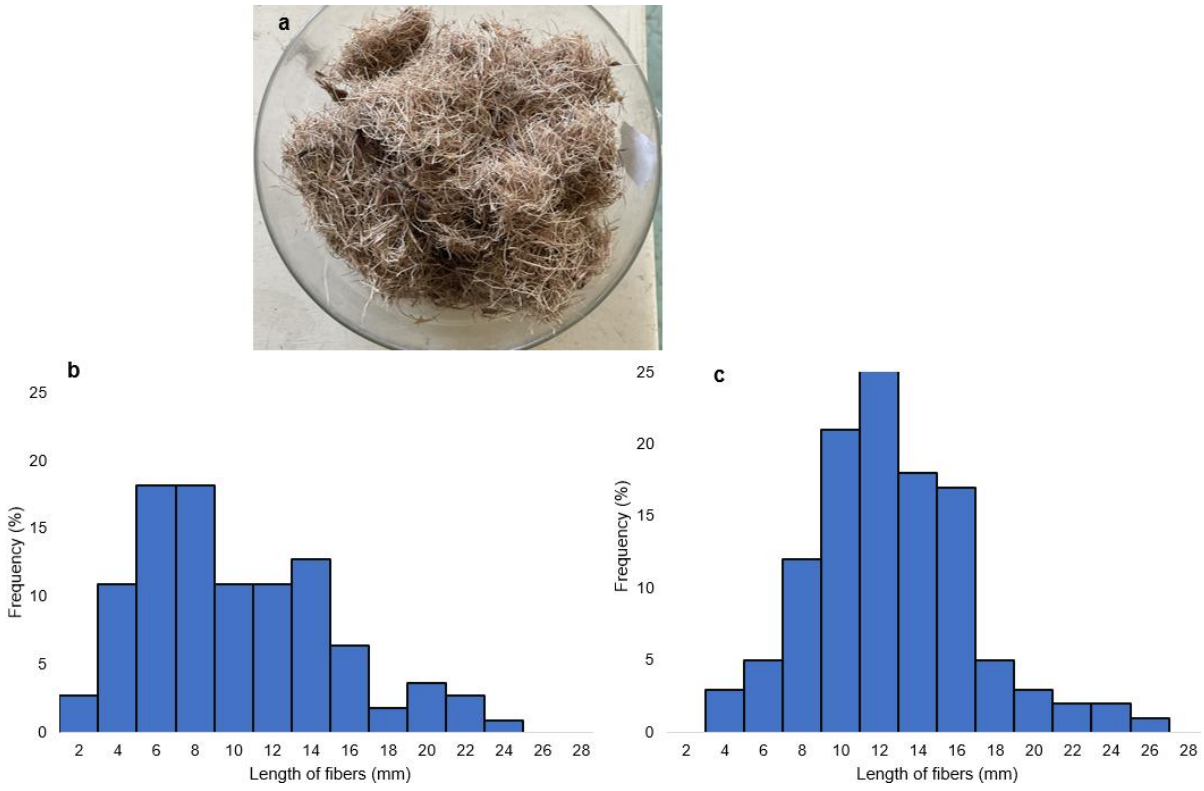

Figure 4. 14. POFL fibers (a), length distribution of G-2cm (b) and G-3cm long fibers (c).

Average length of POFL fibers is shown in Table 4.5.

Table 4. 5. Length distribution of POFL fibers

Grid size	Average length (mm)	Maximum length (mm)
G-2cm	9.48	24.05
G-3cm	11.5	32.96

Thermal conductivity of natural fibers is usually low and the addition of natural fibers in earth bricks improves their thermal characteristics. Heat flow method was used to find the thermal conductivity of POFL fibers by using polystyrene moulds having dimensions of 15*15*3 cm^3. Thermal conductivity and thermal resistivity of POFL are shown in Table 4.6.

Table 4. 6. Thermal conductivity and resistivity of POFL

Fibers	Thermal conductivity (W/mK)	Thermal resistivity (m^2K/W)
POFL	0.058	0.80

Natural fibers and tropical fibers characteristics reported in literature in Table 4.7.

Table 4. 7. Review of physical and mechanical properties of natural fibers (Bui et al., 2022).

Type of fiber	Density (g/cm^3)	Absorption coefficient (%)	Elasticity modulus (GPa)	Tensile strength (MPa)
Temprerature climate and subtropical fibers				
Bamboo	0.45-1.3	40-145	2.82-54	39.5-1000
Cotton	1.21-1.6	-	1.1-13	265-800
Flax	1.19-1.55	63-330	4.4-110	93-2000
Hemp	1.07-1.50	85-415	10-90	159-1264
Jute	1.23-1.50	84-281	2.5-78	300-800
Palm date	0.902	133-140	1.9-85	58-678
Ramie	1-1.58	-	23-128	400-1620
Reed	0.54-0.94	-	35.9	112-503
Rice straw	0.86-1.11	52-84	3.3-26.3	435-450
Sisal	1.2-1.50	110-230	1.46-38	80-1002.3
Wheet straw	1.14-2.05	96-320	1.4-4.8	3.45-140
Tropical fibers				
Banana spine	0.31-1.36	134-282	3-32	49.3-914
Coconut-coir	0.67-0.52	63-180	0.628-28	15-593
Palm oil*	0.1-1.55	54-120	0.5-25	147-400
Sugar cane	0.31-1.31	102-219	15-27.1	20-290.5

4.3 Earth bricks

The importance of earth bricks is increasing due to climate changes and huge energy consumption by construction materials such as concrete. Earth bricks are green products, and their thermal conductivity is considerably lower than modern construction materials. Less energy consumption, easier recycling, and abundant raw material reduce the production cost and make adobe bricks an economical choice in developing countries. Usumacinta bricks were manufactured by mixing Usumacinta River sediments with POFL fibers and Mexican lime as the stabilization of bricks improves their strength and characteristics. Figure 4.15 show the different sorts of bricks manufactured with Usumacinta River sediments.

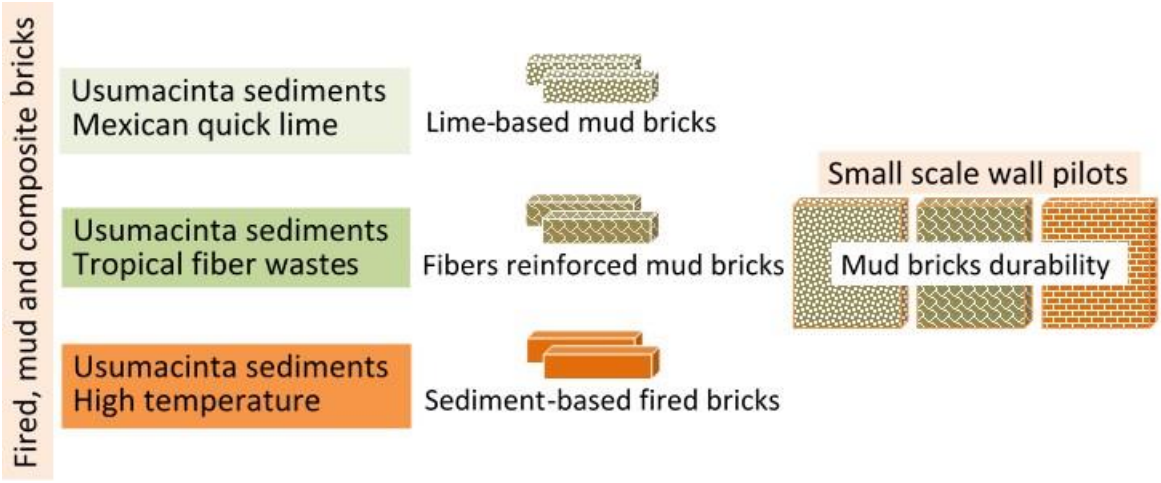

Figure 4. 15. Usumacinta River sediments use in bricks

4.3.1. Manufacturing of earth bricks

Mud bricks manufacturing process consists of material preparation (sediments, fibers and water mixing) moulding and drying. Usumacinta River sediments bricks were manufactured with J3 sediments and POFL fibers. J3 sediments were selected due to their suitability for earth bricks on the base of their grain size and Atterberg limits according to standards (AFNOR XP P13-901, 2001, MOPT, 1992). Furthermore, J3 sediments have a low organic matter which is essential for the strength of bricks. In addition, Presence of contaminants in these sediments is also negligible except Ni which can be neutralized with addition of lime. Usumacinta River sediment's physico-chemical properties are within line with soils used for bricks.

(a) Material preparation

Usumacinta River sediments were dried in the oven at 40 °C to eliminate the water. Dried sediments were passed through a 2 mm sieve after crushing. After sieving, sediments were mixed with POFL fiber with moulding moisture content. POFL fibers act as reinforcement in earth bricks and increase the strength and durability of bricks. Moulding moisture content is critical for mixing fibers and sediments. At high and low water content, the compaction of bricks becomes difficult. Moreover, higher water content disrupts the distribution of fibers in bricks and compaction of bricks becomes difficult due to which tensile and compressive

strength of bricks decreases (Fgaier et al., 2016). Higher moulding moisture content leads to significant shrinkage and cracks development in bricks on drying which reduces the strength of bricks.

Optimum moisture content of the soil is commonly used as moulding moisture content (Mellaikhafi et al., 2020). Therefore, optimum moisture content of Usumacinta River sediments determined with Proctor test was used as moulding moisture content. Optimum moisture content of J3 sediments is 19.4%. Additional water in mixture is needed to saturate the fibers. However, fibers water absorption in mixture is not instantaneous and there is excessive water in the mixture at high fiber content. At higher fibers content, the solution tends to be very liquid which hinders the compaction of bricks. To avoid this problem, Fibers were saturated in water for 24 hours before their use in bricks to avoid this problem.

Prismatic moulds of size 4*4*16 cm^3 were used to manufacture Usumacinta bricks. To prepare a prismatic bricks sample, mass of sediments used is around 450 g after AFNOR standard (AFNOR EN196-2016). Amount of water needed to be mixed with dry sediments and fibers was calculated with equation 4.1.

$$m_{water} = \frac{m_{sediments} \times \%\ of\ water}{100} \quad (4.1)$$

Quantity of fibers for material preparation is another important parameter. Fiber's addition is done with percentage by mass or by volume. In the case of fiber addition with the percentage by mass, fibers content of earth bricks varies from 1% to 5% (Hakkoum et al., 2017; Azhary et al., 2017; Saleem et al., 2016). Excessive fiber content decreases the adhesion between sediments and fibers. Density of bricks also decreases with increasing fiber content. Usumacinta bricks were manufactured with Usumacinta River sediments and POFL fibers at 0%, 1%, 2%, 3%, 4% and 5% fibers addition by mass of sediments. Quantity of fibers to be used for each brick was calculated with equation 4.2.

$$m_{fiber} = \frac{m_{sediments} * \%\ of\ fibre}{100} \quad (4.2)$$

Homogenous sediments and fiber mixture is important because the presence of lumps, fibers clusters and voids inside the mixture decreases the efficiency of bricks. Usumacinta River sediments and POFL fibers were mixed with an electric mixer for 5 minutes. Initially, dry sediments and fibers were added and then moulding moisture content was added to the mixing bowl. Electric mixer with small blades gets choked in sediments matrix while it is difficult to mix the sediments at the bottom and sides of the bowl with big blades. Therefore, sediments and fibers were mixed with a blade of medium size to prepare a homogenous mixture and avoid clustering of fibers inside the sediment matrix. Usumacinta River sediments, POFL fibers and mixer are shown in Figure 4.16.

Figure 4. 16. Usumacinta River sediments and POFL fibers

(b) Moulding

The sediments mixture was moulded into bricks specimens of size 4*4*16 cm^3 in a prismatic steel mould. The inner surface of moulds was oiled to facilitate demoulding and prevent sediments adherence with moulds.

(c) Compaction of bricks

Sediments moulding was followed by the compaction of bricks. Compaction of bricks eliminates the pores in bricks, enhances the density of bricks and decreases their drying time, water absorption and permeability. Compaction technique has a considerable effect on tensile and compressive strength of earth bricks. Static compaction, dynamic compaction and tamping are common compaction techniques. However, dynamic compaction of bricks substantially increases the tensile and compressive strength of bricks (Dormohamadi and Rahimnia, 2020; Hussain et al., 2020).

Dynamic compaction of prismatic earth bricks was performed with miniature compaction test apparatus. Moulds were filled in two layers. First sediment layer surface was scratched to increase the surface roughness and adhesion between the two layers. A wooden plate was used at the top surface of sediments and each sediments layer was compacted with 42 blows with a mass of 1.043 kg falling from the height of 17.8 cm.

Prismatic mould with compaction rod and compaction plan for dynamic compaction is shown in Figures 4.17a and 4.17b. Wooden plate of a size similar to the brick size was kept on the top of sediments fibers mixture and compacted with strokes in the order shown in Figure 4.17b. Initially, 4 strokes are applied on four equal parts of bricks (1,2,3 and 4) and then three strokes 5,6,7 at the top in the mid-parts 1-2, 2-3 and 3-4.

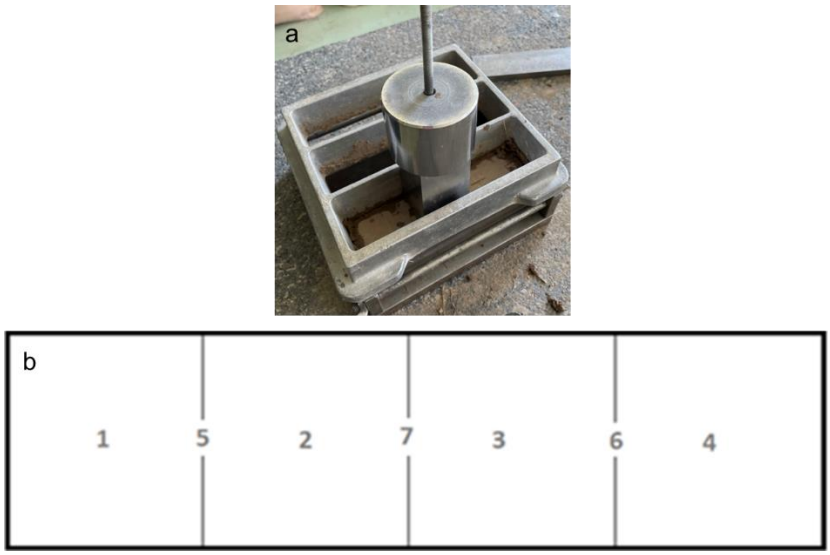

Figure 4. 17. Compaction apparatus (a) and compaction plan of bricks (b)

Dynamic compaction of Usumacinta bricks is shown in Figure 4.19c.

Compaction energy used in this test was the same as the normal proctor test *i.e. 600 kN.m/m^3*. Compaction energy was calculated with equation 4.3.

$$Et = M*g*h*n*N/V \quad (4.3)$$

where M = falling mass =1.043 kg, g= 9.8 m/s^2, h= height of falling mass = 17.8 cm, n= number of layers= 2, N= number of strokes and V= volume of mould= 4*4*16 cm^3.

(d) Drying of bricks

Usumacinta bricks were oven and air dried. Oven drying of bricks was done at 40 °C and Usumacinta bricks were dried completely in 3-4 days while air drying of bricks at room temperature (20±2°C) lasted for 2-3 weeks and depends on weather conditions. Bricks are considered dry when their mass variation is below 1%.

Oven drying pattern of Usumacinta bricks is shown in Figure 4.18. It can be seen in Figure 4.18 that the mass of Usumacinta bricks gets stabilized after 3 days of drying time and the curve becomes flat.

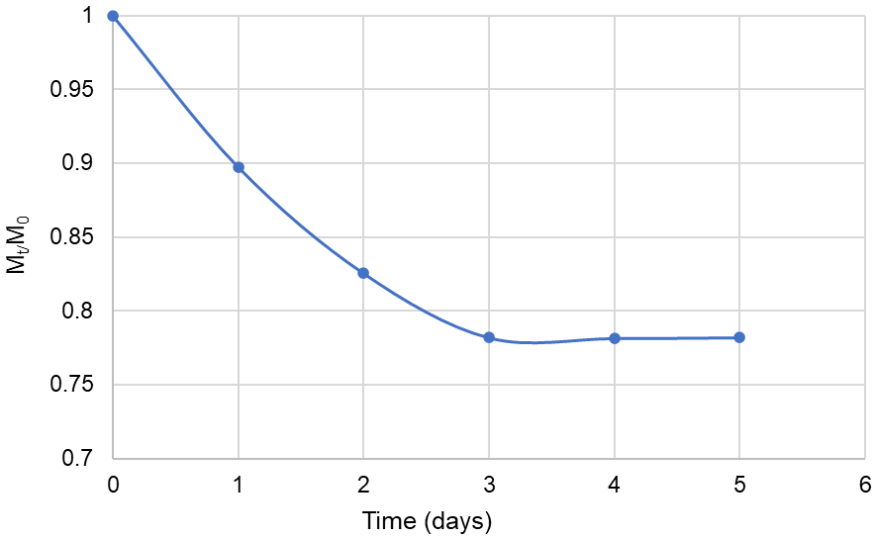

Figure 4. 18. Oven drying pattern of earth bricks

Earth bricks manufacturing process and steps are shown in Figure 4.19. Usumacinta River sediments and POFL fibers are shown in Figure 4.19a, their mixing is shown in 4.19b, dynamic compaction in 4.19c, drying in 4.19d and tensile strength testing is shown in 4.19e.

Figure 4. 19. Earth bricks manufacturing process

Earth bricks samples manufactured with varying fiber percentages are shown in Figure 4.20.

Figure 4. 20. Earth bricks samples

4.4 Testing of earth bricks

Testing of bricks was done to examine the physical and mechanical characteristics of earth bricks. These characteristics were investigated with different tests such as ultra-sonic pulse velocity (UPV) test, tensile strength, compressive strength, thermal conductivity and fibers distribution.

4.4.1 Ultrasonic pulse velocity (UPV)

UPV test was performed to see the uniformity of the structure of bricks and observe the presence of pores and cracks. Propagation of P and S waves inside the brick's changes with the presence of voids and fibers clusters inside the bricks. UPV of Usumacinta bricks was measured with a portable ultrasonic pulse velocity meter according to AFNOR standard (AFNOR NF P 12504-4, 2005). UPV apparatus and bricks testing with direct method are shown in Figure 4.21.

Figure 4. 21. Ultrasonic pulse velocity test set up

4.4.2 Linear shrinkage

Shrinkage of bricks occurs due to evaporation of water from sediments and fibers. Mould of 16cm in length was used in this study to manufacture bricks. Linear shrinkage of bricks was determined for bricks with 0% to 5% fiber content. The following formula was used to find the linear shrinkage.

$$LS\ (\%) = \frac{L_0 - L}{L_0} * 100 \qquad (4.4)$$

In this equation, L_0 stands for the initial length of bricks before drying and L is the final length after drying.

4.4.3 Density of bricks

Mass of earth bricks is measured when it becomes constant after the gradual loss of moisture during the drying process (Calatan et al., 2016). Apparent density of bricks is found by the ratio of the mass of bricks and the volume of bricks.

4.4.4 Distribution of fibers

Uniform distribution, position and alignment of fibers are essential for tensile and compressive strength of bricks. Fibers are usually randomly distributed in earth bricks. In this study, the distribution of fibers and cross-sectional area occupied by POFL fibers were found with ImageJ software. Prismatic brick specimens were cut with an electric saw into 4 equal parts with 6 cross sections having dimensions of 4*4*4 cm^3. 4 parts of bricks *i.e. 1, 2, 3 and 4* have six cross sections. These cross sections were named 1, 2S1, 2S2, 3S1, 3S2 and 4 as shown in Figure 4.22. 2S1, 2S2, 3S1 and 3S2 indicate the front and rear cross section of the second and third part of brick. The first and fourth part has only one cross section as their second side is in contact with the boundary of the mould.

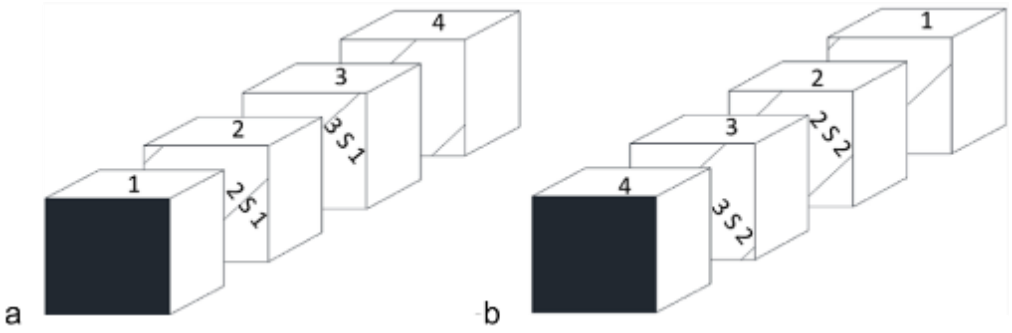

Figure 4. 22. Cross sections in a brick sample.

Surface of the brick cross section was brushed to remove loose sediments accumulated at the top. Picture of each brick section was obtained by scanning the brick cross section with a digital microscope (Figure 4.23a) and analyzed with ImageJ software. After introducing the right scale in software, fibers were highlighted with a red color threshold as shown in Figure 4.23c. The number of fibers and their respective areas were found for each cross section which helped to observe the fiber's distribution and orientation.

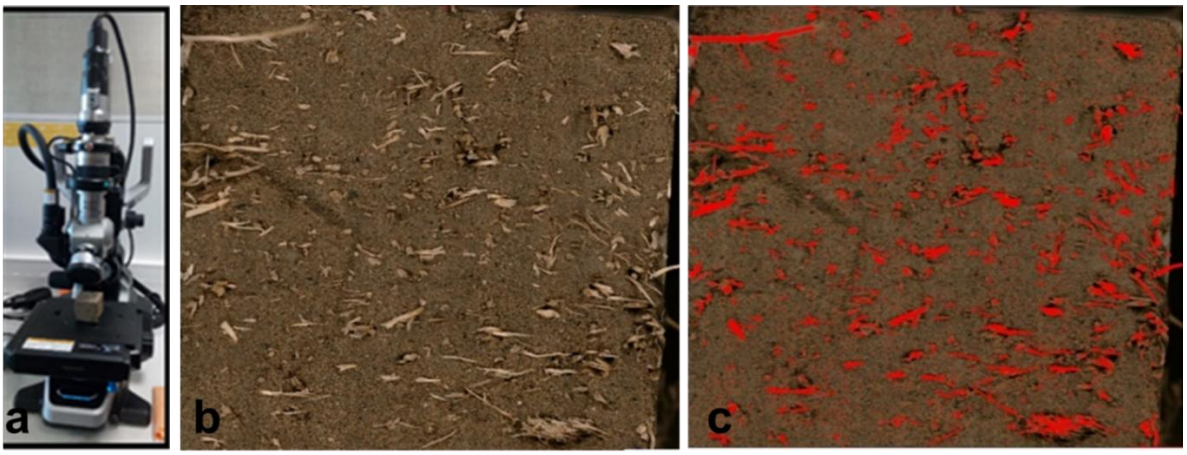

Figure 4. 23. Digital microscope (a) brick cross section (b), brick cross section after processing (b)

4.4.5 Thermal conductivity (ʎ)

Earth bricks have good heat insulation due to which heat transfer in adobe bricks is low and prevents the structure from becoming warm in summer and cool in winter. Thermal conductivity testing mechanism is shown in Figure 2.24a. Thermal analysis of two soil specimens of the size of 15*15*3 cm^3 was done with heat flow method. Specimens were manufactured G-2cm long fibers with 4% fiber content by mass and compacted with energy of 600 $kN.m/m^3$. Usumacinta brick specimen preparation is shown in Figure 4.24b.

Figure 4. 24. Thermal conductivity testing design and sample preparation.

Specimens used for testing thermal conductivity are shown in Figure 4.25.

Figure 4. 25. Sample preparation for thermal conductivity test

4.4.6 Pull out test of fibers

Pull out test was performed on earth bricks samples made with Usumacinta River sediments (J3) and POFL fibers to examine the performance of fibers under loading. For this purpose, a special prismatic wooden mold with holes on the sides was made as shown in Figure 4.26a. Brick was formed with two layers of sediment matrix. Palm oil fibers were inserted from the side with a needle after the first layer. Then second layer was added, and compaction was applied. The final product is shown in Figure 4.26b. Pull out testing of fibers is shown in Figure 4.26c.

Figure 4. 26. Wooden mould with holes (a) earth brick with fibers (b) and tensile testing (c).

Distance between the upper face of the brick and upper jaw is fixed at 10mm and the other conditions are travel speed: 1mm / min, pre-loading: 5mm / min, up to 0.5N.

4.4.7 Durability of earth bricks

Earth bricks have durability issues. Their performance decreases in a humid environment as expansion and contraction of fibers take with moisture which affects the strength of bricks. Bricks expand by absorbing moisture while on drying, moisture is released in the air and fibers shrink which induces microcracks. This is a slow process and increases the deterioration of bricks. Durability of earth bricks was observed with abrasion test, capillarity water absorption and inundation tests.

(a) Abrasion test

Abrasion test was performed on Usumacinta bricks by brushing 30 times the wire brush on the front surface of the bricks with one round of brushing each second. Abrasion resistance is estimated by the mass difference before and after the test (ASTM D559, 1994). Figure 4.27 shows the abrasion test on Usumacinta bricks.

Figure 4. 27. Abrasion testing of earth bricks

(b) Capillary water absorption (Ca)

Water absorption of adobe is important for durability of these bricks. Water absorption test for Usumacinta bricks was performed by capillary action method. Brick sample face was dipped in water up to the height of 0.5mm for 10 minutes (BS EN 772-2011).

Capillary water absorption coefficient was determined with the following formula.

$$C_w = \frac{Mw - Md}{A\sqrt{t}} \quad (4.5)$$

In this equation C_w is capillary water absorption coefficient ($kg/m^2min^{0.5}$), Mw and Md are wet and dry mass in kg. A is the surface area of earth brick in cm^2, and t is the time of water absorption in minutes. Capillary water absorption test on Usumacinta bricks is shown in Figure 4.28.

Figure 4. 28. Capillarity water absorption test

(c) Inundation of earth bricks

Earth bricks were immersed in water for 24 hours at room temperature to see the behavior of bricks in case of inundation. Damage to bricks can be light, moderate and severe. Inundation of the earth brick sample with 2cm long fibers and 4% fiber content is shown in Figure 4.29. Bubbles in the top left corner indicate the presence of voids inside the brick.

Figure 4. 29. Adobe brick immersion in water

4.4.8 Mechanical testing

Mechanical testing of bricks was performed to understand the effect of fibers content on the strength of bricks. Three-point bending tests were done on prismatic brick samples to observe the indirect tensile strength of bricks samples. Earth bricks after flexural strength test were cut into cubes of 4*4*4 cm^3, which were subjected to a compression test.

(a) Flexural strength of earth bricks

Flexural strength test was done on bricks to find the indirect tensile strength of bricks. Flexural strength of bricks was found by a 3-point bending test in which load is applied at the center of brick (ASTM D790-03, 2003). Flexural strength of dynamically compacted bricks was observed at 0%, 1%, 2%, 3%, 4% and 5% fiber content. Equation 4.6 was used to calculate the flexural strength of bricks.

$$\text{Flexural strength} = \frac{1.5*F*l}{bd^2} \quad (4.6)$$

F= flexural force, l= supported span length, b= width of earth bricks, d= height of earth brick

Failure in unreinforced compressed earth blocks in three-point loading is rapid with no toughness. Deflection before complete failure in fibers reinforced compressed earth bricks is higher than the compressed earth bricks without fibers (Mostafa and Nasim, 2015).

Flexural strength testing and failure surface of Usumacinta earth brick specimen are shown in Figure 4.30a. Rupture starts from the bottom of brick and grows upward. Load deflection curve of Usumacinta brick reinforced with 3% POFL addition is also shown in Figure 4.30b.

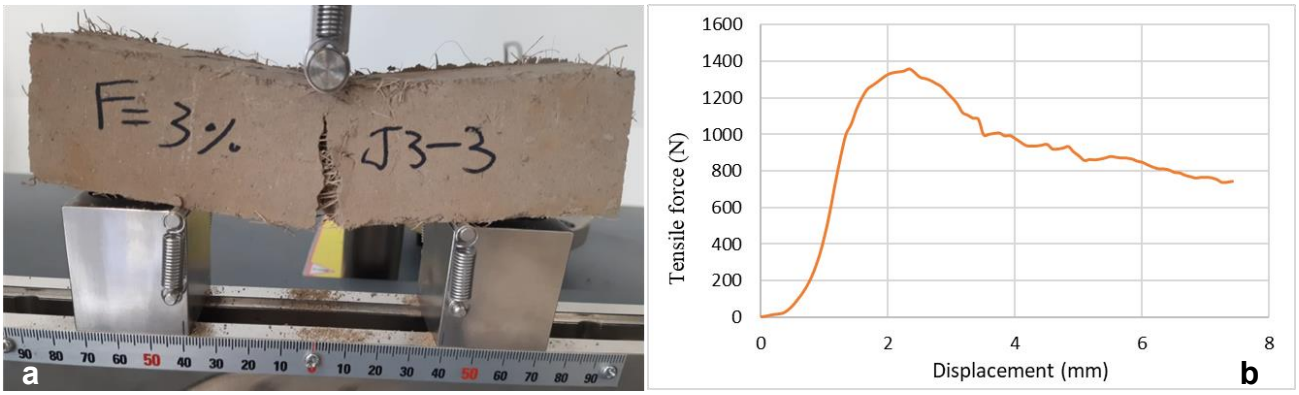

Figure 4. 30. Flexural strength testing and load deflection curve of earth bricks

(b) Toughness index (I5) of earth bricks

Fibers addition in earth bricks increases the post crack load bearing capacity of bricks as after initial cracking fibers take the load and transform the brittle failure into ductile failure. Toughness index of Usumacinta bricks was calculated with load-deflection curve by using ASTM standard (ASTM C 1018-97, 1997) as shown in Figure 4.31a.

There is usually no toughness in unreinforced bricks as bricks fail after initial cracking. It can be observed from Figure 4.31 that the post crack strength bearing capacity of brick is nearly zero and the failure mechanism is brittle. Compressive failure pattern in controlled brick specimens with 0% fiber content is similar to the failure pattern of plain concrete. In reinforced earth bricks, fibers hold the pieces of block and prevent spalling. (Mostafa and Nasim, 2015). Toughness index value for plain concrete and bricks is 1 and the addition of natural fibers increases the toughness of these materials.

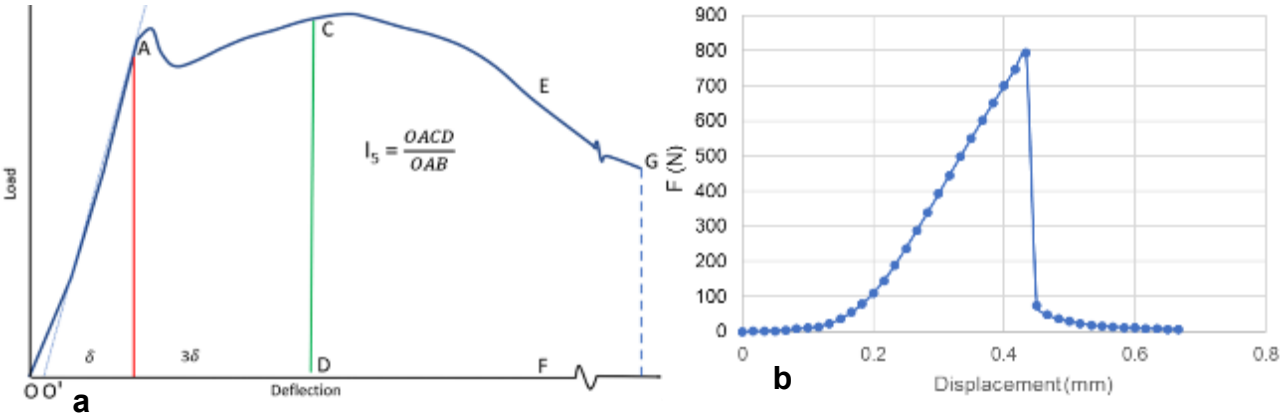

Figure 4. 31. Toughness calculation (a) and toughness of unreinforced Usumacinta bricks (b)

(c) Compressive strength

After flexural strength test, two halves of earth bricks were cut into cubic specimens of size 4*4* cm^3 with an electric saw. Compressive strength of brick specimens was tested with a Universal testing machine. Cubic specimen after flexural strength test and their loading under compression is shown in Figure 4.32.

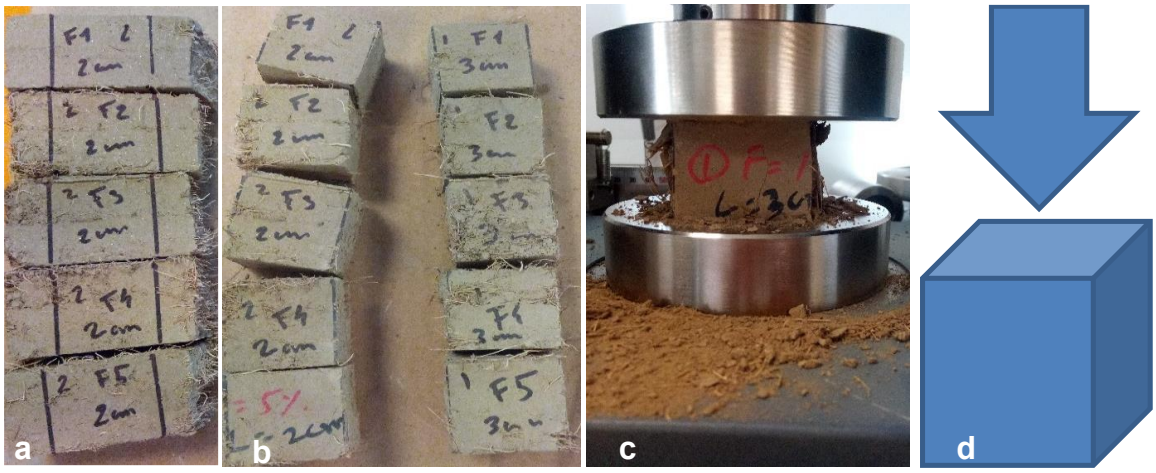

Figure 4. 32. Samples for compressive strength and their testing

Compressive strength of bricks was calculated with equation 4.7.

$$\text{Compressive strength} = \frac{\text{Compressive force}}{\text{Area}} \quad (4.7)$$

4.4.9 Earth bricks for numerical modeling

Earth bricks were manufactured for numerical modeling. For homogenous distribution of fibers, 64 flax fibers of length 16 cm were added in 8 layers through holes in bricks wooden mould of size 4*4*16 cm^3. Fibers layers spacing is kept at 5mm while the spacing for initial and bottom layers is 2.5mm for mould corners. Fibers were inserted in mould having holes of 1.5mm. Prismatic mould and fibers distribution pattern by Alioune (2022) is shown in Figure 4.33.

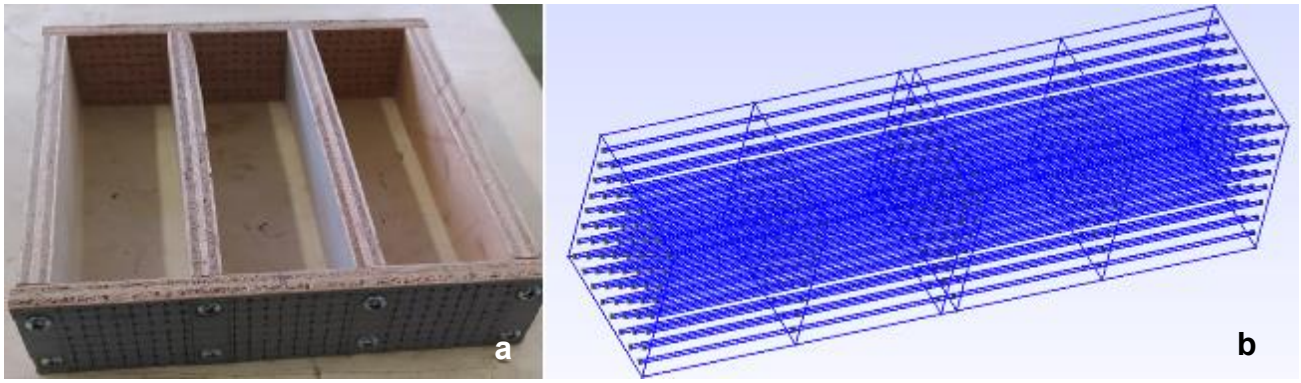

Figure 4. 33. Wooden mould (a) and fibers distribution pattern (b)

Earth bricks were dynamically compacted with the energy of 600 $kN.m/m^3$ in two layers. Each layer is supposed to incorporate 32 fibers at regular spacing. However, with compaction of

bricks, fibers layers are shifted downward due to hammering. As optimum moisture content was used to mould sediments, quantity of water is not sufficient to support the upward movement of fibers with compaction. Compacted bricks were demoulded and dried in oven. Tensile strength of oven dried bricks samples was determined with three-point bending test. The manufacturing of bricks is shown in Figure 4.34.

Figure 4. 34. Earth bricks numerical modeling samples

In parallel, Numerical modeling of earth bricks was done with code_Aster and numerical behavior of bricks was observed with numerical simulations. Finally, experimental and numerical results will be compared with experimental results

4.4.10 Fibers based bricks for wall construction

Palm oil flower fibers reinforced 40 earth bricks of dimension 4*4*16 cm^3 were manufactured with J3 sediments to construct earth bricks wall and observe its behavior. Bricks samples are shown in Figure 4.35.

Figure 4. 35. Earth bricks samples

The dry mass of each brick and dimensions were measured. Density and linear shrinkage of these bricks were also calculated. Average values of density, linear shrinkage, mass, length, width and height of 40 brick samples at 4% fiber content are shown in Table 4.8.

Table 4. 8. Dimensions of and physical parameters of bricks.

Usumacinta bricks	**Average**
Density (kg/m^3)	1524.17±36.54
mass (kg)	0.370±0.02
Linear shrinkage (cm)	0.36±0.15

4.4.11. Lime based bricks for wall construction

Cement, lime and gypsum are common stabilizing agents used for earth bricks (Adam and Agib, 2001). Earth bricks of dimension 4*4*16 cm^3 were manufactured from Usumacinta River sediments (T6) with the addition of lime. The percentage of lime used is 1.5% which is the amount of lime required to initiate pozzolanic reaction (Djeran-Maigre et al. 2022). Bricks samples were left for curing for 60 days and 1.5 year. Earth bricks samples stabilized with lime under packing are shown in Figure 4.36.

Figure 4. 36. Lime stabilized earth bricks samples

4.4.12. Masonry wall

Laboratory scale masonry walls of dimensions 50 x 67 x 4 cm3 (width, height and thickness respectively) were constructed with three types of Usumacinta River sediments bricks which are fired bricks (T10), lime-based bricks (T6) and bio-based bricks (J3) reinforced with palm oil flower fibers. Pushout test was done on walls built on foundation beams by applying lateral load with loading speed of 1mm/min on the top of the wall with hydraulic apparatus (Djeran-Maigre et al. 2022).

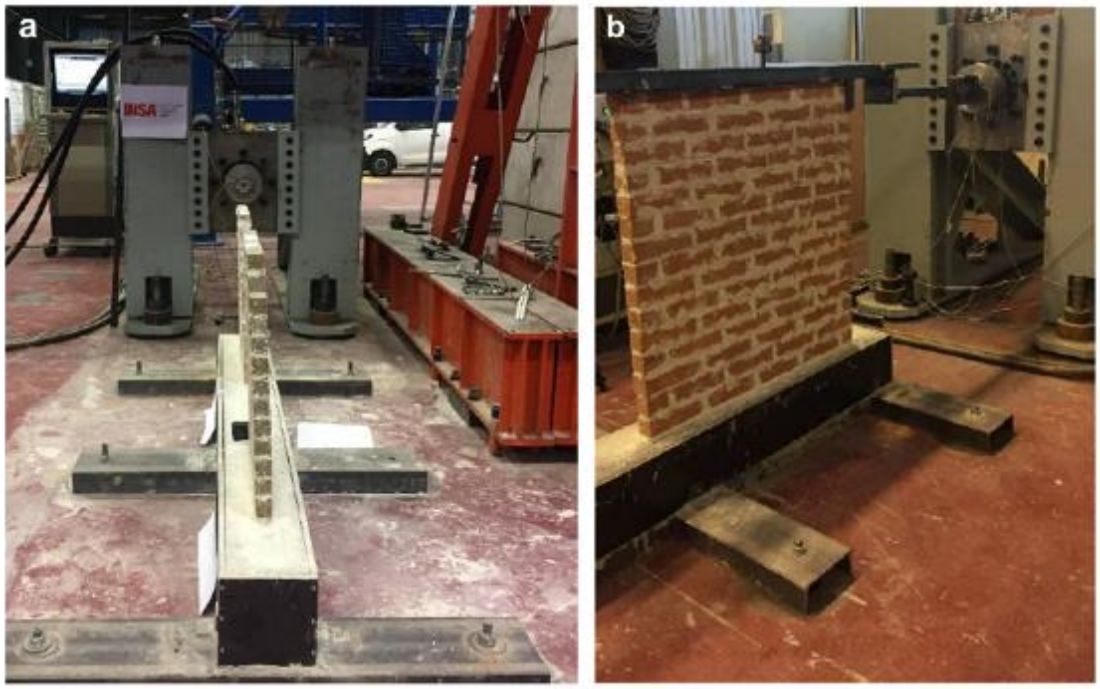

Figure 4. 37. Positioning of wall (a) and its horizontal loading (b) (Djeran-Maigre et al. 2022).

4.5 Results and discussion

4.5.1. Linear shrinkage (LS)

The average linear shrinkage of 3 Usumacinta bricks samples on drying is shown in Table 4.9.

Table 4. 9. Linear shrinkage in bricks with G-2cm and G-3cm long fibers

Brick	DC 0%	DC 1%	DC 2%	DC 3%	DC 4%	DC 5%
LS $_{G-2cm}$ (mm)	1.5	1.88	2.63	1.88	1.88	1.88
LS $_{G-3cm}$ (mm)	1.5	2.19	2.81	2.5	1.09	1.63

Note: DC = dynamic compaction, LS = linear compaction

The value of linear shrinkage for G-2cm long fibers is below 2mm in most of the bricks except for the brick with 2% fibers. This indicates that shrinkage is nearly constant. Linear shrinkage of bricks with G-3cm long fibers varies from 1.09 to 2.81. Linear shrinkage of bricks varies with clay content, moisture content and fiber content. Shrinkage of bricks increases with increasing clay and moisture content. Addition of natural fibers controls the growth of cracks and shrinkage on drying. However, fibers contribution to control shrinkage in earth bricks is more evident in clayey soils (Tavares and Magalhães, 2019). The impact of POFL fibers addition on shrinkage in Usumacinta River sediments bricks is trivial as Usumacinta earth bricks have very low shrinkage. Moreover, in manual manufacturing, it is difficult to control the quantity of sediments and fibers during the filling of moulds.

4.5.2. Density of brick

Density of earth bricks decreases with increasing natural fibers as density of fibers is less than the density of sediments and pores are induced in bricks with swelling and shrinking of fibers during saturation and drying of bricks. Average density of three Usumacinta bricks samples with G-2cm and G-3cm long fibers is shown in Table 4.10.

Table 4. 10. Density variation of Usumacinta bricks with fiber content

Brick	DC 0%	DC 1%	DC 2%	DC 3%	DC 4%	DC 5%
Density G-2cm (kg/m^3)	1521	1510	1538	1536	1494	1479
Density G-3cm (kg/m^3)	1521	1525	1503	1475	1430	1429

Density of Usumacinta bricks decreases with increasing fiber content and fluctuates between 1525 kg/m^3 and 1430 kg/m^3. Common density values of adobe bricks in literature range from 1260 kg/m^3 to 1950 kg/m^3 (Illampas et al. 2011, Salih, et al. 2019).

Relationship between density and fibers content for Usumacinta bricks is shown in figure 4.38.

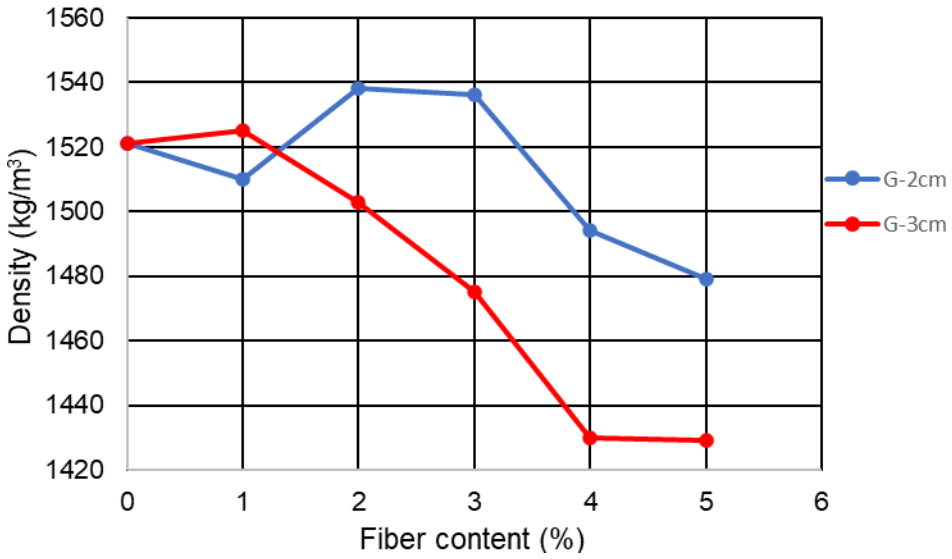

Figure 4. 38. Density variation with fiber content for G-2cm and G-3cm long fibers

It can be seen from figure 4.38 that density of bricks decreases with the addition of fibers and its value is minimum with 5% fibers content for G-2cm and G-3cm long fibers. Density values of bricks for bricks with G-2cm long fibers are slightly higher than density values of bricks with G-3cm long fibers. In case of Usumacinta bricks, it is difficult to fit a linear trend as it is difficult to control the quantity of sediments mixture during manual manufacturing of earth bricks.

Ige and Danso (2021) found that the density of earth bricks decreases linearly with increasing fibers content and equation 4.8 describes the relationship between density and fiber content with R^2 value of 0.97.

$$Y = -66.4X + 1628.6 \quad (4.8)$$

where Y = density kg/m^3 and X = fiber content (0%, 0.25%, 0.5%, 0.75 and 1%)

Relation between the density and fiber content varies for different sediments, natural fibers and manufacturing conditions such as moulding moisture content, fiber content and compaction etc.

4.5.3. Fibers distribution in bricks

Number of fibers and area occupied by POFL fibers in each cross section of Usumacinta brick at 3% fiber content is shown in Table 4.11. Number of fibers and area occupied by fibers is nearly similar in both types of bricks i.e. *G-2cm and G-3cm long fibers*. Each brick is cut into 4 parts with 6 exposed cross sections. Number of fibers observed with a digital microscope in each cross section is shown in Table 4.11. Similarly, area of each cross section occupied is also shown in Table 4.11.

Table 4. 11. Number of fibers and area occupied by fibers in a cross section

Cross sections	1	2	3	4	5	6
Number of fibers G-2cm	76	390	297	314	280	326
Number of fibers G-3cm	280	288	249	276	252	288
Area of G- 2cm fibers (%)	2.68	7.12	7	7.25	6.05	8.69
Area of G-3cm fibers (%)	5.88	7.25	6	6.5	6.5	8.5

Each cross section of G-2cm long fibers bricks consists of 272 fibers on average similarly G-3cm bricks have 280 fibers. Average area occupied by G-2cm long fibers is 6.71% and G-3cm long fibers are 6.46%. Area occupied by fibers is similar in both types of bricks as the fiber content is the same in both bricks.

Fibers distribution is anisotropic inside the earth bricks. Fibers are randomly distributed in earth bricks in all directions and prevent the transverse and longitudinal deformation of earth bricks. Longitudinally distributed fibers significantly increase the tensile strength of building composites and prevent transverse and longitudinal deformation in bricks. Properties of fibers having random orientation are in between the longitudinally and transversely distributed fibers. Alberti et al., 2018, found through numerical simulations of fiber reinforced concrete that the orientation of fibers is usually good in short fibers. The fibers which are in vertical directions are torn apart on applying force. Fibers distribution in bricks is affected by moulding moisture content, the filling of moulds and compaction method. In case of dynamic compaction of bricks with excessive moulding moisture content, fibers move toward the top surface of bricks which affects the distribution of fibers and strength of bricks.

4.5.4. Thermal conductivity of bricks

Thermal conductivity of bricks from Usumacinta bricks is around 0.23 W/m-K. Thermal conductivity of these is substantially lower as addition of natural fibers in adobe bricks increases the porosity of bricks and decreases the thermal conductivity of bricks. Moreover, thermal conductivity of natural fibers is also significantly low. Usually, thermal conductivity of earth bricks ranges from 0.18 to 1.13 W/m-K (Revuelta-Acosta et al., 2010; Bahobail, 2011; Calatan et al., 2016) and that of concrete is around 1 W/m-K (Kanbur et al., 2013). Low thermal conductivity is essential to minimize the energy consumption of buildings.

4.5.5. Pull out strength

Fibers inside the bricks are fails by rupture or by sliding inside bricks on applying external traction force which depends on fibers embedded length and adhesion between fibers and sediments. Fibers in Usumacinta River sediments bricks tend to slide in bricks which shows the weak adhesion between fibers and sediments. Pull out strength of POFL fibers at failure is shown in Table 4.12

Table 4. 12. Pull out strength of POFL fibers at different depths

Embedded depth (cm)	Pull out strength (MPa)
1	77.92
2	72.11
3	61.19
4	64.15

POFL fibers were embedded at a depth of 1cm to 4cm in earth bricks and their pull-out strength range is around 61 MPa to 77 MPa. All the fibers fail by sliding in matrix before reaching their tensile strength limit which is around 119 MPa. Rupture of fibers or sliding depends on embedded lengths and tensile strength of fibers. Deeply embedded fibers incline towards the rupture while fibers with less embedded length slide due to short length and weak interfacial adhesion. Danso et al., 2017 performed experiments on earth bricks to observe the pull out and rupture length of fibers in earth bricks. Tests were performed on sugarcane bagasse, coconut and palm oil fibers and it was observed that natural fibers in adobe bricks slide when they are embedded at a depth of 3 mm and ruptured when they have an embedded depth of 5mm.

4.5.6. Ultrasonic pulse velocity (UPV)

Average UPV values of two earth brick samples with G-2cm and G-3cm long fibers and fiber content from 0% to 5% are shown in Table 4.13. UPV value decreases with addition of fibers due to voids and cracks which are induced after addition of fibers. Compaction of bricks also influence the results. UPV variation with fiber content is shown in Table 4.13.

Table 4. 13. Ultrasonic pulse velocity of bricks with G-2cm and G-3cm long fibers

Brick	DC 0%	DC 1%	DC 2%	DC 3%	DC 4%	DC 5%
UPV (m/s) -2cm	1261	1510	1538	1536	1494	1479
UPV (m/s) -3cm	1261	1548	1446	924	1046	1012

UPV values at 0% fiber content are slightly lower than other values. This is because POFL fibers were kept in water before using them in bricks. Presence of water in fibers influence the moulding moisture content. Slight variation in moulding moisture of sediments mixture changes the compaction and density of bricks. Variation in compaction, changes UPV values of bricks. From 1% to 5% fibers addition, variation in UPV values of bricks is more obvious and it decreases with fibers addition. UPV values of Usumacinta bricks range from 924 m/s to 1548 m/s. UPV values of earth bricks in the literature vary between 1086 m/s to 1251 m/s at varying fiber content (Türkmen et al., 2017). Table 4.13 shows some exceptions for a decrease in UPV with fiber content. Manual compaction of bricks and sediments quantity used during moulding of bricks varies with operators as it is difficult to control sediments amount which affects the results. In addition, uneven brick surfaces and faulty mixing and manufacturing procedure are contributing to imprecise results.

4.5.7. Flexural strength of bricks

Load deflection curves for bricks with 0% to 5% fiber content of G-2cm and G-3cm long fibers are shown in Figures 4.39 and 4.40.

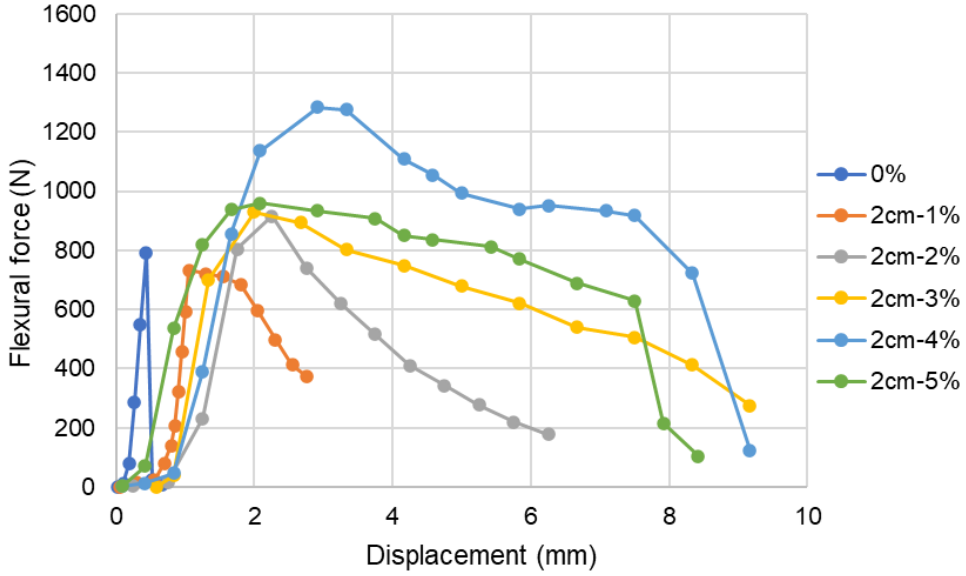

Figure 4. 39. Flexural load deflection curves with G-2cm long fibers

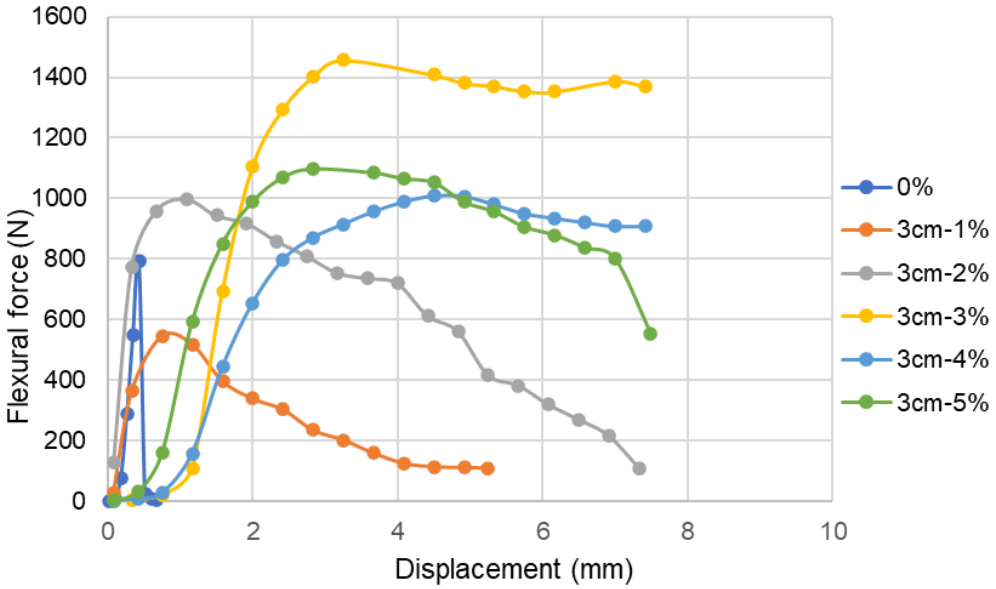

Figure 4. 40. Flexural load deflection curves with G-2cm long fibers

Average flexural strength of 3 earth bricks samples made with G-2cm and G-3cm long fibers at different fiber percentages are given in Table 4.14.

Table 4. 14. Flexural strength of earth bricks at different lengths and fiber content

Fiber content (%)	**0%**	**1%**	**2%**	**3%**	**4%**	**5%**
σ_t (MPa)-2cm	1.79±0. 01	1.56± 0.2	2.37± 0.3	2.37± 0.35	2.93± 0.03	2.38 ± 0.2
σ_t (MPa)-3cm	1.79±0. 01	1.79± 0.3	2.56± 0.2	3.19± 0.4	2.02± 0.2	2.59± 0.1

Table 4.14 and figure 4.39 show that the addition of fibers increases the tensile strength of Usumacinta bricks and improves the load bearing capacity of bricks after initial cracking. After the initial crack, fibers help the bricks to withstand the load. It can be observed in Figures 4.39 and 4.40 that failure in Usumacinta bricks with 0% fiber content is brittle as the strength of bricks drops rapidly after initial cracking. Fiber addition changes their behavior to ductile failure in which load bearing capacity gradually decreases.

It can be observed from Table 4.14 that with the addition of 4% fiber content of G-2cm long fibers, earth bricks have maximum flexural strength. For 3cm long fibers, bricks have maximum flexural at 3% fiber content. Earth bricks have maximum tensile strength with G-2cm long POFL fibers at 4% addition of fibers and this value is 2.93 MPa. Similarly, Usumacinta bricks with 3cm long POLF fibers have maximum tensile strength at 3% addition of fibers and their strength is 3.19 MPa. Flexural strength increases with fiber addition but after optimum fiber percentage, flexural strength starts to decrease. This is because, with a higher percentage of fibers, adhesion between sediments and fibers starts to decrease. Clusters of fibers are another phenomenon associated with higher fiber quantity. Tensile strength for G-2cm long fibers and G-3cm long fibers increases by 39% and 78% respectively from unreinforced bricks manufactured with Usumacinta River sediments. Ige and Danso (2021) observed a 53% increase in tensile strength of adobe bricks with the addition of 0.5% plantain pseudo-stem fibers of length 75mm.

It can be seen in table 4.14 that bricks have higher flexural strength with long fibers. Long fibers prevent the spalling of brick during flexural strength test and their longitudinal distribution in bricks maximizes the reinforcing influence of fibers. However, increasing the length of fibers decreases the compressive strength of bricks and the orientation of fibers is better in short fibers (Binici et al., 2005; Alberti et al., 2018).

Minimum tensile strength recommended for earth bricks varies in different standards and it ranges from 0.012 MPa to 0.25 MPa in French, Mexican and other standards (NZS, 1998, NORMA E.080, 2017; AFNOR XP, P13-901, 2001). In Table 4.14, all the bricks from Usumacinta River sediments have significantly higher flexural strength which is indirect tensile strength. Tensile strength of natural fibers reinforced earth bricks varies significantly and depends on different factors such as percentage of fibers, nature of sediments, compaction and moulding moisture content etc. Table 4.15 shows the tensile strength of earth bricks reported in the literature.

Table 4. 15. Tensile strength of fiber reinforced earth bricks

Fibers	Fiber content (wt.%)	Tensile strength (MPa)	Reference
Jute	0.5-2	0.55-0.66	Araya-Letelier et al., 2021
Seagrass	0.5-3	0.4-0.6	Olacia et al., 2020
Straw	0.5	0.71	Abdulla et al., 2020
Sugarcane bagasse	0-1	0.29-0.89	Kumar and Barbato, 2022
Date palm waste	0-10	0.29-2.26	Khoudja et al., 2021

Note: References of table 4.15 are given in chapter 1.

It can be seen from Table 4.15 that Usumacinta bricks have considerably higher strength than literature values.

4.5.8. Bending stiffness

Bending stiffness of Usumacinta bricks is the slope of flexural load deflection curves in Figure 4.39. Table 4.16 shows the average flexion stiffness value of earth bricks

Table 4. 16. Flexion stiffness of earth bricks

Fiber content (%)	**0**	**1**	**2**	**3**	**4**	**5**
E-2cm (N/mm)	3080	1913	2287	1335	1185	1151
E-3cm (N/mm)	3080	2400	2541	1526.5	965	1051

Bending stiffness of bricks is heavily influenced by the sediment's nature and addition of fibers. With increasing palm oil fiber content, flexural modulus decreases. This is because the peak value of flexural load is achieved after high deflection with high fiber content and a vertical rise of the curve is gradual while it is sharp in the case of the controlled specimen with 0% fiber content.

4.5.9. Toughness index of bricks

Toughness of earth bricks increases with addition of natural fibers. Toughness index values of earth brick at different fiber lengths and fiber content are presented in Table 4.17. Toughness of brick is maximum at 3% fiber content for G-2cm long fibers and 3% fiber content for G-3cm long fibers. Usually, both toughness index and tensile strength are maximum at optimum fiber percentage.

Table 4. 17. Toughness index of Usumacinta bricks

Fibers content (%)	**1**	**2**	**3**	**4**	**5**
Length= 2 cm	3.95	4.02	4.38	4.24	4.73
Length= 3 cm	2.58	4.18	4.42	3.83	3.89

4.5.10. Compressive strength

Compressive strength of Usumacinta bricks with G-2cm and G-3cm long fibers with addition of 0 to 5% fibers were tested with Universal testing machine on pieces of 4*4*4 cm^3. Graphs in Figures 4.41 and 4.42 show the compressive load deflection curves of Usumacinta bricks.

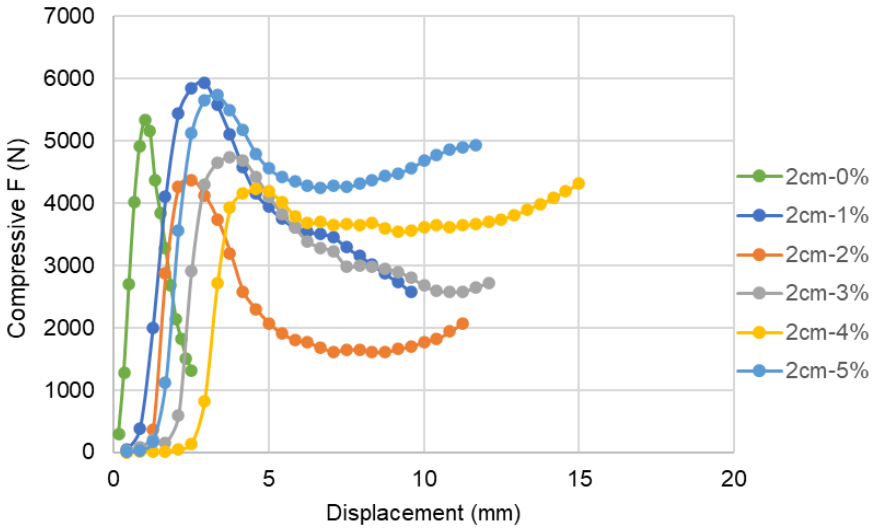

Figure 4. 41. Compressive load and deflection curve for G-2cm long fibers.

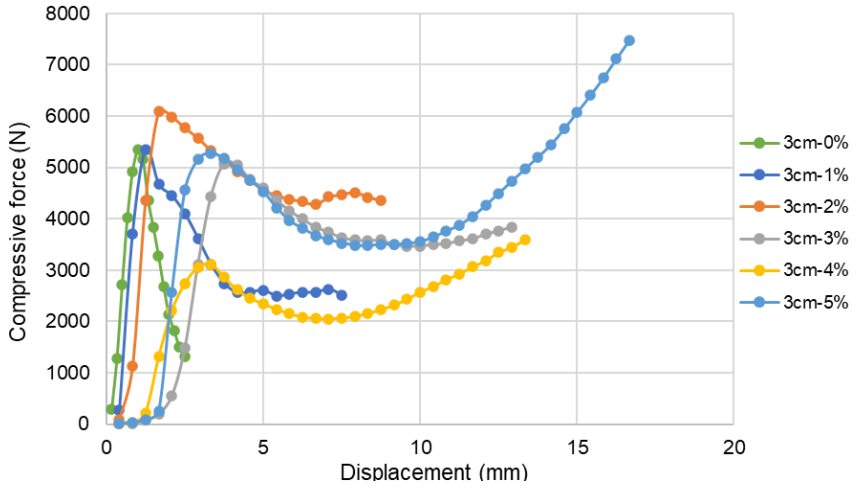

Figure 4. 42. Compressive load and deflection curve for G-3cm long fibers.

In Figure 4.41 and 4.42, compressive load of bricks has two peaks. In bricks with 0% fibers, compressive load decreases continuously after initial failure. With increasing fibers content, we can see from the curves that the strength of bricks decreases after initial failure and start to rise again as the load is shifted on fibers. This plateau behavior is associated to the good adhesion between fibers and sediments. Average compressive strength of 4 brick samples at initial failure is shown in Table 4.18.

Table 4. 18. Compressive strength of earth bricks at initial cracking

Fiber content (%)	**DC 0%**	**DC 1%**	**DC 2%**	**DC 3%**	**DC 4%**	**DC 5%**
σ_c (MPa)-2cm	3.03 ± 0.2	3.72 ±0.2	2.77 ±0.7	2.97 ±0.1	2.75 ±0.3	3.59 ±0.2
σ_c (MPa)-3cm	3.03 ± 0.2	3.34 ±0.1	3.84 ±0.2	3.21 ±0.4	2.29 ±0.2	3.29 ±0.3

Compressive strength of earth bricks increases randomly with increasing fiber content. Compressive strength is maximum at 1% fiber content for G-2cm long fibers and its value is 3.72 MPa while for G-3cm long fibers its value is maximum at 2% fiber content which is 3.84

MPa. Recommended compressive strength of earth bricks is 1 MPa in French and Mexican standards (AFNOR XP, P13-901; NORMA E.080, 2017).

Relationship between fiber content and compressive strength for Usumacinta River sediments with G-2cm and G-3cm is shown in Figure 4.43.

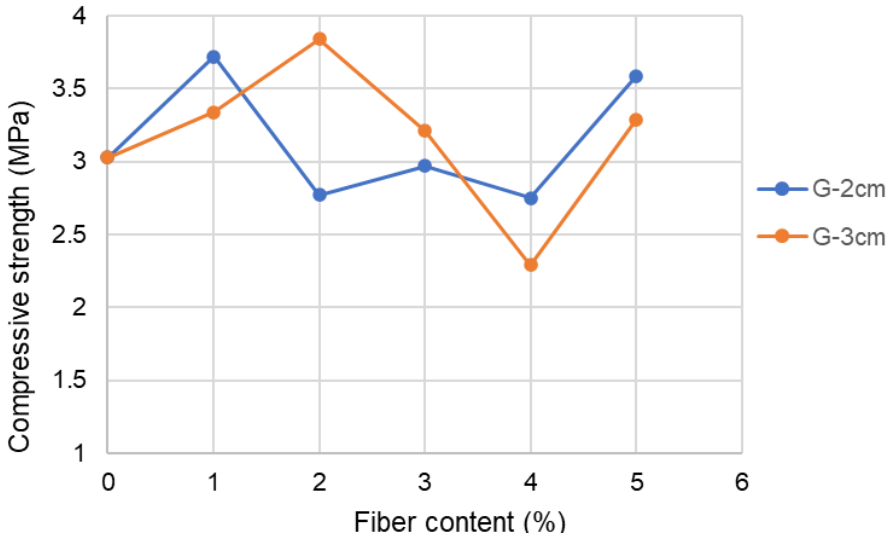

Figure 4. 43. Compressive strength variation for G-2cm and G-3cm long fibers

Caporale et al., 2014 reported compressive strength relation with fiber content by mass. 0.6% of straw fibers of 70 mm length and 3mm diameter were used to make earth bricks. The following equation explains the decrease of compressive strength with increasing fiber content.

Compressive strength = 2.16 exp (-0.33*fiber content by mass) (4.9)

The ratio between compressive strength and tensile strength of Usumacinta bricks with G-2cm and G-3cm long fibers at different fibers content is shown in Table 4.19.

Table 4. 19. Ratio between compressive strength and tensile strength

Fiber content (%)	**0**	**1**	**2**	**3**	**4**	**5**
σ_c/σ_{tb}-2cm	1.70	2.40	1.17	1.25	0.94	1.50
σ_c/σ_{tb}-3cm	1.70	1.86	1.50	1.00	1.13	1.87

Compressive and flexural strength values range from 0.94 to 2.4 MPa for 2cm long fibers and 1 to 1.87 MPa for 3cm long fibers. For unreinforced bricks at 0% fiber content, ratio of compressive and tensile strength is 1.70. These values are far less than the typical concrete value of 10. Table 4.20 shows the compressive and tensile strength and their ratio for earth bricks tested in different parts of the world.

Table 4. 20. Compressive and tensile strength of earth bricks observed in different studies

Location	σ_c	σt	σ_c/σ_{tb}	Reference
Portugal	1.17	0.19	6.16	Silveira et al. 2012
Mexico	0.51-1.57	0.20-0.43	2.55 to 3.65	Meli, 2005
Colombia	3.04	0.41	7.415	Rivera and Muñoz, 2005
Morroco	2.83	0.18-0.35	15.72 to 8.08	Baglioni et al. 2010
Itlay	0.29-1.56	0.17-0.40	1.70 to 3.90	Liberatore et al. 2006

Compressive and tensile strength have huge variations as the strength of bricks is influenced by heterogenous nature of sediments, fibers and manufacturing conditions of earth bricks.

4.5.11. Durability testing of bricks

(a) Inundation of bricks in water

Bricks samples were inundated for 24 hours. After 2 hours of inundation, bricks were severely degraded which shows the vulnerability of earth bricks to inundation. Fibers in adobe bricks act as a channel for water and dislodge quickly. In areas with heavy rains and floods, adobe bricks should be stabilized with cement and lime and if possible to protect the adobe walls against rains.

(b) Abrasion testing

Abrasion test on Usumacinta River sediments shows that mass loss of Usumacinta River sediments bricks is around 14%. The acceptable mass loss range in cement stabilized earth blocks ranges from 6% to 12% (ASTM D559, 1994).

(c) Capillary water absorption (Ca)

Water absorption by capillarity action for Usumacinta River sediments earth bricks after 10 minutes immersion time is around 1.56 $\frac{kg}{cm^2}.min^{0.5}$. French standrd (AFNOR NF EN 1015-18, 2003) recommends capillary water absorption below 0.4 $\frac{kg}{cm^2}.min^{0.5}$ for mortar. However, earth bricks are different from mortar and vulnerable to water.

4.5.12. Earth bricks stabilized with lime

Usumacinta bricks were stabilized with addition of 1.5% lime. Tensile and compressive strength of lime stabilized bricks was determined after a curing time of 60 days and 1.5 year. Flexural strength testing of earth bricks can be seen in Figure 4.44a. Flexural load deflection curves of lime stabilized bricks with a curing time of 1.5 year are also shown in 4.44b.

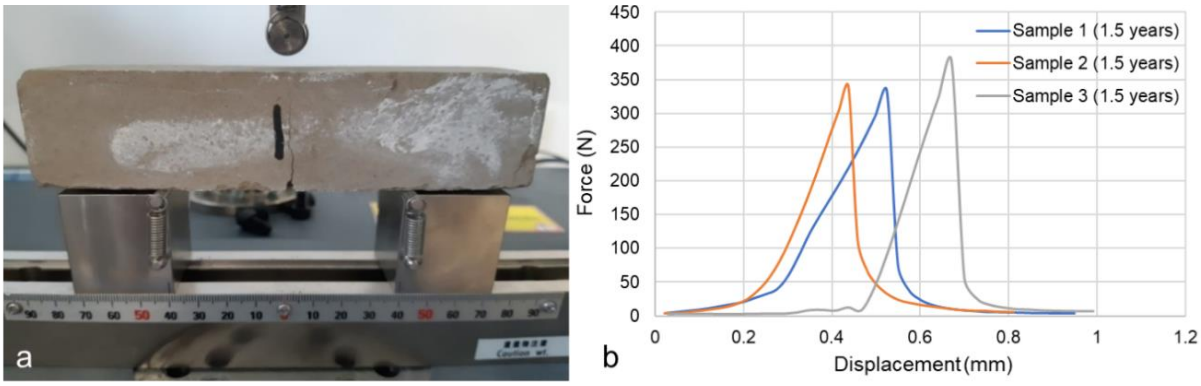

Figure 4. 44. Flexural strength test on earth bricks (a) and load deflection curves (b)

Whitening on the surface of bricks indicates the efflorescence which occurs on drying after evaporation of water. Average flexural strength of brick samples at different curing times is shown in Table 4.21.

For compressive strength test, each brick is divided into 2 cubes of size 4*4*4 cm^3. Brick cubes and their compressive strength testing in Figure 4.45.

Figure 4. 45. Cubic brick samples (a) and compression testing (b)

Load deflection curves for compressive strength for brick samples are shown in Figure 4.46.

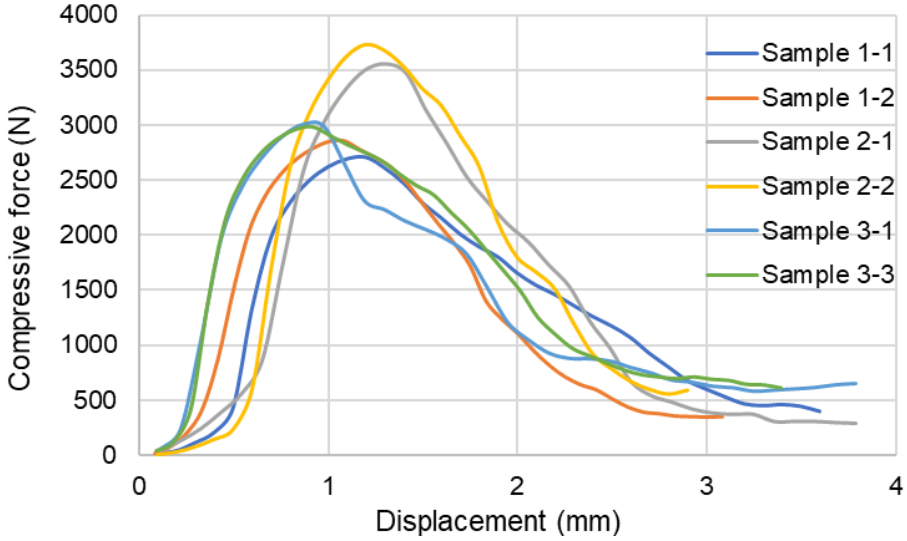

Figure 4. 46. Compressive load deflection curves of bricks after 1.5 year

Compressive strength variation of lime stabilized bricks with time is shown in Figure 4.47.

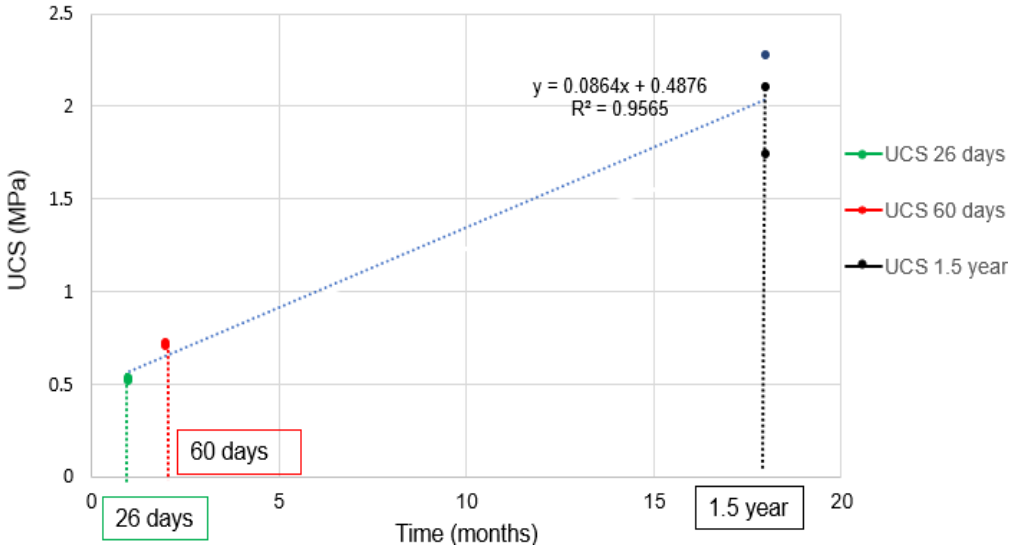

Figure 4. 47. Compressive strength variation with time

Figure 4.47 shows that compressive strength of lime stabilized bricks increases with time. Compressive and tensile strength of lime stabilized bricks is shown in Table 4.21.

Table 4. 21. Compressive and tensile strength of lime-based bricks

Strength	**60 days = 2months**	**1.5 years =18 months**
σc	0.71	2.03
σt	0.31	0.67

4.5.13. Masonry wall of Usumacinta River sediments bricks

During pushover test, wall constructed with fired bricks shows initially elastic behavior. However initial cracking in mortar transforms it into inelastic linear behavior and horizontal pushover force shows a plateau behavior at a load of 140 N. After that, load decreases suddenly and the wall collapse through sliding failure with displacement of 4mm. Maximum load observed is around 146 N. Load displacement behavior of fired bricks wall is shown in Figure 4.48. In case of lime-based bricks, initially load increases elastically, followed by a plateau. Load increases slowly and the wall collapse at a load of 120 N. In case of fiber reinforced bricks, initial cracking occurs at 15 kN. However, load starts to increase linearly and rapidly. With increasing load, the width of initial crack also increases and the elastic phase ends near 100 N with rotation of wall. However, load continues to increase slowly. Test was stopped after vertical displacement of the bottom side lifted by 4cm. Figure 4.48 shows the load deflection curves of masonry walls (Djeran-Maigre et al. 2022).

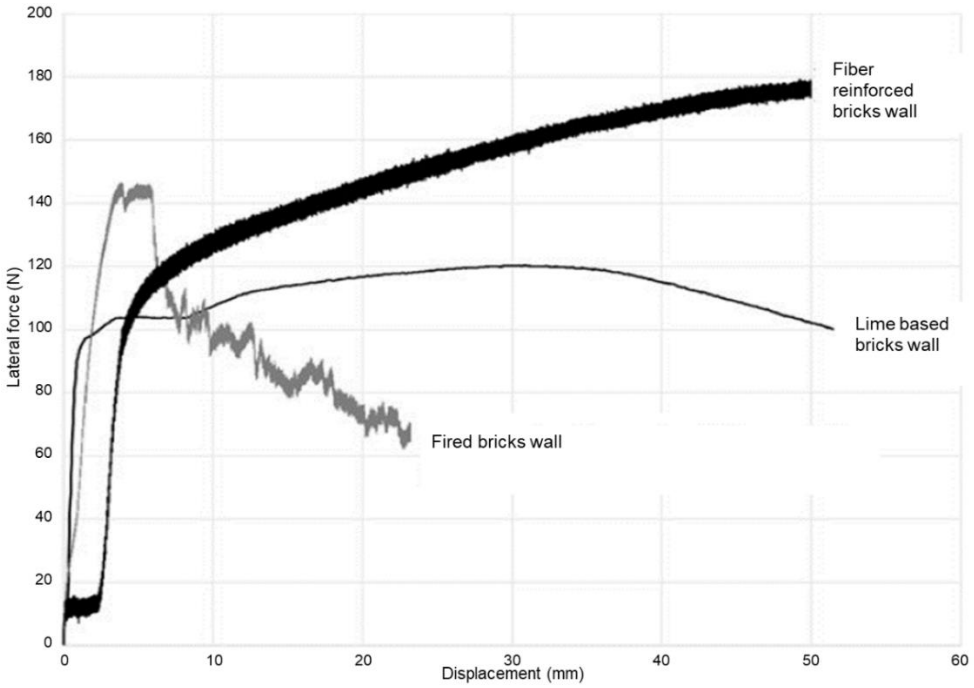

Figure 4. 48. Load deflection behavior of Usumacinta sediments-based bricks (Djeran-Maigre et al. 2022).

Figure 4.48 shows that fired bricks wall has maximum resistance against horizontal loading. However, fiber-based bricks also show good resistance. Final load withheld by bricks wall is shown in Table 4.22.

Table 4. 22. Maximum horzental load and failure mode (Djeran-Maigre et al. 2022)

Wall nature	**Maximum load (N)**	**Failure mode**
Fired bricks	146	Sliding
Lime bricks	120	Rotation F*
Fiber bricks	Not measured	Rotation F*

*Note: *Rotation near foundation*

4.6 Earth bricks limitations

Earth bricks are less resistant to weathering actions. The compressive strength and durability of earth bricks are limited when compared with other building materials such as fired bricks and concrete.

Natural fibers are used as reinforcement in earth bricks. These fibers swell when they are saturated with water and contract when water is evaporated during drying process of bricks. After water evaporation, cracks are developed at the periphery of fibers which affects the strength of bricks. Degradation of natural fibers is another drawback of crude brisk. Strength of natural fibers deteriorates with time which affects the strength of bricks. Degradation of fibers increases in alkaline environments. Fibers start to decompose due to humidity and microorganism activities after some time.

4.7 Conclusion

Earth bricks manufactured with Usumacinta River sediments represent one of the suitable recovery solutions and offers the possibility of constructing ecological buildings with local resources and materials. In this chapter, Usumacinta River sediments characteristics were investigated for their use in earth bricks. According to AFNOR and MOPT standards, granulometry and Atterberg limits of Usumacinta River sediments are within the range recommended for earth bricks.

Earth bricks were manufactured with J3 sediments with 0%, 1%, 2%, 3%, 4% and 5% fiber content and compacted dynamically with energy of 600 kN.m/m^3. Physical and mechanical characteristics of earth bricks such as shrinkage, density, fibers distribution, capillary absorption, thermal conductivity, tensile strength and compressive strength were investigated.

Linear shrinkage in earth bricks is very small and ranges from 1.55mm to 2.81mm. Density of Usumacinta bricks ranges from 1429 kg/m^3 to 1538 kg/m^3 and is lowest at 5% fiber content. Fibers distribution is anisotropic in brick cross sections they occupy 6 to 7% area of a brick cross section. Thermal conductivity of Usumacinta bricks is considerably low and its value is around 0.23 W/m-K which is important thermal comfort of buildings.

Ultrasonic pulse velocity of Usumacinta bricks ranges from 1012 m/s to 1538 m/s. Earth bricks have durability issues. Usumacinta bricks mass loss is around 14% with abrasion test which is considerably higher. Inundation of bricks also shows their vulnerability to water.

Pull out strength test shows the failure of fibers inside the bricks with sliding and pull out strength of fibers increases with increasing embedded length of fibers inside the bricks. Pull out resistance of POFL fibers ranges from 61.19 MPa to 77.92 MPa.

Usumacinta bricks have a maximum tensile strength at 4% fiber content with G-2cm long fibers which is 2.93 MPa. Similarly, G-3cm long fibers, bricks have maximum tensile strength at 3% fiber content which is 3.19 MPa. With G-2cm long fibers, at 4% fiber content, tensile strength of bricks is 39% higher than the controlled samples with 0% fiber content. Bricks with G-3cm long fibers tensile strength at 3% fiber content is 78% higher than controlled sample. Compressive strength of bricks is maximum at 1% fiber content for G-2cm long fibers and its value is 3.72 MPa while for G-3cm long fibers, it is maximum at 2% fiber content and its value is 3.84 MPa. Usumacinta bricks good tensile and compressive strength and satisfy the recommended strength limitations. Recommended tensile strength of earth bricks varies from 0.12 MPa to 1 MPa while recommended compressive strength of earth bricks is around 1 MPa (NZS, 1998, NORMA E.080, 2017; AFNOR XP, P13-901, 2001).

Masonry wall with Usumacinta sediments bricks shows that the fired bricks-based masonry wall has maximum resistance against lateral loading which is 146 N while lime-based bricks wall supports the load up to 120 N. Fibers reinforced brick have shown significant rotation at 100 N, however, load continues to increase. Masonry wall testing shows that fiber reinforced earth bricks have good resistance and they can be a sustainable solution for small-scale buildings.

References

Adam, E.A., Agib, A.R.A. (2001). Compressed stabilised earth block manufacture in Sudan. United Nations Educational, Scientific and Cultural Organization UNESCO, Paris, 11. Open Access Library Journal, Vol.1 No.5, August 27, 2014.

AFNOR XP P13-901 (2001). Compressed earth blocks for walls and partitions: definitions – Specifications – Test methods – Delivery acceptance conditions. Saint-Denis La Plaine Cedex, France.

AFNOR NF EN 1015-18 (2003). Méthodes d'essai des mortiers pour maçonnerie - Partie 18 détermination du coefficient d'absorption d'eau par capillarité du mortier durci.

AFNOR EN196-1 (2016). Méthodes d'essais des ciments - Partie 1 : détermination des résistances.

AFNOR NF P 12504-4 (2005). Essais pour béton dans les structures - Partie 4 : détermination de la vitesse de propagation du son.

Aguilar-Rivera, N., Rodrıguez, L. D. A., Enriquez, R. V. Castillo M. A., Herrera, A. S. (2012). The Mexican Sugarcane Industry: Overview, Constraints, Current Status and Long-Term Trends. Sugar Tech 14(3): 207–222. DOI 10.1007/s12355-012-0151-3

Alberti, M.G., Enfedaque, A., Gálvez, J.C., (2018). A review on the assessment and prediction of the orientation and distribution of fibres for concrete, Composites Part B: Engineering, Volume 151, 2018, 274-290, https://doi.org/10.1016/j.compositesb.

Alioune, N. (2022). Modélisation des briques crues à base de sédiments et renforcées par des fibres de lin, coco, banane, palmier: analyse par éléments finis et transformée de Fourier Rapide. Rapport de stage de fin de cycle Master2 Mécanique, Université de Caen, France.

Aoual-Benslafa, F.K. Ameur, M., Mekerta, B., Semcha, A. (2014): Caractérisation des sédiments de dragage du barrage de Bouhanifia pour une réutilisation. *XIII*^{èmes} *Journées Nationales Génie Côtier – Génie Civil Dunkerque*, 2-4 juillet 2014. DOI:10.5150/jngcgc.2014.11

ASTM D559 (1994). Methods of Wetting and Drying Test of Compacted Soil-Cement Mixtures.

ASTM D 790 – 03 (2003). Standard Test Methods for Flexural Properties of Unreinforced and Reinforced Plastics and Electrical Insulating Materials. American Society for Testing and Materials.

ASTM C 1018 – 97 (1997). Standard Test Method for Flexural Toughness and First-Crack Strength of Fiber-Reinforced Concrete (Using Beam with Third-Point Loading).

ASTM C1557-03 (2003). Standard test methods for tensile strength and young's modulus of fibers, American Society for Testing and Materials: West Conshohocken, PA, USA

ASTM D7357–07 (2012). Standard specification for cellulose fibers for fiber-reinforced concrete. American Society for Testing and Materials: West Conshohocken, PA, USA

Azhary, K.E., Chihab, Y., Mansour, M., Laaroussi, N., Garoum, M. (2017). Energy efficiency and thermal properties of the composite material clay-straw. Energy Procedia, 141, 160–164.

Baglioni, E., Fratini, F., Rovero, L. (2010). The materials utilised in the earthen buildings sited in the Drâa Valley (Morocco): mineralogical and mechanical characteristics. In: Proceedings of 6 Seminário de Arquitectura de Terra em Portugal and 9 Seminário Ibero-Americano de Construção e Arquitectura com Terra [CD-ROM], Coimbra, Portugal.

Bahobail, M.A. (2011). The mud additives and their effect on thermal conductivity of adobe bricks. Journal of Engineering Sciences, Assiut University, Vol. 40, No 1, pp.21-34, January 2012.

Binici, H., Aksogan, O., Shah, T. (2005). Investigation of fibre reinforced mud brick as a building material. Construction and Building Materials, Volume 19, pp. 313–318. https://doi.org/10.1016/j.conbuildmat.2004.07.013

BS EN 772-11 (2011). Methods of test for masonry units. Determination of water absorption of aggregate concrete, autoclaved aerated concrete, manufactured stone and natural stone masonry units due to capillary action and the initial rate of water absorption of clay masonry units. European Standards adopted by British Standards Institution.

Bui, H, Hussain, M., Levacher, D. (2022). Recycling of tropical natural fibers in building materials. Natural fibers, Intechopen book. DOI: 10.5772/intechopen.102999.

Calatan, G., Hegyi, A., Dico, C., Mircea. C. (2016). Determining the Optimum Addition of Vegetable Materials in Adobe Bricks. Procedia Technology 22, 259 – 265. doi: 10.1016/j.protcy.2016.01.077

Caporale, A., Parisi, F., Asprone, D., Luciano, R., Prota, A. (2014). Critical surfaces for adobe masonry: Micromechanical approach. Composite Part B: Engineering, Vol. 56, pp. 790-796. https://doi.org/10.1016/j.compositesb.2013.08.087

Danso, H., Martinson, D.B., Ali, M., Williams, J.B. (2017). Mechanisms by which the inclusion of natural fibres enhance the properties of soil blocks for construction. Journal of Composite Materials 51(27). DOI: 10.1177/0021998317693293

Defoirdt, N., Biswas, S., Vriese, L.D., Tran, L.Q.N., Acker, V., Ahsan, Q., Gorbatikh, L., Vuure, A.V., Verpoest, I. (2010). Assessment of the tensile properties of coir, bamboo and jute fibre. Composites: Part A 41, 588–595. https://doi.org/10.1016/j.compositesa.2010.01.005

Djeran-Maigre, I., Morsel, A., Hussain, M., Levacher, D., Razakamanantsoa, A., Delfosse , E. (2022). Murs pilotes à base de briques élaborées avec des sédiments du fleuve Usumacinta du

Mexique. 11èmes journées nationales de géotechnique et de géologie de l'ingénieur, Lyon, France. ffhal-03720264f.

Dormohamadi, M. and Rahimnia, R. (2020). Combined effect of compaction and clay content on the mechanical properties of adobe brick. Case Stud. Constr. Mater., 13, e00402.

Fgaier, F.E., Lafhaj, Z., Chapiseau, C., Antczak, E. (2016). Effect of sorption capacity on thermo-mechanical properties of unfired clay bricks. J. Build. Eng., 6, 86–92.

Ghavami, K., Filho, R.D.T., Barbosa, N.P. (1999). Behaviour of composite soil reinforced with natural fibres. Cement and Concrete Composites, 21, 39–48. https://doi.org/10.1016/S0958-9465(98)00033-X

Hakkoum, S., Kriker, A., Mekhermeche, A. (2017). Thermal characteristics of Model houses Manufactured by date palm fiber reinforced earth bricks in desert regions of Ouargla Algeria. Energy Procedia, 119, 662–669.

Houben, H., Guillaud, H. (1994): Earth construction: A comprehensive guide. Intermediate Technology Publications, London.

Hussain, M., Saouti, L., Levacher, D., Djeran-Maigre, I., Razakamanantsoa, A., Leblanc, N., Zmamou, H. (2020). Production of waste fiber-reinforced raw earth specimens by controlled compaction. 3rd Euromaghreb Conference, Sustainability and Biobased Materials on the road of Bioeconomy, October 2020, Rouen.

Ige, O., Danso, H. (2021). Physcio-mechanical and thermal gravimetric analysis of adobe masonary units reinforced with plantain pseudo-stem fibers for sustainable construction. Construction and Building Materials, Vol. 273, 121686. https://doi.org/10.1016/j.conbuildmat.2020.121686

Illampas, R., Ioannou, I., Charmpis, D.C. (2011). A study of the mechanical behaviour of adobe masonry. Structural Repairs and Maintenance of Heritage Architecture XII 485. WIT Transactions on The Built Environment, Vol 118. doi:10.2495/STR110401

Kanbur, B.B., Atayilmaz, S.O., Demir, D., Koca, A., Gemici, Z. (2013). Investigating the thermal conductivity of different concrete and reinforced concrete models with numerical and experimental methods, in: Proceeding of the 4th European Conference of the Mechanical Engineering (ECME-13), Paris. ISBN: 978-960-474-345-2

Khennache, M., Mahieu, A., Ragoubi, M., Taibi, S., Poilane, C., Leblanc, N. (2019). Physicochemical and mechanical performances of technical flax fibers and biobased composite material: effects of flax transformation process. Journal of Renewable Materials 7(9), 821–838, doi:10.32604/jrm.2019.06772

Khoudja, D., Taallah, B., Izemmouren, O., Aggoun, O., Herihiri, O., Guettala, A. (2021). Mechanical and thermophysical properties of raw earth bricks incorporating date palm waste. Constr. Build. Mater. 270, (2021) 121824. https://doi.org/10.1016/j.conbuildmat.2020.121824.

Lagunes-Fortiz, E.R., Gómez-Gómez, A, A., Leos-Rodríguez, J. A., Omaña-Silvestre, J.M., Lagunes-Fortiz, E. (2021). Analysis of Copra and Coconut Oil Markets in Mexico. Agroproductividad: Vol. 14, Núm. 4, abril. 2021. pp: 11-20. DOI: 10.32854/agrop.v14i4.1806

Liberatore, D., Spera, G., Mucciarelli, M., Gallipoli, M.R., Santarsiero, D., Tancredi, C. (2006). Typological and experimental investigation on the adobe buildings of Aliano (Basilicata, Italy).

Meli, R. (2005). Experiences in Mexico on the reduction of seismic vulnerability of adobe constructions. In: Proceedings of Sismo Adobe[CD-ROM], Lima, Peru.

Mellaikhafi, A., Tilioua, A., Souli, H., Garoum, M., Hamdi, M.A. (2020). Characterization of different earthen construction materials in oasis of south-eastern Morocco (Errachidia Province). Case studies in Construction Materials, Volume 14, e00496. https://doi.org/10.1016/j.cscm.2021.e00496.

Montfort, G.R.C, Santana, T.J.M., Barrera, M.A.F., Valencia, R.A.S. (2021). Prospectiva de la producción de coco en Yucatán, México. región Y Sociedad, 33, e1467. DOI: 10.22198/rys2021/33/1467

MOPT (1992): Bases para el diseno y construccion con tapial. Madrid, Spain: Centro de Publicaciones, Secretarıa General Tecnica, Ministerio de Obras Publicas y Transportes.

Mostafa, M., Nasim, U. (2015). Effect of banana fibers on the compressive and flexural strength of compressed earth blocks. Buildings 2015, 5: 282-296. doi:10.3390/buildings5010282

NORMA E.080 (2017). Diseño y construcción con tierra reforzada. Ministerio de Vivienda, Construcción y Saneamiento. Anexo-Resolución Ministerial, 21-2017-Vivienda. Available online: https://procurement-notices.undp.org/view_file.cfm?doc_id=109376

NZS 4298 (1998). Materials and workmanship for earth buildings [Building Code Compliance Document E2 (AS2)]

Picandet, V. (2017). Bulk density and compressibility. In: Amziane, S., Collet, F. (eds) Bio-aggregates based building materials. RILEM State-of-the-Art Reports, vol 23, Springer, Dordrecht. https://doi.org/10.1007/978-94-024-1031-0_5

Pradeep, P., Dhas, J.E.R., Suthan R., Vijayarangam, J. (2016). Characterization of palm fibers for reinforcement in polymer matrix. ARPN Journal of Engineering and Applied Sciences. VOL. 11, NO. 12. ISSN 1819-6608.

Revuelta- Acosta, J.D., Garcia- Diaz, A., Soto- Zarazua, G.M, Rico- Garcia, E., (2010). Adobe as a Sustainable Material: A Thermal Performance. Journal of Applied Sciences, 10: 2211-2216. DOI: 10.3923/jas.2010.2211.2216

Rivera, J.C. and Muñoz, E.E. (2005). Structural characterization of materials of earth structural systems: adobe, Revista Internacional de Desastres Naturales. Accidentes e Infraestructura Civil, 5(2):135–48.

Saleem, M.A., Abbas, S., Haider, M. (2016). Jute Fiber Reinforced Compressed Earth Bricks (FR-CEB) – A Sustainable Solution. Pak. J. Eng. & Appl. Sci, Vol. 19, p. 83–90.

Salih, M.M., Osofero, A. I., Imbabi, M. S. (2018). Mechanical properties of fibre-reinforced mud bricks. 2nd Conference of Civil Engineering Sudan, 2018. https://www.researchgate.net/publication/329786369

Salih, M.M., Osofero, A.I., Imbabi, M.S. (2019). Critical review of recent development in fiber reinforced adobe bricks for sustainable construction. Front. Struct. Civ. Eng., 14(4): 839–854 https://doi.org/10.1007/s11709-020-0630-7

Seifi, S., Sebaibi, N., Levacher, D., Boutouil, M., 2018. Mechanical performance of a dry mortar without cement, based on paper fly ash and blast furnace slag. J. Build. Eng. 22, 113–121. https://doi.org/10.1016/j.jobe.2018.11.004.

Silveira, D., Varum, H., Costa, A., Martins, T., Pereira, H., Almeida, J. (2012). Mechanical properties of adobe bricks in ancient constructions. Construction and Building Materials (28): 36-44. doi:10.1016/j.conbuildmat.2011.08.046

Tavares, G.R.L., Magalhães, M.S. (2019). Effect of recycled pet fibers inclusion on the shrinkage of adobe brick. 3 rd International Conference on Bio-Based Building Materials June 26 th - 28th, Belfast, UK

Türkmen, I., Ekinci, E., Kantarcı, F., Sarıc, T. (2017). The mechanical and physical properties of unfired earth bricks stabilized with gypsum and Elazıg Ferrochrome slag. International Journal of Sustainable Built Environment 6, 565-573. https://doi.org/10.1016/j.ijsbe.2017.12.003

Van Soest, P.J., Robertson, J.B., Lewis. B.A. (1991). Methods for dietary fiber, neutral detergent fiber, and non-starch polysaccharides in relation to animal nutrition. Journal of Dairy Science, 74(10), 3583–3597

Chapter 5. Local sustainable applications

In this chapter, Usumacinta River sediments (USU) agronomic characteristics were investigated for recovery of these sediments to grow plants. Usumacinta River sediments were mixed with local industrial potting soil (*terreau, in French*) to sow ryegrass in green house. Ryegrass was cultivated at different sediments and soil compositions and local climatic conditions. Germination of ray grass, its growth over time and fresh biomass of grass were investigated to observe the sediments suitability for agronomic applications.

Furthermore, local French sediments recovery in sustainable building materials such as earth bricks was investigated. Methodology developed from Usumacinta River sediments reuse in earth brick was applied to French sediments from Dunkirk port and Garonne River sediments from Saint-Vidian reservoir. Characteristics of Dunkirk port and Garonne River sediments were investigated for their reuse in earth bricks. Hemp shiv which is a local waste plant aggregate was used as reinforcement in bricks. Earth bricks were manufactured at different hemp shiv content to optimize the strength and durability of bricks.

5.1 Sediments reuse in agronomy

5.2.1 Introduction of sediments agronomic recovery

Dredged sediments are naturally occurring waste material and can be recycled in different sectors. Among all the known recycling areas (Anger, 2014; Rakshith et al, 2016, the reuse of dredged sediments in the creation of vegetative supporting soils seems relevant for several reasons which include lack of topsoil and supporting soil for the establishment of green spaces, landscaping and restoration of degraded sites (Fourvel (2018). Sediment agronomic reuse is one of the sustainable recovery methods (Levacher, 2021) and is interesting from a technical, economic and ecological perspective.

Freshwater sediments constitute a secondary raw material for agronomic use such as the development of vegetative soil which helps to reduce the extraction of nonrenewable soil resources. Sediments reuse in agronomy helps to increase the crop yield as sediments act as fertilizing agents by providing nutrients to the plants. Soil fertility decreases with time due to the use of fertilizers and pesticides, so as the crop production. Fresh sediment cover provides nutrients and increases the performance of soil. Agricultural soils can be partially or fully replaced with dredged sediments. Rearrangement of soil particles takes place with the addition of sediments which improves the soil quality and positively influence the growth of crops.

Different plants and vegetables such as ryegrass, pepper and vegetables can be grown in sediment-based soils. The choice of plants depends on local climatic conditions and the environment (Kiani et al. 2021, Baran et al. 2016, Brigham et al. 2021).

Reusing sediments for agronomic purposes, such as soil fertilization, is also relevant for development projects requiring vegetative cover, such as landscape models (Lalaut, 2014; Bataillard et al., 2017), for protective developments (dikes, embankments), erosion prevention (vegetation with rooting), rehabilitation sites (mining quarries, industrial sites) and creation of recreational areas (golf courses, etc.). Vegetation cover on riverbanks helps to curb the erosion of riverbanks and immobilize possible contaminants which may leak into the environment due to leaching.

Agronomic valorization of sediments is based on the following conditions *i.e. sediments must have agronomic interest, be harmless to human beings, flora, fauna and environment and lie within prescribed norms*. Sediment characteristics such as the presence of primary nutrients like phosphorus (P) potassium (K) and the presence of pollutants are deciding factors for their recovery in growing crops (Fourvel, 2018). Sediments addition as soil amendment contributes to the fertilizing effects by increasing the nutrients of mineral and organic origin and secondary fertilizing agents, improving physical (cohesion, porosity etc.), chemical (pH, cation exchange capacity) and biological (microbial biomass) characteristics. These aspects are interesting for ecological rehabilitation of degraded sites that require the creation of substrate favorable to re-vegetation.

The feasibility study can be established concisely according to Figure 5.1.

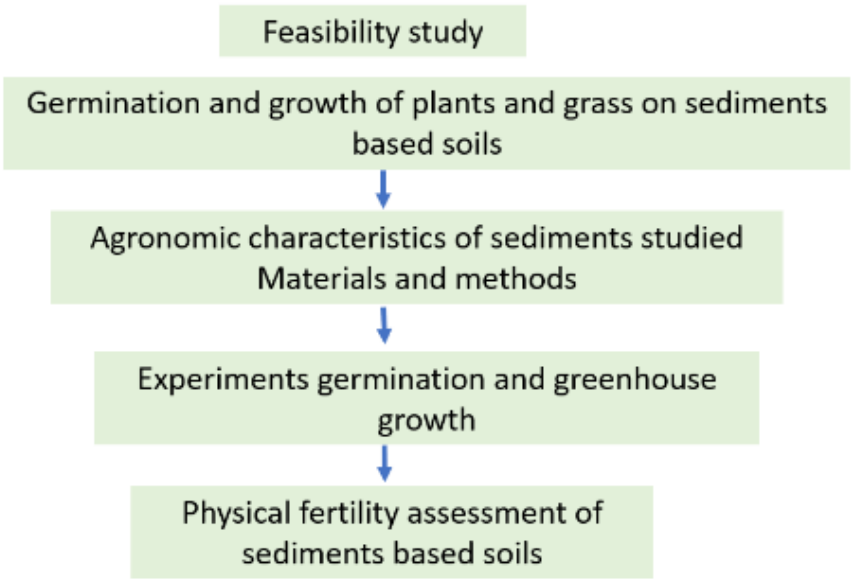

Figure 5. 1. Plant fertility phases study for sediments-based soils

In case of polluted sediments, treatment of sediments becomes necessary as polluted sediments recycling in agronomy is dangerous for the environment. Presence of salts and metals increases the level of toxicity of amended soils (Canet et al. 2003). Reuse of freshwater sediments in agronomy is comparatively simpler as the salinity of freshwater sediments is usually low. However marine sediments have higher salinity. Presence of salts in sediments reduces plant growth as saline soils decrease the capacity of plants to uptake the water and generates water stress conditions (Munns, 2002). Salt concentration of saline sediments is diluted with leaching to minimize the salinity. Dredged sediments have higher initial water content. Drainage of marine sediments acts as a pretreatment as it removes the dissolved salts and contaminants.

Dredged sediments reuse in agronomy and landscaping is relatively unexplored. This is because current regulations are a significant barrier to this value-adding industry. This is paradoxical as sediments have been used for soil amendments for decades on several occasions (Bourret, 1997). There exist limited studies on sediment reuse in agronomy to improve the nutrients in soil and meet the plant's requirements. Mainly these studies are focused on particular sediments and demonstrate that sediments can be used alone or combined with organic materials such as compost for the development of vegetative soil.

Regulatory framework for sediments recovery for soil amendments for agriculture is nonexistent in France. In France and most other countries, sediments are not included in the materials suitable which have the potential to improve the soil quality (AFNOR NF U44-551, 2002). Some common waste recycled in agronomy in France includes mud, green waste compost, bio-waste compost, and residual household waste compost etc. (ADEME, 2001). However, in research studies, it has been observed that sediment recovery in the cultivation of crops is possible by spreading sediments layer on the soil. Dredged sediments can be spread on agricultural soil to increase their performance. However, sediment's characteristics and quantity are important for their large-scale reuse. Similarly, analysis of soil characteristics on which

sediments will be spread is also essential. Compatibility of sediments with planned soil increases the prospects of sediments recovery in agro sector (Djeran-Maigre et al. 2022). Further separation of fine and coarse sediments facilitates the sediments reuse to improve the quality of agricultural soils.

Water soluble macro and micronutrients move downstream with the erosion of soil and settled in dams and riverbeds. Soil amendments with these sediments, fulfill the deficiency of soil nutrients and ameliorate the water retention and cation exchange capacity of the soil sediments mixture. Sediments act as a fertilizing agent and growing media for the cultivation of crops (Kiani et al. 2021, Canet et al. 2003).)

For sustainable development and circular economy, dredged sediments reuse is viable locally in areas close to the dredging sites as transportation and dewatering of sediments increase the cost. For example, in the Brittany region of France, 33% of marine dredged sediments are stored on land sites and 15% of stored sediments are reused in agronomy (Bénédicte 2017).

Some studies have been conducted in the recent past for sediments reuse in the construction of soils for agronomy and research work is going on in different parts of the world on this matter. Table 5.1 shows the agronomic valorization of sediments in different applications.

Table 5. 1. Studies on the agronomic valorization of sediments

Project or study	Objectives	Results	Reference
Marine sediments agronomic valorisation	Study of the agronomic interest	Spreading on agricultural plots. Investigation of the appropriate conditions for using sediments in thick layers in order to rehabilitate degraded soils: quarries, industrial sites, roadsides. Verification of the behavior of lawns, annual plants and shrubs for green spaces. Creation of beds and embankments, and implementation of experiments on composting with sediments. Amendment of agricultural land is possible.	4Vaultx-Jardin (1998), Ferreira (2003)
Creation of artificial soil with dredged sediments	Making fertile soils	Mixtures of dredged material and materials, such as green waste, compost, sawdust, bio-solids (WWTP sludge, slurry) and industrial by-products with cellulose. Stage 1: physico-chemical characterization of the different materials and mixtures and germination and growth tests on a laboratory scale. If the results are positive for producing fertile soil: Step 2: creation of a demonstration project or marketing of the process	Sturgis et Lee (1999) ; Sturgis et al., (2001a, 2001b, 2002)
Vegetation of a fly ash park with river sediments	Use of sediments to revegetate part of a fly ash park	5 ha of an ash park covered with sediments from deepening dredging of the channeled Moselle, spread over 40cm. The deposition of mud coupled with sowing is a success from the point of view of plant development (sown or spontaneous species) on the site thanks to the deposition of sediments and the creation of favorable micro-habitats.	ESCOPE/ASCAL (2008)
Agricultural recovery of waterways dredged sediments	Finding a durable solution to the stockpiles of dredged river sediments	Dredged sediments can have properties similar to soils, even in some cases, fertile agricultural soils	Bernes Cabanne, (2009)
Use of sediments for the production of topsoil substitute- Manufactured soil	Development of a topsoil substitute from marine sediments from the port of Waterford (Ireland)	14 mixtures of compost (=6% OM) and desalinated or non-desalinated sediments with the addition of aluminum sulphate to adjust the pH (6.75 desired) and improve the availability of nutrients	Sheehan et al., (2010a, 2010b)
On-site spreading of canal sediments	Implementation of an agricultural experiment on site to confirm the agronomic potential of sediments	1.75cm of sediment over 2.58ha. Absence of soil and plant contamination. Agronomic potential of sediments for a restructuring of a skeletal soil.	Sheehan et al., (2010a, 2010b)
Study of the potential release of inorganic elements from an agricultural soil-sediment complex from the dredging of uncontaminated canals	Development of an experimental protocol in the laboratory to determine the environmental risks associated with the agricultural spreading of uncontaminated canal sediments	Receiving soils: sandy agricultural soil from Saône-et-Loire (71), silty-clay soil from the lower Ain valley (01), control soil consisting of sand from Fontainebleau. Mixtures of sediments and soils: Ratios 2 to 15/25: contribution of 2 to 5cm of sediment on 25 cm of cultivated soil. For a spreading of 2 cm, the potential for release is identical to that of the soil, there is no influence of sediments; the increase in the sediment/soil ratio leads to a greater potential for the release of inorganic elements.	Cantegrit et Eisenlohr, (2012)
Floor construction feasibility study - Technosols	Evaluation of the agronomic fertility of marine sediments in soil construction as plant support	Need for desalting, lowering the pH and/or adding exogenous organic matter. Improved germination thanks to the addition of sludge-based compost. The drainage of the amended soil seems insufficient, explained by the weak structuring of the materials of the amendment soil.	Macia et al., (2014) Koropchak et al. (2015)
Experimenting with the recycling of ditch cleaning sediments as planting substrate	Recycling of cleaning sediments to limit the extraction of arable land. Offers better agronomic properties to ensure planting of vegetation.	Control substrate (arable soil), substrate with 50% sediment and 50% green compost. Good root colonization of the plant cover. The homogeneity of the mixed soil can pose a problem or limits the recovery of shrubs.	Damas et Coulon, (2016)
Spreading of estuarine mud	Implementation of agronomic valuation	Possibility of spreading the mud up to 500 tons / ha, there would be no delay in germination or drop in yield. Encouraging results, but without forgetting the salt content of the Vilaine estuary, twice as high as that of the Rance.	Chourre (2016), CA Côtes d'Armor (2016), Quideau (2016), Dawid (2017)

(a) Agronomic characteristics of dredged sediments

Fertility of sediments depends on physico-chemical and biological parameters of soil. Agronomic soils must have characteristics favorable to metabolic activity and mineral supply of plants. Freshwater sediments (rivers, lakes, dams) have physico-chemical characteristics similar to agricultural soil. These characteristics include particle size, pH, electrical conductivity, organic matter, salts, minerals, organisms and carbonates content etc.

Fresh water sediments contain elements such as P and K which are important nutrients in the soil from the perspective of agronomy while elements such as Fe, S, Mn, Mg and B are minor and secondary nutrients in sediments (Darmody and Marlin, 2002). These sediments can be a possible source of nutrients for plants (Kiani et al. 2021). Sediment addition modifies the physical (cohesion, porosity), chemical (pH, cation exchange capacity) and biological (microbial biomass) characteristics of soil and provides nutrients and organic minerals to the plants (Levacher et al. 2022). Dredged sediments usually consist of minerals such as silica and quartz, fine particles in the form of clay, and chemical components such as calcite etc.

Granulometry of soil and is very important for agronomy as infiltration of water and leaching of minerals in the soil is mainly associated with sediments and soil grain size distribution. Clay soil and sediments absorb a higher amount of water. Drainage and water absorption of soil are important for crop yield. Higher pH and electric conductivity of sediments lead to the problem of phototoxicity in crops. The main agronomic characteristics of fine sediments studied for soil amendment are shown in Table 5.2.

Table 5. 2. Characteristics of fine sediments used for soil amendment (Fourvel, 2018)

Origin	**pH**	**CE ($\mu S\ cm^{-1}$)**	**Texture**	**$CaCO_3$ ($g\ kg^{-1}$)**	**CO ($g\ kg^{-1}$)**	**OM ($g\ kg^{-1}$)**	**N total ($g\ kg^{-1}$)**
Brackish	8,3	4170	silt clayey-sandy	346	55,2	-	1,34
Continental	7,9	470	silt clayey-sandy	58	33,3	-	1,54
Continental	7	2060	Medium silt	177	80,9	-	2,07
Brackish	9	510	Sandy-clayey	346	74,4	-	3,91
Continental	7,2	1890	Clayey loam	120	111,6	-	6,82
Continental	7,8	740	Clayey sandy loam	199	96,2	-	2,7
Marine	8,2	170	Clayey sandy loam	514	93,4	-	2,74
Brackish	8,8	250	Clay sand	309	39,6	-	0,22
Brackish	8,1	1640	Silty clay	329	48,8	-	1,01
Continental	7,4	190	Medium silt	97	60,5	-	4,01
Continental	6,9	-	Medium sandy loam	-	18	-	0,4
Marine	38	36000	Sandy clayey loam	101	-	-	45
Marine	9,9	37000	Fine (clay+silt >80%		-		-
Marine	7,6	15360	Medium sandy loam	0,9	-	5,3	0,364
Marine	8,2	19260	Medium sandy loam	1,1	-	25	1,259
Continental	7,2	-	Medium sandy loam	-	-	18	0,319
Continental	7	1696	Clay sandy loam	7,3	33	-	2,9

Even if it is challenging to describe the ideal physico-chemical characteristics of fertile soil given that they depend on the planned plant cover and the application (agriculture, landscape gardening, etc.). Table 5.3 shows the recommended values of soil physico chemical parameters, identified in the literature.

Table 5. 3. Threshold values of soil parameters to assess its fertility (Fourvel, 2018)

Parameters	**Optimum value**	**Unfavorable value**
Volumic mass (g cm^{-3})	< 1.2	> 1.7
Macro porosity (m^3m^{-3})	> 0.2	< 0.05
Hydraulic conductivity (cm s^{-1})	> $1.4*10^{-3}$	< $4.2*10^{-4}$
Useful reserve for plants (mm cm^{-1})	> 1.5	< 0.5
aggregate stability (mm)	> 2	< 0.8
pH	6.5 to 7.5	<6.5 and 7.5>
Organic matter (g kg^{-1})	40 to 100	<10 and 100>
Total nitrogen (g kg^{-1})	10 to 20	<2and > 20
CEC ($cmol^1$ kg^{-1})	> 40	< 12
$CaCO_3$ (g kg^{-1})	10 to 50	> 500
Electric conductivity (µS cm^{-1})	< 500	> 2000

(b) Objectives

Val-Uses project consists of Usumacinta River sediments valorization in diverse applications for their sustainable and eco-friendly reuse.

The objective of this study is recycling of Usumacinta River sediments in agronomy. Soil amendments with Usumacinta River sediments to grow crops must be investigated through the germination and growth of plants.

Germination and growth of ryegrass are planned on Usumacinta River sediments and the study is based on knowledge of the agronomic potential of sediments namely the agronomic and technical feasibility of constructed soils. These constructed soils are a mixture of sediments and potting soils having higher organic matter. A comparison will be drawn between the established soils and reference sediments. This comparison helps to observe the fertility of sediments alone and the improvement in constructed soil with the addition of potting soil. Germination and plant growth over time allows to observe the suitability of constructed soils and sediments for vegetation.

5.2.2 Materials and methods

Potting soil (*terreau in French*) was amended with Usumacinta River sediments and ryegrass was sown to observe its germination and growth to evaluate the potential of Usumacinta River sediments reuse in agronomy.

5.2.1 Characteristics of Usumacinta River

Usumacinta sediment's physico-chemical, environmental and mineralogical characteristics were investigated for their use in agriculture to improve the quality of soil. J4 sediments were selected for this purpose, based on their characteristics, availability and proximity to the agricultural areas.

(a) Grain size analysis

Grain size of Usumacinta sediments was observed with laser granulometry. Table 5.4 shows the percentage of clay, silt and sand particles in Usumacinta sediments along with median diameter.

Table 5. 4. Characteristics of Usumacinta River sediments

Sediment	pH	Clay (%)	Silt (%)	Sand (%)	D50 (µm)	classification (GTR)
USU	8.51	13.4	62.5	24.1	14.12	Clayey soil

Note: USU = Usumacinta River sediments,

Characteristics of J4 sediments show that these sediments have a higher percentage of fine particles and according to GTR classification of soils, Usumacinta sediments are clayey soil. Fine sediments with a lower percentage of coarse particles are suitable and recommended for agronomic applications (Darmody and Marlin, 2002).

Texture of soil is helpful to deduce the fertility potential of soil. It also influences the other parameters of soil such as porosity, aeration and water retention capacity of soil (Anger, 2014). USDA soil texture ternary diagram was used to see the nature of sediments. Usumacinta River sediments position in USDA texture diagram is shown in Figure 5.2.

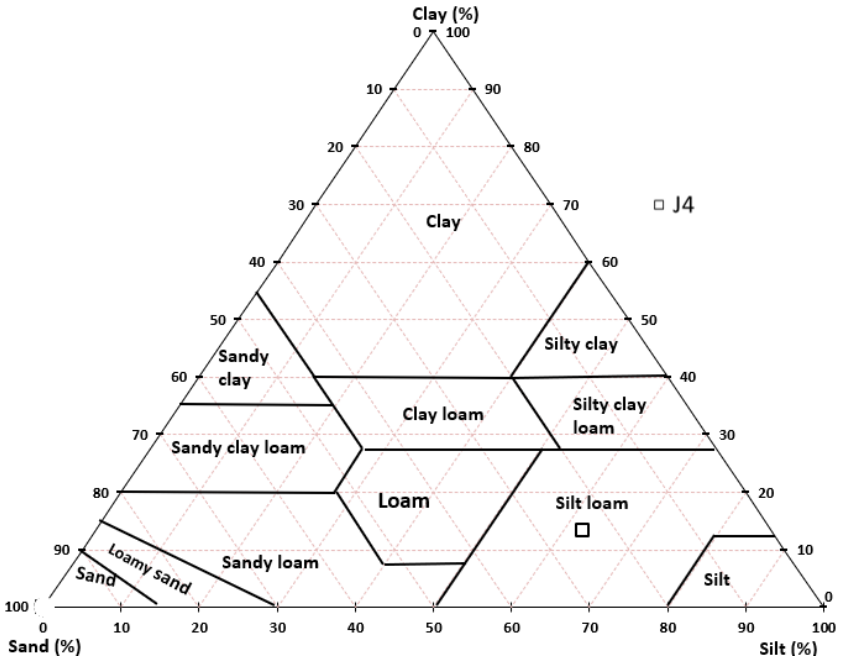

Figure 5. 2. Usumacinta River sediments soil texture (USDA texture diagram)

USDA soil texture ternary diagram shows that J4 sediments lie in the silt loam region. Higher fine particle percentage of sediments allows them to retain water and nutrients contrary to the coarse particle which is susceptible to leaching (Jadczyszyn et al. 2016). Loam is considered the ideal soil for agriculture. It contains 40% sand, 40% silt and 20% clay (USDA NRCS 1999).

Grain size analysis of sediments is also useful to correlate the porosity and permeability with granulometry. Ternary diagram in Figure 5.3 shows the different zones to describe the porosity and permeability of the soil. Porosity is high in the top WS section, low in the middle zones (PS and MWS) and moderately high in the bottom zones (WS, MWS and WS). Permeability is very low in top WS zone, low in the middle zones (PS and MWS) and moderate high in bottom MWS zone. High permeability in the bottom WS zone and moderate permeability in bottom WS zone (McManus, 1998).

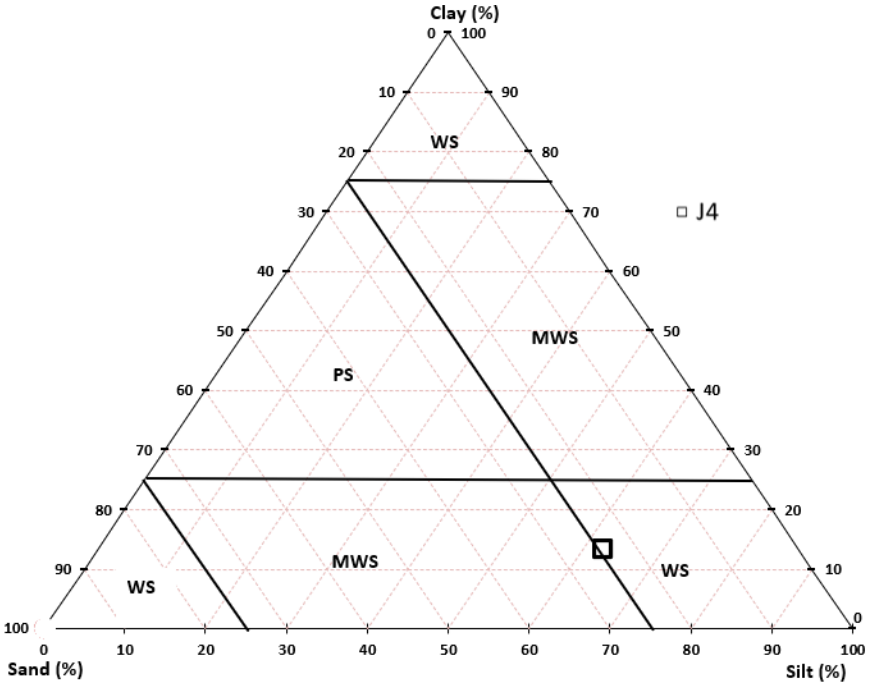

Note: WS, MWS and PS stand for well sorted, moderately well sorted and poorly sorted.

Figure 5. 3. Usumacinta River sediments soil texture (USDA texture diagram)

J4 sediments lie in WS zone which means that these sediments are well sorted with moderately high porosity and higher permeability. Porosity of sediments helps to circulate water and air.

(b) Organic matter

Organic matter in soil helps for soil stability as it binds the soil particles. Higher organic matter is suitable for sediments use in agriculture applications for growing crops as it is helpful for the mineralization of plants and increases the biological activity of crops. Organic matter in Usumacinta sediments is shown in Table 5.5.

Table 5. 5. Organic matter of Usumacinta River sediments

Sediment	OM (%)	Sediments nature
J4	5.72	Low organic

Note: OM = organic matter

Organic matter of Usumacinta River sediments is 5.72% which is an intermediate value and sediments are classified into low organic sediments (AFNOR XP P 94-011, 1999).

(c) pH and electrical conductivity of Usumacinta sediments

pH and electrical conductivity (EC) of Usumacinta sediments were determined with pH meter. pH value of sediments was also observed with pH paper. Results are shown in Table 5.6.

Table 5. 6. pH and electrical conductivity of Usumacinta River sediments

Sediment	pH (pH meter)	pH (pH paper)	Electrical conductivity (mS/cm)*
J4	8.51	7	0.02

pH values with pH meter are more precise. Higher pH value of J4 sediments shows that they have a slightly alkaline nature. Carbonate minerals in sediments are mainly responsible for the alkalinity of sediments. pH value between 5 to 10 does not significantly influence the germination of ryegrass (Javaid et al. 2022).

Furthermore, the salinity of soil is measured with electrical conductivity. Electrical conductivity recommended for agronomic use of soil varies from crop to crop. However recommended threshold is below 1 mS/cm (Kotuby-Amacher, 2000). It is hard for the plant to obtain water in saline soils which leads to a water stress situation. Electrical conductivity of Usumacinta sediments is considerably lower than the maximum authorized limit which means that Usumacinta Rivers sediments are not saline.

(d) Carbonate content of sediments

Carbonate ($CaCO_3$) is a basic component of soil and its higher quantity affects the agronomic characteristics of sediments. Carbonate content of Usumacinta sediments was determined with Bernard calcimeter method (AFNOR NF ISO 10694, 1995). Results are shown in Table 5.7.

Table 5. 7. Carbonate content of Usumacinta River sediments

Sediment	$CaCO_3$ (%)	Sediments nature
J4	8.49	Non marly

J4 sediments have non marly nature according to French standards (AFNOR XP P 94-011, 1999).

(e) Mineralogy of sediments

Analysis of oxides such as SiO2, Al_2O_3, CaO, N, P_2O_5, helps to understand the composition of sediments and their compatibility with soil. Nitrogen, Phosphorous and potassium are three main nutrients responsible for plant growth. Micronutrients in soil suitable for plants are Fe, S, Mn, Mg and B etc. Table 5.8 shows the oxide composition of Usumacinta River sediments.

Table 5. 8. Oxide composition of Usumacinta River sediments

Sediments	SiO_2 (%)	Al_2O_3 (%)	CaO (%)	TiO_2 (%)	Fe_2O_3 (%)	K_2O (%)
J4	56.3	16.1	6.4	1.9	16.1	2.6

Table 5.8 shows the presence of primary nutrients in the form of potassium oxide and secondary nutrients such as iron oxide.

Clay minerals are also important for sediment reuse in agronomy. Table 5.9 shows the percentage of different minerals *i.e. silicates, and carbonates* in Usumacinta River sediments.

Table 5. 9. Dominant clay minerals in Usumacinta River sediments

	Mnt (%)	Ilt (%)	Vrm (%)	Kao (%)	Qz (%)	Cal (%)	Dol (%)	Bt (%)	Crs (%)	Or (%)	Ano (%)	Ab (%)	Others
J4	10	6.4	17.1	4.9	21.4	2.2	10.1	7	1.6	5.3	9.6	4.3	5

Note: Mnt = Montmorillonite; Ilt = Illite ; Kao; Kaolinite ; Qz = Quartz; Cal = Calcite ; Dol = Dolomite ; Vrm = Vermiculite ; Bt = Biotite; Crs = Cristobalite ; Or = Orthoclase ; Ano = Anorthoclase; Ab = Albite ; others = Non identified minerals

Usumacinta River sediments (J4) are clayey sediments in which the percentage of clay is around 13.4%. Dominant clay minerals are montmorillonite, illite, Vermiculite and kaolinite.

(f) Cation exchange capacity (CEC)

Cation exchange capacity of Usumacinta River sediments was determined with methylene blue values. Results of CEC of J4 sediments with methylene blue value and direct measurement are shown in Table 5.10.

Table 5. 10. Cation exchange capacity of Usumacinta River sediments

Sediments	CEC_{MBV} (meq/ 100 g)	$CEC_{measured}$ (meq/ 100 g)
J4	25.01	35.7

CEC value varies with the quantity of clay in sediments and presence of organic matter.

(g) Sodium absorption ratio (SAR)

Sodium absorption ratio (SAR) of Usumacinta River sediments was determined by using following equation.

$$SAR = \frac{Na}{\sqrt{0.5*(Ca+Mg)}} \quad (5.1)$$

Quantity of sodium (Na), calcium (Ca) and magnesium (Mg) in sediments was determined with Coupled Plasma/Atomic Emission Spectrometry (ICP/AES). Table 5.11 shows the sodium absorption ratio of Usumacinta River sediments.

Table 5. 11. Quantity of Na, Ca and Mg in J4 sediments and sodium absorption ratio

	Na (mg/kg)	Ca (mg/kg)	Mg (mg/kg)	SAR
J4	241	59800	15400	1.24

Salinity of soils can be assessed with chart salinity based on sodium absorption ratio (SAR) and electrical conductivity (EC) as shown in Figure 5.4 (USSLS, 1954; EC, 2012).

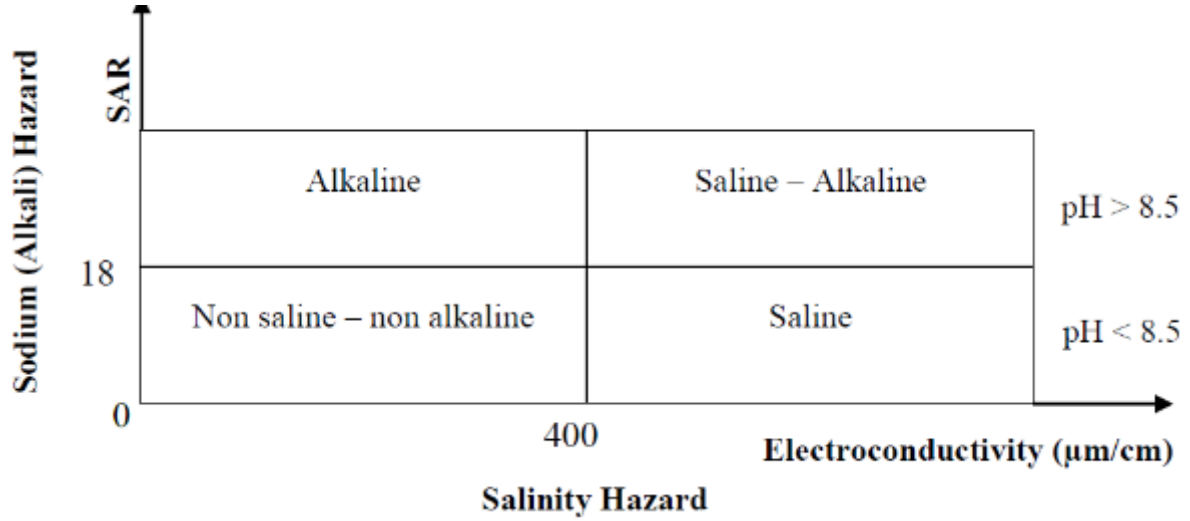

Figure 5. 4. Soil salinity assessment (USSLS, 1954; EC, 2012)

Usumacinta River sediments have SAR value of 1.24 and EC value of 0.02 which classify them into non-saline soils.

(h) Contaminants in Usumacinta River sediments

Presence of pollutants is one of the important hurdles for sediments recycling in agronomy. Heavy metals, poly aromatic hydrocarbons (PAHs) and polychlorinated biphenyls (PCB) are common pollutants in sediments generated from industrialization and the use of pesticides in agriculture. Table 5.12 shows the heavy metals in Usumacinta River sediments and thresholds recommended by French authorities for sediments reuse in agronomy.

Table 5. 12. Chemical composition of Usumacinta sediments

Parameters	**Level S1**	**J4**
Arsenic (As) mg/kg	30	5.19
Cadmium (Cd) mg/kg	2	<0.4
Chromium (Cr) mg/kg	150	131
Copper (Cu) mg/kg	100	20.5
Mercury (Hg) mg/kg	1	<0.1
Nickel (Ni) mg/kg	50	256
Lead (Pb) mg/kg	100	11.3
Zinc (Zn) mg/kg	300	40.2
PCB total mg/kg	0.68	<0.001
HAP total mg/kg	22.8	0.014

In Usumacinta River sediments, heavy metal contaminants are negligible except Ni. Higher Ni concentration in Usumacinta River sediments is associated with mining activities in upstream in Guatemala and its percentage is high in rainy seasons. Sediments Ni content can be minimized by dredging in dry seasons to reuse them in agronomy while for sediments reuse in bricks, Ni can be neutralized with addition of lime. Low concentration of other heavy metals in Usumacinta River sediments is due to the absence of industry across the Usumacinta River.

Lower concentration of metals in sediments does not require any additional treatment to remove contaminants which are important for their recycling in agriculture as it is cost-effective.

PAHs and PCB values of Usumacinta River sediments were also determined. Results of PAHs and PCB values of Usumacinta River sediments are shown in Tables 5.13 and 5.14. PAHs values below Level N1 are acceptable and above N2 are considered dangerous (JORF, 2013).

Table 5. 13. PAHs values of Usumacinta River sediments (Del Negro, 2019)

PAHs (mg/kg)	N1	N2	J4
Naphtalene	0.16	1.13	0.0024
Acenaphtylene	0.015	0.26	<0.0023
Acenaphtene	0.04	0.34	<0.0023
Fluorene	0.02	0.28	<0.0023
Phenanthene	0.085	0.59	0.0031
Anthracene	0.24	0.87	0.0043
Fluoranthene	0.6	2.85	<0.0023
Pyrene	0.5	1.5	0.0042
Benzo anthracene	0.26	0.93	<0.0023
Chrysene	0.38	1.59	<0.0024
Benzo pirene	0.43	1.01	<0.0027
Dibenzo anthracene	0.06	0.16	<0.0028
Benzo perylene	1.7	5.56	<0.0029
Indono pyrene	1.7	5.56	<0.0030

Table 5. 14. PCBs values of Usumacinta River sediments

PCB	J4
PCB congeneric 28	<0.001
PCB congeneric 52	<0.001
PCB congeneric 101	<0.001
PCB congeneric 118	<0.001
PCB congeneric 138	<0.001
PCB congeneric 153	<0.001
PCB congeneric 180	<0.001
Sum PCB	<0.001

Similarly, sum of PCBs values in Usumacinta River sediments is below 0.001 mg/kg which is substantially lower than the threshold of 0.02 mg/kg (VROM, 2000).

Tables 5.12, 5.13 and 5.14 shows that the presence of metallic, PAHs and PCBs contaminants in Usumacinta River sediments are negligible, except Ni. Absence of contaminants in sediments allows reusing these sediments in agronomy without additional treatment.

5.2.2 Potting soil (terreau in French)

Usumacinta River sediments were mixed with potting soil named *terreau*. The *terreau* is commercially available potting soil in France. It consists of peat, wood fibers, green compost, organic fertilizer and agro-minerals. Peat is essential for the aeration of potting soil and retaining water. Wooden fibers maintain porosity of soil to circulate water and air. Green compost is essential to provide nutrients to the plants while organic fertilizer and agro-minerals are essential for plant growth. Characteristics of the *terreau* are described in Table 5.15.

Table 5. 15. Characteristics of potting soil

Soil	Dry matter (%)	Organic matter (%)	Conductivity (mS/m)	Water retention capacity (ml/L)	pH
Potting soil	38	72%	36	780	6.5

It is important to note that soil in fields is different from the one available as an industrial product as industrial soils are usually for a small area to be cultivated and it is very costly to change the soil composition of an entire area with industrial soil specially designed for plants.

5.2.3 Ryegrass

Choice of plants to grow with amended soils is very important. Ryegrass (*Lolium perenne*) was sown in this study to observe the influence of Usumacinta River sediments on growth and germination of ryegrass. Ryegrass has been previously used to observe the sediment's suitability for agronomic applications (Kiani et al. 2021, Fourvel, 2018). Ryegrass is used in a wide range of applications such as landscaping, golf courses, roadways and to stabilize the soils. Erosion of riverbanks and shores can also be effectively controlled by the cultivation of ryegrass on riverbanks.

Some literature studies on sediment reuse for growing crops in different cultivation conditions are shown in Table 5.16. Ryegrass used in this study has an industrial name, *Gazon Anglais Carrefour*. Ryegrass seeds cultivated for trial studies are shown in Figure 5.5.

Figure 5. 5. Ryegrass seeds sowed in greenhouse

5.2.4 Local climatic conditions

Climatic conditions are also important for the cultivation of any crops. Sediments based amended soils have been used to grow crops in different regions of the world and under controlled conditions. Table 5.16 shows different crops successfully cultivated with sediment-based soils under different cultivation conditions.

Table 5. 16. Dredged sediments and cultivation conditions

Sediments	**Sediments (%)**	**Crops**	**Conditions**	**T* (°C)**	**RH** (%)**	**Time**	**Reference**
Lake	75cm thick layer	Ryegrass	Farmland	-	-	243 days	Kiani et al. 2021
Reservoir	5,10,30,50,100	Maize	Farmland	-	-	70 days	Baran et al. 2016
Lake	0,10,20,100	Soybean	Greenhouse	31.5	43.6	123 days	Brigham et al. 2021
River	0,10,25,50,75,100	Cucumber	Chamber	25	-	4 weeks	Urbaniak et al. 2019
Lake	5,10,20	Lettuce	Greenhouse	-	-	2 months	Canet et al. 2003
Lake	12 to 18 inches thick layers	Corn	Farmland		-	4 months	Lembke et al. 1983

Note: T = temperature, RH = relative humidity

In Tabasco region of Mexico, Usumacinta riverbanks have abundant natural vegetation and cultivated plants such as sunflowers. Tropical crops in this region include palm oil, coconut coir, banana and sugarcane (Hussain et al, 2021b). Figures 5.6a and 5.6b show the cultivated crops (*sunflowers*) and natural greenery on the banks of Usumacinta River.

Figure 5. 6. Crops cultivation (a) and natural vegetation (b) on Usumacinta Riverbanks, Jonuta

Grass cover in Figure 5.6b helps to prevent the erosion of soil and stabilizes the river's banks slopes.

To grow ryegrass in the greenhouse, local climatic conditions of Tenosique and Jonuta towns were observed and replicated. Annual temperature, humidity and rainfall data of the Tenosique region in Mexico are shown in Figure 5.6.

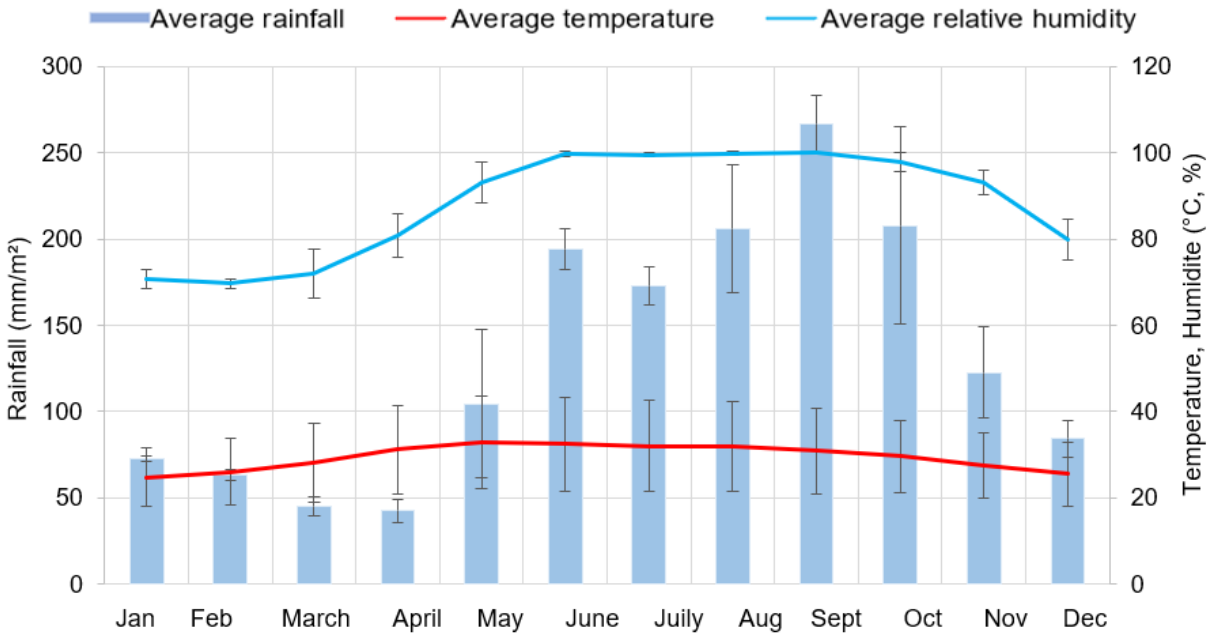

Figure 5. 7. Annual rainfall and temperature variation in Tenosique in 2020 (Weather spark, 2021)

5.2.5 Experimental setup

Agronomic potential of Usumacinta River sediments was investigated by mixing these sediments with potting soil and growing ryegrass in greenhouse. Usumacinta River sediments and potting soil were mixed at different proportions to sow ryegrass and observe its growth. Table 5.17 shows the composition of sediments and soil mixtures based on their dry mass.

Table 5. 17. Sediments and potting soil ratio

Type	Composition 1 (C1)	Composition 2 (C2)	Composition 3 (C3)
Sediments (%)	0	50	100
Terreau (%)	100	50	0

Mixing percentages of sediments and potting soil were taken in mass. Similar combinations of dredged sediments and potting soil are used in literature studies to grow plants by amending soil with sediments (Urbaniak et al. 2019, Martínez-Nicolás et al. 2020, Baran et al. 2016).

Sediments and potting soil were mixed manually and filled in pots of dimensions (20*20*70 cm^3) with drainage holes at bottom of the pots. Usumacinta River sediments have negligible contaminants. However, mixing of sediments and soil also decreases the percentage of pollutants in the mixture. Mixing of sediments and potting soil and filling of pots is shown in Figure 5.8.

Figure 5. 8. Sediments - potting soil mixing (a) and pots filled with soil mixtures (b)

Ryegrass was germinated under controlled conditions in the greenhouse. Conditions of the greenhouse were adjusted similar to the tropical environment. Germination and growth of ryegrass over a period of 2 months in the greenhouse were analyzed to observe sediment's suitability for agronomy. Temperature of the greenhouse was fixed to 30°C and relatively humidity was initially kept at 90% but was lowered to 70% after a week due to a very humid environment. Temperature and relative humidity were measured automatically throughout the cultivation period. Graph in Figure 5.9 shows the relative humidity variation in the greenhouse

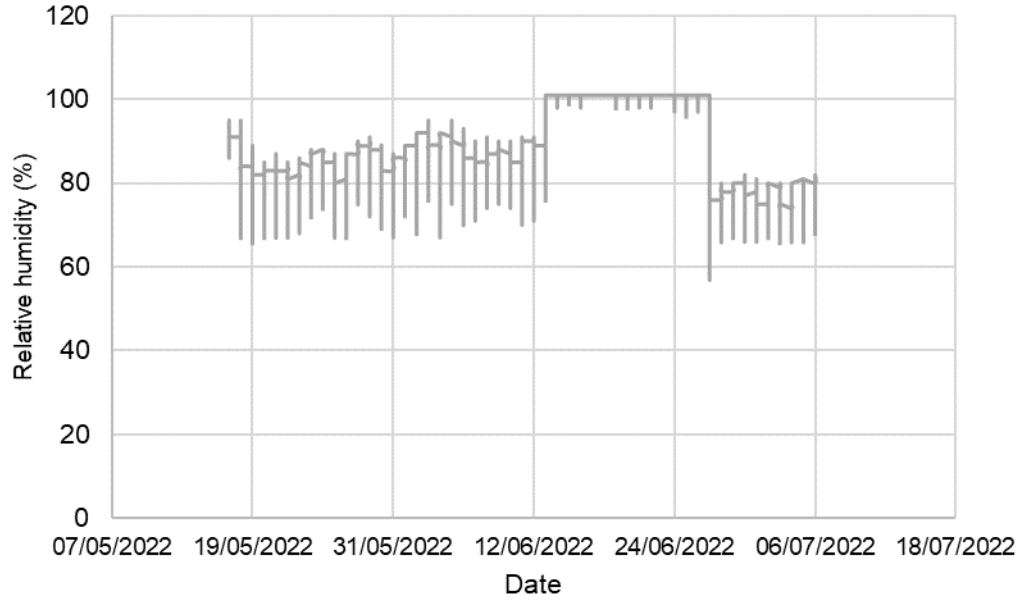

Figure 5. 9. Relative humidity recorded in greenhouse during experiments in 2022.

There is a variation of relatively humidity after one week as it was lowered from 90% to 70%.

Temperature variation in the greenhouse is shown in Figure 5.10.

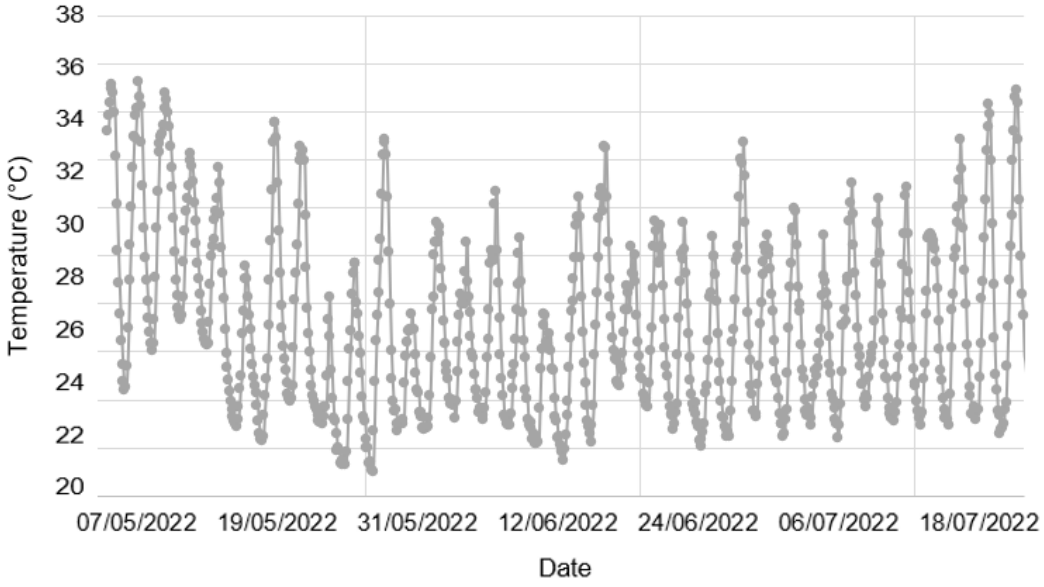

Figure 5. 10. Temperature recorded in greenhouse during experiments in 2022.

Temperature variations in Figure 5.10 are related to the day and night temperature variations.

In literature, growth of plants and crops is observed at a time ranging from several days to a few months (Baran et al. 2016). Furthermore, ryegrass germination is ideal at a humidity of 95% in greenhouse at a temperature of 25°C. Germination of ryegrass decreases significantly at a temperature above 35°C and below 15°C (Javaid et al. 2022).

5.2.6 Ryegrass cultivation

Ryegrass seeds were sown at a depth of 3cm to 5cm within pots of volume 20*20*70 cm^3. Ryegrass sowing in Usumacinta based soil is shown in Figure 5.11 followed by burying the seeds with potting soil and sediments.

Figure 5. 11. Ryegrass sowing and watering in greenhouse

Watering of ryegrass was done on the first day followed by watering every week. Figure 5.12 shows the different combinations of soil with 100% potting soil (C1) (a), 50% potting soil (C2) (b) and 100% sediments (C3) (c).

Figure 5. 12. Sowing of ryegrass on day 1.

Ryegrass seed weight and sowing depth are two important factors for its germination. Common range of ryegrass seed weight is 0.9mg to 3.6mg. Arnott 1969 observed that light and heavy weight seeds show similar germination. Furthermore, germination of lightweight and heavyweight ryegrass seeds is good and quite similar at a depth of 1.25cm to 7cm. However, the number of seeds germinated reduces after the depth of 7cm.

5.2.7 Ryegrass germination and growth

Ryegrass growth was measured continuously. After the height of 10cm, ryegrass was cut to the height 5cm. Welsch-Pausch et al. 1995 in their research cut the ryegrass in greenhouse to a height of 4cm after regular intervals. The fresh biomass of ryegrass was also observed to analyze the performance of sediments. Ryegrass germination and growth are shown in Figures 5.13a and 5.13b.

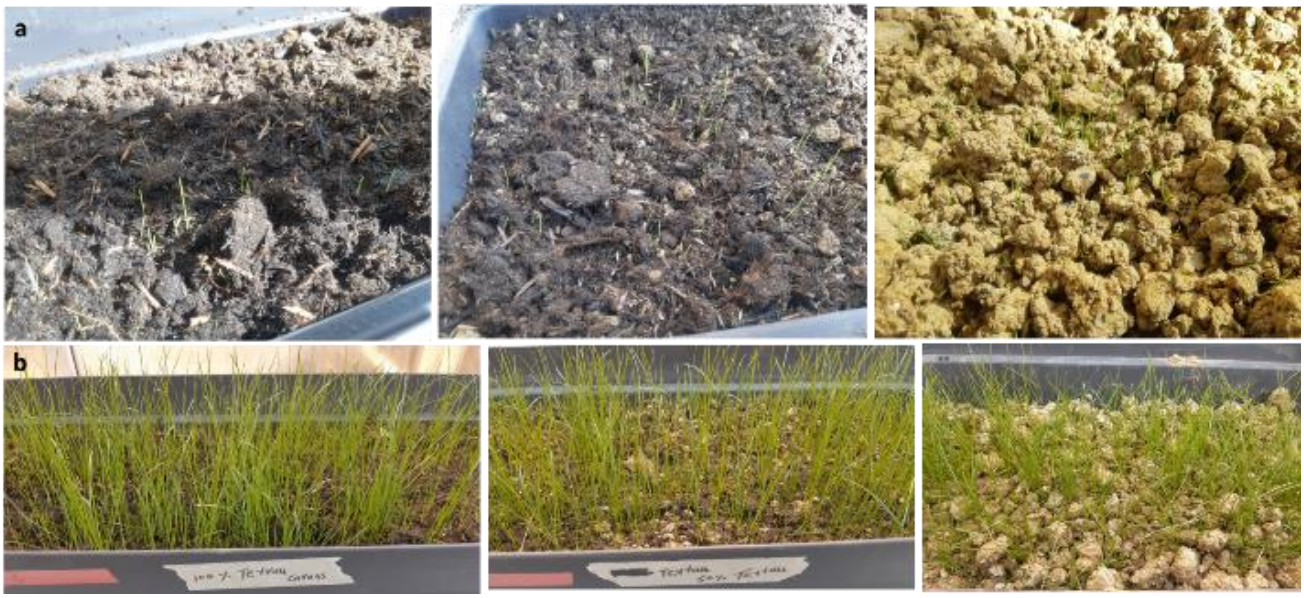

Figure 5. 13. Germination of ryegrass at day 5 (a) and ryegrass at day 14 (b), from left to right C1, C2 and C3 compositions respectively

Few seeds of ryegrass germinated on the 4th day. However, on day 5, considerable seeds have been germinated. Ryegrass height was measured continuously at intervals of 2-3 days. Test was terminated after 66 days. Figure 5.14 shows the ryegrass at day 66.

Figure 5. 14. Germination of ryegrass day 66, from left to right C1, C2 and C3 compositions respectively

The roots of ryegrass after 66 days are shown in the soil block of C2 composition in Figure 5.15.

Figure 5. 15. Roots observation of ryegrass (C2 composition)

Ryegrass growth and germination are similar in both mixture C1 (100% Terreau) and mixture C2 (50% Terreau and 50% sediments). However, in mixture C3 with 100% sediments, grass is thin and its growth is slow. Industrial potting soil is specifically designed for small-scale plantations with higher organic matter, higher conductivity and low pH value which increase the growth of plants.

5.2.8 Results and discussions

Ray grass growth with time was measured at different compositions. In addition, fresh biomass of ryegrass was measured at different intervals of time.

(a) Ryegrass growth analysis

Ryegrass germination and growth are parameters that allow assessing the suitability of sediments. Germination and growth are influenced by the pH, temperature, weight of seed, burial depth, water and presence of salts (Javaid et al. 2022, Arnot, 1969).

Growth of ryegrass was observed with time which increases with increasing time. Ryegrass growth with time is shown in Table 5.18.

Table 5. 18. Ryegrass growth with time

Days	h_{C1} (cm)	h_{C2} (cm)	h_{C3} (cm)
0	0		0
5	Germination	Germination	Germination
9	4	3	3 to 4
12	7	6	4 to 5
15	9	7	5 to 6
17	11*	10*	6 to 7
19	8	7	6 to 7
22	15*	13*	7 to 9
23	7	6	9 to 11*
24	11*	10*	5 to 6
27	9	8	7 to 8
29	12*	11*	9 to 10
36	14*	12*	10 to 11*
38	9	8	5 to 6
43	16*	15*	6 to 7
45	8	7	7 to 8
47	13*	12*	9 to 11*
55	12*	11*	6.5
60	9	9	7.5
66	12*	11*	7.5

** At this height ryegrass was cut up to the height of 5cm.*

Ryegrass was cut after the height of 10 cm every time. Height of adult ryegrass in literature studeis ranges from 30cm to 40 cm (Gnis, 2008).

Graph in Figure 5.16 shows the variation in height with time. In Figure 5.16, red lines indicate the decrease in growth after cutting the grass to 5cm.

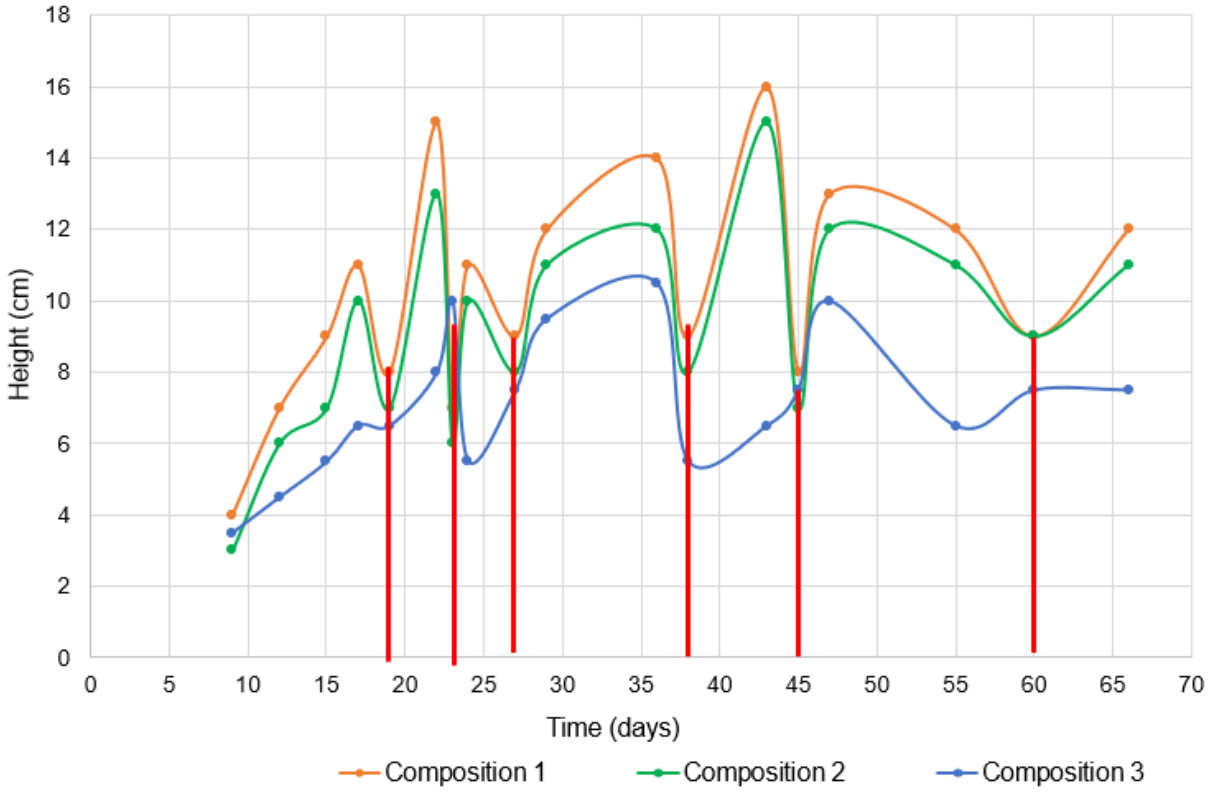

Figure 5. 16. Ryegrass height variation with time

Ryegrass height and fresh biomass in Tables 5.18 and Figure 5.16 are low for 100% sediments when compared with 50% sediments and 0% sediments soil. Lower organic matter of sediments is one of the reasons. Moreover, electric conductivity and pH values of potting soil are specially designed for plant growth and soil is rich in nutrients. Higher pH values of sediments can be reduced with the addition of aluminum sulphate (Sheehan et al. 2010b).

Salt deposition on wet sediments surface shows the higher soluble salt content in tap water used. SAR and electrical conductivity of Usumacinta River sediments indicate that salt presence in Usumacinta River sediments is negligible. Figure 5.17 shows the presence of salts on the surface of the sediment which is due to a higher percentage of salts in local underground water.

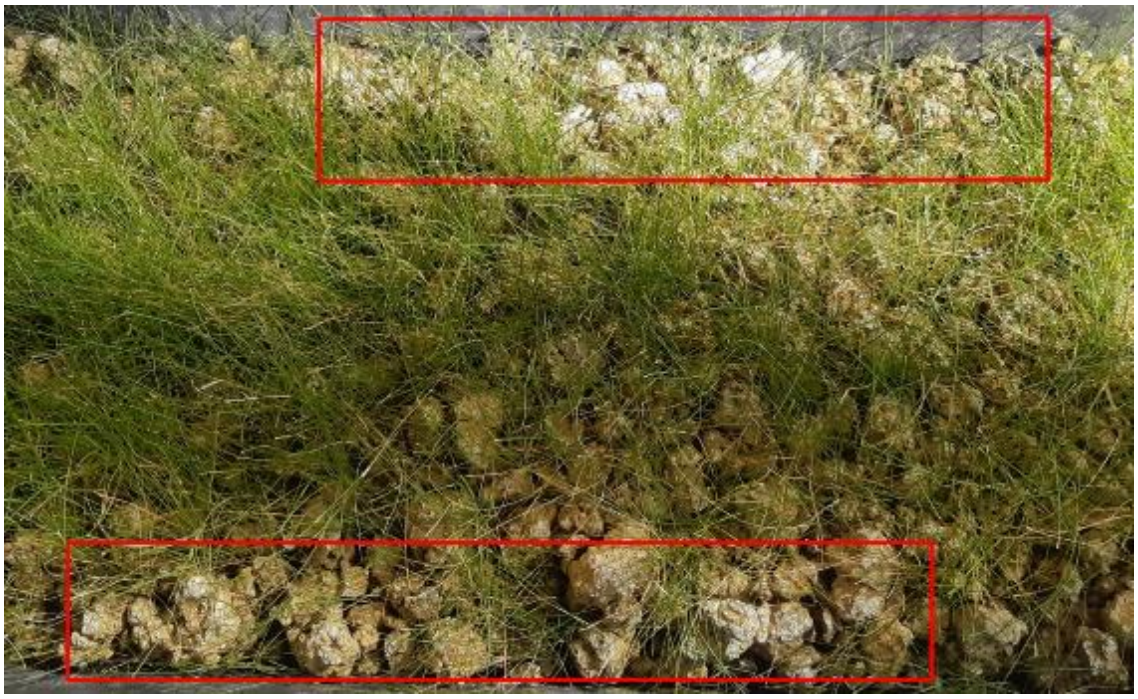

Figure 5. 17. Presence of salts on sediments surface

Presence of salt in soil or water used for crops has a negative influence on the germination and growth of grass as it becomes hard for grass to absorb water from the sediments (Macía et al. 2014). Additionally, Usumacinta River sediments have higher percentage of fine particles which affects the porous matrix. Addition of coarse particles do the aeration of soil by improving its texture.

The height of plants for 50% Terreau and 50% sediments (C2) is similar to the height of plants with 100% Terreau (C1). This is because, at 50% mass of sediments, sediments volume is considerably lower than the volume of potting soil which is very lightweight due to higher organic matter. With 50% potting soil addition by mass, the texture of the sediment's mixture is improved and its performance is similar to the potting soil. Volume of potting

This observation shows that agronomic soil (topsoil layer) can be replaced with dredged sediments in the Usumacinta basin up to 50% sediments addition by mass. Soil replacement in saline soils can improve the productivity of soils by minimizing the percentage of salts.

(b) Ryegrass biomass

Fresh biomass of ryegrass was calculated at the end of the test. Biomass of ryegrass with100% potting soil (C1) and 50% Terreau (C2) is considerably higher than the biomass of 100% sediments (C3). Table 5.19 shows the biomass of ryegrass at the different cutting of soil.

Table 5. 19. Fresh biomass growth with cutting in grams

Cutting	1	2	3	4	5	6	7	8
Composition C3	3.49	5.06	6.88	-	-	-	-	-
Composition C2	6.25	9.75	7.85	9.83	27.83	21.06	8.79	26.3
Composition C1	8.27	9.34	10.6	11.24	38.4	24.3	11.72	34.41

Table 5.20 shows the biomass of ryegrass at the end of the test.

Table 5. 20. Final height and biomass yield at the end of the test

Composition	Mass (g)	Average height (cm)	Yield (kg/m^2)
Composition C3	6.88	7 to 8	0.05
Composition C2	26.3	11 to 12	0.18
Composition C1	34.41	11 to 12	0.25

Ryegrass fresh biomass variation with time observed in literature is shown in Figure 5.18 (Kiani et al. 2021).

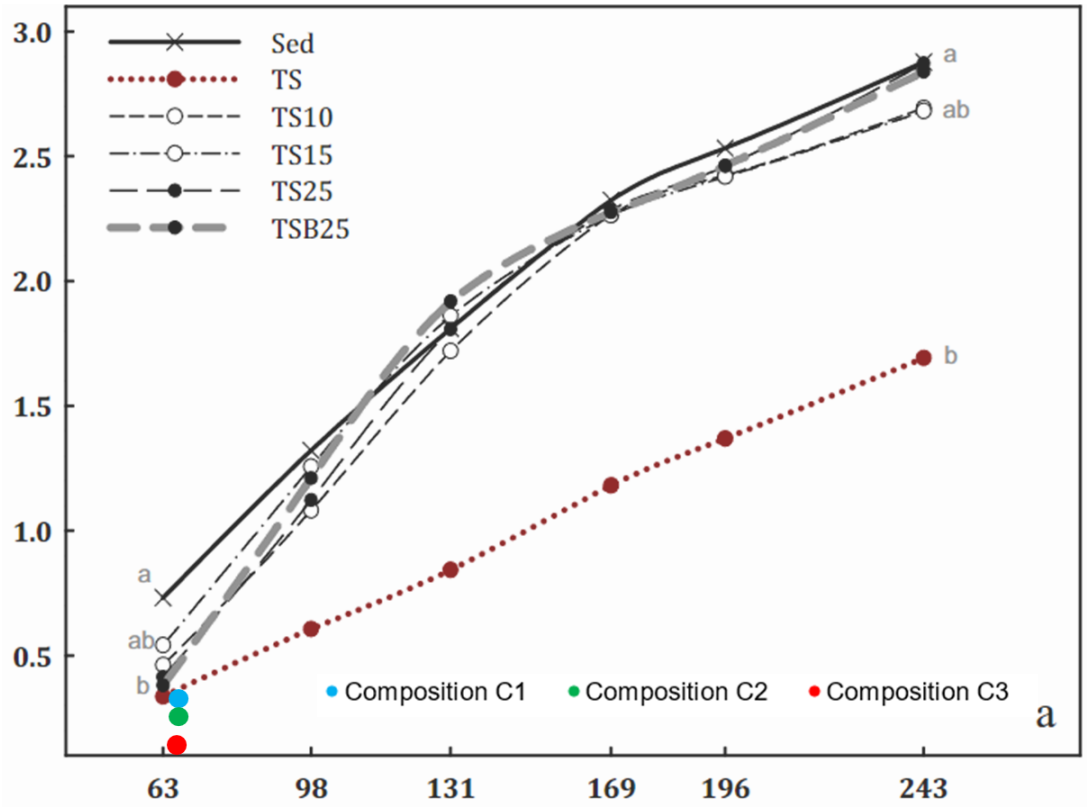

Note: Sed = sediments; TS = topsoil; TS10= 10 cm of soil on 90 cm of sediment; TS15= 15 cm of soil on 85 cm of sediment; TS25= 25 cm of soil on 75 cm of, sediment; TSB25: 23 cm of soil plus 2 cm of biochar on 75 cm of sediment.

Figure 5. 18. Ryegrass biomass variation with time, (Kiani et al. 2021).

Ryegrass mass in Figure 5.18 at 63 days is around 0.5 kg/m^2 and is maximum at 243 days and its value is 2.88 kg/m^2. Usumacinta sediments composition C1, C2 and C3 are also shown in

Figure 5.18. However, ray grass with Usumacinta River sediments was cut every 2 to 3 days when it reaches 10 cm length while Figure 5.18 presents results in which ray grass was cut only after 63 days due to which fresh biomass of research conducted in Figure 5.18 is higher than the fresh biomass shown in Table 5.20. Furthermore, the nature of sediments, watering of plants and plants seeds change the growth of plants significantly.

5.2.9 Conclusion about sediments reuse in agronomy

Dredged sediments reuse in agronomy provides a sustainable solution for sediment management. In this study, Usumacinta River sediments characteristics were investigated for their reuse in agronomy. Physico-chemical and mineralogical characteristics of Usumacinta sediments are similar to soils used for agronomy. Clay content of sediments is 13.4% and organic matter is around 5.72%. Usumacinta sediments have alkaline nature, and their pH value is around 8.5. Electrical conductivity (EC) and sodium absorption value of Usumacinta sediments shows that the presence of salts in Usumacinta River sediments is negligible. Environmental characteristics of sediments show that the presence of contaminants in Usumacinta sediments is smaller than recommended thresholds except Ni which needs further considerations.

Usumacinta River sediments were used with potting soil (terreau) to grow ryegrass within greenhouse at a temperature of 30°C and relative humidity of 70 °C. Three soil compositions were tested with 0% sediments (C1- with terreau), 50% sediments (C2) and 100% sediments (C3) addition to potting soil. It was observed that the germination of ryegrass is similar in all three mixtures. However, growth of ryegrass is significantly lower with 100% sediments. 50% potting soil replacement with sediments shows similar growth to 100% potting soil, which indicates the sediment's potential to partially replace even the commercial soil. Furthermore, the germination of ryegrass similar is also similar in all three compositions which is encouraging for sediments recovery in agronomy.

Pilot study on ryegrass germination and growth in greenhouse by using Usumacinta River sediments highlights the potential of these sediments as a sustainable resource for agronomy where these sediments can be used to improve the quality of degraded soils by excessive exploitation and use of commercial fertilizers. Inert nature of Usumacinta sediments and presence of primary and secondary nutrients such as potassium and iron in Usumacinta sediments makes them suitable for soil amendments to grow crops, vegetation covers to prevent erosion and for soil aeration purposes.

5.2 French sediments reuse in earth bricks

5.2.1 Introduction

Sediments are dredged from seaports, rivers, dams and waterways in France every year. Every three million m^3 sediments are dredged from Dunkirk port in which 500000 m^3 are contaminated sediments stored on land sites while only 50000 m^3 to 60000 m^3 sediments are recycled in roads, landscaping, concrete and aggregates etc. (Robin, 2017; Agence conseil en développement des entreprises, 2022). Unpolluted sediments from ports are immersed in the sea and river sediments are stored on land sites. Land stie storage is costly, therefore, sediment recycling must be considered. Sediment valorization in different sectors is decided after analysis of sediments characteristics and local demands. Dredged sediments reuse in construction materials such as earth bricks can be an environmentally friendly and sustainable way of reusing sediments.

Sediments reuse in earth bricks is limited due to the heterogeneous nature of sediments and the presence of contaminants in sediments. Some important pollutants in sediments are As, Ni, Pb etc. which are removed by treatment of sediments to use these sediments in earth bricks. Sediments based earth brick strength and characteristics depend on the characteristics of raw material. Earth bricks are reinforced with natural fibers, mostly waste from agri-industry. In France, hemp and flax fibers are common natural fibers. The cultivated area of hemp in France is 17000 ha. This plant produces 3 tons/ha as plant particles. 51 000 tons is annual hemp shiv production in France (Lenormand and Leblanc, 2020, Ziapkoff et al. 2022).

In this study, sediments from Dunkirk port and Garonne River, France were used to manufacture earth bricks along with hemp shiv. Characteristics of sediments and hemp shiv were investigated for their recovery in earth bricks. Laboratory scale experiments were conducted to manufacture earth bricks from these sediments and investigate the characteristics of these bricks.

5.2.2 Materials and methods

Dunkirk port and Garonne River sediments were used in manufacturing earth bricks along with hemp shiv as reinforcement. Characteristics of sediments and hemp shiv were investigated for their reuse in earth bricks.

(a) Dredged sediments

Marine and freshwater sediments were used in this study. Marine sediments are dredged from Dunkirk port France and freshwater sediments are taken from Saint-Vidian reservoir, Garonne River (GAR) France. Physio-chemical, geotechnical and mineralogical characteristics of Dunkirk sediments (DK) and Garonne River sediments (GAR) were investigated so as their suitability for earth bricks based on granulometry and consistency limits. Consistency limits, grain size, chemical composition, percentage of clay and organic matter have a significant influence on the strength and quality of earth bricks.

Characteristics of DK and GAR sediments are given in Table 5.21.

Table 5. 21. Characteristics of DK and GAR sediments

Sediments	Clay (%)	Silt (%)	Sand (%)	LL (%)	PI	OM (%)	ρ_{sed} (g/cm^3)	W_{opt} (%)
DK	4.29	24.78	70.92	18.92	8.20	5.29	2.55	20.50
GAR*	3.40	60.60	36.00	76.00	26.00	9.10	2.65	24.00

*Note: *GAR sediments characteristics are investigated by Anger, 2014.*

Table 5.21 shows that DK sediments have slightly higher clay content than GAR sediments but the percentage of sand in DK sediments is significantly higher. Organic matter in GAR sediments is considerably high as its value is 9.1%. Similarly, consistency limits and optimum moisture content of GAR sediments are also high. Consistency limits and optimum moisture contents are influenced by the percentage of fine particles and organic matter.

Sediment's suitability for earth bricks was observed with their granulometry and Atterberg limits by using AFNOR (AFNOR, XP P13-901, 2001) and Spanish (MOPT, 1992) standards. Figure 5.19 shows the recommended zones for earth bricks based on sediment grain size after French and Spanish standards.

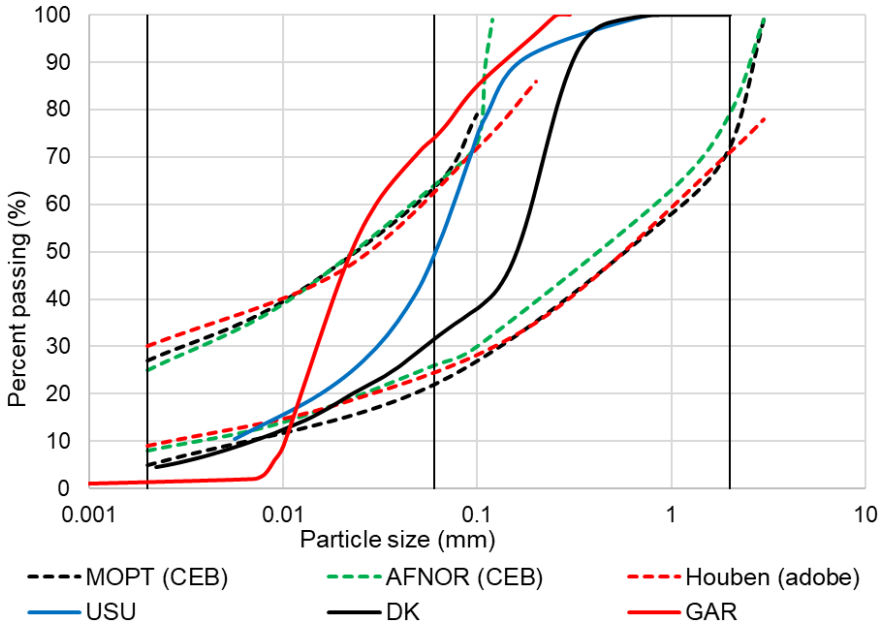

Note: CEB = compressed earth blocks

Figure 5. 19. Sediments suitability for earth bricks with grain size

Figure 5.19 shows that DK and USU sediments are in the zone suggested for earth bricks. GAR sediments slightly deviate from the proposed zone due to unsuitable grain size distribution.

Figure 5.20 shows the recommended zones for earth bricks based on Atterberg limits after the French standard and recommendation by Houben and Guillaud (1994).

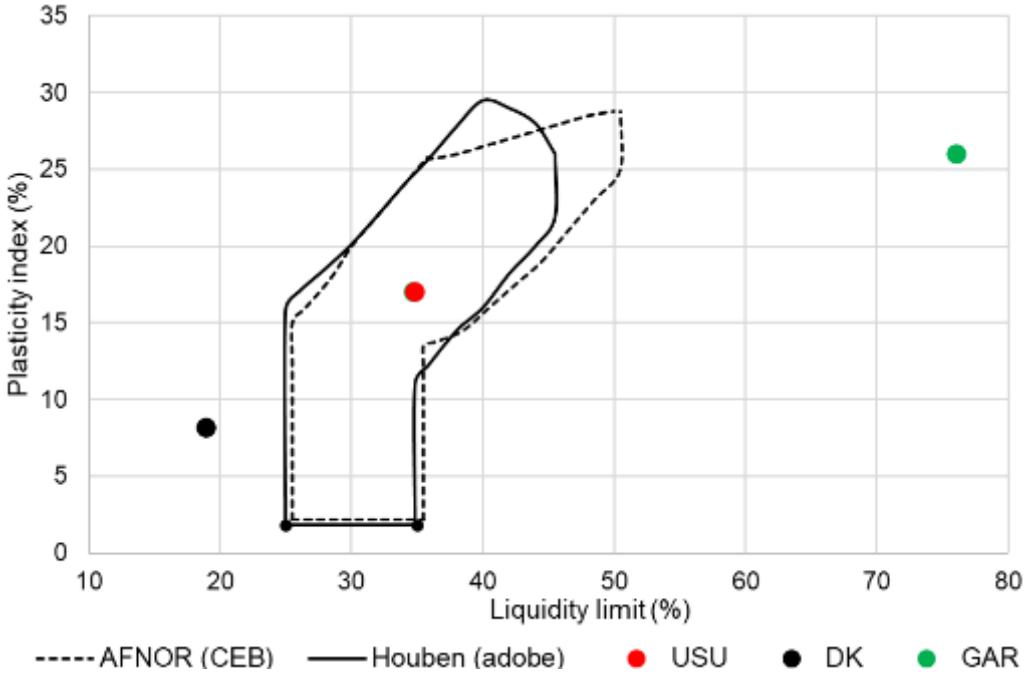

Figure 5. 20. Sediments suitability for earth bricks with consistency limit

In Figure 5.20, it can be observed that USU sediments are inside the zone recommended for earth bricks. However, DK sediments are outside the zone due to low PI index and LL values. Higher sand content of DK sediments affects their moulding characteristics. GAR sediments are also outside the zone recommended for bricks as their Atterberg limits are very high due to a higher organic matter content.

(b) Hemp shiv

Hemp shiv was used as reinforcement in earth bricks as hemp shiv is local agriculture waste produced at an industrial scale in Normandy, France. Hemp shiv used in this study has a controlled and constant particle size, and dust rate passing through the sieve of 0.25 mm, less than 2%. Characteristics of hemp shiv such as tensile strength, length, density and water absorption were investigated as they play an important role in the strength and durability of earth bricks.

Hemp shiv used in this study has length variation and consist of thick wooden and thin fibrous part as shown in Figure 5.21. Length and thickness of hemp shiv were found through ImageJ software. 100 hemp shiv particles were distributed on the plan sheet as shown in Figure 5.21. Hemp shiv was treated with ImageJ software to find the length and thickness of fibers. This process was repeated three times to get an average value.

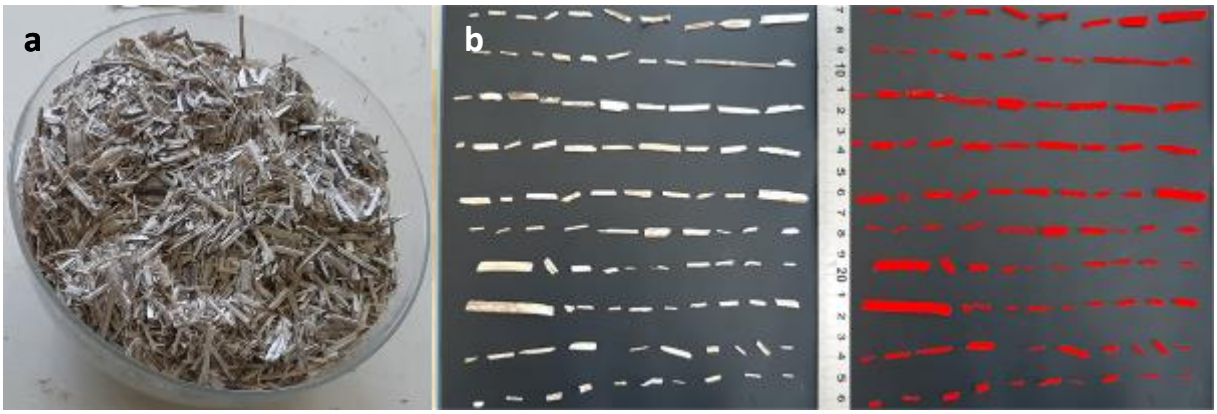

Figure 5. 21. Hemp shiv (a) and length and thickness estimation of hemp shiv (b)

Grain size distribution of length of hemp shiv is shown in Figure 5.22.

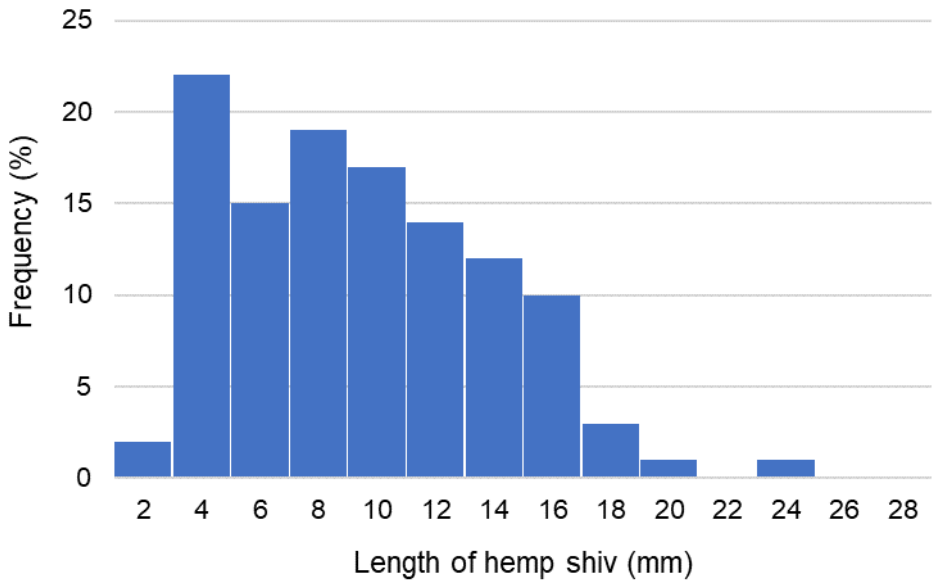

Figure 5. 22. Grain size distribution of length of hemp shiv

Grain size distribution of length and thickness of hemp shiv is shown in Figure 5.23.

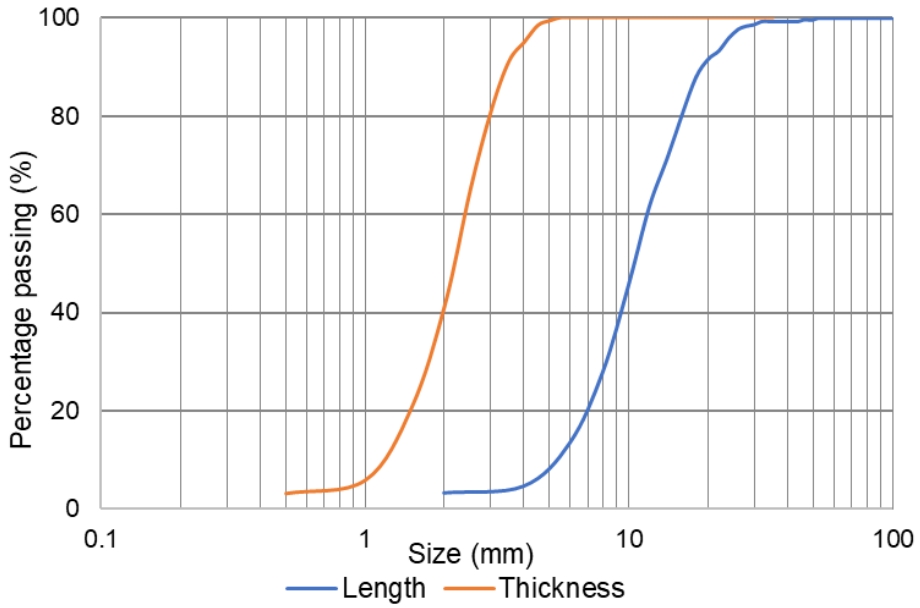

Figure 5. 23. Grain size distribution of length and thickness of hemp shiv

Average and maximum length of hemp shiv is shown in Table 5.22. Water absorption of hemp shiv was found by immersing fibers in water for 24 hours. Physical and mechanical characteristics of hemp shiv are summarized in Table 5.22.

Table 5. 22. Characteristics of hemp shiv

Plant Aggregates	Average length (mm)	Maximum length (mm)	Average thickness (mm)	Skeletal density (g/cm^3)	σt (MPa)	WA (%)
Hemp shiv	11.67	50.46	2.24	1.44-1.52*	960 +/-220 **	2.98

*Note: WA = water absorption, σt = tensile strength, * Jiang et al., 2018; ** Thygesen et al., 2008*

Average length of hemp shiv is around 11.67 mm which is lower than 25 mm, the length of natural fibers recommended for building composites such as concrete (ASTM D7357-07, 2012). Maximum length observed for hemp shive is around 50.46 mm. Hemp shiv is very thick as compared to natural fibers and the average thickness is 2.24 mm. Skeletal density of hemp shiv ranges from 1.44 to 1.52 which is similar to the density of the tropical fibers. Water absorption capacity of hemp shiv is around 298%. Bui et al. 2022, reports these values between 85 MPa-415 MPa. Water absorption of tropical natural fibers used in earth bricks as reinforcement is around 235% (Hussain et al. 2021a). Variation in water absorption is associated with heterogenous nature of natural fibers and the method adopted to find the water absorption of natural fibers. Tensile strength of hemp shiv is considerably higher due to the thickness of hemp shiv.

5.2.3 Manufacturing of bricks

DK and GAR sediments and hemp shiv were mixed with optimum moisture content to make a homogenous mixture with an electric mixer. Optimum moisture content of DK and GAR sediments is 20.54% and 24% respectively and it varies with the percentage of fine particles

and organic matter in sediments. Sediments mixture was moulded into prismatic brick specimens of size 4*4*16 cm^3 and compacted in two layers with dynamic compaction energy of 600 $kN.m/m^3$ which is proctor normal energy (Bruno et al., 2018). Quantity of sediments needed for 4*4**16 cm^3 is around 450 g (AFNOR EN 196-1, 2016). Earth bricks were manufactured with hemp shiv content of 0%, 1%, 2%, 3%, 4% and 5% by mass of sediments which is a common range for natural fibers and plant aggregate in earth bricks (AZHARY *et al*., 2017; ISMAIL *et al*., 2011). Finally, Bricks were dried at 40 °C in oven. Oven drying of bricks takes place in 2 -3 days. The manufacturing process of earth bricks with DK and GAR sediments is shown in Figure 5.24.

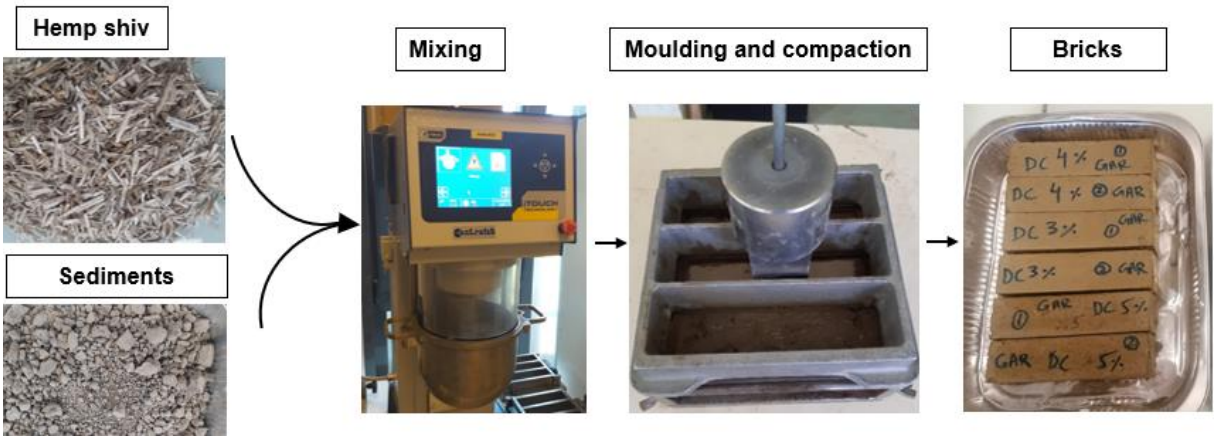

Figure 5. 24. Manufacturing of earth bricks with DK and GAR sediments.

5.2.4 Testing of bricks

Earth brick's physical and mechanical characteristics were investigated and the influence of hemp shiv content on mechanical characteristics was examined.

(a) Mechanical testing of bricks

Indirect tensile strength of bricks was found with a three-point bending test by using ASTM standard (ASTM C1557-03, 2004). After three points bending test, compressive strength test was performed on cubic bricks specimens of dimensions 4*4*4 cm^3, obtained from two halves of bricks after 3 points bending test.

Distribution of fibers in bricks was observed by dividing the bricks into 4 parts with 6 cross-sections as shown in Figure 5.25. Each brick cross-section has dimensions of 4*4*4 cm^3. Brick cross sections were analyzed with ImageJ software to observe the distribution of fibers (Bui, 2021).

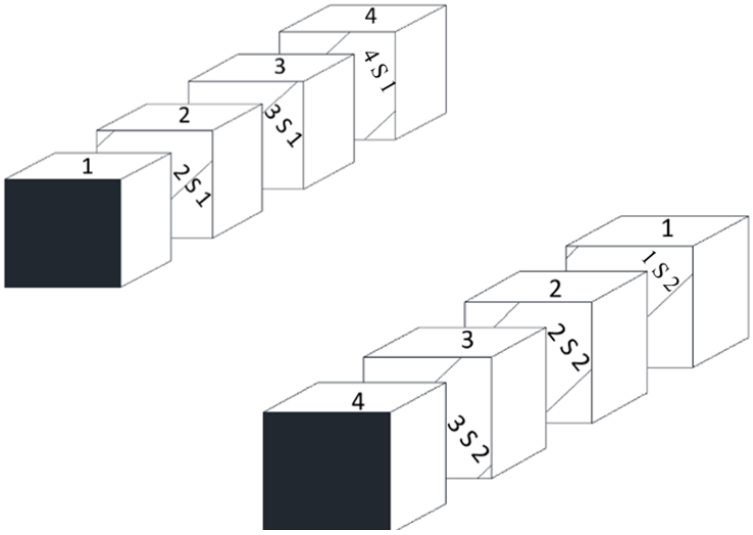

Figure 5. 25. Cross sections and division of each section in a section of 1cm.

Figures 5.26a and 5.26b show the hemp shiv distribution and binarization with ImageJ software of a bricks cross-section with 3% hemp shiv content.

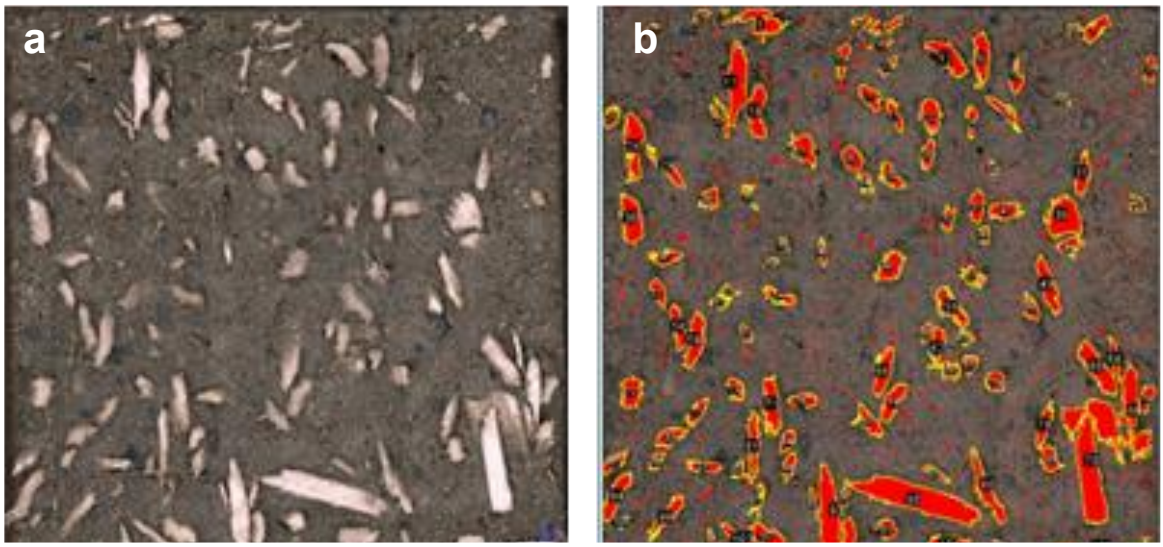

Figure 5. 26. Brick cross section microscopic image and its treatment with ImageJ software

Brick cross section was further divided into 4 layers of dimensions 4*1cm^2 with 16 squares of size 1cm^2 as shown in Figure 5.27. ImageJ software was used to calculate the area of fibers by counting the number of fibers in each square and calculating the area of the fiber through binarization. Equation 5.2 was used to find the area occupied by fibers in each square.

$$\text{Area occupied by fibers (\%)} = \frac{\text{Area of fibers in a square}}{\text{Area of square}} * 100 \qquad (5.2)$$

With the area of each square, the area occupied by fibers in each layer of dimension 4*1 cm^2 was determined. DK sediments bricks cross sections and their division into squares are shown in Figure 5.27.

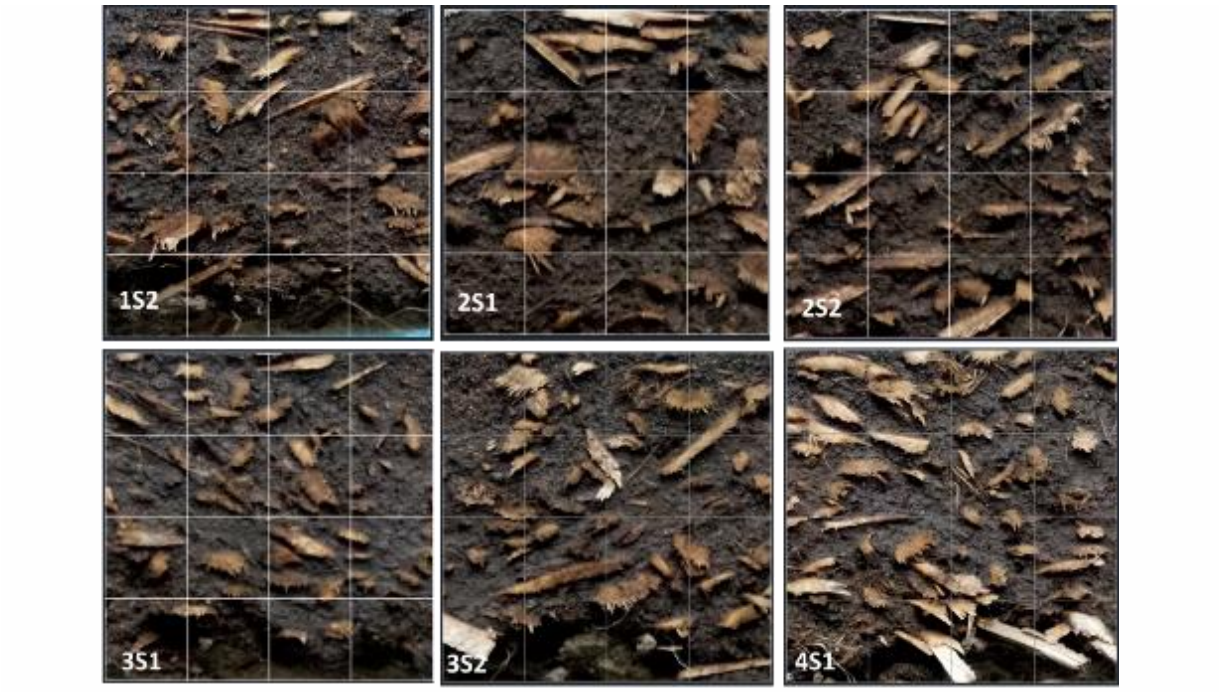

Figure 5. 27 . Fibers distribution and counting in DK sediments bricks

Number of hemp shiv aggregates and the area occupied by aggregates for hemp shiv is shown in Table 5.27.

5.2.5 Results and discussion

(a) Density of bricks

Dry density of DK and GAR bricks was found after drying the bricks. Density of DK and GAR sediments bricks with different hemp shiv content is shown in Table 5.23.

Table 5. 23. Density variation of earth bricks

Dry Density (kg/m^3)	DC 0%	DC 1%	DC 2%	DC 3%	DC 4%	DC 5%
DK	1585	1549	1428	1478	1282	1329
GAR	1291	1174	1323	1296	1218	1187

Density of earth bricks is influenced by fiber content and organic matter. Density of earth bricks generally decreases with increasing natural fiber content as fibers have low density and incorporation of increases voids in earth bricks which decreases the density of bricks (Calatan et al., 2016). Density of GAR sediments is considerably lower than DK bricks due to the higher organic matter. For unreinforced bricks, Usumacinta and DK bricks density is approximately 18% and 22% higher than GAR sediments bricks. Density of GAR bricks is higher at 2% and 3% hemp shiv content which is associated with uneven shrinkage of bricks. Furthermore, in manual manufacturing of bricks, it is difficult to control the quantity of sediments mixture in bricks. Density of adobe bricks varies with the nature of sediments and fibers addition, compaction and moulding moisture content. Common density values of adobe bricks in the

literature range from 1260 kg/m^3 to 1950 kg/m^3 (Illampas et al. 2011, Salih, et al. 2019). Density of most of the bricks from DK and GAR sediments lies within this range.

(b) Flexural strength of bricks

Addition of fibers increases the flexural strength of earth bricks. Unreinforced DK and GAR bricks have brittle behavior. Addition of natural fibers increases the stiffness of these bricks by transforming bricks behavior into ductile. After initial cracking, load is taken by fibers. Flexural load-deflection curves of DK and GAR bricks are shown in Figures 5.28 and 5.29.

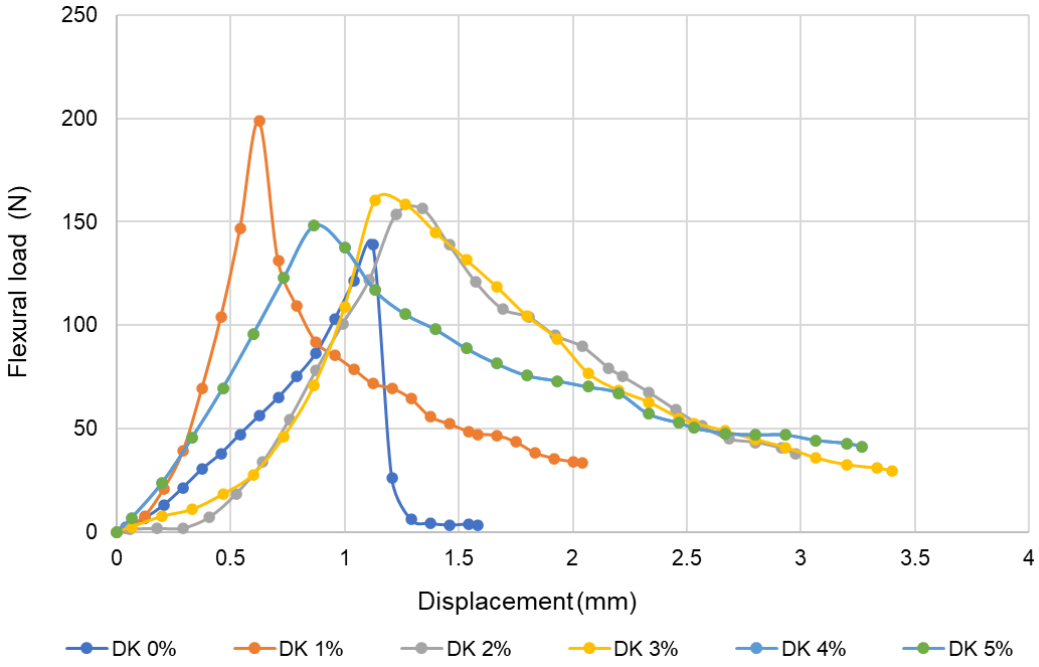

Figure 5. 28. Flexural load deflection curves of Dunkirk port sediments bricks

Figure 5.28 shows that failure in bricks with 0% fiber is brittle and gradually transforms to ductile with addition of hemp shiv. Flexural load increases linearly in all bricks before reaching peak load and after peak load, plastic deformation starts as fibers take the load.

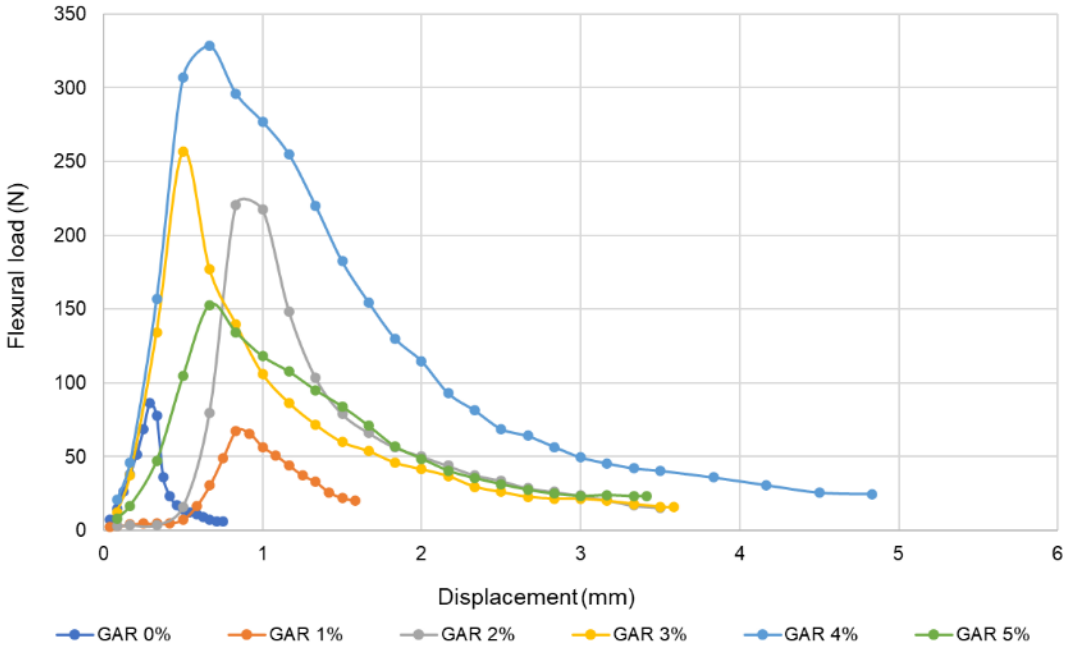

Figure 5. 29. Flexural load deflection curves of Garonne River sediments bricks

Figure 5.29 shows that deflection after the initial crack is higher in GAR bricks. Maximum load in GAR bricks is observed with a 4% hemp shiv addition.

Load bearing capacity and deflection in DK and GAR bricks is lower than Usumacinta bricks. This is due to higher clay content, low organic matter and morphology of POFL fibers which are soft and short when compared with hemp shiv. In case of bricks from DK and GAR sediments, tensile strength of the hemp shiv is higher and it does not fail but the sediments detach from hemp shiv when failure happens and deflection is limited. Average tensile strength of USU, DK and GAR sediments bricks is summarized in Table 5.24.

Table 5. 24. Flexural strength (indirect tensile strength) of earth bricks

Fiber content (%)	**F = 0%**	**F = 1%**	**F = 2%**	**F = 3%**	**F = 4%**	**F = 5%**
σ_t (MPa) $_{USU}$	1.79	1.79	2.56	3.19	2.02	2.59
σ_t (MPa) $_{DK}$	0.35	0.48	0.41	0.39	0.35	0.34
σ_t (MPa) $_{GAR}$	0.19	0.16	0.51	0.52	0.60	0.32

Note: σ_t = tensile strength.

Tensile strength of USU sediments is high and its value is 3.19 MPa with 3% fibers addition. Tensile strength of bricks starts to decrease after optimum moisture content as at high fiber content adhesion between sediments and fibers decreases. Tensile strength of DK and GAR sediments is very low. Both DK and GAR sediments have similar tensile strength and load deflection behavior. Maximum tensile strength in the case of DK bricks is at 1% hemp shiv addition while in GAR sediments strength is maximum at 4% fibers addition. In the case of DK and GAR sediments, the low percentage of fine particles and higher organic matter in GAR sediments are important reasons behind the low strength of bricks. Furthermore, morphology,

particle size and tensile load behavior of hemp shiv are quite different from palm oil flower fibers which also influence the performance of DK and GAR sediments bricks. Usually, earth bricks without using stabilizing agents have low strength and tensile strength suggested for adobe bricks varies from 0.012 MPa to 0.25 MPa (NZS, 1998, NORMA E.080, 2017, AFNOR XP, P13-901, 2001). DK sediments bricks have tensile strength higher than this range at all hemp shiv content. However, Garonne River sediments have lower strength from this range at 0% and 1% hemp shiv addition. Table 5.25 shows the tensile strength of earth bricks manufactured with different natural fibers.

Table 5. 25. Tensile strength of fiber reinforced earth bricks

Fibers	**Fiber content (wt.%)**	**Tensile strength (MPa)**	**Reference**
Jute	0.5-2	0.55-0.66	Araya-Letelier et al., 2021
Seagrass	0.5-3	0.4-0.6	Olacia et al., 2020
Straw	0.5	0.71	Abdulla et al., 2020
Sugarcane bagasse	0-1	0.29-0.89	Kumar and Barbato, 2022
Date palm waste	0-10	0.29-2.26	Khoudja et al., 2021

Note: Reference of Table 5.25 are given in chapter 1.

Maximum tensile strength of DK bricks (0.48 MPa) at 1% hemp shiv and GAR bricks (0.60 MPa) at 40% hemp shiv content have strengths similar to the values reported in the literature.

(c) Bending stiffness of bricks

Bending stiffness of earth bricks manufactured with GAR and DK bricks was determined from flexural load deflection curves in Figures 5.28 and 5.29. Table 5.26 shows the average flexion stiffness value of earth bricks.

Table 5. 26. Flexion stiffness of DK and GAR sediments bricks

Hemp shiv (%)	**0**	**1**	**2**	**3**	**4**	**5**
DK (N/mm)	109	416	198	262	182	269
GAR (N/mm)	306	207	844	670	904	378

Flexural stiffness of earth bricks is maximum at the highest tensile strength. Stiffness in GAR sediments bricks is higher than DK sediments bricks. This is due to higher tensile strength of GAR sediments bricks. Furthermore, flexural load curves of DK sediments bricks show that load increases gradually before it reaches the final value. Gradual rise of load leads to lower stiffness in DK bricks.

(d) Distribution of fibers in bricks

Dunkirk sediments were used to define the compaction method to manufacture earth bricks. Earth bricks were manufactured with Dunkirk sediments with different compaction techniques such as dynamic compaction, static compaction and tamping. Compaction of bricks changes the distribution of fibers inside the matrix as lightweight fibers move toward the top surface of

composite materials with water (Bui, 2021). Distribution of hemp shiv in Dunkirk sediments bricks was investigated with ImageJ software. The number of fibers and area occupied by fibers in DK bricks are shown in Table 5.27.

Table 5. 27. Fibers distribution in bricks cross sections – case of Dunkirk bricks

	Dynamic compaction		**Static compaction**		**Tamping**	
Plane	**Fibers**	**Area (%)**	**Fibers**	**Area (%)**	**Fibers**	**Area (%)**
1	91	14.18	90	15.94	70	13.76
2	91	17.16	92	16.13	94	13.91
3	95	15.66	87	14.93	88	13.77
4	100	17.26	102	17.68	110	14.21
5	107	13.6	104	14.29	87	14.56
6	104	14.23	94	13.78	94	13.12

On average, hemp shiv occupies 15.35% of bricks cross section with 3% hemp shiv addition by mass in static compaction. For static compaction and compaction by tamping, at 3% hemp shiv addition in earth bricks from Dunkirk sediments, hemp shiv occupies nearly 13.89% and 13.39 % area of cross section respectively. In Figure 5.30, a cross section of bricks is divided into 4 layers of 1 cm height and size 4*1cm^2. Each 1cm of bricks layer is further divided into 4 squares of size 1*1 cm^2.

1-1	1-2	1-3	1-4
2-1	2-2	2-3	2-4
3-1	3-2	3-3	3-4
4-1	4-2	4-3	4-4

Figure 5. 30. Layers and squares in a brick section

Graph in Figure 5.31 shows the area occupied by fibers in each cross section at different depths described in Figure 5.30.

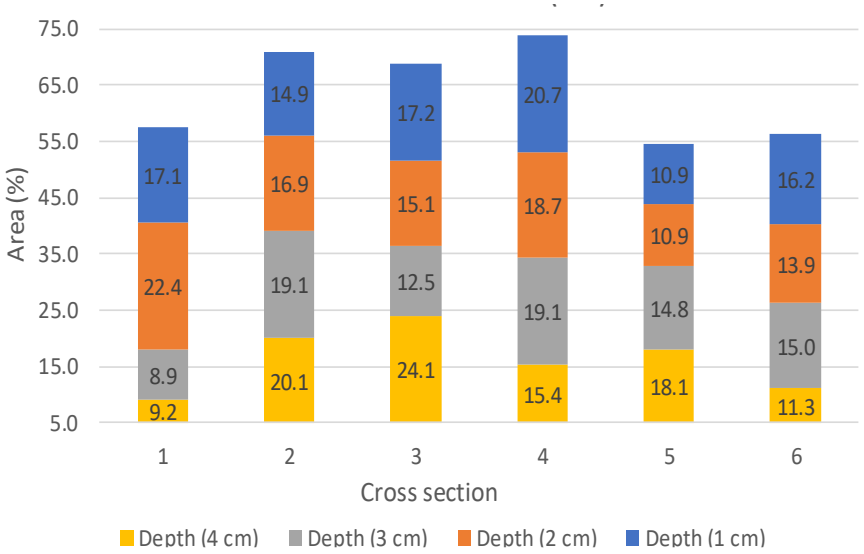

Figure 5. 31. Fibers distribution in bricks with dynamic compaction at 3% fiber content

(e) Microcracks development

Hemp shiv particles swell with their interaction with water. However, due to the evaporation of water during the drying of bricks, plant aggregates shrink and small pores are developed around the surface of fibers. Development of cracks reduces the adhesion between plant aggregates and sediments matrix. Cracks growth in DK bricks around hemp shiv is shown in Figure 5.32.

Figure 5. 32. Micro cracks development around hemp shiv.

(f) Compressive strength of bricks

Dunkirk sediments bricks were tested only for flexural strength to optimize fibers addition and define the compaction method as the influence and contribution of fibers are more apparent with tensile strength test. Earth bricks from DK sediments and hemp shiv were compacted with static compaction, dynamic compaction and tamping. Earth bricks with DK sediments have maximum strength with dynamic compaction (Hussain et al. 2021b). Dynamic compaction was applied to manufacture earth bricks from GAR sediments. Compressive strength tests were only performed on Garonne River sediments and Usumacinta River sediments bricks. Load deflection curves of GAR bricks are shown in Figure 5.33.

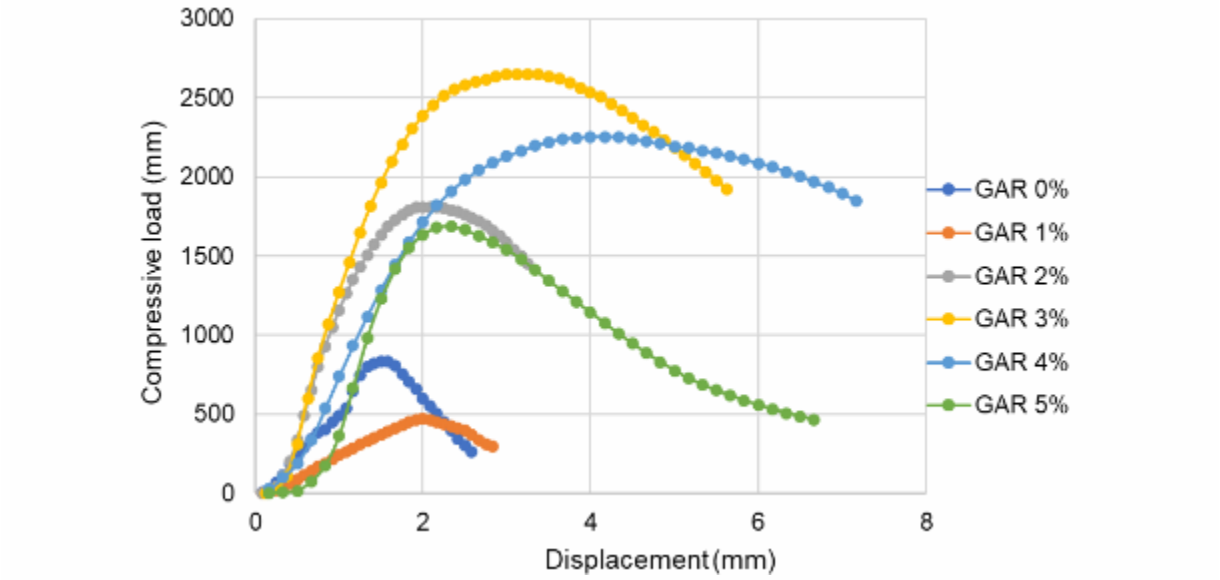

Figure 5. 33. Compressive load deflection curves of Garonne River sediments bricks

In Figure 5.33, after the initial failure, compressive load of earth bricks decreases gradually due to low adhesion between sediments and hemp shiv. Adhesion of fibers depends on the nature of sediments *i.e. plasticity* and morphology of fibers. Compressive strength of Garonne River sediments and Usumacinta River sediments bricks and bricks is shown in Table 5.28.

Table 5. 28. Compressive strength of Usumacinta bricks (USU) and GAR bricks

Sediments	**F= 0%**	**F= 1%**	**F= 2%**	**F= 3%**	**F= 4%**	**F= 5%**
σ_c (MPa)-2cm $_{USU}$	3.03	3.72	2.77	2.97	2.75	3.59
σ_c (MPa)-3cm $_{USU}$	3.03	3.34	3.84	3.21	2.29	3.29
σc (MPa) $_{GAR}$	0.41	0.39	1.14	1.52	1.2	1.02

Compressive strength of USU sediments is high and ranges from 2.29 to 3.84 MPa. French and Spanish standards recommend 1 MPa compressive strength for earth bricks (AFNOR XP, P13-901; NORMA E.080, 2017). However, compressive strength of GAR sediments is low but GAR bricks have higher strength than 1 MPa at 2%, 3%, 4% and 5% fibers addition. Higher organic matter, hemp shiv morphology and mechanical characteristics are some of the reasons behind the low strength of GAR sediment bricks.

5.2.6 Conclusion

In this section, characteristics of DK and GAR sediments and hemp shiv were investigated to use them in earth bricks. DK sediments have suitable grain size distribution for earth bricks. However, GAR sediments slightly deviate from recommended zones based on granulometry. Consistency limits of both DK and GAR sediments are unsuitable for bricks due to higher sand content and organic matter. Hemp shiv studied along with these sediments has an average length of 11.66 mm and water absorption of 298%.

Earth bricks were manufactured from DK and GAR sediments at hemp shiv addition of 0%, 1%, 2%, 3%, 4% and 5%. Density of bricks decreases with increasing fiber content. Dunkirk bricks have a higher density than GAR sediment bricks due to higher organic matter. Fibers distribution analysis in DK bricks shows that fibers occupy nearly 15% area of the brick cross section.

Tensile strength of both DK and GAR bricks is low. It is maximum for DK bricks at 1% hemp shiv addition and its value is 0.48 MPa. GAR bricks have a maximum tensile strength at 4% hemp shiv content and their tensile strength is 0.60 MPa. Compressive strength of GAR bricks is low and its value is maximum at 3% hemp shiv addition which is 1.52 MPa. Compressive and tensile strength of DK and GAR bricks is low but GAR bricks satisfy the tensile and compressive strength requirements at 2 to 5% hemp shiv addition while DK bricks satisfy the tensile strength requirement at 0% to 5% hemp shiv addition (NZS, 1998; AFNOR XP P13-901, 2001; NORMA E.080, 2017). Tensile and compressive strength of Usumacinta bricks is very high. Tensile strength of Usumacinta bricks approaches to 3.19 MPa at 3% POFL fiber content while maximum compressive strength is observed at 2% POFL fiber content and its value is 3.84 MPa. Higher percentage of fine particles, low organic matter and nature of POFL fibers contribute toward the higher strength of Usumacinta bricks.

Low strength of earth bricks with DK and GAR sediments is due to higher organic matter and low clay content. Strength of DK bricks can be improved with low-cost solutions such as replacing a proportion of these sediments with clayey sediment which can improve the granulometry and plasticity of Dunkirk sediments. Garonne River sediments have a higher organic matter which is around 9%. Addition of lime can stabilize the organic matter and increase the strength of these bricks. Furthermore, rigid fibers like hemp shiv have weak adhesion with sediments which is evident by the compressive load behavior of GAR sediments bricks in Figure 5.33. Use of soft fibers from hemp, flax etc. is recommended rather than shiv as the flexibility of soft fibers reinforces the bricks with a significant contribution to tensile and compressive strength.

References

4Vaultx-Jardin (1998). Valorisation agronomique des sédiments marins et fluviaux de la Rance Etudes et expérimentations préalables - Rapport final. 34 p.

ADEME (2001). Les boues d'épuration municipales et leur utilisation en agriculture : 58 p.

AFNOR XP P13-901 (2001). Compressed earth blocks for walls and partitions: definitions – Specifications – Test methods – Delivery acceptance conditions. Saint-Denis La Plaine Cedex.

AFNOR NF ISO 10694, (1995). Qualité du sol–dosage du carbone organique et du carbone total apres combustion seche (Analyse Elementaire).

AFNOR XP P 94-011 (1999). Sols : reconnaissance et essais, Description – Identification-Dénomination des sols.

AFNOR NF U44-551 (2002). Supports de culture – dénomination, spécifications, marquage.

AFNOR EN 196–1, Méthodes d'essais des ciments - 2016 Partie 1: détermination des

résistances.

Agence conseil en développement des entreprises (2022). Dunkirk promotion. https://www.dunkerquepromotion.org/2018/07/dunkerque-port-valorisation-sediments-non-immergeables/. Consulted on 11/07/2022

Anger B. (2014). Caractérisation des sédiments fins des retenues hydroélectriques en vue d'une orientation vers des filières de valorisation matière. Thèse de doctorat, Université de Caen Normandie, 302 p. https://hal-normandie-univ.archives-ouvertes.fr/tel-01938082

Arnot, R. (1969). The effect of seed weight and depth of sowing on the emergence and early seedling growth of perennial ryegrass (Lolium perenne). Grassland Research Institute, Hurley, Berkshire. DOI: 10.1111/j.1365-2494.1969.tb01053.x

ASTM C1557-03, 2004. Standard test methods for tensile strength and young's modulus of fibers. American society for testing and analysis.

ASTM D7357 07. (2012). Standard specification for cellulose fibers for fiber-reinforced concrete.

Azhary, K. E., Chihab, Y., Mansour, M., Laaroussi, N., Garoum, M. (2017). Energy efficiency and thermal properties of the composite material clay-straw. Energy Procedia 2017, vol. 141, pp. 160–164. https://doi.org/10.1016/j.egypro.2017.11.030

Bataillard P., Chevrier B., Hoang V. (2017). Valorisation à terre des sédiments de dragage : retour d'expérience en France et à l'international, rapport final, BRGM/RP-67329, 117p.

Bernes Cabanne C. (2009). Valorisation agricole des sédiments de dragage des voies navigables. Rapport de Stage, ENTPE, 148 p.

Bénédicte, D. (2017). La faisabilité de la valorisation des sédiments de dragage de l'estuaire de la Vilaine, une démarche territoriale. PhD thesis, Institution d'Aménagement de la Vilaine, France.

Baran, A., Tarnawski, M., Koniarz, T., Jasiewicz, C. (2016). Agricultural use of sediments from narożniki reservoir – yield and concentration of macronutrients and trace elements in the plant. Nr IV/1/2016, POLSKA AKADEMIA NAUK, Oddział w Krakowie, s. 1217–1228. DOI: http://dx.medra.org/10.14597/infraeco.2016.4.1.089

Bourret J. (1997). La valorisation agronomique des sédiments marins de la Rance. Courrier de l'environnement de l'INRA n°31, août 1997, pp.66-69.

Brigham, R.D., Pelini, S., Xu, Z., Vázquez-Ortega, A., (2021). Assessing the effects of lake-dredged sediments on soil health: Agricultural and environmental implications for northwestern Ohio. Journal of Environmental Quality, 50; 494-503. DOI: 10.1002/jeq2.20199.

Bruno, A.W., Gallipoli, D., Perlot, C., Mendes, J., 2019. Optimization of bricks production by earth hypercompaction prior to firing. Journal of Cleaner Production 214:475-482. DOI: 10.1016/j.jclepro.2018.12.302

Bui, H. (2021). Study on performance enhancement of coconut fibres reinforced cementitious composites. PhD thesis. Caen Normandie University, France

Bui, H, Hussain, M., Levacher, D. (2022). Recycling of tropical natural fibers in building materials. Natural fibers, Intechopen book. DOI: 10.5772/intechopen.102999.

Calatan, G., Hegyi, A., Dico, C., Mircea, C., (2016). Determining the optimum addition of vegetable materials in adobe bricks. Procedia Technology 22: 259 – 265. https://doi.org/10.1016/j.protcy.2016.01.077

Canet, R., Chaves, C., Pomares, F., Albiach, R. (2003). Agricultural use of sediments from the Albufera Lake (eastern Spain). Agriculture, Ecosystems and Environment 95, 29–36. doi:10.1016/S0167-8809(02)00171-8.

Cantegrit L., Eisenlohr L. (2012). Potentialité de relargage en éléments inorganiques d'un complexe sol agricole-sédiments de dragage de canaux non contaminés. Présentation orale, Intersol'2012, 27-30 mars 2012.

Chambre d'agriculture des Côtes d'Armor-CACA (2016). Utilisation des vases de la Rance sur les terres agricoles. Septembre 2016. Op.cit. p.8.

Chourre G. (2016). Modalités de dragage de la Sèvre niortaise domaniale : enjeux, techniques et valorisation, Colloque Rennes dragages, 22 novembre 2016, Institution Interdépartementale du Bassin de la Sèvre Niortaise – IIBSN.

Damas O., Coulon A. (2016). Créer des sols fertiles: du déchet à la végétalisation urbaine. Editions Le Moniteur, 335 p.

Darmody, G. R., Marlin, J.C. (2002). Sediments and sediment-derived soils in Illinois: pedological and agronomic assessment. Environmental Monitoring and Assessment 77: 209–227. https://doi.org/10.1023/A:1015880004383

Dawid B. (2017). La faisabilité de la valorisation des sédiments de dragage de l'estuaire de la Vilaine, une démarche territoriale. Rapport de mastère spécialisé en économie circulaire, 143p. EME Bruz-Rennes.

Del Negro, R. (2019). Characterization of Usumacinta River's sediments, Master thesis, Université de Nantes-IFSTTAR Nantes, 18p.

Djeran-Maigre, I., Levacher, D., Hussain, M. (2022). Valorisation des sédiments en matériaux de construction durables, Valorisation agronomique en soutien à la biodiversité et à l'agriculture riveraine. WP4 - Rapport de synthèse. INSA Lyon, France

EC, European Commission, van Beek C. and Toth G., 2012. Risk Assessment Methodologies of Soil Threats in Europe - Status and options for harmonization for risks by erosion, compaction, salinization, organic matter decline and landslides. JRC Scientific and Policy Reports. EUR 24097 EN, 84p.

ESCOPE/ASCAL (2008). Suivi de la végétalisation du parc à cendres de la centrale thermique EDF à Blénod-lès-Pont-à-Mousson - Rapport provisoire, 73p.

Ferreira V. (2003). Valorisation agricole des sédiments marins de la Rance : Bilan des premières opérations et perspectives agronomiques. Rapport de stage, ENSAR, 50 p.

Fourvel G. (2018). Valorisation agronomique des sédiments fins de retenues hydroélectriques en construction d'anthroposols fertiles. Thèse de doctorat Agrocampus Ouest, 2018. 397p. https://tel.archives-ouvertes.fr/tel-02136422

Gnis (2008). Cultivons l a diversité des plantes cultivées, Ryegrass Anglais. Techniques de culture et activités pédagogiques. www.semencemag.fr.

Houben, H., Guillaud, H., 1994. Earth Construction: A Comprehensive Guide. Intermediate Technology Publications, London.

Hussain, M., Levacher, D., Leblanc, N., Zmamou, H., Djeran-Maigre, I., Razakamanantsoa, A., Saouti, L. (2021a). Properties of Mexican tropical palm oil flower and fruit fibers for their perspective use in eco-friendly construction material. Fibers, 9(11), 63. https://doi.org/10.3390/fib9110063

Hussain, M., Levacher, D., Saouti, L., Leblanc, N., Zmamou, H., Djeran-Maigre, I., Razakamanantsoa, A., (2021b). Implementation on a Preparation and Controlled Compaction Procedure for Waste-Fiber-Reinforced Raw Earth Samples. J. Compos. Sci., 6(1), 3; https://doi.org/10.3390/jcs6010003

Illampas, R., Ioannou, I., Charmpis, D.C. (2011). A study of the mechanical behaviour of adobe masonry. Structural Repairs and Maintenance of Heritage Architecture XII 485. WIT Transactions on The Built Environment, Vol 118. doi:10.2495/STR110401

Ismail, S., Yaacob, Z. (2011). Properties of laterite brick reinforced with oil palm empty fruit bunch fibres. Pertanika Journal of Science and Technology, Vol. 19, pp. 33 – 43. doi: 10.1016/j.protcy.2016.01.077

Jadczyszyn, j., Niedźwiecki, j., Debaene, g. (2016). Analysis of agronomic categories in different soiltexture classification systems. Polish Journal of Soil Science, vol. XLIX/1 2016 PL ISSN 0079-2985. DOI: 10.17951/pjss/2016.49.1.61

Javaid, M.M., Mahmood, A., Alshaya, D.S., AlKahtani, M., Waheed, H., Wasaya, A., Aslam, S., Naqve, M., Haider, I., Shahid, M.A., Nadeem, M.A., Azmat, S., Bilal, A.K., Bilal, R.M., Attia, K., Fiaz, S. (2022). Influence of environmental factors on seed germination and seedling characteristics of perennial ryegrass (Lolium perenne L.). Scientific Reports 12(1). Nature portfolio. DOI: 10.1038/s41598-022-13416-6

Jiang, Y., Lawrence, M., Ansell, M.P., Hussain, A. (2018). Cell wall microstructure, pore size distribution and absolute density of hemp shiv. Royal Society Open Sciience, 5 (4), 171945. https://doi.org/10.1098/rsos.171945.

JORF (2013). Arrêté du 8 février 2013 complémentaire à l'arrêté du 9 août 2006 relatif aux niveaux à prendre en compte lors d'une analyse de rejets dans les eaux de surface ou de sédiments marins, estuariens ou extraits de cours d'eau ou canaux relevant respectivement des rubriques 2.2.3.0, 3.2.1.0 et 4.1.3.0 de la nomenclature annexée à l'article R. 214-1 du code de l'environnement. Journal Officiel de la République Française

Lalaut Y. (2014). Valorisation à terre des sédiments non immergeables : l'action du Grand Port de Dunkerque, 4èmes Assises du Port du Futur, 8-9 septembre 2014, Paris.

Kiani, K., Raave, H., Simojoki, A., Tammeorg, O., Tammeorg, P. (2021). Recycling lake sediment to agriculture: Effects on plant growth, nutrient availability, and leaching. Science of the Total Environment, 753, 141984. https://doi.org/10.1016/j.scitotenv.2020.141984

Koropchak S.C., Daniels L.W., Wick A., Whittecar R.G., Haus N. (2015). Beneficial use of dredge materials for soil reconstruction and development of dredge screening protocols. Journal of environmental quality, 45:62-73.

Kotuby-Amacher, J., Koenig, R., Kitchen, B., (2000). Salinity and plant tolerance. AG-SO-03. Utah state university extension.

Lembke, W.D., Mitchell, J.K. (1983). Dredged sediment for agriculture: Lake Paradise , Mattoon, Illinois. Transactions of the ASAE. American Society of Agricultural Engineers. DOI: 10.13031/2013.34027.

Lenormand H., Leblanc N. (2020). Des particules végétales en abondance et renouvelables.6p. https://www.construction21.org.

Levacher D. (2021). Sediment beneficial use: Sediment as natural resource. L'Usumacinta en 12 questions. 2p., (version anglaise). Projet Val Uses (voir Val Uses, 2017).

Levacher, D., Hussain, M., Zmamou, H. (2022). Etude de germination et de croissance de plantes mexicaines sur terreau et sédiment mexicain. ANR-CONACYT: VAL-USES Project 2018-2022. Task 4: Characteristics, future uses and valorization of sediments.

Martínez-Nicolás, J.J., Legua, P., Núñez-Gómez, D., Martínez-Font, R., Hernández, F., Giordani, E., Melgarejo, P. (2020). Potential of dredged bioremediated marine sediment for strawberry cultivation. Scientific Reports volume 10, Article number: 19878. https://doi.org/10.1038/s41598-020-76714-x

Macía, P., Fernández-Costas, C., Rodríguez, E., Sieiroc, P., Pazos, M., Sanromána, M.A. (2014). Technosols as a novel valorization strategy for an ecological management of dredged marine sediments. Ecological Engineering 67, 182-189. http://dx.doi.org/10.1016/j.ecoleng.2014.03.020.

McManus, J. 1988. Grain size distribution and interpretation, in M.E. Tucker (Ed.),Techniques in Sedimentology, pp. 63–85.

MOPT (1992): Bases para el diseno y construccion con tapial. Madrid, Spain: Centro de Publicaciones, Secretarıa General Tecnica, Ministerio de Obras Publicas y Transportes.

Munns, R. (2002). Comparative physiology of salt and water stress. Plant Cell Environ. 2002 Feb;25(2):239-250. doi: 10.1046/j.0016-8025.2001.00808.x.

NORMA E.080 (2017): Diseño y construcción con tierra reforzada. Ministerio de Vivienda, Construcción y Saneamiento. Anexo-Resolución Ministerial, 21-2017-Vivienda. Available online: https://procurement-notices.undp.org/view_file.cfm?doc_id=109376

NZS 4298 (1998): Materials and workmanship for earth buildings [Building Code Compliance Document E2 (AS2)]

Quideau P. (2016). Utilisation des vases de la Rance sur les terres agricoles. Septembre 2016, Chambre d'agriculture.

Rakshith S., Singh D. N. (2016). Utilization of dredged sediments: Contemporary issues. Journal of Waterway, Port, Coastal, and Ocean Engineering, Volume 143 Issue 3, May 2017, American Society of Civil Engineers. https://doi.org/10.1061/(ASCE)WW.1943-5460.0000376.

Robin, P. (2017). Valorisation des sédiments marins. Port Autonome de Dunkerque. Sediments marins, Cerema. Colas. https://www.cerema.fr/system/files/documents/2017/10/3-Sediments_marins_P_ROBIN.pdf

Salih, M.M., Osofero, A.I., Imbabi, M.S. (2019). Critical review of recent development in fiber reinforced adobe bricks for sustainable construction. Front. Struct. Civ. Eng., 14(4): 839–854 https://doi.org/10.1007/s11709-020-0630-7

Sheehan C., Harrington J., Murphy J. (2010a). A technical assessment of topsoil production from dredged material. Resources, Conservation and Recycling, vol. 54, pp 1377-1385. doi:10.1016/j.resconrec.2010.05.012.

Sheehan C., Harrington J., Murphy J. (2010b). An environmental and economic assessment of topsoil production from dredge material. Resources, Conservation and Recycling, vol. 55, pp 209-220. doi : 10.1016/j.resconrec.2010.09.011.

Sturgis T.C., Lee C.R. (1999). Manufactured soil screening test, DOER Technical Notes Collection TN DOER-C6, U.S. Army Engineer Research and Development Center, 9 p.

Sturgis T.C, Lee C.R, Banks H.C, Jr. (2001a). Evaluation of Toledo harbor dredged material for manufactured soil, Phase 1: Greenhouse Bench-Scale Test, Technical Report ERDC/EL TR-01-25,U.S. Army Engineer Research and Development Center, 31 p.

Sturgis T.C, Lee C.R., Banks H.C, Jr., Burchell M.R., II, Johnson K. (2001b). Evaluation of manufactured soil using dredged material from New York/New Jersey Harbor Newton Creek Site; Phase 1: Greenhouse bench-scale test. ERDC/ELTR-01-35, U.S. Army Engineer Research and Development Center, 48 p.

Sturgis, T.C., Lee, C.R., Banks, H.C., Jr., Johnson, K., Langan, J.P., Rees, S.I., Dyess, C. (2002). Evaluation of manufactured soil using dredged material from confined placement facilities in Mobile, Alabama; Phase 1: Greenhouse bench-scale test. Technical Report ERDC/ELTR-02-12, U.S. Army Engineer Research and Development Center, Vicksburg.

Thygesen, A., Daniel, G., Lilholt, H., Thomsen, A.B., 2008. Hemp fiber microstructure and use of fungal defibration to obtain fibers for composite materials. Jouranl of Natural Fibers 2 (4), 19–37. https://doi.org/10.1300/J395v02n04_02.

USSLS, United States Salinity Laboratory Staff, 987 1954. Diagnosis and Improvement of Saline and Alkali Soils. United States Department of Agriculture. Agriculture Handbook, n°60. L.A. Richards, Editor. 166p.

USDA-NRCS (1999). U.S. Department of Agriculture, National Resources and Conservation Service). 1999. Guide to Texture by Feel. www.nrcs.usda.gov/wps/portal/nrcs/ detail/soils/edu/?cid=nrcs142p2_054311.

Urbaniak, M., Lee, S., Takazawa, M., Mierzejewska, E., Baran, A., Kannan, K. (2019). Effects of soil amendment with PCB-contaminated sediment on the growth of two cucurbit species.

Environmental Science and Pollution Research 27:8872–8884. https://doi.org/10.1007/s11356-019-06509-9

VROM. (2000). Circular on target values and intervention values for soil remediation. Ministry of Housing, spatial Planning and Environment DBO/1999226863.

Weatherspark (2021). https://fr.weatherspark.com/y/11302/Météo-moyenne-à-Tenosique-de-Pino-Suárez-Mexique-tout-au-long-de-l'année. Consulted on 26/10/2021

Welsch-Pausch, K., Mclachlan,M.S. Umlauf, G. (1995). Detentrination of the Principal Dibenzo-p-dioxins and Di s to Lolium muMorum (Welsh Ray Grass). Environ. Sci. Techno., 29, 1090- 1098.

Ziapkoff, M., Robin, G., Duigou, L., Daya, E.M., Cadou, J.M. (2022). Etude numérique de l'amortissement de structures composites à fibre de lin par une méthode itérative d'ordre élevé. CSMA, 15ème Colloque National en Calcul des Structures 16-20 mai 2022, Presqu'île de Giens (Var)

Summary of thesis

For sediments reuse in fired and earth bricks, physico-chemical, mineralogical, hydromechanical and environmental characteristics of Usumacinta River sediments were investigated. Granulometry of Usumacinta River sediments indicates that most of these sediments are silty with low clay content. Clay content of T5 and J4 sediments is relatively higher. Organic matter in Usumacinta River sediments is also low and below 6%. Presence of contaminants in Usumacinta River sediments is negligible.

For Usumacinta River sediments reuse in fired bricks, their suitability for fired bricks was analyzed with industrial approaches. Augustinik diagram based on sediment's chemical composition shows that these sediments are suitable for fired bricks. In plasticity chart, sediments moulding characteristics are also appropriate for bricks. However, in the Winkler diagram, sediments grain sizes are outside the recommended zones for fired bricks. Fired bricks cubic and prismatic specimens of sizes 20*20*20 mm^3 and 15*15*60 mm^3 were manufactured for compressive and tensile strength testing bricks and fired at a temperature range of 700 °C to 1100 °C. Bricks were made with individual sediments and different sediments mixtures based on-site, mineralogy, oxides and specific surface area.

Physical and mechanical characteristics of bricks were investigated through different tests. Linear shrinkage in Usumacinta bricks ranges from 0.56 to 13.5%. Density of Usumacinta bricks ranges from 994 kg/m^3 to 1888 kg/m^3 and increases with increasing temperature. Loss on ignition (LOI) of fired bricks ranges from 0.56% to 13.51% and it is highest for clayey sediments such as T5 and J4. Water absorption of bricks ranges from 10.71% to 22.39%. Water absorption is highest in T1 sediments and lowest in T5 sediments. Mechanical testing shows that the flexural and compressive strength of Usumacinta bricks is maximum at 1100 °C and at moulding moisture content of 0.25PI and 0.5PI in the Sembenelli diagram. Sediments mixtures with specific surface area and mineralogy approaches have low flexural and compressive strength. Flexural strength of J4 (12.82 MPa at 1000 °C) and T5 (6.60 MPa at 1100 °C) sediments is the highest. T5, J3, J4 and mixes suggested with Winkler diagram and site-based approach have good flexural and compressive strength. Compressive strength of T5 and J4 sediments is 15.51 MPa and 17.04 MPa at a moderate temperature of 700 °C and satisfies the compressive strength requirement of fired bricks which is usually between 5 to 15 MPa. T3, T5, J3 and J4 sites sediments have good compressive strength at a moderate temperature of 850 °C. At 1100 °C compressive strength of most of the bricks is higher than 5 MPa except for T1 and T2 which are sandy sediments.

In case of earth bricks, sediments suitability was observed with AFNOR and MOPT standards. Granulometry and Atterberg limits of Usumacinta River sediments are suitable for earth bricks. Prismatic earth bricks of size 4*4*16 cm^3 were manufactured with J3 sediments with addition

of 0% to 5% palm oil flower fibers (POFL). Testing of bricks shows that Usumacinta bricks have a maximum tensile strength at 4% POFL fibers addition with G-2cm fibers and its value is 2.93 MPa. For G-3cm long fibers bricks have a maximum tensile strength at 3% fibers addition and its value is 3.19 MPa. Compressive strength of Usumacinta bricks is maximum at 1% fiber content for G-2cm long fibers and its value is 3.72 MPa while for G-3cm long fibers, compressive strength is maximum at 2% fiber content and its value is 3.84 MPa. Recommended tensile strength of earth bricks varies from 0.12 MPa to 1 MPa while recommended compressive strength of earth bricks is 1 MPa (NZS, 1998, NORMA E.080, 2017; AFNOR XP, P13-901, 2001). Usumacinta earth bricks have considerably higher strength and satisfy the recommended strength limitations.

Usumacinta River sediments characteristics were investigated to explore their agronomic potential. Physico-chemical and mineralogical characteristics of Usumacinta sediments are similar to soils used for agronomy. Electrical conductivity (EC) and sodium absorption value of Usumacinta sediments show that Usumacinta sediments are non-saline sediments. Usumacinta River sediments were used with potting soil to grow ryegrass within the greenhouse.

Three soil compositions were tested with 0% sediments, 50% sediments and 100% sediments (C3) addition to potting soil. Germination of ryegrass is similar in all three mixtures. However, the growth of ryegrass is significantly lower with 100% sediments. 50% potting soil replacement with sediments shows similar growth to 100% potting soil, which indicates the sediment's potential to partially replace even the commercial soil. Furthermore, the germination of ryegrass similar is also similar in all three compositions which is encouraging for sediments recovery in agronomy. Ryegrass germination and growth with Usumacinta River sediments highlights the potential of these sediments as a sustainable resource for agronomy to improve the quality of degraded soils by excessive exploitation and use of commercial fertilizers to grow crops. Usumacinta sediments have the potential to be used for vegetation covers to prevent erosion and for soil aeration purposes.

Experimental research on Usumacinta River sediments shows that Usumacinta River sediments reuse in agronomy and manufacturing fired and earth bricks are suitable recovery solutions for these sediments and offer the possibility of ecological building material and agronomic raw material with local resources in the context of a circular economy.

Finally, local sediments from Dunkirk port (DK) and Garonne River (GAR) France were investigated for their recovery in earth bricks along with hemp shiv. DK sediments have suitable granulometry for earth bricks. However, GAR sediments slightly deviate from recommended zones based on granulometry. Consistency limits of both DK and GAR sediments are unsuitable for bricks due to higher sand content and organic matter.

Earth bricks were manufactured with DK and GAR sediments with hemp shiv addition of 0%, 1%, 2%, 3%, 4% and 5%. Mechanical testing of bricks shows that the tensile strength of both

DK and GAR bricks is low. It is maximum for DK bricks at 1% hemp shiv addition and its value is 0.48 MPa. GAR bricks have a maximum tensile strength at 4% hemp shiv addition and their tensile strength is 0.60 MPa. Compressive strength of GAR bricks is low and its value is maximum at 3% hemp shiv addition which is 1.52 MPa. GAR bricks satisfy the tensile and compressive strength requirements at 2 to 5% hemp shiv addition while DK bricks satisfy the tensile strength requirement at 0% to 5% hemp shiv addition (NZS, 1998; AFNOR XP P13-901, 2001; NORMA E.080, 2017). Low strength of earth bricks with DK and GAR sediments is due to higher organic matter and low clay content. Strength of DK bricks can be improved by mixing them with clayey sediments to improve the granulometry and plasticity. GAR sediments have a higher organic matter which is around 9%. Addition of lime can stabilize the organic matter and increase the strength of these bricks. Furthermore, the use of soft fibers from hemp, flax etc. is recommended rather than hemp shiv to improve the adhesion of fibers and sediments.

Prospective

Crude and fired bricks were manufactured and tested in laboratory conditions. Further analysis and experimental work are suggested at industrial scale for large-scale production. Furthermore, it is important to evaluate the influence of climatic conditions on durability of bricks and socio-economic acceptance of fired and earth bricks manufactured with dredged sediments.

Numerical modelling of earth bricks is also an interesting tool as it gives the idea of the strength of bricks without manufacturing bricks through sediments and fibers characteristics. Further research is needed to validate the experimental results with numerical modelling to establish a model for earth bricks.

For sediments reuse in agronomy, experiments with local plants and soil are recommended in real conditions as greenhouse testing is done in controlled conditions while the real conditions of field vary significantly with time. In addition, the use of local soil with Usumacinta River sediments is suggested as potting soil is commercial soil with higher organic matter which is not the case with most of the soil in fields

List of figures

List of tables

Annex

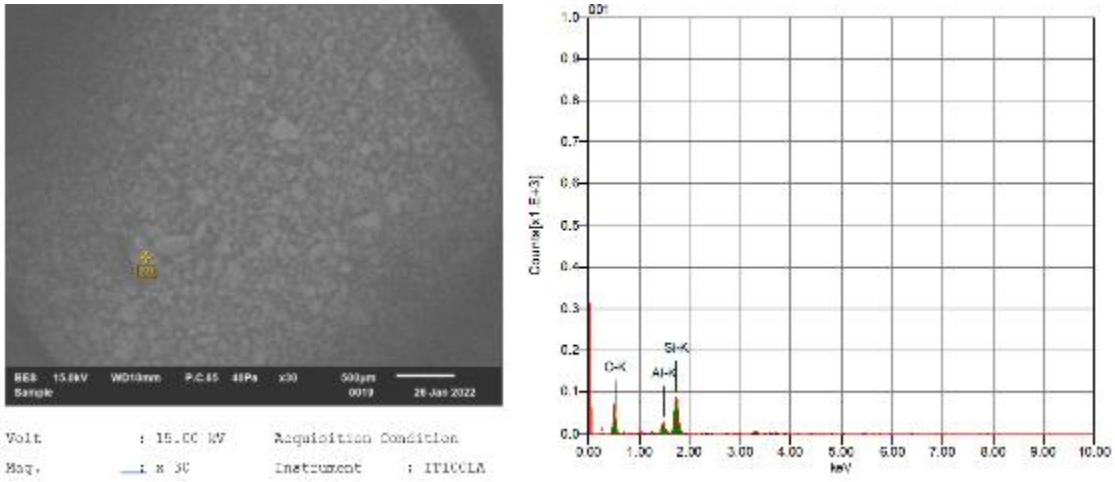

Figure A. 1. SEM image and spectrum of T1 sediments

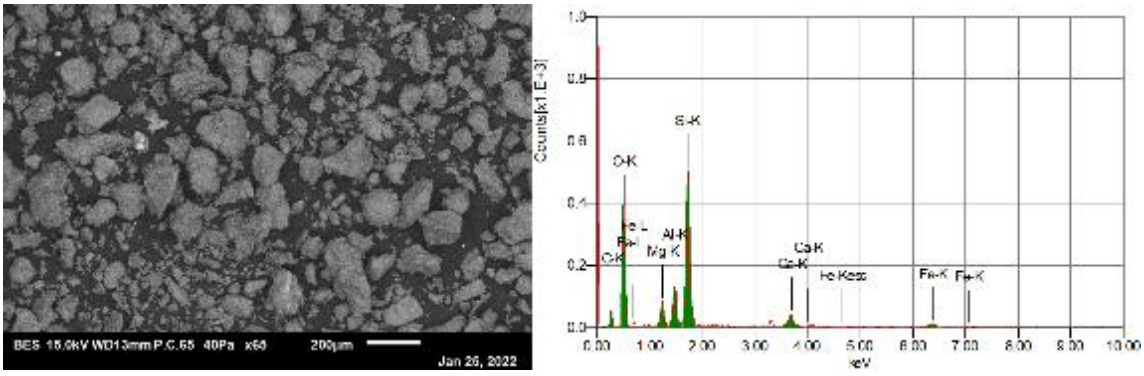

Figure A. 2. SEM image and spectrum of T2 sediments

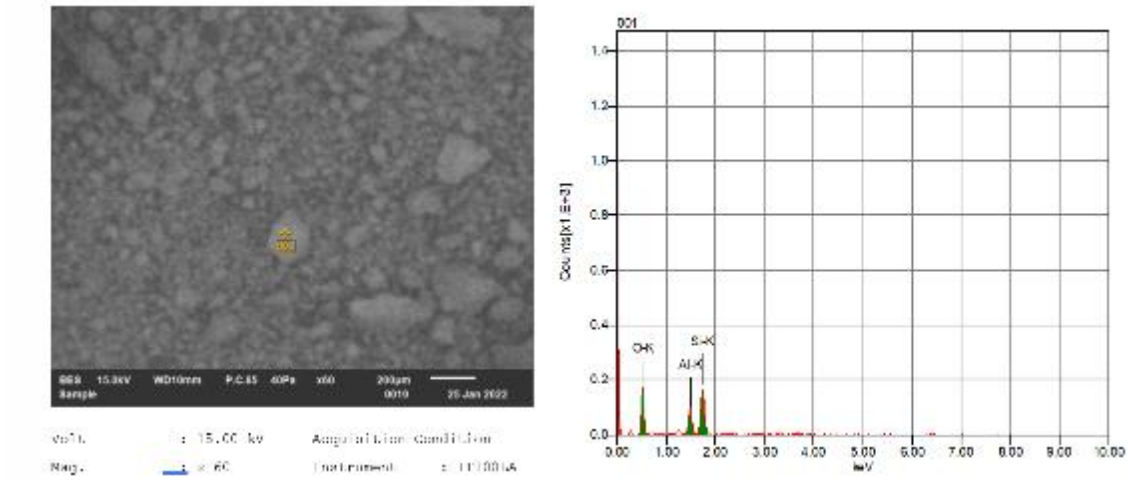

Figure A. 3. SEM image and spectrum of T5 sediments

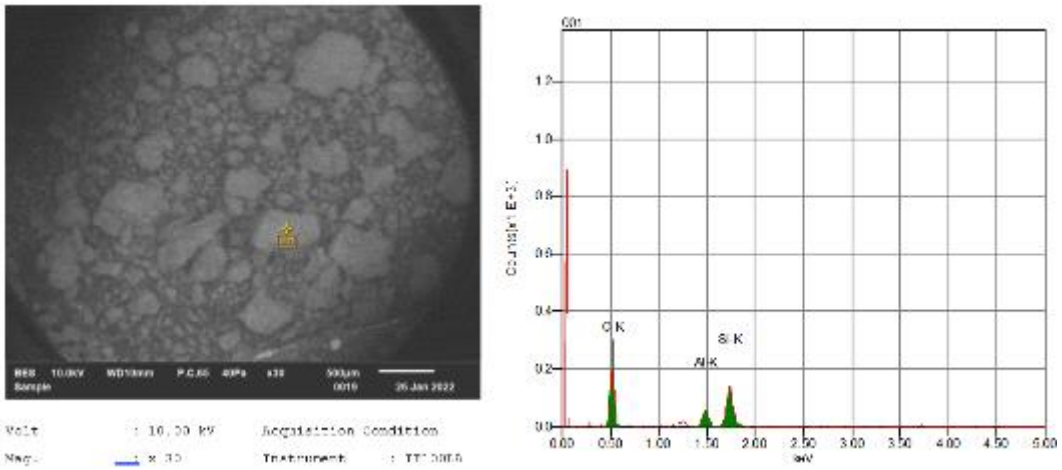

Figure A. 4. SEM image and spectrum of T6 sediments

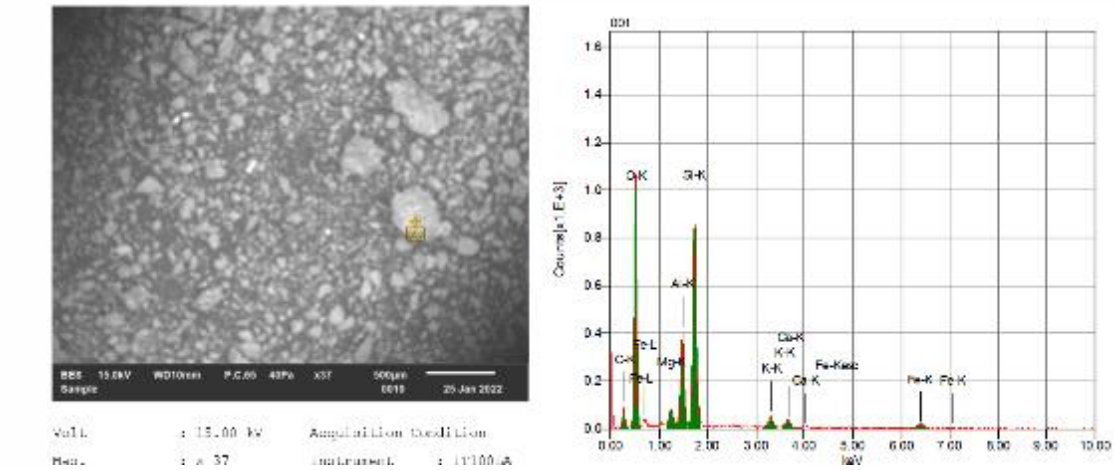

Figure A. 5. SEM image and spectrum of J3 sediments

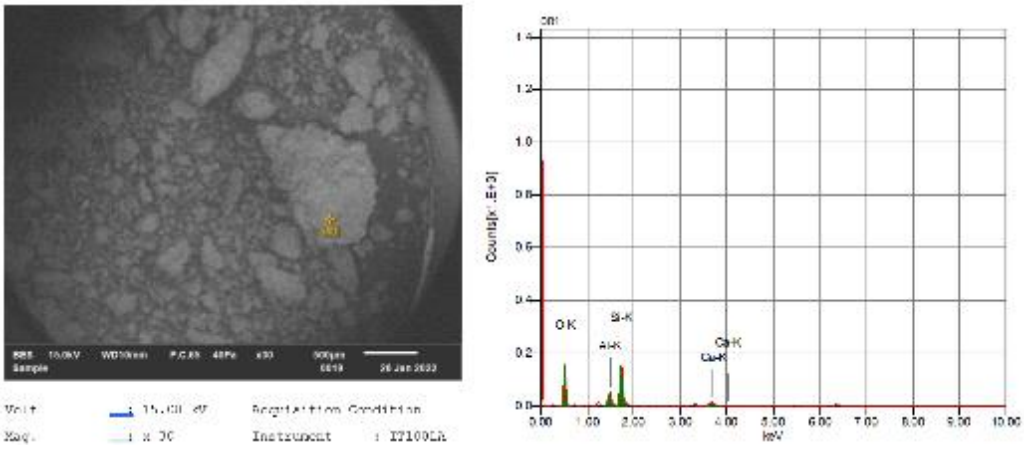

Figure A. 6. SEM image and spectrum of J4 sediments

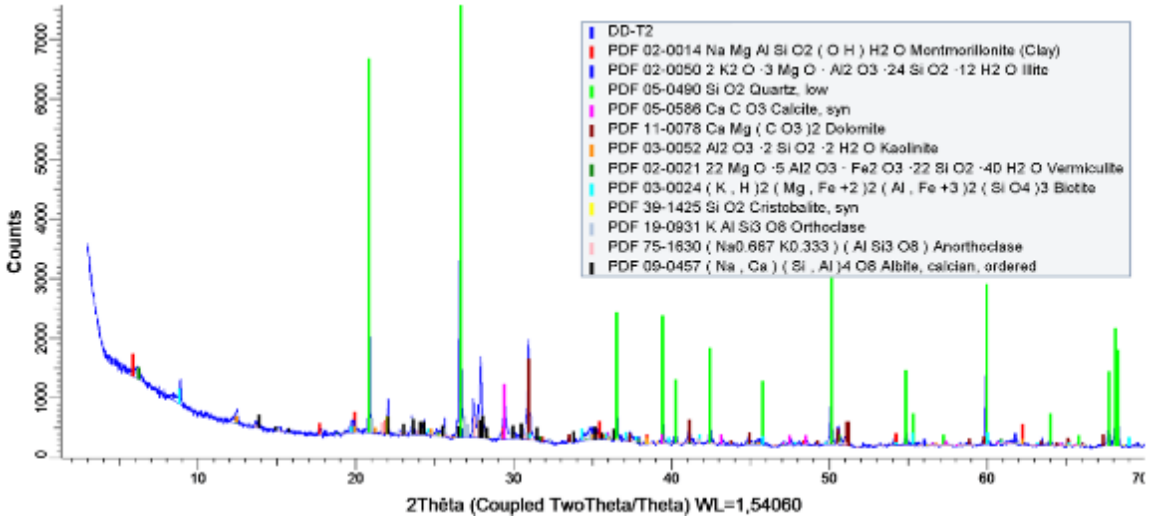

Figure A. 7. XRD spectrum of T2 sediments

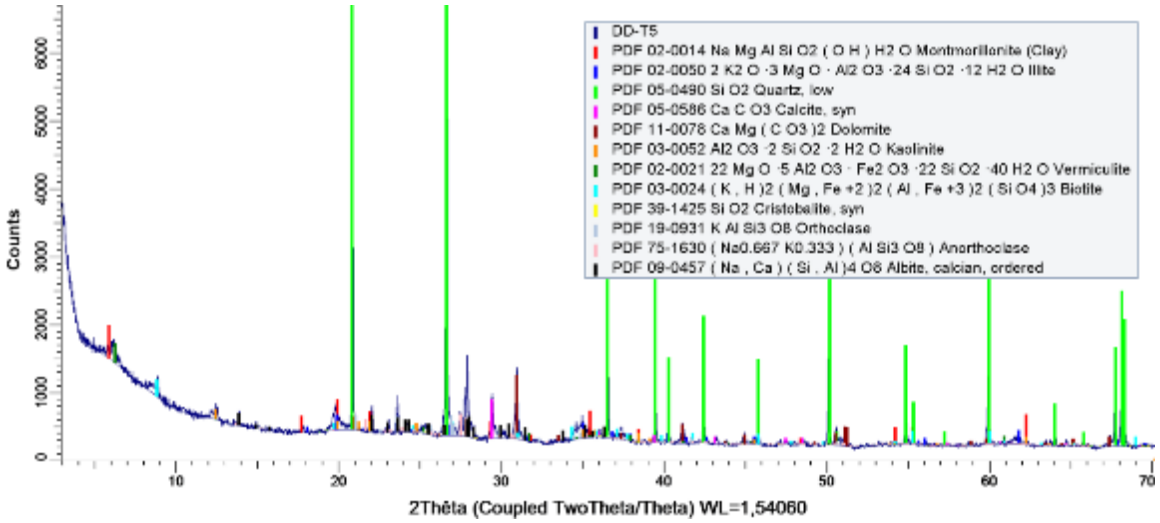

Figure A. 8. XRD spectrum of T5 sediments

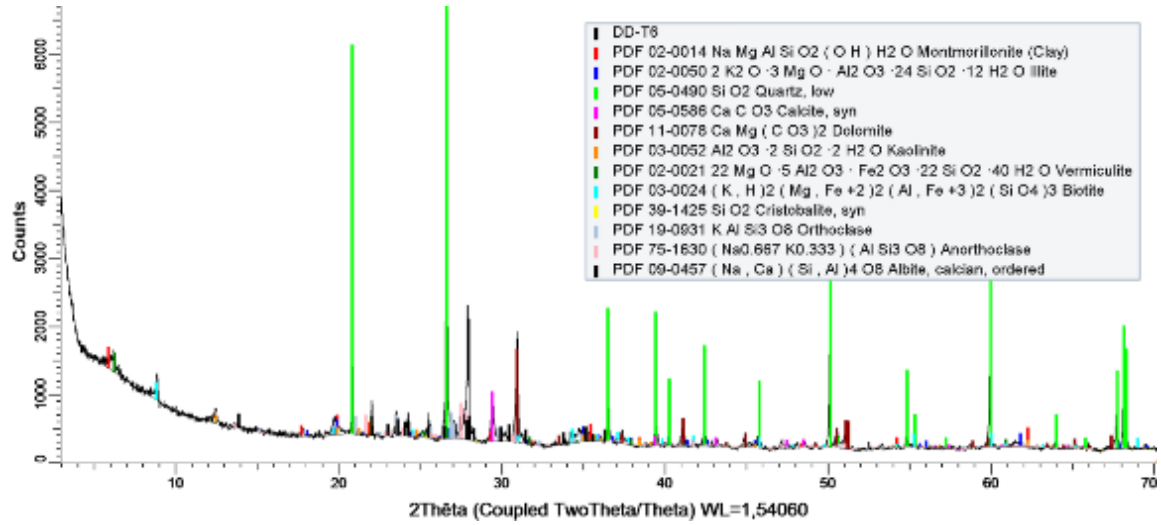

Figure A. 9. XRD spectrum of T6 sediments

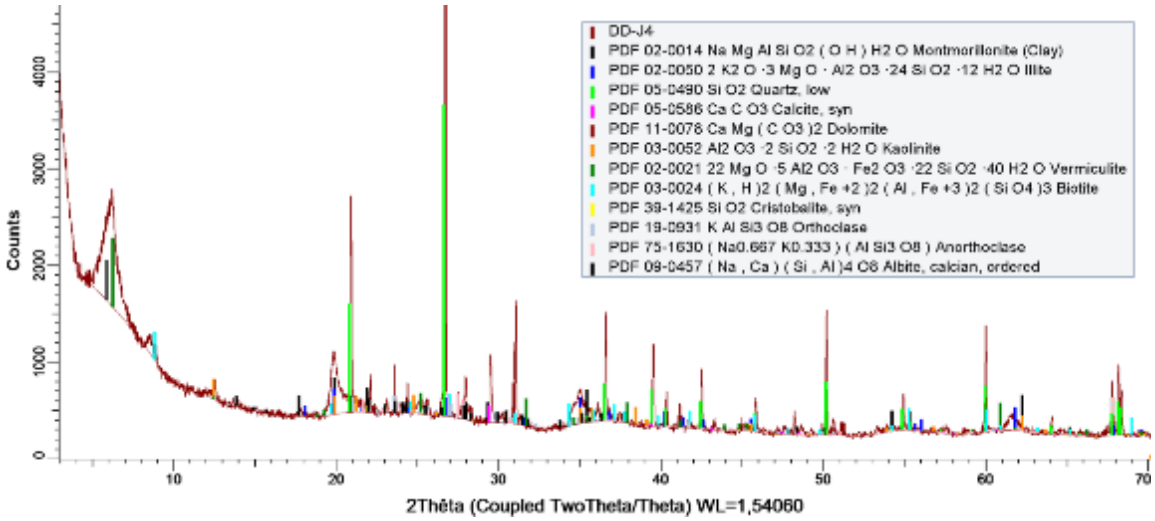

Figure 2. XRD spectrum of J4 sediments

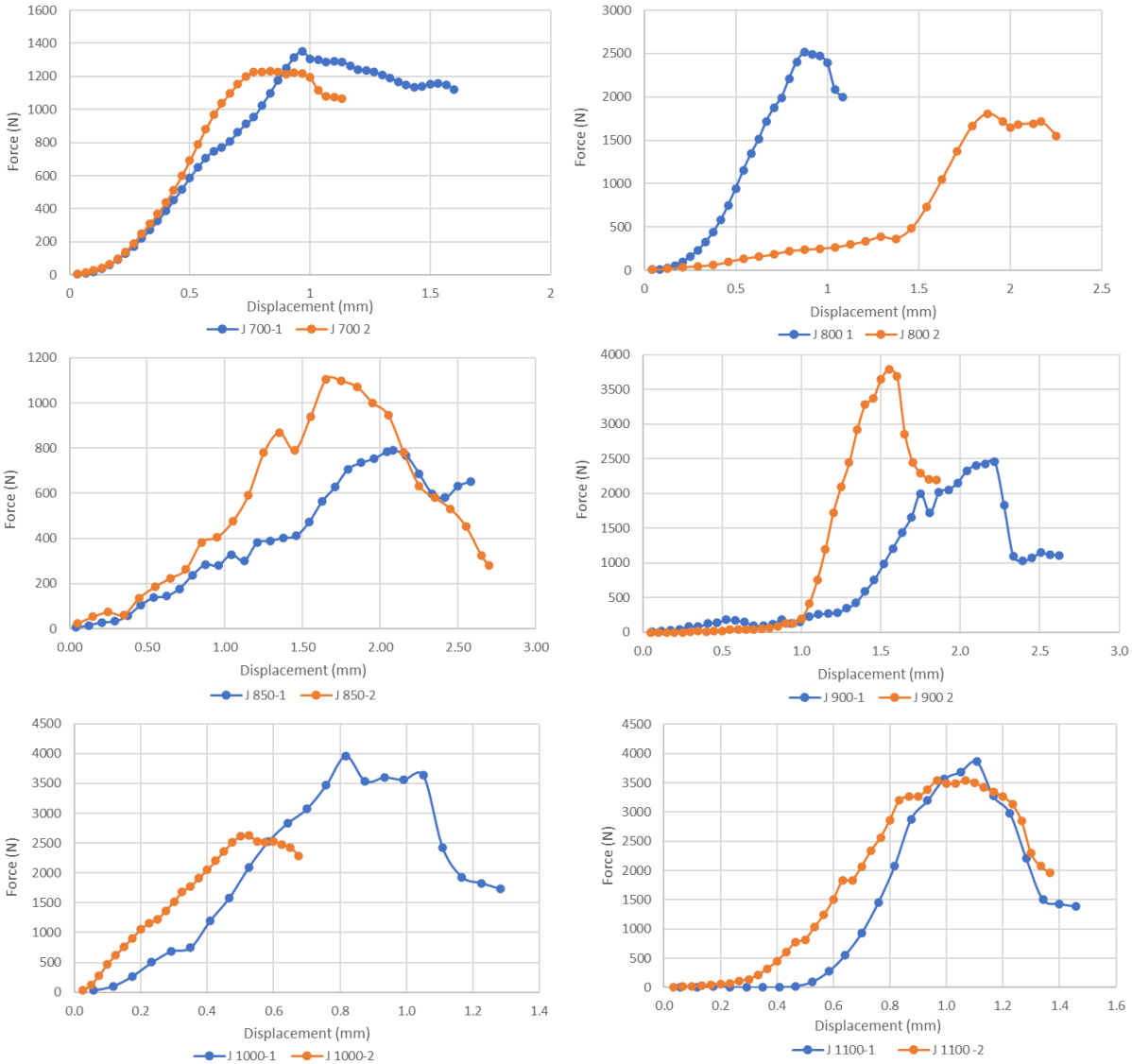

Figure A. 10. Flexural strength curves of fired brick